

Paramagnetic NHC Complexes of Chromium and Titanium - Synthesis and Chemistry

by

Tracy Hamilton MChem (Hons.)

Submitted in fulfilment of the requirements of degree of

Doctor of Philosophy



School of Chemistry
Cardiff University
Wales, UK

2010

UMI Number: U516904

All rights reserved

INFORMATION TO ALL USERS

The quality of this reproduction is dependent upon the quality of the copy submitted.

In the unlikely event that the author did not send a complete manuscript and there are missing pages, these will be noted. Also, if material had to be removed, a note will indicate the deletion.



UMI U516904

Published by ProQuest LLC 2013. Copyright in the Dissertation held by the Author.
Microform Edition © ProQuest LLC.

All rights reserved. This work is protected against
unauthorized copying under Title 17, United States Code.



ProQuest LLC
789 East Eisenhower Parkway
P.O. Box 1346
Ann Arbor, MI 48106-1346

Acknowledgements

Firstly, I would like to thank my supervisors: Professor Kingsley J. Cavell for his expert guidance, but more importantly for his patience and support throughout my PhD; Dr Damien M. Murphy for his advice and helpful discussions on the EPR spectroscopy side of my project. I also thank Woody for his help over the past few years, not least for reading my thesis and reminding me when to calm down and go to the pub.

Thanks must also go to the technical staff at Cardiff University; I am particularly grateful for the help of Robyn in attaining mass spec data for some very sensitive complexes, Rob for his help with many analytical techniques and crystallographer Dr Benson Kariuki for his excellent skills with the handling of air sensitive complexes.

A special mention to the many members of the Cavell group past and present who have made coming in into the lab such a joy, thanks for making me laugh every day and especially for all the lost Friday nights in the Pen and Wig. Thanks also to Lucia, for all the help with EPR, Sasol Technology for providing financial support and Dr Dave McGuinness for the catalysis study.

I am lucky to say that I have many people to thank for making my time at Cardiff University so enjoyable; Baz, Andrew, Chris, Emma, Dan, Mandeep, Adrien, Manuel, Debs, Gareth, Laura, Jess, and everyone involved with ChemSoc-thank you for many fun years!

I would like to express my appreciation for the support from all those outside of Cardiff University, of which there are too many to mention, but particular thanks must go to Becky and Hayley for always being there. For his patience, understanding and encouragement I would like to thank Richard-you may not realise how much you have helped me, and I am very grateful.

Finally, and most importantly, I would like to thank my parents who have supported me in every way-this thesis certainly would not have been possible without their help.

Thank you both for everything.

DECLARATION

This work has not previously been accepted in substance for any degree and is not concurrently submitted in candidature for any degree.

Signed *Hamidhan*..... (candidate) Date *10.10.2010*.....

STATEMENT 1

This thesis is being submitted in partial fulfillment of the requirements for the degree of PhD

Signed *Hamidhan*..... (candidate) Date *10.10.2010*.....

STATEMENT 2

This thesis is the result of my own independent work/investigation, except where otherwise stated. Other sources are acknowledged by explicit references.

Signed *Hamidhan*..... (candidate) Date *10.10.2010*.....

STATEMENT 3

I hereby give consent for my thesis, if accepted, to be available for photocopying and for inter-library loan, and for the title and summary to be made available to outside organisations.

Signed *Hamidhan*..... (candidate) Date *10.10.2010*.....

Abbreviations

Ar	aryl group
Av	Average
b	broad
δ	chemical shift (ppm)
d	doublet
dd	double-doublet
DCM	dichloromethane
DIPP	2,6-Diisopropylphenyl
DMSO	dimethylsulfoxide
EPR	electron paramagnetic resonance
ES-MS	electrospray mass spectrometry
Et	ethyl group
Et ₂ O	diethyl ether
HRMS	high resolution mass spectrometry
ⁱ Pr	<i>iso</i> -propyl
IR	infra red
KHMDS	Potassium hexamethyldisilazide
L	neutral, 2 electron donor ligand
LAO	linear alpha olefin
m	multiplet
M	metal
MAO	methylaluminoxane
Me	methyl
MeCN	acetonitrile
md	medium
Mes	mesityl, 2,4,6-trimethylphenyl
NHC	N-heterocyclic carbene
NMR	nuclear magnetic resonance
ORTEP	oak-ridge thermal ellipsoid plot
Ph	phenyl
q	quartet

R	alkyl or aryl group
s	singlet
sh	shoulder
st	strong
r.t.	room temperature
t	triplet
^t Bu	<i>tertiary</i> -butyl
THF	tetrahydrofuran
TON	turnover number
UV	ultraviolet visible spectroscopy
w	weak
X	halogen
Xyl	xylyl

Abstract

This thesis focuses on the synthesis of early transition metal complexes. A unique series of chromium complexes in oxidation states 0, +I, +II and +III containing N-heterocyclic carbenes have been prepared, as well as titanium complexes in the +III oxidation state. A series of bis(phosphine) complexes of chromium in oxidation states 0 and +I have also been synthesised, and all paramagnetic compounds have been analysed by EPR spectroscopic techniques.

Chapter one provides an introduction to the chemistry of N-heterocyclic carbenes, and their crucial role in organometallic chemistry. A background to the use of early transition metal complexes in the ethylene oligomerisation process is described, along with recent advances in selective ethylene trimerisation and tetramerisation catalysis. An overview of Electron Paramagnetic Resonance spectroscopy is provided as a brief theoretical background to the technique and the applications relevant to the synthetic work presented in this thesis.

Chapter two introduces a novel series of donor-functionalised imidazolium salts and their structural characterisation. Synthesis of the corresponding free NHC ligands is described, and the synthesis of silver(I) complexes reported. This chapter provides an insight into the bonding of these new ligands, allowing comparison to similar compounds.

In chapter three, the synthesis of a series of bis(phosphine) chromium(0) and chromium(I) complexes is described, along with their characterisation and EPR analysis. This work was sponsored by Sasol Technology, and was carried out in order to gain vital skills and experience in the preparation and handling of these sensitive compounds.

Chapter four describes the synthesis of a series of low oxidation state chromium complexes. Chromium(0) and novel chromium(I) complexes were prepared using a similar methodology described in chapter three. EPR analysis of the resulting paramagnetic complexes is included, and represents the first series of chelating NHC-Cr(I) complexes to be studied in this way. An interesting reaction is described, in which a NHC ligand is found to decompose in an unexpected manner upon attempted coordination to chromium(0). A novel series of chromium(II)-NHC complexes have also been prepared and are thought to be the first of their type reported.

Chapter five describes the synthesis of a novel series of NHC containing Cr(III) and Ti(III) complexes. Analysis by EPR spectroscopy was carried out and the resulting data is reported, confirming the electronic structures of the complexes. The catalytic activity of a

selection of complexes in ethylene oligomerisation reactions were tested and found to give mostly polymeric product, with little selectivity toward linear alpha olefins. The variation in observed activities is attributed to the different ligands systems involved.

Table of Contents

Chapter One: Introduction	1
1.1 N-Heterocyclic Carbenes	2
1.1.1 Chemistry of NHCs	3
1.1.2 NHC Complexes in Homogeneous Catalysis	6
1.2 Ethylene Oligomerisation	9
1.2.1 Selective Ethylene Trimerisation	9
1.2.2 Mechanistic Considerations	11
1.2.3 Selective Ethylene Tetramerisation	12
1.3 Electron Paramagnetic Resonance Spectroscopy	15
1.3.1 Basic Principles	16
1.3.2 Real Systems	18
1.3.3 Transition Metal Complexes	21
1.4 References	22
Chapter Two: Functionalised N-Heterocyclic Carbenes and Silver(I) Complexes	31
2.1 Introduction	32
2.1.1 Silver(I) NHC complexes	32
2.1.2 Functionalised N-Heterocyclic Carbenes	36
2.2 Results and Discussion	38
2.2.1 Synthesis of Functionalised Imidazolium Salts	38
2.2.2 Preparation of Free Carbenes	47
2.2.3 Silver(I) Carbene Complexes	47
2.2.4 Structural Characterisation of Silver(I) Complexes	49
2.2.5 Transmetallation	53
2.3 Conclusion	54
2.4 Experimental Section	55
2.5 References	65

Chapter Three: Preparation and EPR analysis of Cr(I) bis(phosphine) complexes	69
3.1 Introduction	70
3.1.1 Role of Chromium(I) in the Ethylene Trimerisation Process	70
3.1.2 Background (previous work)	72
3.1.3 Use of EPR for d^5 Complexes of Chromium	76
3.2 Results and Discussion	78
3.2.1 Synthesis and Characterisation of Chromium(0) Compounds	79
3.2.2 Synthesis and Characterisation of Chromium(I) Compounds	81
3.2.3 EPR Studies	84
3.3 Conclusion	86
3.4 Experimental Section	88
3.5 References	93
Chapter Four: Low oxidation state chromium complexes	97
4.1 Introduction	98
4.1.1 Cr(0)-NHC Complexes	98
4.1.2 Cr(I) and Cr(II)-NHC Complexes	99
4.1.3 Role of Chromium(II) in the Ethylene Trimerisation Process	101
4.2 Results and Discussion	102
4.2.1 Cr(0)-NHC Complexes	102
4.2.2 Functionalised NHC-Cr(0) Complexes	108
4.2.3 Synthesis and Characterisation of Chromium(I)-NHC Complexes	113
4.2.4 EPR Studies	117
4.2.5 Cr(II)-NHC Complexes	122
4.3 Conclusion	127
4.4 Experimental Section	128
4.5 References	136

Chapter Five: Synthesis, Characterisation and Catalytic Testing of Some Novel Chromium(III) and Titanium(III)-NHC complexes	141
5.1 Introduction	142
5.1.1 Role of Cr(III) in the Trimerisation Process	142
5.1.2 Role of Other Metals in the Trimerisation Process	144
5.1.3 Cr(III)-NHC Complexes	146
5.1.4 Ti(III)-NHC Complexes	147
5.2 Results and Discussion	149
5.2.1 Synthesis of Cr(III)-NHC Complexes	150
5.2.2 EPR Studies	156
5.2.3 Catalysis	158
5.2.4 Synthesis of Ti(III)-NHC Complexes	160
5.2.5 EPR Studies	163
5.2.6 Catalysis	165
5.3 Conclusion	166
5.4 Experimental Section	167
5.5 References	173
Appendix A	179
EPR Spectra	
Appendix B	183
X-ray data	
Appendix C	203
Publication from this thesis	

Chapter One

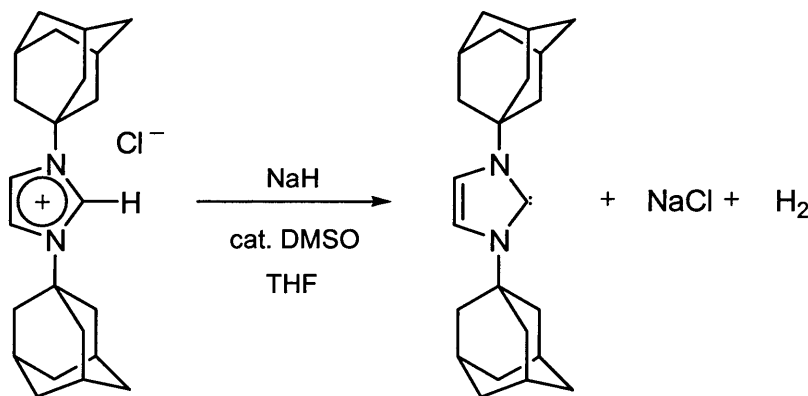
Introduction

Chapter One

Introduction

1.1 N-Heterocyclic Carbenes (NHCs)

Despite early reports by Wanzlick and co-workers¹ postulating the presence of NHCs, it was not until the isolation of the first free NHC, reported by Arduengo² and co-workers in 1991, that these ligands became a real synthetic target and important ligand in organometallic chemistry (Scheme 1.1). A large number of NHCs were subsequently isolated and reported, along with an even larger number of complexes containing NHC ligands.³ Reports describing the catalytic properties of this new class of complexes established these ligands within the area of homogeneous catalysis as potentially very useful and interesting compounds, and imidazol-2-ylidene carbenes of the type described by Arduengo are still the most commonly studied class of carbene.



Scheme 1.1 Synthesis of the first isolated free NHC by Arduengo in 1991.

In this introduction, the chemistry and properties of N-heterocyclic carbenes will be discussed, and their use as ancillary ligands in different types of homogeneous catalysis reactions is discussed.

1.1.1 Chemistry of N-Heterocyclic Carbenes

Carbenes are generally defined as neutral compounds of divalent carbon with two non-bonding electrons; they display either linear (sp) or bent (sp^2) geometries. The carbon atom has only six valence electrons and carbenes are therefore electron deficient and usually very reactive species.

N-heterocyclic carbenes are carbenes originally based on N-containing heterocycles (figure 1.3). They contain an sp^2 hybridized carbon atom, with two non-bonding orbitals, where the two non-bonding electrons occupy one orbital with paired spin orientations ($\sigma^2 p\pi^0$). This results in a singlet ground state multiplicity (1A_1),³ as opposed to a triplet ground state where each electron is in a different orbital ($\sigma^1 p\pi^1$).

The ground state multiplicity (singlet or triplet) is a consequence of the relative energies of the non-bonding σ - and $p\pi$ -orbitals. A singlet ground state is observed if there is a large enough energy gap between them.^{3,4} The size of this energy gap, and therefore the multiplicity, is controlled by the steric and electronic effects of substituents at the carbene carbon atom.

The presence of nitrogen atoms adjacent to the carbene centre results in a large energy gap between the two non-bonding orbitals (σ and $p\pi$), by removing the degeneracy through a combination of both inductive and mesomeric effects⁶ (figure 1.1).

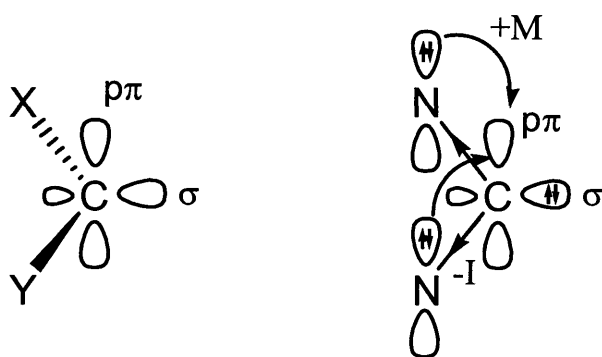


Figure 1.1 Stabilisation of free carbene through mesomeric and inductive effects.

The inductive effect caused by the σ -electron withdrawing nature of the electronegative nitrogen atom lowers the energy of the σ -orbital by increasing its s-character. Meanwhile, donation of electron density from the nitrogen atom lone pair into the carbene empty $p\pi$ -orbital by mesomeric effect destabilises the carbene $p\pi$ -orbital.^{4,6,7} This interaction

of π -electrons of the nitrogen atoms with the p_{π} -orbital on the carbene carbon results in a delocalised system in which the N-C bonds have partial double bond character (figure 1.2).

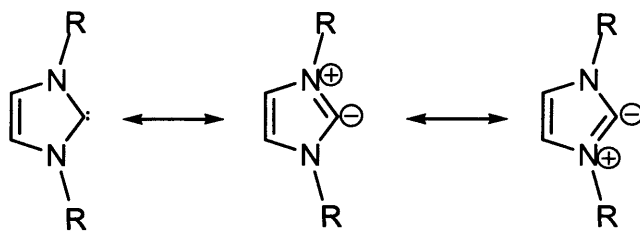


Figure 1.2 Resonance structures of five-membered N-heterocyclic carbenes.

The first isolated NHC was based on an imidazole ring where the carbene centre is adjacent to two nitrogen atoms, and included a 6- π -electron, 5-membered ring arrangement (figure 1.2). This results in stabilisation of the carbene,⁸ and NHCs of this type with many R-group variations have been reported including alkyl, aryl, alkyloxy, alkylamino, and chiral N-substituents. Bulky N-substituents have been reported to help kinetically stabilise carbenes,^{5a} but are not necessary for isolation. Figure 1.3 displays just some of the variations of NHC ligands reported in the literature including the “saturated” 5-membered imidazolin-2-ylidenes and expanded 6- and 7-membered ring carbenes⁹ which have recently become more accessible following the report of a new method of synthesis by Bertrand and co-workers.⁹ Donor functionalised expanded NHC complexes were reported by Cavell and co-workers to show excellent catalytic activity in hydrogenation reactions under very mild conditions.^{10,11} Carbenes based on triazoles,¹² benzimidazoles¹³ and oxazoles¹⁴ are known, and following the report of an NHC ligand bound via the C₄ “backbone” position by Crabtree,¹⁵ there have been several so-called abnormal carbene complexes reported.^{16,17}

The 5-membered imidazole-2-ylidenes of the type first described by Arduengo, along with some expanded NHCs will remain the focus of this thesis.

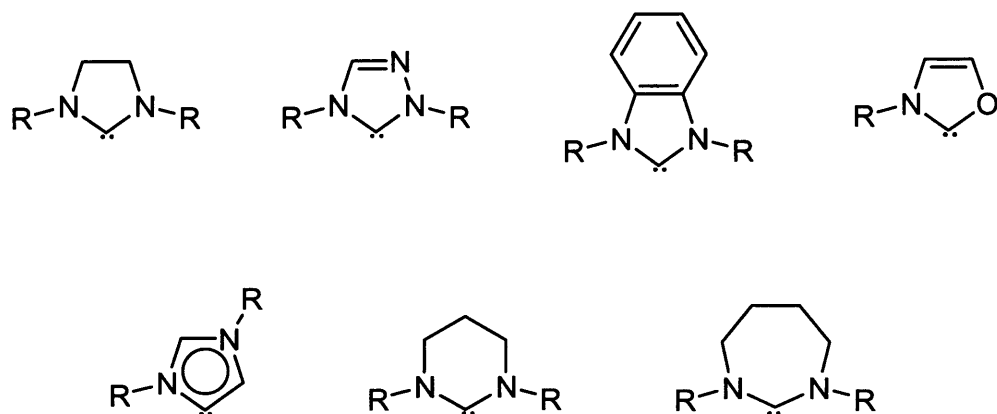


Figure 1.3 Some common types of N-heterocyclic carbene.

NHCs are frequently compared to phosphines as ligands in transition metal chemistry and were originally considered to be phosphine mimics.¹⁸ Like phosphine ligands, NHCs are neutral 2-electron donor ligands that can be easily sterically and electronically modified, and also support catalysis when coordinated to catalytically active metals.

However, the high basicity and different structural features of NHCs sets them apart from the more established phosphines. NHCs are now considered to behave more like tertiary alkyl phosphines in some respects. They exhibit stronger σ -donor properties,²⁰ and in some instances are thought to surpass phosphines in both catalytic activity and scope,^{12,19,21} due to advantages such as increased thermal and oxidative stability of complexes and the fact that they exhibit limited decomposition reactions associated with ligand dissociation as a result of tighter ligand binding.¹⁷

One major difference between phosphines and carbenes is the ability to undergo π -backbonding. Phosphines are known to extensively backbond with certain metals, and although there is some debate about the ability of NHCs to undergo backbonding,²² it is certainly not necessary for back-bonding to occur to produce stable metal complexes.

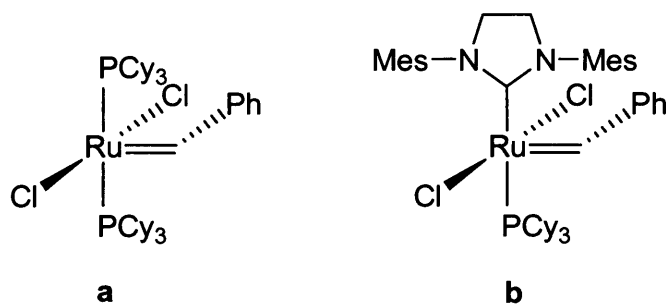


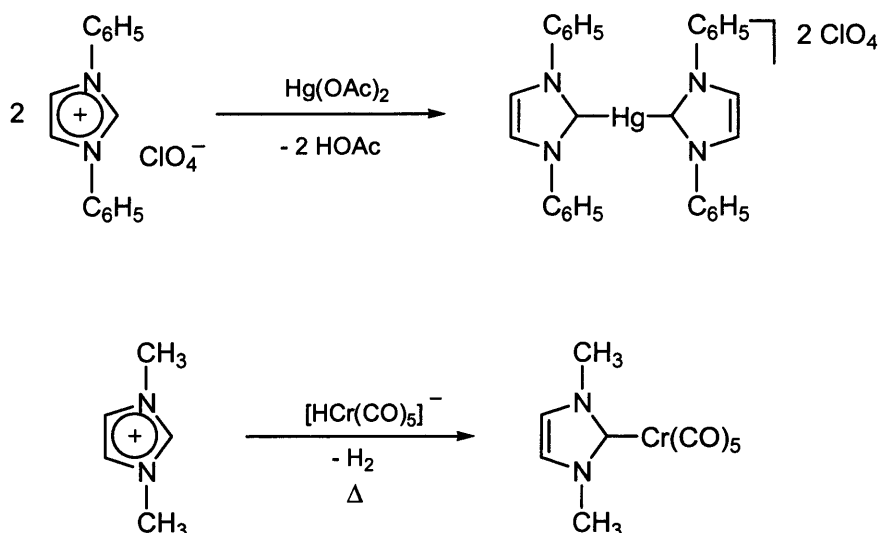
Figure 1.4 Grubbs' first (a) and second (b) generation metathesis catalysts.

In the early years of development of NHC complexes, a wide range of palladium and ruthenium complexes were isolated and studied as homogeneous catalysts. The substitution of tricyclohexylphosphine by an NHC ligand in the so-called 2nd generation Grubbs' catalyst²³ (figure 1.4), and the subsequent improvement in catalytic activity (~100 times) was reported in both ring closing metathesis (RCM) and ring opening metathesis polymerisation (ROMP) led to increased interest in the use of NHCs as ancillary ligands in transition metal catalysis.^{23a,24}

1.1.2 NHC Complexes in Homogeneous Catalysis

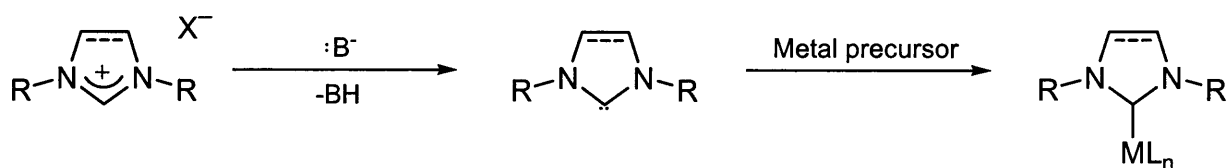
The application of NHCs in transition metal chemistry, particularly in homogeneous catalysis began with the first reports of NHC-Metal complexes independently by Wanzlick²⁵ and Öfele²⁶ in 1968, long before the isolation of the first free NHC. The mercury (Hg(II)) and chromium-NHC complexes were formed by deprotonation of the imidazolium cation by a basic ligand of the metal precursor (scheme 1.2), and this method remains a commonly utilised route to transition metal complexes of NHCs.^{3, 20a, 27-31}

Prior to the isolation of free NHCs, carbenes were classified as either Fischer or Schrock-type carbenes according to the nature of the carbene-metal bond formed.^{32,33} These carbenes form double bonds with metals and require π -backbonding to stabilise metal complexes, in contrast to NHCs where a strong σ -bond is generally sufficient to stabilise a variety of oxidation states.¹⁸



Scheme 1.2 Synthesis of first NHC-transition metal complexes.^{25,26}

The isolation of stable free carbenes has opened up new routes for the synthesis of metal-carbene complexes, and while numerous complexes have been prepared via different methods, the most common route is via the addition of an external base such as NaH, KO^tBu or KHMDS (potassium hexamethyldisilazide), to deprotonate the azolium precursor. Very often the free carbene is prepared *in situ*, i.e. it is not isolated as a solid, but prepared in solution, and added directly to a metal precursor. This tends to be the preferred route to many metal complexes (scheme 1.3), as it allows the use of a greater variety of metal precursors that do not necessarily contain basic ligands required to deprotonate the salt.



Scheme 1.3 *in situ* preparation of NHC complexes.

A wide variety of NHC complexes have been prepared in this way, with most metals in the periodic table, including alkali metals, main group and transition metals, and even lanthanide and actinide complexes reported. Due to their catalytic importance, the majority of reported NHC complexes are based on catalytically active late transition metals such as Pd, Ru, Ir and Rh.

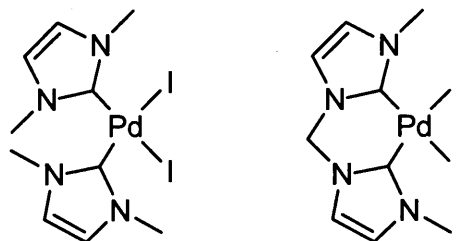


Figure 1.5 First NHC-Pd complexes employed in the Heck reaction.

After some early examples of the use of NHCs as ligands in catalysis,²⁹ the real potential of NHC complexes in homogeneous catalysis was realised after the report by Herrmann and co-workers in 1995 describing palladium complexes as very active catalysts for the Heck reaction^{29b} (figure 1.5). NHCs have since been employed in a wide variety of catalytic reactions,¹⁹ including polymerisation, hydrogenation, hydrosilylation and hydroformylation. However, there are problems associated with using NHC complexes in catalysis; they are susceptible to loss by reductive elimination leading to decomposition of the catalyst sometimes before effective catalysis can take place.^{22,34,35}

It was not until more recently that NHC complexes of early transition metals have been used as olefin oligomerisation and polymerisation catalysis.^{36,37,38} A series of chelating CNC-pincer ligands (figure 1.6), reported by Gibson and co-workers,³⁸ were the first NHC based complexes to display excellent activity for olefin oligomerisation reactions, and demonstrates the exciting potential for this ligand class in early transition metal olefin polymerisation.

NHC complexes of early transition metals have been less widely reported than other transition metals; they represent the main focus of this thesis.

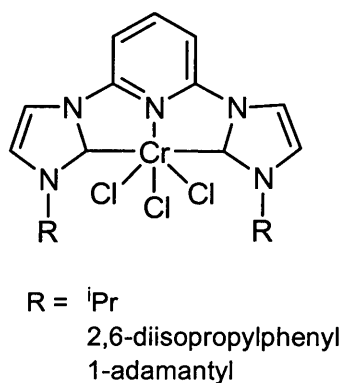
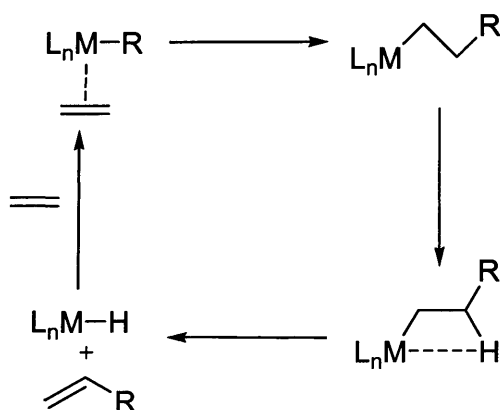


Figure 1.6 First Cr(III)-NHC complexes reported to be excellent olefin oligomerisation catalysts.

1.2 Ethylene Oligomerisation

Linear α -olefins (LAOs) are 1-alkenes that are particularly valuable in the chemical industry as intermediates in the manufacture of co-polymers among other products.³⁹ Metal catalysed ethylene oligomerisation is the conventional route to LAOs, a process which commonly results in a ‘Schulz-Flory’ distribution of olefins, due to the linear chain growth mechanism under which they operate (scheme 1.3). This mixture of olefins must be then separated to give specific carbon number products.⁴⁰⁻⁴² Industrially, olefins containing 6 and 8 carbon atoms (1-C₆ and 1-C₈) are in much higher demand than other carbon numbers, due to their importance as co-monomers in the polymer industry. This presents a challenge to LAO producers, and there is great interest in the development of a series of selective processes in order to match production to market demand.



Scheme 1.3 Ethylene insertion/β-elimination mechanism proposed by Cossee and Arlman for the oligomerisation process.^{43,44}

1.2.1 Selective Ethylene Trimerisation

The first report of ethylene trimerisation was published by Manyik and co-workers at Union Carbide Corporation in 1977 where the formation of 1-hexene was observed during the chromium catalysed polymerisation of ethylene.⁴⁵ Since this initial discovery, where only 1.1% 1-hexene was reported, technology has developed significantly with overall selectivity of 1-hexene of more than 99% reported, along with huge improvements in catalyst activities.³⁹

A major contribution toward this progress in selective ethylene trimerisation was the discovery that chromium-pyrrolide compounds were catalytically active towards ethylene oligomerisation producing 1-hexene with greater than 90% selectivities.⁴⁶ Catalyst systems were prepared by combining chromium(III)-2-ethylhexanoate, 2,5-dimethylpyrrole, diethylaluminium chloride and triethylaluminium. This so called 'Phillips system' has since been commercialised and remains the only industrial process for selective oligomerisation in operation. Following this development, many companies filed patents based on slight modifications of the Phillips system,⁴⁷⁻⁵¹ and investigations into different ligand systems began.

A number of different catalyst systems purporting to show selectivity toward trimerisation have been developed (figure 1.7), including those containing maleimide,⁵² boratabenzenyl,⁵³ aryloxide ligands⁵⁴ and substituted cyclopentadienyl ligands.^{39,55} But perhaps the most interesting results come from the use of chromium based catalyst systems containing multidentate heteroatomic ligands. First developed by Amoco Corporation, tridentate phosphine ligands of the type shown in figure 1.7 were found to be active ethylene trimerisation catalysts when activated by a co-catalyst,⁵⁶ and it was proposed that the 1-hexene produced required no further purification, which is a significant advantage.

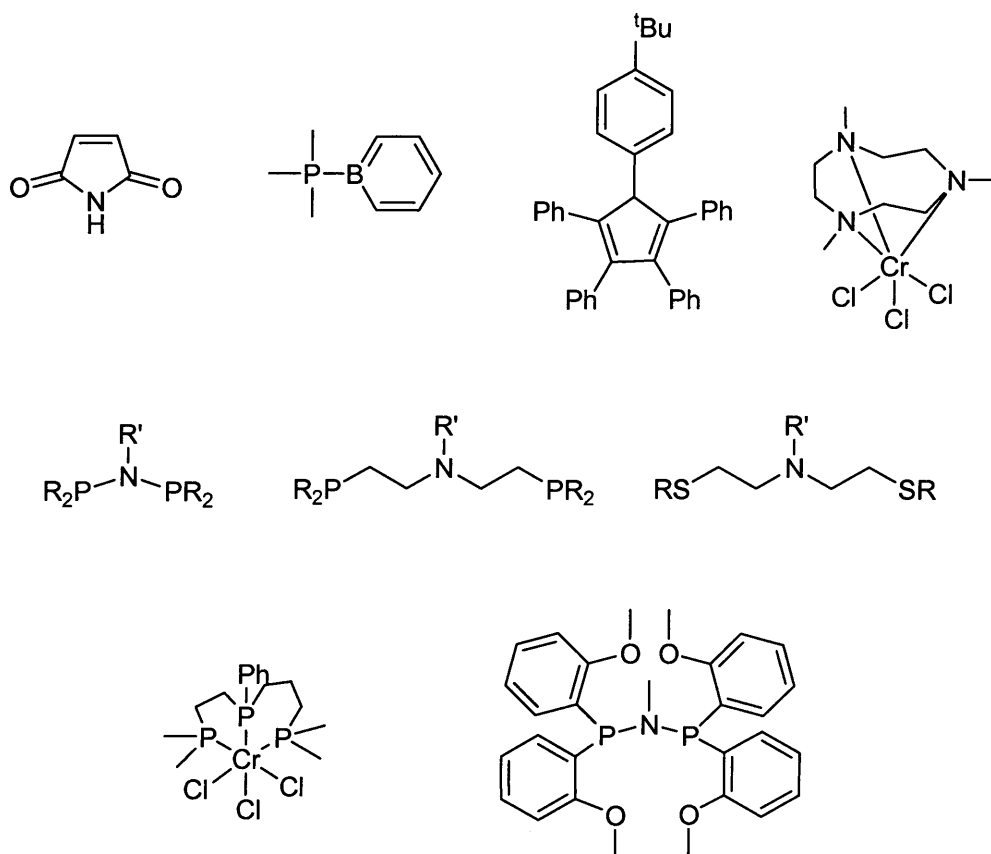


Figure 1.7 Some complexes and ligands reported to show catalytic activity.

BP developed chromium-based trimerisation catalysts with diphosphazane ligands containing an *ortho*-methoxy group (figure 1.7), where the high activity was attributed to the presence of the *ortho*-methoxy groups acting as pendant donors.^{57,58}

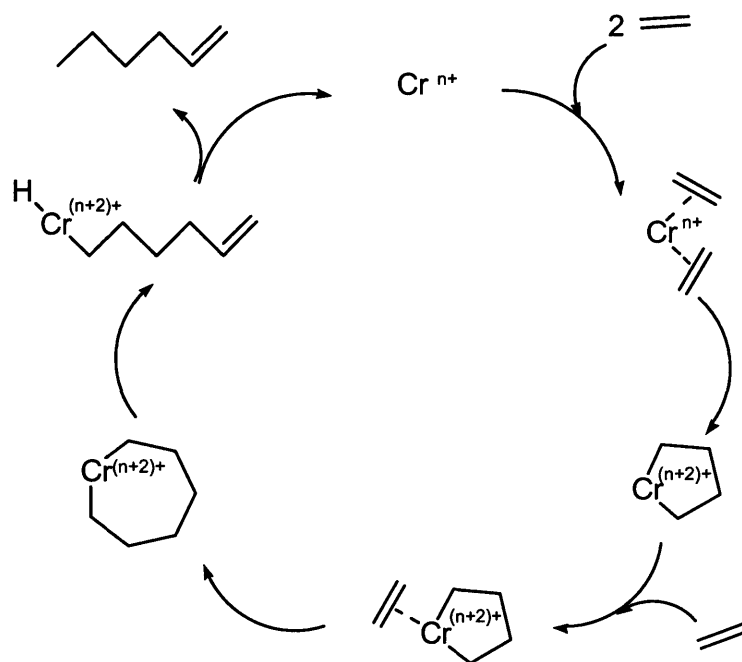
Further studies by Sasol on the *ortho*-substituted catalyst systems showed that the high selectivities previously attributed to the coordination of pendant methoxy groups, were in fact due to steric demand rather than pendant coordination. This was concluded after replacement of the methoxy substituents with ethyl groups resulted in very active and selective catalysts toward ethylene trimerisation.⁵⁹

Complexes containing mixed phosphorus and nitrogen donor atoms are very active and selective trimerisation catalysts, and it has been reported that the inclusion of sterically less demanding R groups, such as ethyl rather than phenyl groups results in much higher activities.^{60,61}

1.2.2 Mechanistic Considerations

The original report⁶² by Manyik and co-workers in 1977, suggested that a metallacyclic mechanism was responsible for the formation of 1-hexene, rather than the linear chain growth mechanism described in scheme 1.3. This was based on the observation that the rate of 1-hexene formation was dependent on the square of the ethylene pressure, suggesting a second order reaction with respect to ethylene.

The postulated metallacyclic mechanism was further expanded by Briggs⁶³ in 1989, and describes the coordination of two ethylene molecules, followed by oxidative coupling to form a metallacyclopentane species, insertion of a third ethylene molecule yields a metallacycloheptane intermediate, which undergoes β -elimination to release 1-hexene. The crucial aspect of this mechanism is the difference in relative stabilities of the 5- and 7-membered ring intermediates with regard to elimination, which accounts for the high selectivity toward 1-C₆ over other olefins⁶⁴ (scheme 1.4). In 2004, Bercaw and co-workers carried out a series of experiments with deuterated ethylene which provided conclusive evidence for the metallacyclic mechanism.^{65,66}



Scheme 1.4 Ethylene trimerisation mechanism proposed by Briggs.⁶³

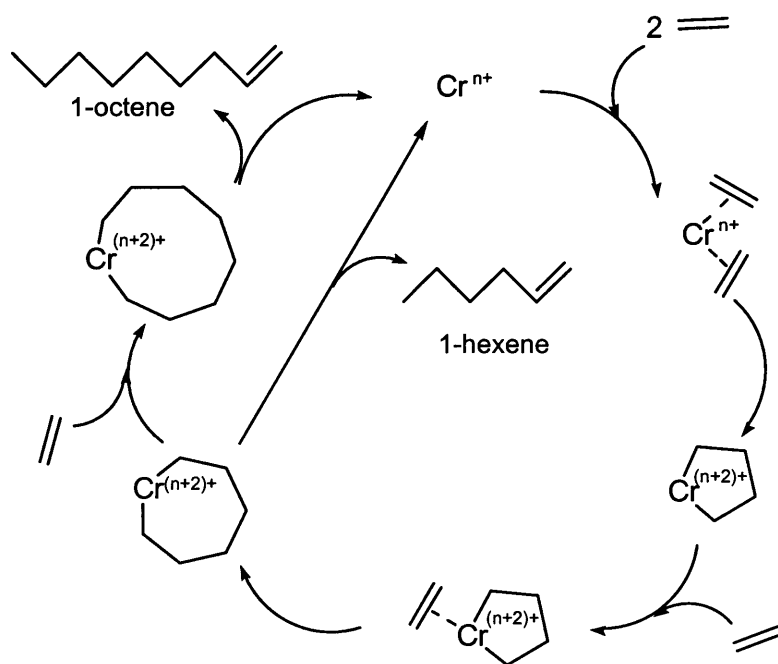
The metallacyclic mechanism (scheme 1.4) involves a change in the formal oxidation state of chromium (Cr^{n+} to $\text{Cr}^{(n+2)+}$) during the addition of the two ethylene molecules and during reductive elimination ($\text{Cr}^{(n+2)+}$ to Cr^{n+}). This is generally accepted to be the case, but the nature of the active species remains unknown, and with different redox pairs proposed in the literature, including $\text{Cr}(\text{I})$ - $\text{Cr}(\text{III})$,^{62,65,67} $\text{Cr}(\text{II})$ - $\text{Cr}(\text{IV})$ ^{68,69} and $\text{Cr}(\text{III})$ - $\text{Cr}(\text{V})$,⁷⁰ this remains an area of ongoing research.

1.2.3 Selective Ethylene Tetramerisation

Sasol Technology recently reported the first catalyst capable of selective ethylene tetramerisation, i.e. the selective production of 1-octene (1-C_8).⁷¹ This is particularly exciting, as 1-octene is also in high demand commercially as discussed in 1.1. The *in situ* catalyst system, based on a PNP ligand, and source of chromium(III), produces 1-octene in up to 70% selectivity.

Given the mechanism described for trimerisation catalysis, ethylene tetramerisation, was initially thought to be highly unlikely, as it would involve insertion of a fourth ethylene

molecule. The resulting metallacyclononane intermediate (scheme 1.5) was previously thought to be extremely unfavoured.^{71,72} Both trimerisation and tetramerisation mechanisms are thought to share a common metallacycloheptane intermediate,^{59,73-76} but in the case of tetramerisation, instead of elimination at this stage, a further ethylene molecule is inserted, forming a nine-membered metallacycle from which 1-octene is reductively eliminated. The main difference between the two mechanisms being that an enhanced stability of the seven-membered intermediate limits 1-hexene elimination, allowing ring growth. This difference is thought to be attributed to subtle steric and electronic effects of the ligand, and a fine balance is required between the relative stability of the intermediates to favour 1-hexene or 1-octene selectivity.⁶⁴ The tetramerisation mechanism has been supported by deuterium labelling studies carried out by Sasol Technology.⁷³



Scheme 1.5 Extended tetramerisation mechanism involving a metallacyclononane intermediate.

A series of PNP type ligand systems have been studied,⁷⁷ and it has been reported that steric bulk on the nitrogen was the predominant factor responsible for the high selectivity in tetramerisation catalysis. It was also found that selectivity, when using *ortho*-alkyl substituents on the phosphorous aryl groups of the diphosphinoamine ligands could be switched from trimerisation toward tetramerisation catalysis by increasing the number of *ortho*-alkyl substituents from 0-4.⁵⁹

Studies into the oxidation state of the catalytic species carried out by Rucklidge and co-workers provided evidence for a Cr(I)-Cr(III) redox couple in the ethylene tetramerisation mechanism.⁷⁸ Studies into tetramerisation are relatively recent, and further studies will undoubtedly follow.

Interestingly, extended metallacyclic mechanisms have been recently reported by both Gibson^{79,80} and McGuinness,⁸¹ resulting in a distribution of higher olefins. Gibson and co-workers demonstrated that a metallacyclic mechanism was responsible for the Schultz Flory distribution of α -olefins produced, using deuterium labelling studies. Large ring metallacyclic intermediates are reported possible when the energy barrier to further insertion and metallacyclic growth is comparable or lower than the barrier for product elimination.⁸¹

While the majority of reported catalysts are based on chromium, some other early transition metal ethylene oligomerisation catalysts have been reported,⁸²⁻⁸⁶ but generally show activities that are much lower than the more established chromium catalysts.⁸⁷ These are described further in section 5.1.

1.3 EPR Spectroscopy

Electron paramagnetic resonance (EPR) is a spectroscopic technique capable of detecting species containing unpaired electrons, such as radicals and other paramagnetic compounds. Important structural and electronic information can be gained from the technique, and it is therefore widely used across the scientific disciplines.

Characterisation of catalytic systems generally involves the use of magnetic resonance techniques, and in the case of the systems we are interested in (i.e. chromium complexes), the commonly used NMR spectroscopic methods are rendered much less effective due to broadening effects caused by the presence of a paramagnetic metal. EPR spectroscopy allows information about the electronic and structural environment of the complex to be collected, making the investigation of such systems feasible. Similar to NMR, EPR techniques can be used to study the catalyst systems under a variety of conditions, including variable temperatures, variable pressures, in solution, etc. Analysis of the spectra provides information not only on the oxidation states of the complex, but also a structural description of the complex in solution.

In most molecules electrons are paired, with opposite spins, as required by the Pauli exclusion principle and EPR experiments cannot be performed on them, as they are EPR silent.⁸⁸ Molecules containing one or more unpaired electrons, including transition metal ions which contain unpaired d-electrons are particularly suited for EPR studies, and this introduction includes a brief overview of the theory and applications of EPR spectroscopy in transition metal complexes.

A detailed account of the physics behind EPR can be found in one of the numerous textbooks on the subject that go into more detail on the practicalities of the technique, and also give a detailed account from different areas of chemistry.⁸⁹⁻⁹³ The experiments discussed in this thesis have all been performed using continuous wave EPR (cw-EPR) spectroscopy at X-band frequency (~9.5 GHz), and the theory discussed in this brief introduction will focus only on this methodology.

1.3.1 Basic Principles

As a negatively charged particle spinning on its axis, an electron will produce a magnetic moment, μ_s , which is co-linear and anti-parallel to its spin angular momentum (or 'spin') S :

$$\mu_s = -g_e \mu_B S$$

The energy of interaction between the magnetic moment and an external magnetic field is given by:

$$E = -\mu_s B$$

therefore

$$E = g_e \mu_B S B$$

The magnetic moments align along the direction of the field and assume one of two orientations, since S can only take one of two values in a given direction, designated by the spin angular momentum quantum number, $M_s = \pm 1/2$. In the absence of an external magnetic field, these states are degenerate. However, in the presence of a field the states split in energy, the high energy position, where the magnetic dipole is orientated anti-parallel to the magnetic field, and the low energy, more stable orientation where the dipole is aligned parallel to the external magnetic field. The resulting energy levels are called Zeeman energy levels (figure 1.8), and are separated by the Zeeman splitting:

$$\Delta E = (\pm 1/2) g_e \mu_B B$$

(where g_e = free electron g value = 2.0023, B = applied field (or magnetic flux density, in units of Tesla (T) or Gauss (G)), μ_B = Bohr magneton ($\mu_B = em/4\pi mc$, where e = electron charge, m = electron mass, c = speed of light) = 9.27×10^{-24} J T⁻¹)

The Zeeman splitting (energy difference between the spin states) is directly proportional to the magnitude of the applied magnetic field (B) (figure 1.8), and a transition between the two Zeeman levels can be induced by the absorption of a photon of the correct frequency, ν , given by:

$$E = h\nu$$

(where h = Planck's constant and ν = frequency of electromagnetic radiation)

Under the influence of an external magnetic field, and at thermal equilibrium, the spin population is split between the two energy levels according to the Maxwell-Boltzmann distribution law:

$$\frac{n_1}{n_2} = e^{-(g_e \mu_B B/kT)}$$

(where, k = Boltzmann constant (1.381×10^{-23} J K⁻¹), T = absolute temperature (K), n_1, n_2 = spin population characterised by the M_s values of $+\frac{1}{2}$ and $-\frac{1}{2}$ respectively.)

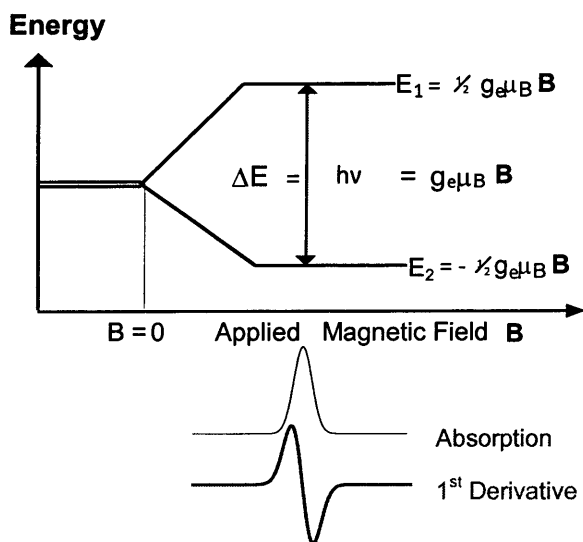


Figure 1.8 The electronic Zeeman effect.

(energy level diagram for a system with 1 unpaired electron ($S = \frac{1}{2}$) and no interacting nuclei)

The transition of an electron from the lower to upper Zeeman level is the basis of the EPR technique. The position of a transition is reported in terms of its g -value, the proportionality constant described in the Zeeman splitting equation, and can be calculated from the combination and re-arrangement of the previous two equations:

$$g = h \nu / \mu_B B$$

The resonance signal is represented by the energy absorption necessary to promote electrons from lower to upper energy levels. The overall net absorption results from the fact that there are more spins in the lower levels than in the upper.

While electrons are promoted to the higher energy level by absorption of a photon of the correct frequency, those in the higher energy state return to the lower level by efficient dissipation of the quantum of energy ($h\nu$). The dissipation process from the excited electron to the ground state is known as relaxation, and is measured in terms of relaxation time.

To maintain a population excess, electrons in the upper level must be able to return to their low energy state. Therefore they must be able to transfer their excess spin energy either to other species or to the surrounding lattice as thermal energy. The time taken for the spin system to lose $1/e$ of its excess energy is called the relaxation time, and there are two types of dissipation mechanisms;

“Spin-Lattice” relaxation: This process is due to the magnetic energy being dissipated within the lattice as vibrational, rotational, or translational energy. Characterised by an exponential decay of energy as a function of time (T_{1e}).

“Spin-Spin” relaxation: The excess energy is exchanged between the spins without transfer of energy to the lattice, which is characterised by a time constant (T_{2e}). This mode of relaxation is important when the concentration of the paramagnetic species is high (spins are close together). If the relaxation time is too fast, then the electrons will only remain in the upper state for a very short period of time and give rise to a broadening of the spectral line width as a consequence of Heisenberg’s uncertainty principle.

Greater sensitivity can be achieved by working at a high resonant frequency ($h\nu$) or by working at low temperature, since, in the Maxwell Boltzmann expression, T is then lower, which increases the difference between n_2 and n_1 so that a larger net absorption occurs.

1.3.2 Real Systems

The discussion thus far has considered the case of the free electron. Electrons in atoms and molecules however are subject to a variety of magnetic interactions which can split the simple Zeeman levels described in figure 1.9.

In any real system, the electron will interact with any associated spin-active nuclei, i.e. where the nuclear spin $\geq 1/2$. An interaction called the nuclear hyperfine interaction (A) takes place, giving origin to splitting of the lines in the spectra, resulting in hyperfine structure, which is very useful in EPR spectroscopy.

Two types of electron spin/nuclear spin interactions occur; an isotropic interaction (A_0) and an anisotropic interaction (B_0).

The isotropic interaction occurs when the electron is located in a spherical s orbital. The spherical nature of the s orbital results in an interaction which is independent of the orientation of the orbital in which the electron is situated and isotropic hyperfine couplings (a_{iso}) are observed.

The anisotropic interaction (B_0) occurs when the electron is situated in directional orbitals such as p, d, and f-orbitals, and the electron is therefore unable to approach the nucleus very closely due to the node of the orbital, and therefore the field it experiences from the nucleus appears to arise from a point magnetic dipole. The interaction is referred to as a dipole-dipole interaction, which is anisotropic, i.e. the magnitude and sign of the interaction is dependent on the orientation of the electrons with respect to the applied magnetic field and to the separation between the two dipoles.

In a system which is highly symmetrical, or where rapid tumbling of the paramagnetic species averages the molecular anisotropies, only the isotropic term is observed.

In most real systems, the isotropic and anisotropic interactions mix due to hybrid orbitals, and therefore the hyperfine interaction contains contributions from both components.

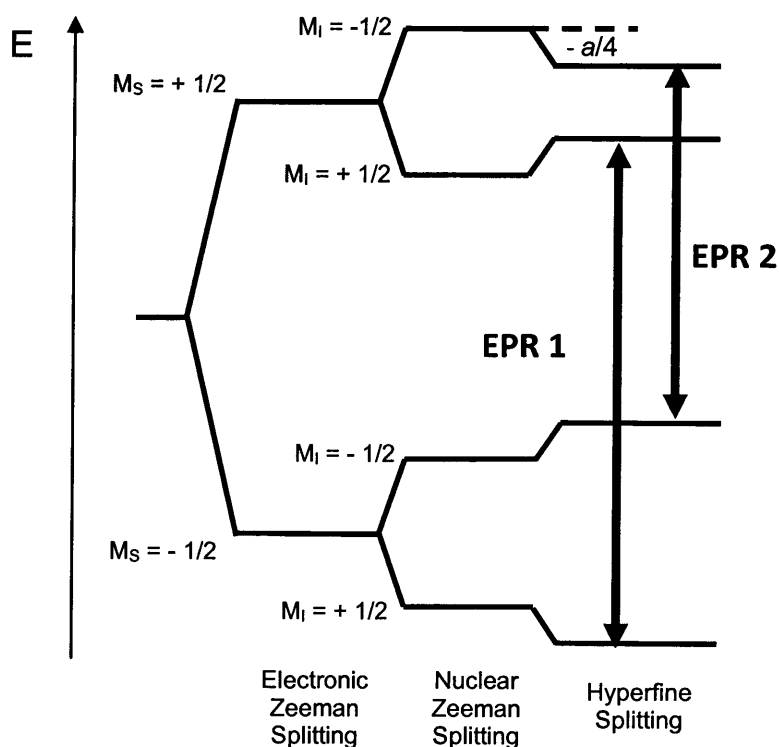


Figure 1.9 Energy level diagram for the interaction of a proton ($I = \frac{1}{2}$) with an unpaired electron ($S = \frac{1}{2}$) in an applied magnetic field.

The profile of the spectrum (figure 1.10), is dependent on the symmetry of the system. An isotropic profile is observed for systems that have perfect cubic symmetry, such as octahedral or tetrahedral symmetry. The g tensor is characterised by a single line where $g_{xx} = g_{yy} = g_{zz}$. It is also observed in low viscosity solutions, where the observed g value (g_{iso}) is the result of averaging of the three components by rapid tumbling.

A molecule displays axial symmetry if two of the principle g values are equal. The unique value is referred to as g_{\parallel} (g_{zz}) and is referred to as “ g parallel” (because it is parallel to the direction of the magnetic field) whilst the other value g_{\perp} ($g_{xx} = g_{yy}$) is referred to as “ g perpendicular”.

A system displaying orthorhombic symmetry has three distinct g values, i.e. $g_1 \neq g_2 \neq g_3$. The resulting spectral lines (figure 1.10) can be further split by hyperfine interactions with spin active nuclei as described above.

The paramagnetic species described in this thesis are studied in frozen solution, so all orientations of the molecule with respect to the field are observed in the spectrum.

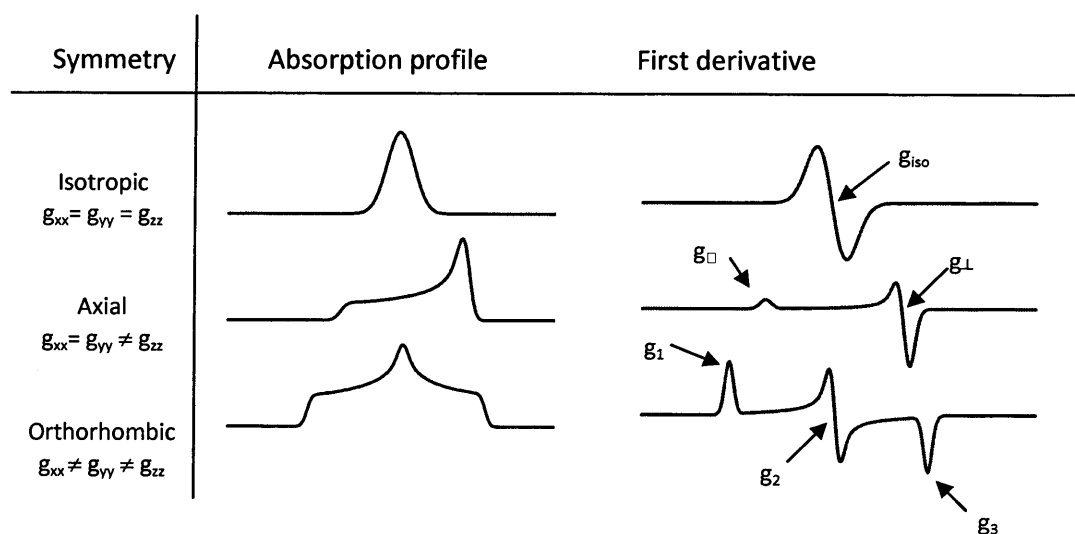


Figure 1.10 Observed spectra for different symmetries.

1.3.3 Transition Metal Complexes

A great deal of information may be obtained about the co-ordination features of transition metal complexes with EPR spectroscopy. The nature of the central ion, type of bonding with the ligands, co-ordination and symmetry of the surroundings, relaxation mechanism and the type of the motion of the paramagnetic species can also be inferred from the EPR spectra. In particular, the g tensor values are characteristic of a given metal complex in a given surrounding (i.e. crystal field symmetry and strength, type of bonding with ligands etc.)

Naturally occurring chromium consists of four isotopes; 90.5% ^{50}Cr , ^{52}Cr and ^{54}Cr with $I = 0$, and 9.5% ^{53}Cr with $I = 3/2$. The observed spectrum of a chromium sample is therefore a superposition of the spectra arising from each isotope. The relative intensity of the lines is approximately proportional to the relative isotopic abundance, and inversely proportional to $2I+1$. For chromium, for every main spectral line arising from electron association with $I=0$ Cr, four satellite lines are generated, arising from the interaction between the electron and the ^{53}C nucleus. However, in practise, due to the low intensity, these hyperfine interactions can rarely be observed.

EPR data has been reported for chromium complexes in the literature, focussing on $\text{Cr(III)}^{94,95}$ and Cr(V)^{96} compounds, and to a much lesser extent on low spin Cr(I)^{97} .

Whilst EPR offers valuable insights into the electronic properties of the Cr complexes, ENDOR (Electron Nuclear DOuble Resonance) provides further complimentary information on the structure of the paramagnetic complex. ENDOR is a sophisticated technique which allows further details about the complex to be gained via analysis of the hyperfine coupling tensor from remote ligand nuclei.^{89,98}

The work reported in this thesis was carried out as part of a synthetic project, where EPR spectroscopy has been used as a method for the characterisation of complexes, rather than in-depth theoretical analysis. However, where relevant to the synthetic work; understanding structure and aspects of reactivity, results obtained using these techniques will be discussed as appropriate. More detailed EPR and ENDOR discussions relating to the work presented in this thesis are reported elsewhere.⁹⁹

1.5 References

- [1] (a) Wanzlick, H. -W.; Schikora, E. *Angew. Chem.* **1960**, *72*, 494. (b) Wanzlick, H. -W.; Kleiner, H. -J. *Angew. Chem.* **1961**, *73*, 493. (c) Wanzlick, H. -W. *Angew. Chem.* **1962**, *74*, 129; *Angew. Chem. Int. Ed.* **1962**, *1*, 75.
- [2] Arduengo III, A. J.; Harlow, R. L.; Kline, M. *J. Am. Chem. Soc.* **1991**, *113*, 361.
- [3] Hahn, F. E.; Jahnke, M. C. *Angew. Chem. Int. Ed.* **2008**, *47*, 3122.
- [4] Hoffmann, R.; Zeiss, G. D.; van Dine, G. W. *J. Am. Chem. Soc.* **1968**, *90*, 1485.
- [5] (a) Bourissou, D.; Guerret, O.; Gabbai, F. P.; Bertrand, G. *Chem. Rev.* **2000**, *100*, 39. (b) Herrmann, W. A.; Köcher, C. *Angew. Chem. Int. Ed.* **1997**, *36*, 2162.
- [6] (a) Harrison, J. F. *J. Am. Chem. Soc.* **1971**, *93*, 4112. (b) Bauschlicher Jr., C. W.; Schaefer III, H. F.; Bagus, P. S. *J. Am. Chem. Soc.* **1977**, *99*, 7106. (c) Harrison, J. F.; Liedtke, R. C.; Liebman, J. F. *J. Am. Chem. Soc.* **1979**, *101*, 7162. (d) Feller, D.; Borden, W. T.; Davidson, E. R. *Chem. Phys. Lett.* **1980**, *71*, 22.
- [7] Baird, N. C.; Taylor, K. F. *J. Am. Chem. Soc.* **1978**, *100*, 1333.
- [8] (a) Heinemann, C.; Müller, T.; Apeloig, Y.; Schwarz, H. *J. Am. Chem. Soc.* **1996**, *118*, 2023. (b) Boehme, C.; Frenking, G. *J. Am. Chem. Soc.* **1996**, *118*, 2039.
- [9] Jazzar, R.; Liang, H.; Donnadiou, B.; Bertrand, G. *J. Organomet. Chem.* **2006**, *691*, 3201.
- [10] Binobaid, A.; Iglesias, M.; Beetstra, D. J.; Kariuki, B.; Dervisi, A.; Fallis, I. A.; Cavell, K. J. *Dalton Trans.* **2009**, 7099.

- [11] (a) Iglesias, M.; Beetstra, D. J.; Knight, J. C.; Ooi, L. -L.; Stasch, A.; Coles, S. J.; Male, L.; Hursthouse, M. B.; Cavell, K. J.; Dervisi, A.; Fallis, I. A. *Organometallics* **2008**, *27*, 3279. (b) Iglesias, M.; Beetstra, D. J.; Kariuki, B.; Cavell, K. J.; Dervisi, A.; Fallis, I. A. *Eur. J. Inorg. Chem.* **2009**, *13*, 1913.
- [12] Herrmann, W. A. *Angew. Chem. Int. Ed.* **2002**, *41*, 1290.
- [13] Huynh, H. V.; Holtgrewe, C.; Pape, T.; Koh, L. L.; Hahn, E. *Organometallics* **2006**, *25*, 245.
- [14] Tubaro, C.; Biffis, A.; Basato, M.; Benetollo, F.; Cavell, K. J.; Ooi, L. -L. *Organometallics* **2005**, *24*, 4153.
- [15] Gründemann, S.; Kovacevic, A.; Albrecht, M.; Faller, J. W.; Crabtree, R. H. *J. Am. Chem. Soc.* **2002**, *124*, 10473.
- [16] Bacciu, D.; Cavell, K. J.; Fallis, I. A.; Ooi, L. -L. *Angew. Chem. Int. Ed.* **2005**, *44*, 5282.
- [17] Arnold, P. L.; Pearson, S. *Coord. Chem. Rev.* **2007**, *251*, 596.
- [18] Green, J. C.; Scur, R. G.; Arnold, P. L.; Cloke, G. N. *Chem. Commun.* **1997**, 1963.
- [19] Crudden, C. M.; Allen, D. P. *Coord. Chem. Rev.* **2004**, *248*, 2247.
- [20] (a) Herrmann, W. A.; Reisinger, C.; Spiegler, M. *J. Organomet. Chem.* **1998**, *557*, 93. (b) Trnka, T. M.; Grubbs, R. H. *Ace. Chem. Res.* **2001**, *34*, 18. (c) Nemcsok, D.; Wichmann, K.; Frenking, G. *Organometallics* **2004**, *23*, 3640.
- [21] (a) Perry, M. C.; Burgess, K. *Tetrahedron: Assymetry* **2003**, *14*, 951. (b) Peris, E.; Crabtree, R. H. *Coord. Chem. Rev.* **2004**, *248*, 2239. (c) César, V.; Bellemin-Laponnaz, S.; Gade, L. H. *Chem. Soc. Rev.* **2004**, *33*, 619. (d) Díez-González, S.; Nolan, S. P. *Ann. Rep. Prog. Chem., Sect. B*, **2005**, *101*, 171. (e)

- Cavallo, L.; Correa, A.; Costabile, C.; Jacobsen, H. *J. Organomet. Chem.* **2005**, *690*, 5407.
- [22] Cavell, K. J. *Dalton Trans.* **2008**, 6676.
- [23] (a) Weskamp, T.; Kohl, F. J.; Hieringer, W.; Gleich, D.; Herrmann, W. A. *Angew. Chem. Int. Ed. Engl.* **1999**, *38*, 2416. (b) Scholl, M.; Ding, S.; Lee, C. W.; Grubbs, R. H. *Org. Lett.* **1999**, *1*, 953.
- [24] (a) Weskamp, T.; Schattenmann, W. C.; Spiegler, M.; Herrmann, W. A. *Angew. Chem. Int. Ed.* **1998**, *37*, 2490. (b) Huang, J.; Stevens, E. D.; Nolan, S. P.; Peterson, J. L. *J. Am. Chem. Soc.* **1999**, *121*, 2674. (c) Fürstner, A.; Ackermann, L.; Gabor, B.; Goddard, R.; Lehmann, C. W.; Mynott, R.; Stelzer, F.; Thiel, O. R. *Chem. Eur. J.* **2001**, *7*, 3236.
- [25] (a) Wanzlick, H. –W.; Schönherr, H. –J. *Angew. Chem.* **1968**, *80*, 154; *Angew. Chem. Int. Ed. Engl.* **1968**, *7*, 141.
- [26] K. Öfele, *J. Organomet. Chem.* **1968**, *12*, 42.
- [27] Wang, H. M. J.; Lin, I. J. B. *Organometallics* **1998**, *17*, 972.
- [28] Hahn, F. E.; Foth, M. *J. Organomet. Chem.* **1999**, *585*, 241.
- [29] (a) Herrmann, W. A.; Elison, M.; Fischer, J.; Köcher, C.; Artus, G. R. *J. Angew. Chem.* **1995**, *107*, 2602; *Angew. Chem. Int. Ed. Engl.* **1995**, *34*, 2371. (b) Hahn, F. E.; Holtgrewe, C.; Pape, T. *Z. Naturforsch. B* **2004**, *59*, 1051. (c) Cardin, D. J.; Doyle, M. J.; Lappert, M. F. *J. Chem. Soc., Chem. Comm.*, **1972**, 927. (d) Lappert, M. F. *J. Organomet. Chem.*, **1984**, *264*, 217. (e) Hill, J. H.; Nile, T. A. *J. Organomet. Chem.*, **1977**, *137*, 293.
- [30] Hahn, F. E.; Holtgrewe, C.; Pape, T.; Martin, M.; Sola, E. Oro, L. A. *Organometallics* **2005**, *24*, 2203.

- [31] Köcher, C.; Herrmann, W. A. *J. Organomet. Chem.* **1997**, *532*, 261.
- [32] Boehme, C.; Frenking, G. *Organometallics* **1998**, *17*, 5801.
- [33] Spessard, G. O.; Miessler, G. L. *Organometallic Chemistry*, Prentice-Hall, New Jersey, **1996**, 302.
- [34] McGuinness, D. S.; Saendig, N.; Yates, B. F.; Cavell, K. J. *J. Am. Chem. Soc.* **2001**, *123*, 4029.
- [35] McGuinness, D. S.; Mueller, W.; Wasserscheid, P.; Cavell, K. J.; Skelton, B. W.; White, A. H.; Englert, U. *Organometallics* **2002**, *21*, 175.
- [36] (a) Döhring, A.; Göhre, J.; Jolly, P. W.; Kryger, B.; Rust, J.; Verhovnik, G. P. J. *Organometallics* **2000**, *19*, 388. (b) Jens, K.-J.; Tilset, M.; Voges, M. H.; Blom, R.; Froseth, M. (Borealis) WO 0001739, **2000**.
- [37] Tilset, M.; Andell, O.; Dhindsa, A.; Froseth, M. (Borealis) WO 0249758, **2002**.
- [38] McGuinness, D. S.; Gibson, V. C.; Wass, D. F.; Steed, J. W. *J. Am. Chem. Soc.* **2003**, *125*, 12716.
- [39] Dixon, J. T.; Green, M. J.; Hess, F. M.; Morgan, D. H. *J. Organomet. Chem.* **2004**, *689*, 3641.
- [40] Schulz, G. V. *Z. Phys. Chem. B.* **1935**, *30*, 379.
- [41] Flory, P. J. *J. Am. Chem. Soc.* **1936**, *58*, 1877.
- [42] Skupinsa, J. *Chem. Rev.* **1991**, *91*, 613.
- [43] Cossee, P. *J. Catal.* **1964**, *3*, 80.
- [44] Arlman, E. J.; Cossee, P. *J. Catal.* **1964**, *3*, 99.

- [45] Manyik, R. M.; Walker, W. E.; Wilson, T. P. (Union Carbide Corporation) US 3300458, **1967**.
- [46] Reagan, W. K. (Phillips Petroleum Company) EP 0417477, **1991**.
- [47] Sato, H.; Nakajima, H. (Idemitsu Chemical Company) JP 06329562, **1994**.
- [48] Wang, G.; Xie, M.; Wang, S.; Qu, J.; Zhao, J.; Zhang, B.; Chen, Q.; Yuan, Z.; Han, X.; Li, L. (Chinese Petroleum Group) CN 1294109, **2001**.
- [49] Tamura, M.; Uchida, K.; Ito, Y.; Iwanga, K. (Sumitomo Chemical Company) EP 0614865, **1994**.
- [50] Dixon, J. T.; Grovč, C.; Ranwell, A. (Sasol Technology (Pty) Ltd) WO 0183447, **2001**.
- [51] Maas, H.; Mihan, S.; Kohn, R.; Seifert, G.; Tropsch, J. (BASF Aktiengesellschaft) WO 2000058319, **2000**.
- [52] Aoyama, T.; Mimura, H.; Yamamoto, T.; Oguri, M.; Koie, Y. (Tosoh Corporation) JP 09176299, **1997**.
- [53] Aoshima, T.; Urata, T. (Mitsubishi Chemical Industries) JP 11181016, **1999**.
- [54] Commereuc, D. C.; Drochon, R. M.; Saussine, C. (Institute Francais du Petrole) US 6031145, **1998**.
- [55] Mahomed, H.; Bollmann, A.; Dixon, J.; Gokul, V.; Griesel, L.; Grove, C.; Hess, F.; Maumela, H.; Pepler, L. *Appl. Catal. A* **2003**, 255, 355.
- [56] Wu, F. J. (Amoco Corporation) US 5811618, **1995**.
- [57] Wass, D. F. (BP Chemicals Ltd) WO 0204119, **2002**.

- [58] Carter, A.; Cohen, S. A.; Cooley, N. A.; Murphy, A.; Scutt, J.; Wass, D. F. *Chem. Commun.* **2002**, 858.
- [59] Blann, K.; Bollman, A.; Dixon, J. T.; Hess, F. H.; Killian, E.; Maumela, H.; Morgan, D. H.; Neveling, A.; Otto, S.; Overett, M. J. *Chem. Commun.* **2005**, 620.
- [60] Dixon, J. T.; Grove, J. J. C.; Wasserscheid, P.; McGuinness, D. S.; Hess, F. M.; Maumela, H.; Morgan, D. H.; Bollmann, A. (Sasol Technology (Pty) Ltd) WO 03053891, **2001**.
- [61] McGuinness, D. S.; Wasserscheid, P.; Keim, W.; Dixon, J. T.; Grove, J. J. C.; Hu, C.; Englert, U. *Chem. Commun.* **2003**, 334.
- [62] Manyik, R. M.; Walker, W. E.; Wilson, T. P. *J. Catal.* **1977**, *47*, 197.
- [63] Briggs, J. R. *J. Chem. Soc., Chem. Commun.* **1989**, *11*, 674.
- [64] Wass, D. F. *Dalton Trans.* **2007**, 816.
- [65] Agapie, T.; Schofer, S. J.; Labinger, J. A.; Bercaw, J. E. *J. Am. Chem. Soc.* **2004**, *126*, 1304.
- [66] Agapie, T.; Labinger, J. A.; Bercaw, J. E. *J. Am. Chem. Soc.* **2007**, *129*, 14281.
- [67] Köhn, R. D.; Haufe, M.; Mihan, S.; Lilge, D. *Chem. Commun.* **2000**, 1927.
- [68] Morgan, D. H.; Schwikkard, S. W.; Dixon, J. T.; Nair, J. J.; Hunter, R. *Adv. Synth. Catal.* **2003**, *345*, 939.
- [69] van Rensburg, W. J.; Grovč, C.; Steynberg, J. P.; Stark, K. B.; Huyser, J. J.; Steynberg, P. J. *Organometallics* **2004**, *23*, 1207.
- [70] Meijboom, N.; Schaverien, C. J.; Orpen, A. G. *Organometallics* **1990**, *9*, 774.

- [71] Bollmann, A.; Blann, K.; Dixon, J. T.; Hess, F. M.; Killian, E.; Maumela, H.; McGuinness, D. S.; Morgan, D. H.; Neveling, A.; Otto, S.; Overett, M. J.; Slawin, A. M. Z.; Wasserscheid, P.; Kuhlmann, S. *J. Am. Chem. Soc.* **2004**, *126*, 14712.
- [72] Blok, A. N. J.; Budzelaar, P. H. M.; Gal, A. W. *Organometallics*, **2003**, *22*, 2564.
- [73] Overett, M. J.; Blann, K.; Bollmann, A.; Dixon, J. T.; Haasbroek, D.; Killian, E.; Maumela, H.; McGuinness, D. S.; Morgan, D. H. *J. Am. Chem. Soc.* **2005**, *127*, 10723.
- [74] Walsh, R.; Morgan, D. H.; Bollmann, A.; Dixon, J. T. *Appl. Catal. A* **2006**, *306*, 184.
- [75] Kuhlmann, S.; Dixon, J. T.; Haumann, M.; Morgan, D. H.; Ofili, J.; Spuhl, O.; Taccardi, N.; Wasserscheid, P. *Adv. Synth. Catal.* **2006**, *348*, 1200.
- [76] Jabri, A.; Crewdson, P.; Gambarotta, S.; Korobkov, I.; Duchateau, R. *Organometallics* **2006**, *25*, 715.
- [77] Kuhlmann, S.; Blann, K.; Bollmann, A.; Dixon, J. T.; Killian, E.; Maumela, M. C.; Maumela, H.; Morgan, D. H.; Pretorius, M.; Taccardi, N.; Wasserscheid, P. *J. Catal.* **2007**, *245*, 277.
- [78] Rucklidge, A. J.; McGuinness, D. S.; Tooze, R. P.; Slawin, A. M. Z.; Pelletier, J. D. A.; Hanton, M. J.; Webb, P. B. *Organometallics* **2007**, *26*, 2782.
- [79] Tomov, A. K.; Chirinos, J. J.; Jones, D. J.; Long, R. J.; Gibson, V. C. *J. Am. Chem. Soc.* **2005**, *127*, 10166.
- [80] Tomov, A. K.; Chirinos, J. J.; Long, R. J.; Gibson, V. C.; Elsegood, M. R. J. *J. Am. Chem. Soc.* **2006**, *128*, 7704.
- [81] McGuinness, D. S.; Suttill, J. A.; Gardiner, M. G.; Davies, N. W. *Organometallics* **2008**, *27*, 4238.
- [82] Deckers, P. J. W.; Hessen, B.; Teuben, J. H. *Organometallics* **2002**, *21*, 5122.

- [83] Deckers, P. J. W.; Hessen, B.; Teuben, J. H. *Angew. Chem., Int. Ed.* **2001**, *40*, 2516.
- [84] Andes, C.; Harkins, S. B.; Murtuza, S.; Oyler, K.; Sen, A. *J. Am. Chem. Soc.* **2001**, *123*, 7423.
- [85] Tobisch, S.; Ziegler, T. *J. Am. Chem. Soc.* **2004**, *126*, 9059.
- [86] Arteaga-Müller, R.; Tsurugi, H.; Saito, T.; Yanagawa, M.; Oda, S.; Mashima, K. *J. Am. Chem. Soc.* **2009**, *131*, 5370.
- [87] Agapie, T.; Day, M. W.; Henling, L. M.; Labinger, J. A.; Bercaw, J. A. *Organometallics* **2006**, *25*, 2733 and references therein.
- [88] Chang, R. *Physical Chemistry for the Chemical and Biological Sciences*, University Science Books, **2000**, 741.
- [89] Schweiger, A.; Jeschke, G. *Principles of Pulse Electron Paramagnetic Resonance*, Oxford University Press, Oxford, **2001**.
- [90] Wertz, J. E.; Bolton, J. R. *Electron Spin Resonance: Elementary Theory and Practical Applications*, McGraw Hill Book Company, New York, **1972**.
- [91] Mabbs, F. E.; Collison, D. *Electron Paramagnetic Resonance of d-Transition Metal Compounds*, Elsevier Science Publisher B. V., Amsterdam, **1992**.
- [92] Assenheim, H. M. *Introduction to Electron Spin Resonance*, J. W. Arrowsmith Ltd, Bristol, **1966**.
- [93] Memory, J. D. *Quantum Theory of Magnetic Resonance Parameters*, McGraw Hill Book Company, New York, **1968**.
- [94] Weyhermüller, T.; Paine, T. K.; Bothe, E.; Bill, E.; Chaudhuri, P. *Inorg. Chimica Acta* **2002**, *337*, 344.

- [95] Bruckner, A.; Jabor, J. K.; McConnell, A. E. C.; Webb, P. B. *Organometallics* **2008**, *27*, 3849.
- [96] (a) Branca, M.; Fruianu, M.; Sau, S.; Zoroddu, M. A. *J. Inorg. Biochem.* **1996**, *62*, 223. (b) Branca, M.; Micera, G.; Sanna, D. *Inorg. Chem.* **1993**, *32*, 578.
- [97] (a) Rieger, P. H. *Coord. Chem. Rev.* **1994**, *135*, 203. (b) Rieger, A. L.; Rieger, P. H. *Organometallics* **2002**, *21*, 5868. (c) Cummings, D. A.; McMaster, J.; Rieger, A. L.; Rieger, P. H. *Organometallics* **1997**, *16*, 4362.
- [98] Murphy, D. M.; Farley, R. D. *Chem. Soc. Rev.* **2006**, *35*, 249.
- [99] McDyre, L. E.; Hamilton, T.; Murphy, D. M.; Cavell, K. J.; Gabrielli, W. F.; Hanton, M. J.; Smith, D. M. *Dalton Trans.*, **2010**, *39*, 7792.

Chapter Two

Functionalised N-Heterocyclic Carbenes and Silver(I) Complexes

Chapter Two

Functionalised N-Heterocyclic Carbenes and Silver(I) Complexes

2.1 Introduction

Functionalised N-heterocyclic carbenes represent an important ligand set in organometallic chemistry. The presence of additional functional groups can complement the strong carbene donor, resulting in very interesting metal complexes with potential to be useful catalytic systems.

A series of imidazolium salts have been prepared as interesting proligands for our work focussing on chromium complexes. Donor-functionalised systems specifically have been included in order to impart extra stability to the more sensitive oxidation states of chromium.

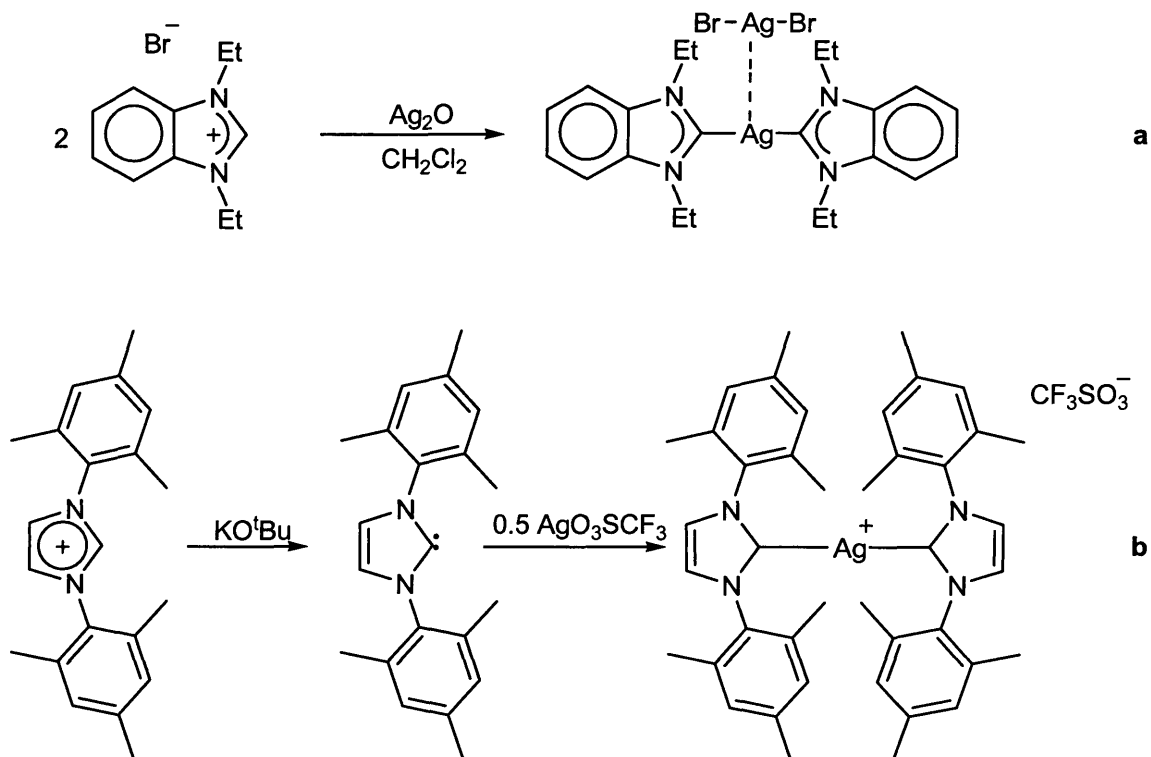
In this chapter we discuss the synthesis, structure and uses of a series of novel NHCs and their silver complexes. Silver(I)-NHC complexes have been fully characterised and are reported to demonstrate the potential use of these ligands in other areas, such as late transition metal chemistry.

2.1.1 Silver(I) NHC Complexes

The vast majority of reported silver(I)-NHC complexes are prepared via the convenient method developed by Lin and co-workers¹ involving the use of Ag₂O as a base (scheme 2.1). The first silver(I)-NHC complex however, was reported by Arduengo² in 1993 and involved the addition of a preformed free carbene to a silver salt, a much more intricate process that requires careful exclusion of moisture and air.

The reaction of imidazolium salts with silver oxide as shown in scheme 2.1a, is a route to NHC complexes with advantageous reaction conditions, i.e. carried out in air, with no need to pre-dry solvents. Following the publication by Lin in 1998, many complexes of this type were reported, including those that could not be obtained using the conventional

method of preparing metal-NHC complexes (Arduengo's method). For example, the presence of additional acidic protons in some imidazolium salts can result in deprotonation at these sites instead of/as well as at the C₂ position. More recently, silver carbonate³ and silver acetate⁴ have been used as bases in the same way to prepare these NHC complexes.



Scheme 2.1 Different routes to Ag(I)-NHC complexes.

The product shown in scheme 2.1b is shown as an ionic compound, however reports have since shown that silver(I) complexes can take on various ionic and neutral structures in the solid state as depicted in figure 2.1. The structure of silver(I)-NHC complexes has been extensively studied, and many different structural conformations have been observed. These differences in solid state structure have been attributed to various factors, including steric effects of the NHC ligand involved, presence of halide or non-halide counterion and the reaction conditions (solvent and temperature) used. Figure 2.1 shows some of the most common structures observed.⁵

This variation in structure is partially due to the ability of Ag(I) to coordinate to either one or two NHC moieties, to form complex anions of the type $[\text{AgX}_2]$ ($\text{X}=\text{halogen}$) and to engage in Ag(I)...Ag(I) interactions in the solid state, such as in Type 4 (figure 2.1).

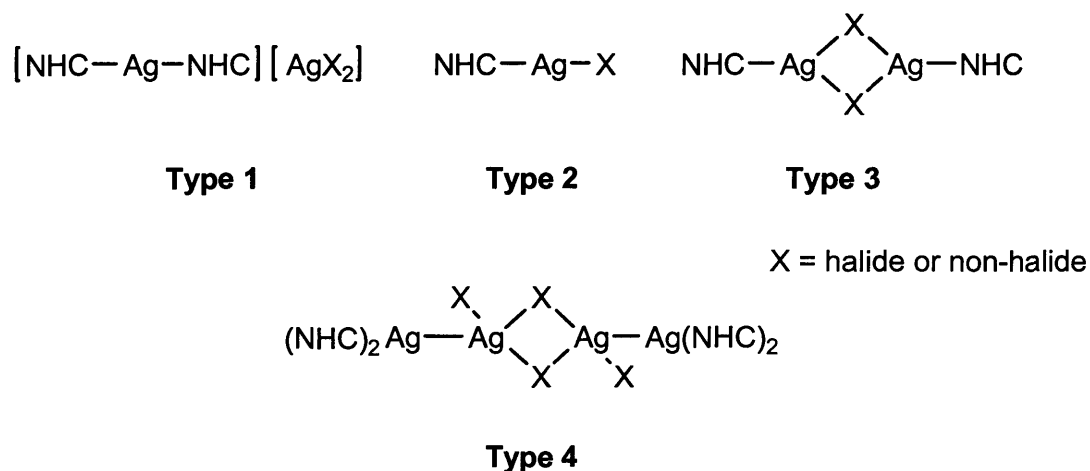
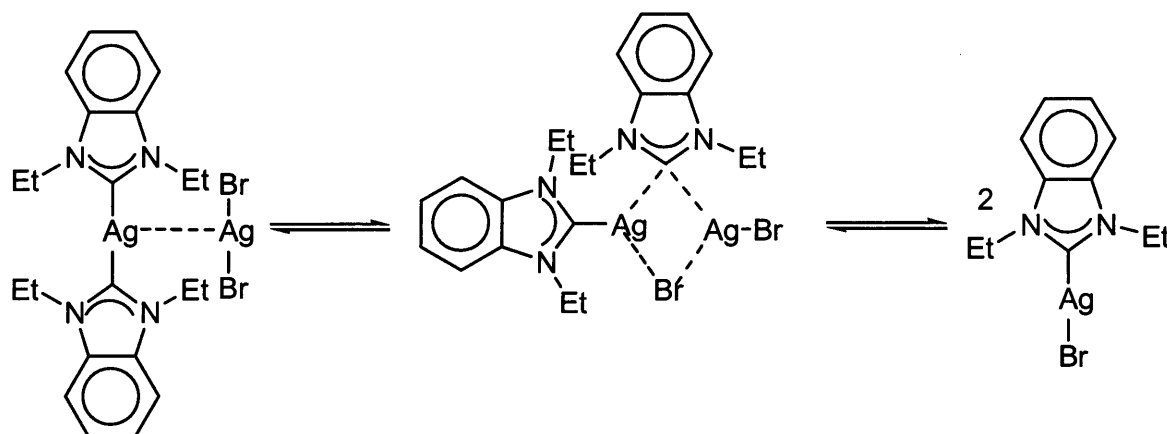


Figure 2.1 Common structures of Ag(I)-NHC complexes.

Generally, the absence of halide ions result in compounds of Type 1 with a quasi-linear geometry.^{1,6-10} The presence of halide ions seems to result in complexes with Type 1 and Type 2 structures, although it has been reported that the presence of iodide is more likely to produce ionic Type 1 complexes, due to the higher polarisability of iodide than chloride or bromide ions.¹ Iodide salts are thought to prefer to form ion-pair complexes rather than neutral species.¹¹ Fluxional behaviour⁵ between ionic and neutral complexes has been commonly observed for these compounds as shown in scheme 2.2, and can lead to ambiguity in structural characterisation.

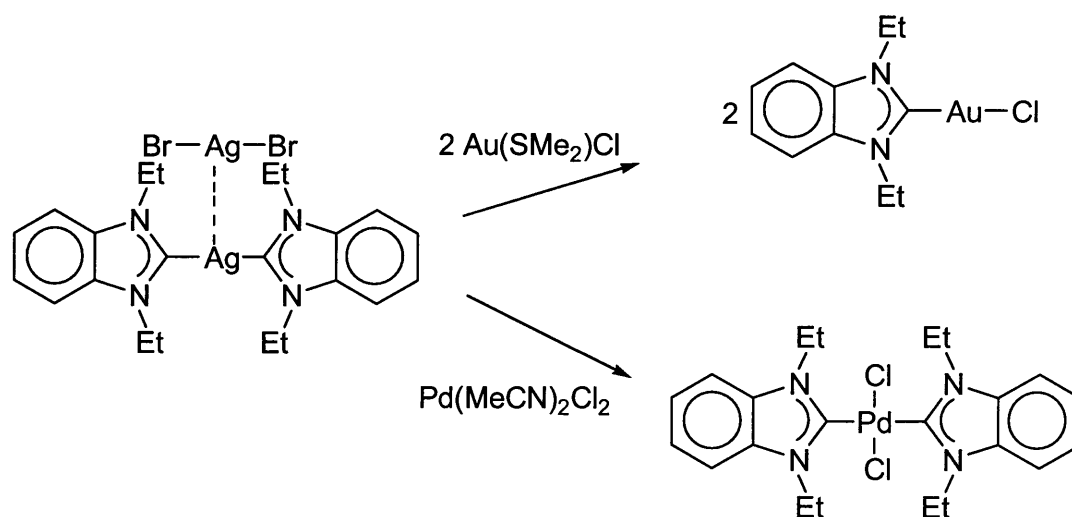
The presence of additional functional groups on the NHC ligand has been shown to have little or no effect on the structure, as they typically remain uncoordinated.^{3,7,8,12-15} Silver(I) has little affinity for additional nucleophilic functional groups when ligated by two NHC ligands,^{3,8,12,15-18} and this lack of interaction confirms the compatibility of the Ag_2O route to complexes of functionalised NHC ligands.

The silver-carbene bond is generally very labile in these complexes, demonstrated by the common lack of ^{13}C - $^{107/109}\text{Ag}$ couplings observed in the ^{13}C NMR spectra. This explains the application of silver(I)-NHC complexes as carbene transfer reagents.



Scheme 2.2 Fluxional behaviour in solution.⁵

First demonstrated by Lin and co-workers to prepare palladium and gold complexes¹ (scheme 2.3), transmetalation is now widely used for the preparation of late transition metal complexes, most commonly Pd(II), Au(I) and Rh(I)-NHCs.⁵ The ambient reaction conditions are often preferable to those required when forming the free carbene, providing a simple route to complexes widely studied in homogeneous catalysis. Until recently, the sole reason for preparing silver(I)-NHC complexes was for transmetalation reactions.



Scheme 2.3 First transmetalation reactions to form gold and palladium complexes.

The antimicrobial properties of silver compounds have been recognized and exploited for hundreds of years.¹⁷ Recently, the pharmaceutical application of silver(I)-NHC complexes has been reported,^{9d,18} describing the antimicrobial activity of these compounds.

One of the main benefits associated with silver(I)-NHC compounds is the ability to prepare a wide range of imidazolium salts of biologically relevant molecules, and this has been carried out with carbene derivatives of caffeine.¹⁹ The application requires the slow release of silver ions, and therefore the strength of the silver-carbene bond is important. Imidazolium salts can be modified quite easily in order to change the stability of the resulting silver complex, and also to ensure that decomposition products are non toxic.

2.1.2 Functionalised N-Heterocyclic Carbenes

The first donor functionalised N-heterocyclic carbenes were described by Herrmann²⁰ *et. al.* in 1996, just five years after the first free carbene was isolated by Arduengo, and have since become an important feature in organometallic chemistry.²¹

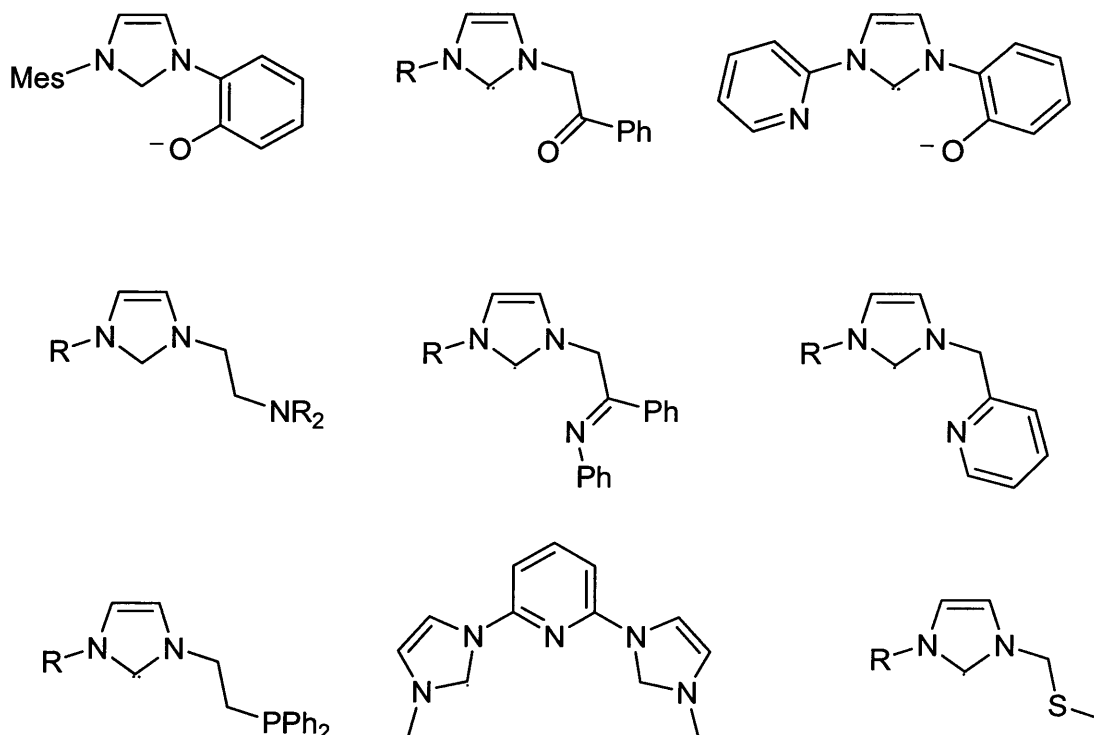
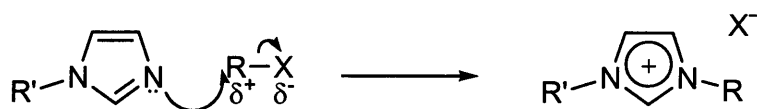


Figure 2.2 Selection of donor functionalised NHCs.

The presence of hemilabile donor functional groups in addition to the strongly binding carbene, results in complexes with added stability which is particularly important for intermediates in catalytic reactions.^{21,22} Many novel and varied mono- and di-functionalised NHC ligands have been reported with C, N, O, S and P donor atoms^{12,21,23-26} a selection of which are shown in figure 2.2.

Facile synthetic methods can account for the vast number of reported NHCs; nucleophilic attack of 1-alkylimidazole on an alkyl halide to produce an N-functionalised carbene precursor (imidazolium salt) is the usual method employed (scheme 2.4). This allows the 'fine-tuning' of ligand systems both electronically and sterically by simple modification of 'R' groups.



Scheme 2.4 General synthetic mechanism.

2.2 Results and Discussion

2.2.1 Synthesis of Functionalised Imidazolium Salts

Our interest in functionalised N-heterocyclic carbenes as ligands for chromium complexes led to the preparation of imidazolium salts containing carbonyl, imine and methoxy functional groups and are displayed in figure 2.3, where previously known compounds²⁵ are labelled (*). These heteroditopic carbene precursors have the potential to act as hemilabile donor ligands with the ability to stabilise a variety of metal complexes, making them very interesting from the point of view of homogeneous catalysis. The presence of the geminal dimethyl group in compounds 1-8 is essential. In related compounds with one or more hydrogens on the carbon alpha to the nitrogen, attempts to prepare the free carbene can result in deprotonation of the methylene linker rather than at the C₂ position.²⁵ This has been reported for several imidazolium salts containing acidic methylene groups.²⁷

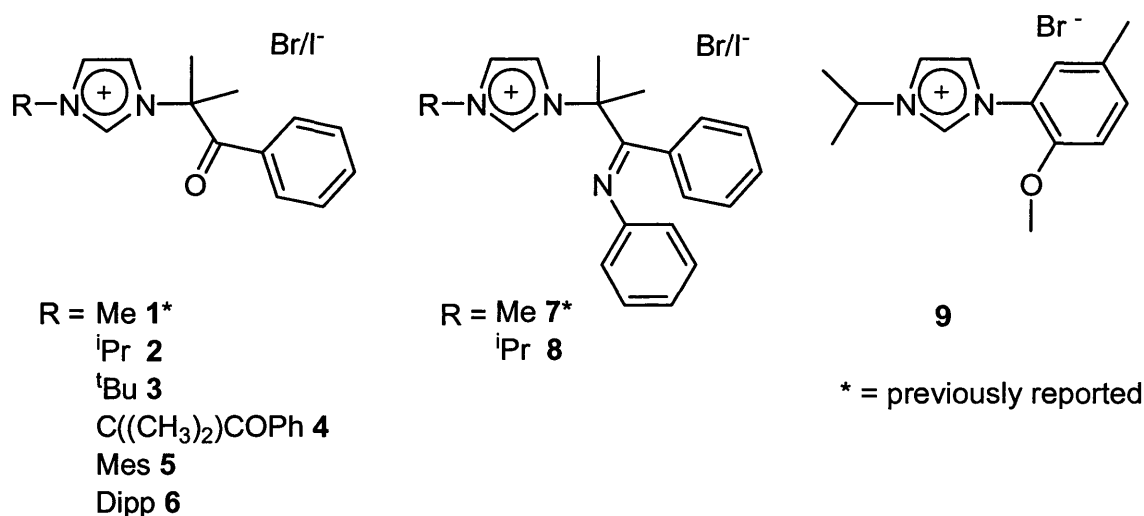
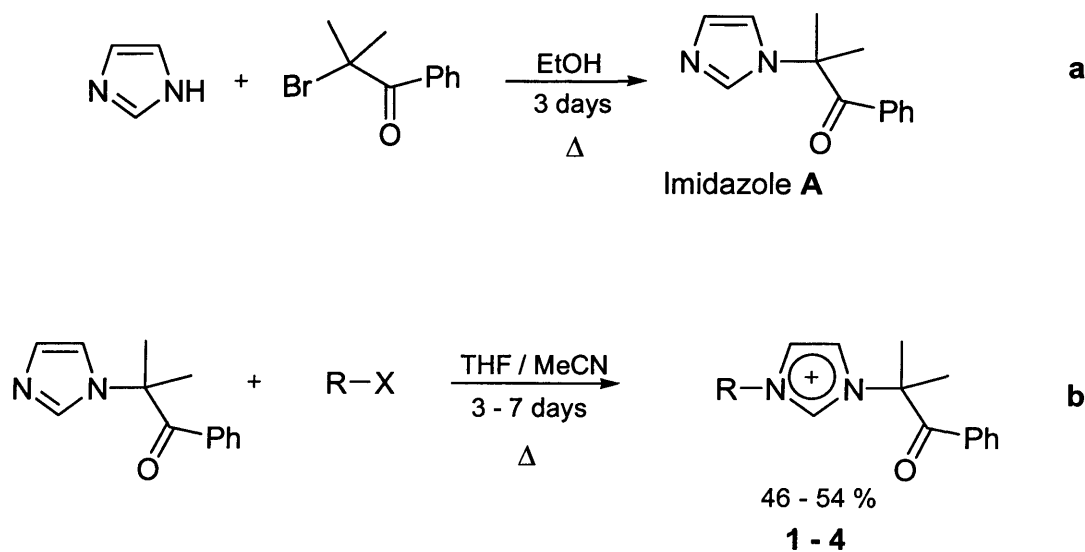


Figure 2.3 Imidazolium salts 1-9.

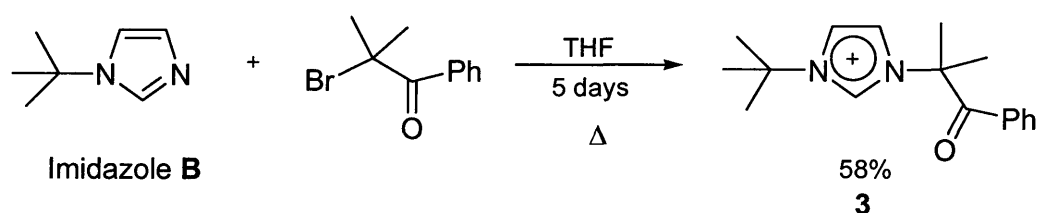
Synthesis of imidazolium salts 1-4 was carried out in a step-wise procedure as shown in scheme 2.5. It was found that isolation and purification of the literature reported substituted imidazole A²⁵ was essential before the second substituent could be added. In the case of the symmetrical salt 4, a one-pot-synthesis reaction with imidazole and 2 equivalents

of 2-bromoisobutyrophenone was attempted, but even after 10 days, only the mono-substituted species imidazole **A** was isolated. The addition of the second substituent (Scheme 2.5b) took between 3 and 7 days to produce the salt in reasonable yields (~50%) understandably, the methyl and isopropyl salts were formed faster. It should also be noted that the methyl substituted salt **1** has an iodide counterion, for no other reason than methyl iodide was readily available.



Scheme 2.5 Step-wise synthesis of imidazolium salts **1-4**.

The tertiary butyl substituted salt **3** was produced only in very poor yields even after extended periods of reflux, due to the obvious steric requirements of the bulky tertiary butyl bromide. Preparation of 1-tertiary butyl-imidazole (imidazole **B**) followed by addition of 2-bromoisobutyrophenone as shown in scheme 2.6, resulted in a significantly better yield in a more modest timeframe.



Scheme 2.6 Improved synthesis to imidazolium salt **3**.

Single-crystal X-ray diffraction data were collected for new salts **2**, **3**, **4** and **9** and their ORTEP plots are shown in figures 2.4, 2.5, 2.6 and 2.8. Selected bond lengths and angles are shown in tables 2.1-2.4. Bond lengths and angles are in the range expected for this type of salt. The internal bond lengths and angles of the imidazolium rings are unexceptional and lie within the range expected.²⁸

As shown in figure 2.4, the isopropyl substituted bromide salt **2** is orientated with the phenyl ring out of the plane of the imidazolium ring, and the carbonyl functionality pointed away from the C₂-proton, suggesting no hydrogen bonding occurs. Comparison of this structure with reported data²⁵ for the precursor imidazole **A** shows significant narrowing of the N-C-N angle in the salt, 109.0(3) ° compared to 113.66(13) °.

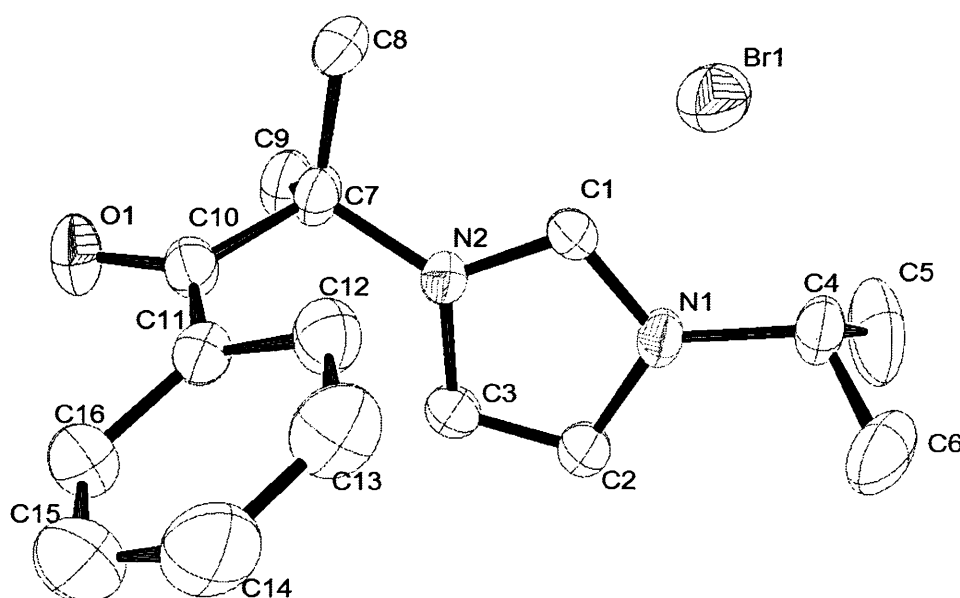


Figure 2.4 ORTEP plot at 50% probability of the molecular structure of **2**.

Bond length (Å)		Bond angle (°)	
C(1)-N(1)	1.320(5)	N(1)-C(1)-N(2)	109.0(3)
C(1)-N(2)	1.330(5)	C(1)-N(1)-C(2)	108.6(3)
C(2)-C(3)	1.337(6)	C(1)-N(2)-C(3)	107.9(3)
C(2)-N(1)	1.386(5)	N(1)-C(2)-C(3)	106.7(4)
C(3)-N(2)	1.380(5)	N(2)-C(3)-C(2)	107.8(4)
N(1)-C(4)	1.476(5)	C(1)-N(1)-C(4)	124.7(3)
N(2)-C(7)	1.478(5)	C(1)-N(2)-C(7)	126.8(3)
C(10)-O(1)	1.222(5)	C(7)-C(10)-C(11)	122.9(4)
		N(2)-C(7)-C(10)	110.6(4)

Table 2.1 Selected bond lengths (Å) and angles (°) for **2**.

Compound **3**, containing the more sterically hindered tertiary butyl group is shown in figure 2.5. We see the same orientation with respect to the phenyl ring and the carbonyl functional group as in salt **2**. The alkyl group is positioned at a slightly larger angle with respect to the ring than the isopropyl group in **2**, and we see that the N-alkyl bond of the tertiary butyl group is slightly longer than that of the isopropyl group in compound **2** (**2** N(1)-C(4) = 1.476(5) Å; **3** N(2)-C(4) = 1.501(4) Å).

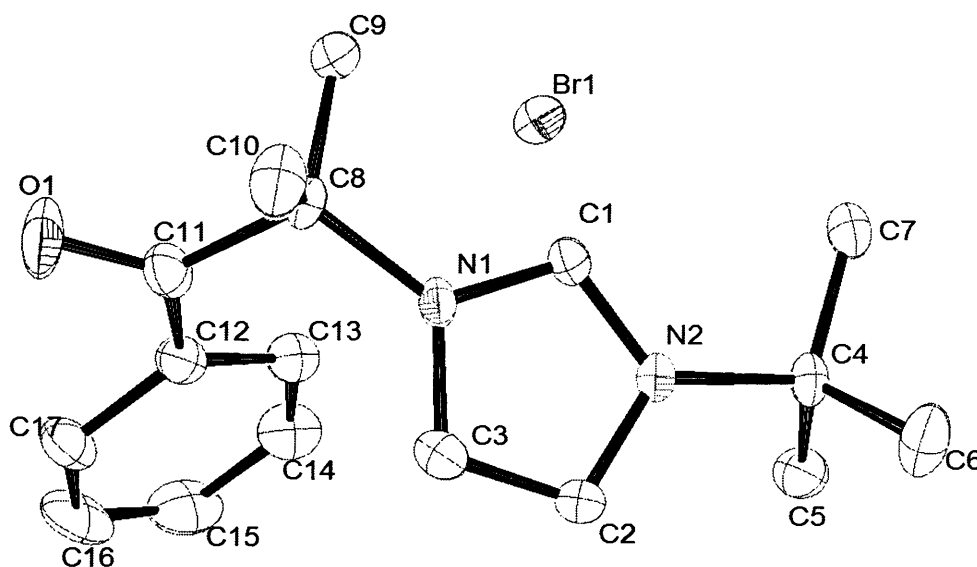


Figure 2.5 ORTEP plot at 50% probability of the molecular structure of **3**.

Bond length (Å)		Bond angle (°)	
C(1)-N(1)	1.338(4)	N(1)-C(1)-N(2)	108.5(3)
C(1)-N(2)	1.328(4)	C(1)-N(1)-C(3)	108.5(2)
C(2)-C(3)	1.354(4)	C(1)-N(2)-C(2)	108.9(2)
C(2)-N(2)	1.387(4)	N(1)-C(3)-C(2)	107.5(3)
C(3)-N(1)	1.377(4)	N(2)-C(2)-C(3)	106.6(3)
N(2)-C(4)	1.501(4)	C(1)-N(2)-C(4)	126.5(3)
N(1)-C(8)	1.485(4)	C(1)-N(1)-C(8)	126.5(3)
C(11)-O(1)	1.224(4)	C(8)-C(11)-C(12)	123.5(3)
		N(1)-C(8)-C(11)	110.5(3)

Table 2.2 Selected bond lengths (Å) and angles (°) for 3.

Salt 4, while found to be symmetrical in solution (NMR spectroscopy) the structure shown in figure 2.6 and data provided in table 2.3 shows that it is not symmetrical in the solid state.

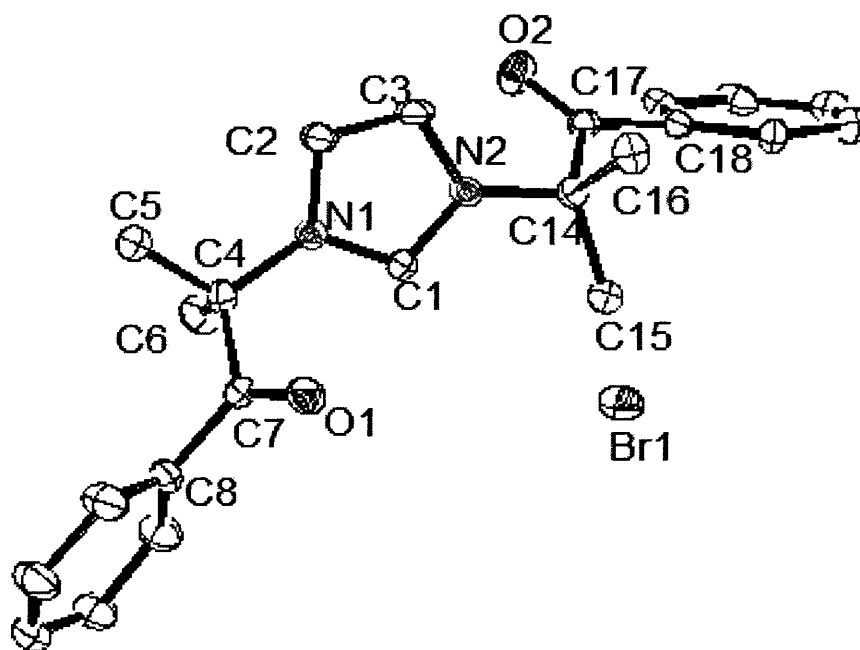


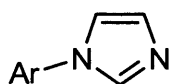
Figure 2.6 ORTEP plot at 50% probability of the molecular structure of 4.

We clearly see each carbonyl group pointing in different directions, and the phenyl rings are closer to the plane of the imidazolium salt than seen in **2** and **3**. We see a difference of 3.2° in the angles of each N-substituent relative to the ring, confirming the unsymmetrical nature of **4** in the solid state. One of the carbonyls is close to the correct position for potential coordination and the differences in solid state and solution structures suggest that rotation is not sterically hindered by the geminal dimethyl group.

Bond length (Å)		Bond angle (°)	
C(1)-N(1)	1.344(5)	N(1)-C(1)-N(2)	108.6(4)
C(1)-N(2)	1.334(5)	C(1)-N(1)-C(2)	108.2(4)
C(2)-C(3)	1.342(6)	C(1)-N(2)-C(3)	108.1(4)
C(2)-N(1)	1.383(5)	N(1)-C(2)-C(3)	107.1(4)
C(3)-N(2)	1.379(5)	N(2)-C(3)-C(2)	108.0(4)
N(2)-C(14)	1.488(5)	C(1)-N(1)-C(4)	123.8(3)
N(1)-C(4)	1.483(5)	C(1)-N(2)-C(14)	127.0(3)
C(7)-O(1)	1.211(5)	C(4)-C(7)-C(8)	120.5(4)
C(17)-O(2)	1.215(5)	C(14)-C(17)-C(18)	121.3(4)
		N(1)-C(4)-C(7)	107.8(4)
		N(2)-C(14)-C(17)	106.2(4)

Table 2.3 Selected bond lengths (Å) and angles (°) for **4**.

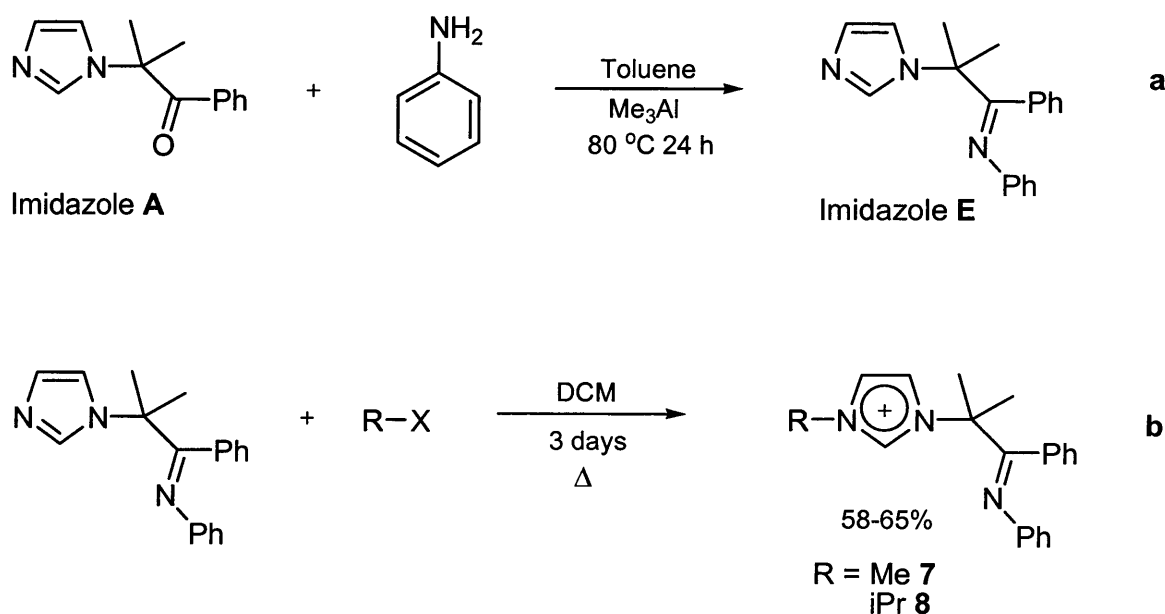
Preparation of aryl substituted salts **5** and **6** was carried out in the same way as for **3**. It is known that nucleophilic attack on such aromatic systems is very difficult,²⁹ so aryl-imidazole compounds **C** and **D** (figure 2.7) were prepared according to literature procedures.³⁰ These compounds are notoriously difficult to prepare in decent yields, with many 'improved' syntheses reported.³¹ The product imidazolium salts were then obtained as white solids in poor yield (~20%) even after extended periods of reflux in different solvents.



Ar = Mes Imidazole **C**
Dipp Imidazole **D**

Figure 2.7 Aryl imidazoles **C** and **D**.

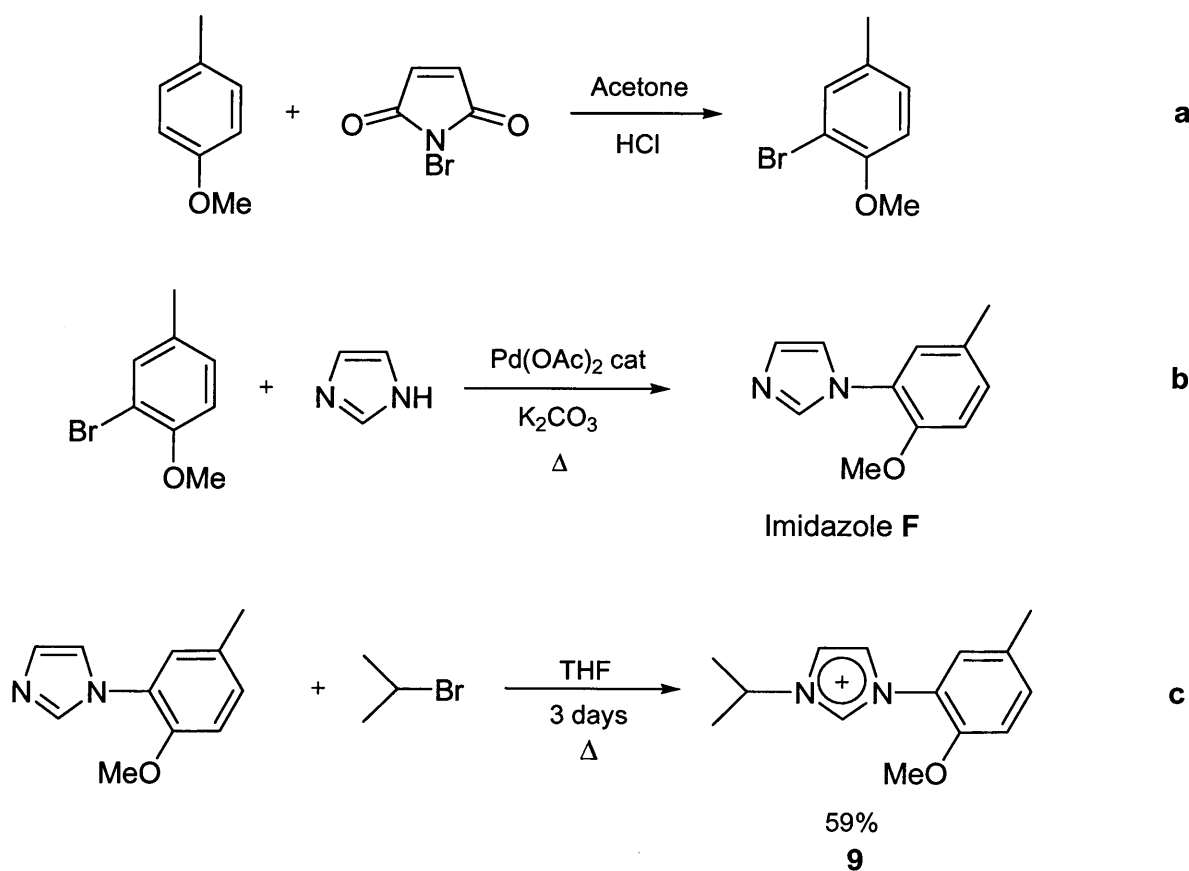
Preparation of **7** and **8** was carried out using a modified literature procedure (scheme 2.7) using imidazole **A** as the starting point to form the ketimine functionalised imidazole **E**,²⁵ where a longer reaction time than the quoted 3 hours at 80 °C was found to be necessary. Addition of methyl iodide or isopropyl bromide, followed by a 3 day reflux in dichloromethane resulted in salts **7** and **8**. When the reflux was performed in THF, no imine was observed, and the carbonyl salts **1** and **2** were recovered. This was attributed to the presence of water in the solvent. No evidence of isomerism was observed in the ¹H NMR spectra for these compounds as might be expected, there is a possibility of two isomers (*E* and *Z*), but it is believed that only one isomer is formed (*E*) due to the sterics involved in the system.³² Attempts to form salts **7** and **8** in a more direct method from carbonyl-functionalised imidazolium salts **1** and **2** were unsuccessful.



Scheme 2.7 Synthesis of imidazolium salts **7** and **8**.

The triflate salt of compound **7** along with the corresponding tungsten complex has been reported previously.²⁵ It has been included in our work as an interesting system for our early transition metal chemistry since only tungsten and no other reported complexes have been prepared, we therefore also report the silver(I) complex. It should be noted that a selection of transition metal complexes containing imine-functionalised NHCs have been disclosed in the patent literature,³³ although these do not contain the steric bulk of the geminal dimethyl group present in **7** and **8**.

Preparation of compound **9** was carried out as shown in scheme 2.8. Bromination of 4-methylanisole using NBS is a standard literature procedure,³⁴ this is followed by reaction with imidazole in the presence of potassium carbonate and a catalytic amount of palladium³⁵ allowing the substituted imidazole **F** to be prepared. Formation of the bromide salt was achieved using 2-bromopropane as described for compound **2**. Crystals suitable for analysis by single crystal X-ray methods were obtained by slow diffusion of diethyl ether into a dichloromethane solution of **9**, and the structure is shown in figure 2.8. Selected bond lengths and angles are shown in table 2.4.



Scheme 2.8 Synthesis of imidazolium salt **9**.

All internal bond lengths and angles lie within reported ranges for five-membered imidazolium salts.³⁶ However, as shown in figure 2.8, we see two molecules in the asymmetric unit, with the phenyl ring and methoxy functional group at different positions relative to the imidazolium ring. This suggests no hydrogen bonding is taking place between the oxygen and the acidic C₂-proton, and also demonstrates the free rotation expected.

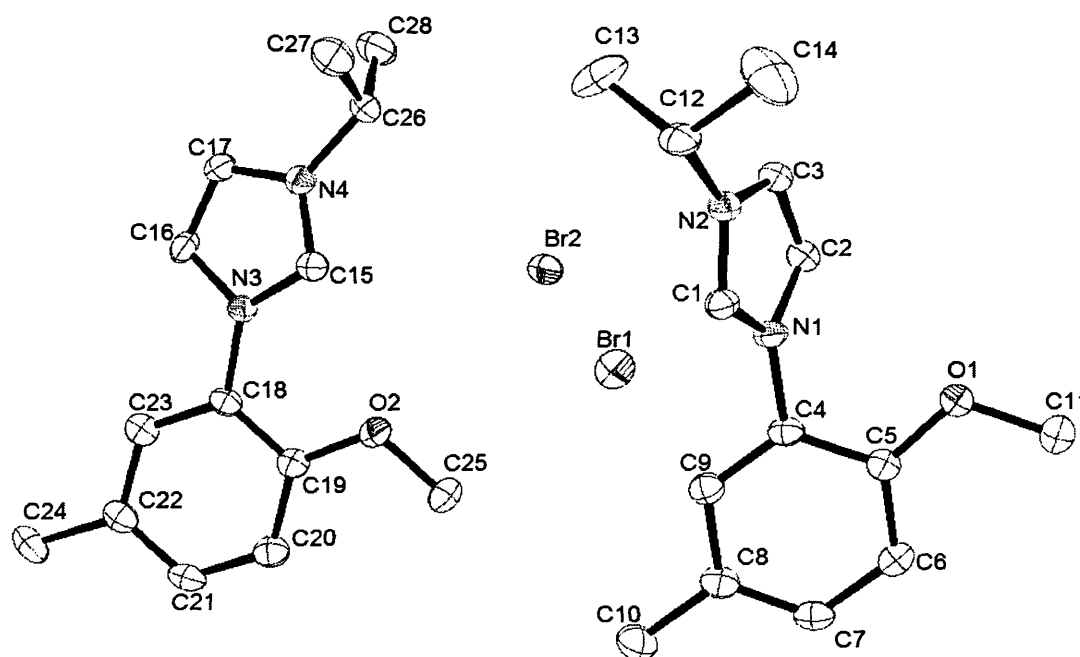


Figure 2.8 ORTEP plot at 50% probability of the molecular structure of 9.

Bond length (Å)		Bond angle (°)	
C(1)-N(1)	1.339(4)	N(1)-C(1)-N(2)	108.5(3)
C(1)-N(2)	1.329(4)	C(1)-N(1)-C(2)	108.3(2)
C(2)-C(3)	1.346(4)	C(1)-N(2)-C(3)	108.8(2)
C(4)-N(1)	1.444(4)	N(2)-C(3)-C(2)	107.2(3)
C(12)-N(2)	1.489(4)	N(1)-C(2)-C(3)	107.2(3)
N(2)-C(3)	1.384(4)	N(1)-C(4)-C(5)	119.9(3)
N(1)-C(2)	1.389(4)	C(1)-N(2)-C(12)	124.9(3)
		C(1)-N(1)-C(4)	124.2(2)

Table 2.4 Selected average bond lengths (Å) and angles (°) for 9.

Imidazolium salts **1-9** were characterised by ^1H and ^{13}C NMR spectroscopy and mass spectrometry and are reported in the experimental section. Simple spectra consistent with the proposed structures were observed in all cases, with characteristic low-field resonances corresponding to the C_2 proton (9-10ppm). The proposed structures were corroborated by X-ray data in the cases of **2**, **3**, **4** and **9**.

2.2.2 Preparation of Free Carbenes

Free carbenes **10-18** were prepared by treatment of imidazolium salts **1-9** with potassium hexamethyldisilylamide [$\text{KN}(\text{SiMe}_3)_2$] in either THF or benzene. Addition of the base to a suspension of the salt at low temperature resulted in an immediate colour change to orange-yellow from colourless, accompanied by complete solubilisation of the partially soluble salt. All free carbenes were found to be relatively stable as solids at low temperature, but decomposed fairly quickly in solution at room temperature. For this reason, future work requiring isolation of the free carbene was carried out *in-situ*.

Reactions were initially carried out on NMR scale in deuterated benzene to identify the product and confirm deprotonation of the salt. The ^1H NMR spectra of the resulting free carbenes lacked the resonance for the C_2 proton at around 9-10 ppm confirming deprotonation of the salt. The ^{13}C NMR spectra confirmed the presence of the free carbene as a large downfield shift of around 80 ppm is observed for the C_2 carbon, which is a relatively weak resonance in the ^{13}C spectra of the free carbene.

2.2.3 Silver(I) Carbene Complexes

Reaction of imidazolium salts **1-9** (figure 2.3) with a small excess of silver oxide in dichloromethane results in formation of the silver(I) complex after stirring at room temperature for 16 hours (Scheme 2.9). Reasonable yields were obtained (~70%), comparable to those reported for functionalised as well as non-functionalised silver-carbene complexes.⁸ The products are stable toward air and moisture, however, decomposition is observed when the complexes are left in solution for a prolonged period (e.g. days), particularly when exposed to light.

Characterisation of products was carried out by ^1H and ^{13}C NMR spectroscopy as well as mass spectrometry (provided in the experimental section). The main feature of the ^1H NMR spectra is the absence of a resonance for the C_2 proton; usually a distinct singlet around 9 ppm in the imidazolium salt. This immediately indicates that the proton has been abstracted, as described for free carbenes, and slight shifts downfield relative to the free carbene are observed for the C_4 and C_5 protons in the azolium ring as a result of coordination taking place.

The signal corresponding to the C_2 carbon in the ^{13}C NMR spectra shifts significantly upon removal of the proton (as discussed in 2.2.2). Generally in silver complexes, a coordination shift of 30-40 ppm upfield is expected relative to the free carbene. A splitting of the signal is also expected as the two main isotopes of silver (^{107}Ag and ^{109}Ag) are NMR active with $I = \frac{1}{2}$, so two doublets are sometimes observed, while the absence of this resonance is attributed to the lability of the carbene ligand.

The ^{13}C NMR spectra for complexes **19-27** are as otherwise as expected, but we see no C_2 resonance. This absence is not uncommon and has been attributed by Lin and co-workers^{1,37} to fluxional behaviour in solution, who report that other structures are likely to be generated in solution due to fluxional changes between the ionic and neutral complexes,^{1,5} i.e. interconversion between the mono- and the bis-carbene, as described in 2.1.1.

2.2.4 Structural Characterisation of Silver(I) Complex 21

As discussed in 2.1.1, silver(I) NHC complexes can adopt a variety of structures (figure 2.1). The NMR data described is not sufficient to determine the structure of compounds **19-27**. High resolution mass spectrometry, in coordination with X-ray crystallography has been used in order to elucidate the molecular structures.

Crystals suitable for X-ray diffraction were grown for compound **21**, and the ORTEP plot is shown in figure 2.9, confirming a neutral compound of Type 2 (NHC-Ag-Br). Selected bond lengths and angles are shown in table 2.5.

The complex has a quasi-linear geometry, with an angle at the metal centre of 174.6° . The carbon-silver bond, at $2.098(5) \text{ \AA}$, is in agreement with the reported average for five-membered carbene complexes ($2.077(8) \text{ \AA}$),³⁸ and the silver-bromide bond is 2.427 \AA which is also perfectly in-keeping with the average of 2.46 \AA .³⁸

On comparison with salt **3**, it can be seen that the NCN angle is much narrower upon coordination, while the other internal angles of the imidazole ring increase slightly. This reduced angle of $104.9(4)^\circ$ is in the range expected for five-membered NHC complexes of silver.² It is also worth pointing out that the carbonyl group points away from the silver atom, confirming the predicted lack of functional group interaction in these complexes, as seen in many other reported complexes of this type.

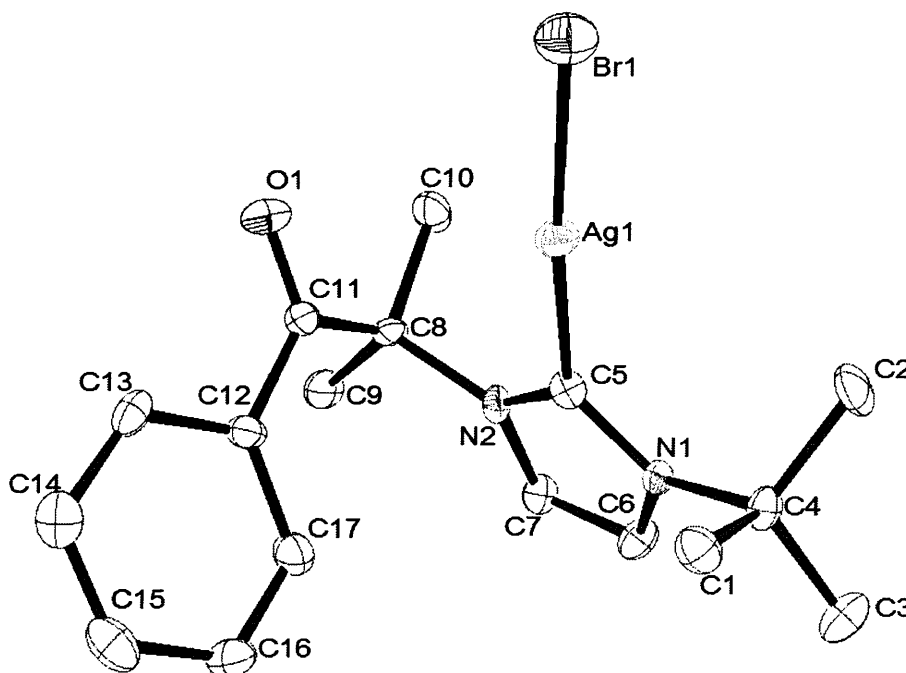


Figure 2.9 ORTEP plot at 50% probability of the molecular structure of **21**.

Bond length (Å)		Bond angle (°)	
C(5)-Ag(1)	2.098(5)	N(1)-C(5)-N(2)	104.9(4)
Ag(1)-Br(1)	2.427(7)	C(5)-N(2)-C(7)	110.5(4)
N(2)-C(5)	1.363(6)	N(2)-C(7)-C(6)	106.5(4)
C(5)-N(1)	1.355(6)	C(5)-N(1)-C(6)	110.3(4)
C(7)-C(6)	1.340(7)	N(1)-C(6)-C(7)	107.7(4)
N(2)-C(7)	1.387(6)	C(5)-N(1)-C(4)	124.6(4)
N(1)-C(6)	1.380(6)	C(5)-N(2)-C(8)	123.5(4)
N(1)-C(4)	1.503(6)	N(2)-C(8)-C(11)	110.4(4)
N(2)-C(8)	1.482(6)	C(5)-Ag(1)-Br(1)	174.6(13)
C(11)-O(1)	1.202(6)		

Table 2.5 Selected bond lengths (Å) and angles (°) for **21**.

Mass spectrometry data for the silver(I)-NHC complexes provides more information on the structures of compounds **19-27**. CH₃CN is used as a carrier solvent, and with the exception of compounds **19** and **25**, the [NHC-Ag-CH₃CN]⁺ fragment is observed. It is common for acetonitrile to displace ligands during analysis, and these results suggest that the halide has been displaced, so these compounds are of Type **2**, [NHC-Ag-X]. This is supported by the X-ray structure shown in figure 2.9. For compounds **19** and **25** however, we see the fragment corresponding to [NHC-Ag-NHC]⁺ suggesting cationic Type **1** structures. Since all compounds were prepared using the same method, i.e. same temperature, solvent and timescale, the different structures observed (figure 2.10) must be a consequence of either steric effects of the ligand, or more likely as a result of the different halide present.

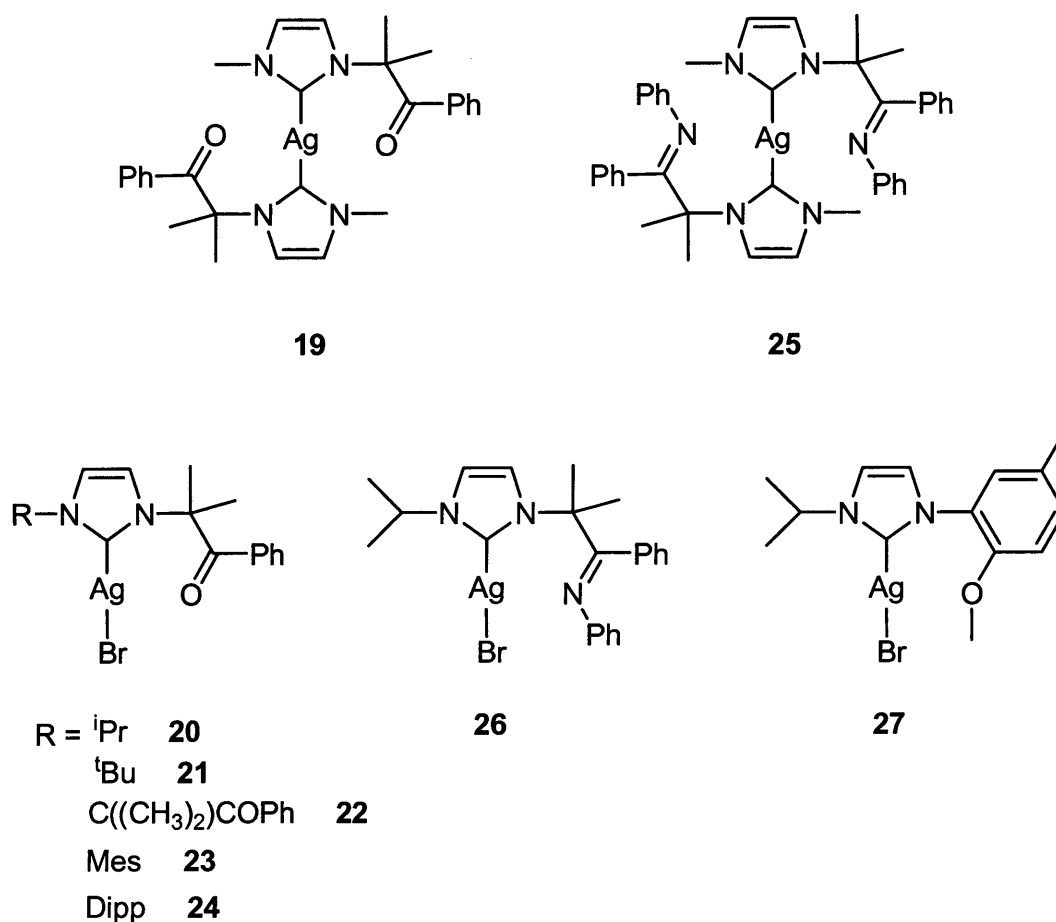


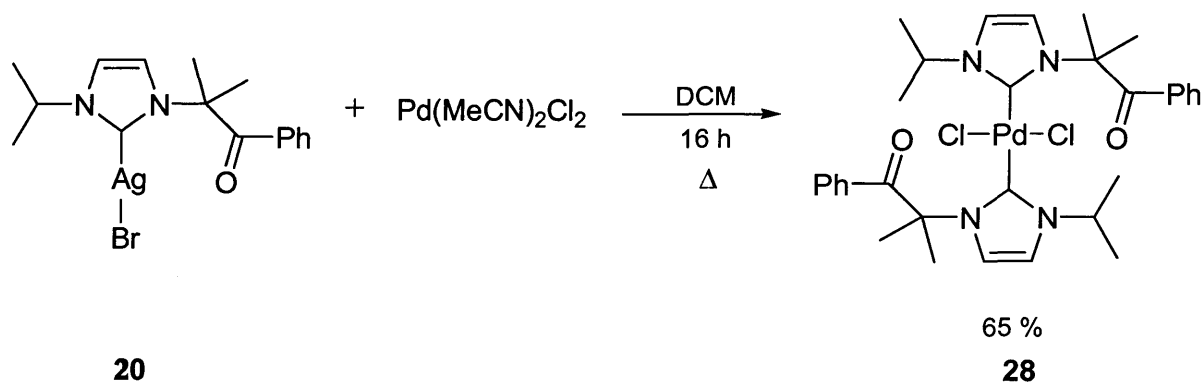
Figure 2.10 Structures of complexes 19-27 as determined by mass spectrometry and X-ray crystallography.

Compound **19** contains a less bulky ligand than the isopropyl and tertiary butyl analogues, and could be reasonably assumed that this reduces the steric interactions enough to allow another NHC to comfortably coordinate to the same metal centre. However, while compound **25** also contains a ligand with one small methyl group, the other half of the ligand is significantly more bulky. This leads to the conclusion that the presence of a different halide in these compounds is responsible for the observed structural differences, and in fact, iodide imidazolium salts have been shown to form ion pair complexes, rather than form the neutral species.¹¹ As described in 2.2.1, imidazolium salts **10** and **16** were prepared using methyl iodide, resulting in an iodide counterion whereas all other salts contain bromide counterions.

2.2.5 Transmetallation

As discussed, one of the main uses of silver(I)-carbene complexes is for transmetallation, where they act as a carbene transfer agent when reacted with late transition metals.¹ This is a well established and convenient method for the preparation of transition metal-carbene complexes of Au(I), Pd(II), Rh, Ir, Cu, Ru, Ni(II), and Pt(II).⁵

The focus of this thesis is early transition metals and as relatively electropositive metals, they are less able to compete with the silver cation for the softer carbene. As a result, transmetallation is generally restricted to late transition metal complexes of the type mentioned. Therefore, the silver(I)-NHC complexes described in this chapter were prepared simply to illustrate a new set of functionalised carbene complexes and gain more understanding about their reactivity, and coordination. One palladium complex has been prepared, to illustrate the transmetallation reaction with these new functionalised carbene systems.



Scheme 2.10 Transmetallation reaction to form palladium(II) complex **28**.

Silver complex **20** and trans-bis(acetonitrile) dichloropalladium (II) were heated in dichloromethane for 16 hours, after which the dark mixture was filtered to remove silver bromide, and the solvent removed. After washing with ethanol and recrystallisation from dichloromethane/ethanol a yellow solid was obtained (scheme 2.10). The palladium complex **28** was isolated and identified by ¹H and ¹³C NMR and mass spectrometry. NMR spectra were as expected, and mass spectrometry showed the fragments corresponding to [NHC-Pd]⁺ as well as [NHC-Pd-(MeCN)₂]⁺. Chloride displacement by acetonitrile (the solvent carrier) is commonly observed and the presence of only one NHC suggests possible coordination of the

ketone functional group. Unfortunately, crystals suitable for X-ray analysis were not obtained so the absolute structure cannot be confirmed. However, the yield obtained suggests that two NHCs are coordinated, and comparison with examples of similar compounds reported suggests that coordination of the carbonyl group is generally not observed in palladium complexes of this type.²⁴

2.3 Conclusion

A series of new imidazolium salts have been prepared and fully characterised. Free carbenes have also been isolated, allowing us to gain valuable information about these sensitive compounds. The free carbenes were found to be quite unstable in solution, but stable as solids at low temperatures for extended periods.

A series of new silver(I) complexes are also reported, along with structural information obtained from X-ray crystallographic data for one complex. This data has been used in collaboration with mass spectrometry and NMR spectroscopy in order to determine the likely structures of the other silver(I) complexes described.

An example of a palladium(II) complex prepared by transmetallation has been described to illustrate the potential use of these versatile N-heterocyclic carbene ligands in other metal complexes.

2.4 Experimental Section

General Remarks. All manipulations were performed in air, unless otherwise stated. Solvents THF and hexane were freshly distilled from sodium/potassium alloy, dichloromethane was distilled from calcium hydride, and all other solvents were used as purchased. Deuterated solvents for NMR measurements were distilled prior to use from the appropriate drying agents. Air sensitive compounds were stored and weighed in a nitrogen atmosphere MBraun UNILAB glovebox with less than 0.1 ppm water and O₂. Compound 7 and imidazoles A-F were prepared according to literature methods, or modifications of literature methods.^{25, 30, 34, 35, 39} All reagents were used as received. ¹H and ¹³C {¹H} NMR spectra were obtained on Bruker Avance AMX 400 and 500 or Jeol Eclipse 300 spectrometers. The chemical shifts δ are given as dimensionless values and are referenced relative to TMS, and coupling constants J are given in Hz. Mass spectra (MS) and high-resolution mass spectra (HRMS) were obtained in positive electrospray (ES) mode unless otherwise reported, on a Waters Q-TOF micromass spectrometer.

1-Methyl-3-(2-isobutyrophenone)imidazol-2-ium iodide (1)

Methyl iodide (1.05 ml, 0.0168 mol) and imidazole A (3.0 g, 0.014 mol) were combined in a Schlenk tube with THF (50 ml) and heated to reflux for 3 days. After cooling to room temperature, the mixture was filtered and the precipitate washed with one portion of THF (20 ml), diethyl ether (2 × 10 ml) and dried *in vacuo*. The salt was recrystallised from dichloromethane/diethyl ether to give the product as a hygroscopic white solid. Yield: 2.35 g (47%). ¹H NMR (d⁶ DMSO, 400 MHz, 298 K): δ (ppm) 9.46 (1H, s, NCHN), 7.84 (2H, d, NCHCHN, ³J_{HH} = 7.52 Hz), 7.69 (2H, d, *ortho*-CH, ³J_{HH} = 7.55 Hz), 7.64 (1H, m, *para*-CH), 7.49 (2H, t, *meta*-CH, ³J_{HH} = 7.71 Hz), 3.90 (3H, s, N-CH₃), 2.01 (6H, s, NC(CH₃)₂). ¹³C {¹H} NMR (d⁶ DMSO, 101 MHz, 298 K): δ (ppm) 197.9 (C=O), 134.92 (NCN), 133.6 (*ipso*-C), 131.6 (*para*-CH), 128.8 (*ortho*-CH), 128.2 (*meta*-CH), 118.4, 116.7 (NCCN), 65.4 (NC(CH₃)₂), 48.9 (NCH(CH₃)₂), 27.9 (NC(CH₃)₂). IR (CH₂Cl₂): ν = 1685 (s) (CO) cm⁻¹. HRMS (ES) (MeCN): found 229.1370 (C₁₄H₁₇N₂O⁺ requires 229.1361 dev: 3.9 ppm).

1-Isopropyl-3-(2-isobutyrophenone)imidazol-2-ium bromide (2)

2-bromopropane (1.06 ml, 0.0112 mol) and imidazole **A** (2.0 g, 0.0093 mol) were combined in a Schlenk tube with THF (30 ml) and heated to reflux for 4 days. After cooling to room temperature, the mixture was filtered and the precipitate washed with one portion of THF (10 ml), diethyl ether (2 × 10 ml) and dried *in vacuo*. The salt was recrystallised from dichloromethane/diethyl ether to give the product as a hygroscopic white solid. Crystals suitable for X-ray crystallography were grown by slow diffusion of diethyl ether into a dichloromethane solution. Yield: 1.45 g, (46%). ¹H NMR (d⁶ DMSO, 400 MHz, 298 K): δ (ppm) 9.24 (1H, s, NCHN), 7.73 (2H, d, NCHCHN, ³J_{HH} = 7.31 Hz), 7.38 (3H, m, *meta*- and *para*-CH), 7.23 (2H, m, *ortho*-CH), 4.42, (1H, sept, NCH(CH₃)₂, ³J_{HH} = 6.72 Hz), 1.79 (6H, s, NC(CH₃)₂), 1.23 (6H, d, NCH(CH₃)₂, ³J_{HH} = 6.66 Hz). ¹³C {¹H} NMR (d⁶ DMSO, 101 MHz, 298 K): δ (ppm) 198.6 (C=O), 134.8 (NCN), 134.4 (*ipso*-C), 132.9 (*para*-CH), 128.7 (*ortho*-CH), 128.0 (*meta*-CH), 121.9, 120.7 (NCCN), 69.2 (NC(CH₃)₂), 52.7 (NCH(CH₃)₂), 25.5 (NC(CH₃)₂), 22.3 (NCH(CH₃)₂). IR (CH₂Cl₂): ν = 1688 (s) (CO) cm⁻¹. HRMS (ES) (MeCN): found 257.1650 (C₁₆H₂₁N₂O⁺ requires 257.1654 dev: -1.6 ppm).

Tert-butyl-3-(2-isobutyrophenone)imidazol-2-ium bromide (3)

2-bromoisobutyrophenone (1.16 ml, 6.87 mmol) and imidazole **B** (0.71 g, 5.73 mmol) were combined in a Schlenk tube with THF (30 ml) and heated to reflux for 5 days. After cooling to room temperature, the mixture was filtered and the precipitate washed with one portion of THF (10 ml), diethyl ether (2 × 10 ml) and dried *in vacuo*. The salt was recrystallised from dichloromethane/diethyl ether to give the product as a hygroscopic white solid. Crystals suitable for X-ray crystallography were grown from slow diffusion of pentane into a chloroform solution. Yield: 1.18 mg, (58%). ¹H NMR (d⁶ DMSO, 400 MHz, 298 K): δ (ppm) 9.27 (1H, s, NCHN), 8.07 (2H, d, NCHCHN, ³J_{HH} = 8.31 Hz), 7.62 (3H, m, *meta*- and *para*-CH), 7.46 (2H, m, *ortho*-CH), 2.05 (6H, s, NC(CH₃)₂), 1.58 (9H, s, NC(CH₃)₃). ¹³C {¹H} NMR (d⁶ DMSO, 400 MHz, 298 K): δ (ppm) 198.7 (C=O), 134.5 (NCN), 134.1, 132.8, 128.6, 128.0 (C₆H₅), 121.9, 120.5 (NCCN), 69.5 (NC(CH₃)₂), 60.1 (NC(CH₃)₃), 29.0 (NC(CH₃)₃), 25.3 (NC(CH₃)₂). IR (CH₂Cl₂): ν = 1687 (s) (CO) cm⁻¹. HRMS (ES) (MeCN): found 271.1802 (C₁₇H₂₃N₂O⁺ requires 271.1810 dev: -3.0 ppm).

1,3-Di-(2-isobutyrophenone)imidazol-2-ium bromide (4)

2-bromoisobutyrophenone (2.83 ml, 0.017 mol) and imidazole A (3.0 g, 0.014 mol) were combined in a Schlenk tube with acetonitrile (101 ml) and heated to reflux for 7 days. After cooling to room temperature, the solvent was removed *in vacuo*, and the residue washed with THF (3 × 20 ml), diethyl ether (2 × 10 ml) and dried *in vacuo*. The salt was recrystallised from dichloromethane/diethyl ether to give the product as a hygroscopic white solid. Crystals suitable for X-ray crystallography were grown by slow diffusion of diethyl ether into a dichloromethane solution. Yield: 3.36 g (54%). ¹H NMR (d⁶ DMSO, 400 MHz, 298 K): δ (ppm) 9.62 (1H, s, NCHN), 8.10 (2H, s, NCHCHN), 7.81 (4H, m, *ortho*-CH), 7.75 (2H, m, *para*-CH), 7.60 (4H, m, *meta*-CH) 2.15 (12H, s, NC(CH₃)₂). ¹³C {¹H} NMR (d⁶ DMSO, 400 MHz, 298 K): δ (ppm) 197.7 (C=O), 135.7 (NCN), 134.3, 133.0, 128.7, 128.7 (C₆H₅), 122.1 (NCCN), 69.7 (NC(CH₃)₂), 25.7 (NC(CH₃)₂). IR (CH₂Cl₂): ν = 1687 (s) (CO) cm⁻¹. HRMS (ES) (MeCN): found 361.1898 (C₂₃H₂₅N₂O₂⁺ requires 361.1916 dev: -5.0 ppm).

1-Mesityl-3-(2-isobutyrophenone)imidazol-2-ium bromide (5)

2-bromoisobutyrophenone (0.54 ml, 3.23 mmol) and imidazole C (500mg, 2.69 mmol) were combined in a Schlenk tube with THF (25 ml) and heated to reflux for 7 days. After cooling to room temperature, the mixture was filtered and the precipitate washed with one portion of THF (10 ml), diethyl ether (2 × 10 ml) and dried *in vacuo*. The salt was recrystallised from dichloromethane/diethyl ether to give the product as a hygroscopic white solid. Yield: 265 mg, (24%). ¹H NMR (d⁶ DMSO, 400 MHz, 298 K): δ (ppm) 9.73 (1H, s, NCHN), 8.15 (2H, m, NCHCHN), 7.72 (2H, m, *meta*-CH), 7.64 (1H, m, *para*-CH), 7.47 (2H, m, *ortho*-CH), 7.16 (2H, s, Mes-CH), 2.34 (3H, s, *para*-CH₃), 2.12 (6H, s, *ortho*-CH₃), 1.89 (6H, s, NC(CH₃)₂). ¹³C {¹H} NMR (d⁶ DMSO, 400 MHz, 298 K): δ (ppm) 198.2 (s, C=O), 137.2 (NCN), 140.4, 134.3, 134.2, 133.1, 131.1, 129.2, 128.8, 128.2 (C₆H₅, C₆H₂), 124.3, 122.5 (NCCN), 69.9 (NC(CH₃)₂), 25.6 (NC(CH₃)₂), 20.6 (*para*-CH₃), 16.8 (*ortho*-CH₃). HRMS (ES) (MeCN): found 333.2037 (C₂₂H₂₅N₂O⁺ requires 333.2043 dev: -1.8 ppm).

1-(Diisopropylphenyl)-3-(2-isobutyrophenone)imidazol-2-ium bromide (6)

2-bromoisobutyrophenone (0.44 ml, 2.63 mmol) and imidazole D (500 mg, 2.19 mmol) were combined in a Schlenk tube with THF (25 ml) and heated to reflux for 7 days. After cooling to room temperature, the mixture was filtered and the precipitate washed with one portion of

THF (10 ml), diethyl ether (2 × 10 ml) and dried *in vacuo*. The salt was recrystallised from dichloromethane/diethyl ether to give the product as a hygroscopic white solid. Yield: 220 mg (22%). ¹H NMR (d⁶ DMSO, 400 MHz, 298 K): δ (ppm) 9.13 (1H, s, NCHN), 7.96 (2H, d, NCHCHN, ³J_{HH} = 7.39 Hz), 7.56 (2H, m, *meta*-CH), 7.41 (1H, m, *para*-CH), 7.32 (2H, m, *ortho*-CH), 7.27 (1H, m, *Mes*-CH), 7.19 (2H, m, *Mes*-CH), 2.13 (2H, sept, CH(CH₃)₂, ³J_{HH} = 6.73 Hz), 1.86 (6H, d, CH(CH₃)₂, ³J_{HH} = 6.76 Hz), 1.72 (6H, d, CH(CH₃)₂, ³J_{HH} = 6.74 Hz), 1.63 (6H, s, NC(CH₃)₂). ¹³C {¹H} NMR (d⁶ DMSO, 101 MHz, 298 K): δ (ppm) 194.2 (C=O), 143.2 (NCN), 137.5, 135.8, 134.1, 132.3, 131.9, 129.8, 129.1, 128.0 (C₆H₅, C₆H₃), 124.8, 123.1 (s, NCHCHN), 68.3 (s, NC(CH₃)₂), 31.2 (s, CH(CH₃)₂), 25.1 (s, NC(CH₃)₂), 23.7 (s, CH(CH₃)₂). HRMS (ES) (MeCN): found 375.1252 (C₂₅H₃₁N₂O⁺ requires 375.1257 dev: -1.3 ppm).

1-Isopropyl-3-(phenylpropylidenebenzenamine)imidazol-2-ium bromide (8)

2-bromopropane (0.4 ml, 4.15 mmol) and imidazole E (1.0 g, 3.46 mmol) were combined in a Schlenk tube with dichloromethane (20 ml) and heated to reflux for 3 days. After cooling to room temperature, the solvent was removed, and the residue washed with diethyl ether (2×10ml) and dried *in vacuo*. The salt was recrystallised from dichloromethane/diethyl ether to give the product as a hygroscopic yellow solid. Yield: 0.83 g (58%). ¹H NMR (d⁶ DMSO, 400 MHz, 298 K): δ (ppm) 9.31 (1H, s, NCHN), 7.12-6.39 (12H, m, C₆H₅, NCHCHN), 4.51, (1H, sept, NCH(CH₃)₂, ³J_{HH} = 6.70 Hz), 1.84 (6H, d, NCH(CH₃)₂, ³J_{HH} = 6.69 Hz), 1.51 (6H, s, NC(CH₃)₂). ¹³C {¹H} NMR (d⁶ DMSO, 101 MHz, 298 K): δ (ppm) 171.8 (s, C=N), 149.5, 138.5, 133.8, 129.7, 128.9, 127.9, 124.0, 120.4 (C₆H₅), 119.9, 118.9 (NCHCHN), 68.7 (s, NC(CH₃)₂), 52.3 (s, NCH(CH₃)₂), 27.6 NCH(CH₃)₂, 27.1 (s, NC(CH₃)₂). HRMS (ES) (MeCN): found 332.2149 (C₂₂H₂₆N₃⁺ requires 332.2156 dev: -2.1 ppm).

1-Isopropyl-3-(2-methoxy-5-methylphenyl)imidazole-2-ium bromide (9)

2-bromopropane (0.6 ml, 6.38 mmol) and imidazole F (1.0 g, 5.32 mmol) were combined in a Schlenk tube with THF (20 ml) and heated to reflux for 5 days. After cooling to room temperature, the mixture was filtered and the precipitate washed with one portion of THF (10 ml), diethyl ether (2 × 10 ml) and dried *in vacuo*. The salt was recrystallised from dichloromethane/diethyl ether to give the product as a hygroscopic white solid. Yield: 0.97 g (59%). ¹H NMR (d⁶ DMSO, 400 MHz, 298 K): δ (ppm) 9.59 (1H, s, NCHN), 8.10 (2H, m, NCHCHN), 7.48 (1H, s, *ortho*-CH), 7.41 (1H, d, *meta*-CH, ³J_{HH} = 8.49 Hz), 7.27 (1H, d,

para-CH, $^3J_{\text{HH}} = 8.51$ Hz), 4.72 (1H, sept, NCH(CH₃)₂, $^3J_{\text{HH}} = 6.62$ Hz), 3.85 (3H, s, O-CH₃), 2.33 (3H, s, *meta*-CH₃), 1.54 (6H, d, CH(CH₃)₂, $^3J_{\text{HH}} = 6.66$ Hz). ¹³C {¹H} NMR (d⁶ DMSO, 101 MHz, 298 K): δ (ppm) 151.3 (C-OMe), 136.9 (NCN), 132.4, 132.0, 126.6, 119.2, 113.0 (C₆H₃), 123.7, 123.4 (NCCN), 57.2 (O-CH₃), 56.7 (NCH(CH₃)₂), 23.3 (*meta*-CCH₃), 20.4 (CH(CH₃)₂). IR (CH₂Cl₂): ν = 1026 (s) (COC) cm⁻¹; HRMS (ES) (MeCN): found 231.1506 (C₁₄H₁₉N₂O⁺ requires 231.1512 dev: -2.6 ppm).

General procedure for the formation of free carbenes. All manipulations for the preparation of the free carbenes were performed using standard Schlenk techniques under an atmosphere of argon. To a suspension of imidazolium salt (1.0 mmol) in THF (10 ml) at -10°C, KN(SiMe₃)₂ (1.2 mmol) was added and the mixture stirred for 30 min. All volatiles were then removed *in vacuo*, the residue extracted with THF (2 × 10 ml) and the solvent removed to leave the product as a solid.

1-Methyl-3-(2-isobutyrophenone)imidazol-2-ylidene (10)

Yield: 166 mg (73%). ¹H NMR (THF, 500 MHz, 298 K): δ (ppm) 7.65 (2H, d, NCHCHN, $^3J_{\text{HH}} = 7.54$ Hz), 7.43 (1H, m, *para*-CH), 7.26 (2H, m, *meta*-CH), 6.95 (2H, m, *ortho*-CH), 3.84 (3H, s, N-CH₃), 1.86 (6H, s, NC(CH₃)₂). ¹³C {¹H} NMR (THF, 125 MHz, 298 K): δ (ppm) 213.8 (NCN), 197.0 (C=O), 134.6 (*ipso*-C), 130.4 (*para*-CH), 128.3 (*ortho*-CH), 126.6 (*meta*-CH), 119.2, 115.8 (NCCN), 36.2 (N-CH₃), 26.3 (C(CH₃)₂), 13.7 (C(CH₃)₂).

1-Isopropyl-3-(2-isobutyrophenone)imidazol-2-ylidene (11)

Yield: 200 mg (78%). ¹H NMR (THF, 500 MHz, 298 K): δ (ppm) 7.64 (2H, d, NCHCHN, $^3J_{\text{HH}} = 7.29$ Hz), 7.43 (3H, m, *meta*- and *para*-CH), 7.28 (2H, m, *ortho*-CH), 4.54 (1H, sept, N-CH(CH₃)₂, $^3J_{\text{HH}} = 6.72$ Hz), 1.92 (6H, s, N-C(CH₃)₂), 1.48 (6H, d, N-CH(CH₃)₂, $^3J_{\text{HH}} = 6.73$ Hz). ¹³C {¹H} NMR (THF, 125 MHz, 298 K): δ (ppm) 210.9 (NCN), 196.5 (C=O), 133.9 (*ipso*-C), 129.7 (*para*-CH), 127.5 (*ortho*-CH), 125.8 (*meta*-CH), 115.8, 114.6 (NCHCHN), 63.5 (NC(CH₃)₂), 50.2 (NCH(CH₃)₂), 25.5 (NC(CH₃)₂), 12.8 (NCH(CH₃)₂).

1-Tertiarybutyl-3-(2-isobutyrophenone)imidazol-2-ylidene (12)

Yield: 185 mg (67%). ¹H NMR (THF, 500 MHz, 298 K): δ (ppm) 7.71 (2H, d, NCHCHN, $^3J_{\text{HH}} = 8.24$ Hz), 7.37 (3H, m, *meta*- and *para*-CH), 7.16 (2H, m, *ortho*-CH), 1.96 (6H, s, NC(CH₃)₂), 1.88 (9H, s, NC(CH₃)₃). ¹³C {¹H} NMR (THF, 125 MHz, 298 K): δ (ppm) 211.7

(s, NCN), 196.5 (C=O), 134.1, 129.3, 127.3, 125.6 (C₆H₅), 114.3, 114.2 (NCCN), 53.8 (NC(CH₃)₂), 48.8 (NC(CH₃)₃), 25.3 (NC(CH₃)₃), 12.8 (NC(CH₃)₂).

1,3-Di-(2-isobutyrophenone)imidazol-2-ylidene (13)

Yield: 276 mg (76%). ¹H NMR (THF, 400 MHz, 298 K): δ (ppm) 7.73 (2H, s, NCHCHN), 7.63 (10H, m, C₆H₅), 1.69 (12H, s, C(CH₃)₂). ¹³C {¹H} NMR (d⁶ DMSO, 101 MHz, 298 K): δ (ppm) 213.1 (NCN), 195.5 (C=O), 132.3, 131.2, 128.4, 128.0 (C₆H₅), 117.6 (NCCN), 66.2 (NC(CH₃)₂), 19.9 (NC(CH₃)₂).

1-Mesityl-3-(2-isobutyrophenone)imidazol-2-ylidene (14)

Yield: 218 mg (66%). ¹H NMR (THF, 400 MHz, 298 K): δ (ppm) 8.09 (2H, m, NCHCHN), 7.66 (1H, m, *para*-CH), 7.65 (2H, m, *meta*-CH), 7.32 (2H, m, *ortho*-CH), 7.08 (2H, s, Mesityl-CH), 2.31 (3H, s, *para*-CH₃), 2.10 (6H, s, *ortho*-CH₃), 1.73 (6H, s, NC(CH₃)₂). ¹³C {¹H} NMR (THF, 101 MHz, 298 K): δ (ppm) 212.6 (NCN), 196.5 (C=O), 138.2, 132.2, 132.0, 131.5, 129.2, 128.8, 128.0, 127.4 (C₆H₅, C₆H₂), 118.7, 115.3 (NCCN), 67.3 (NC(CH₃)₂), 23.8 (NC(CH₃)₂), 18.3 (*para*-CH₃), 14.8 (*ortho*-CH₃).

1-(Diisopropylphenyl)-3-(2-isobutyrophenone)imidazol-2-ylidene (15)

Yield: 235 mg (63%). ¹H NMR (THF, 400 MHz, 298 K): δ (ppm) 7.81 (2H, d, NCHCHN, ³J_{HH} = 7.28 Hz), 7.42-6.91 (8H, m, C₆H₅, C₆H₃), 2.01 (2H, sept, CH(CH₃)₂, ³J_{HH} = 6.70 Hz), 1.59 (6H, d, CH(CH₃)₂, ³J_{HH} = 6.72 Hz), 1.42 (6H, d, CH(CH₃)₂, ³J_{HH} = 6.69 Hz), 1.31 (6H, s, NC(CH₃)₂). ¹³C {¹H} NMR (THF, 101 MHz, 298 K): δ (ppm) 215.2 (NCN), 192.9 (C=O), 135.0, 134.4, 133.5, 131.4, 130.1, 128.70, 128.2, 127.4 (C₆H₅, C₆H₃), 119.6, 117.5 (NCHCHN), 65.3 (s, NC(CH₃)₂), 27.6 (s, CH(CH₃)₂), 24.3 (s, NC(CH₃)₂), 19.2 (s, CH(CH₃)₂).

1-Isopropyl-3-(phenylpropylidenebenzenamine)imidazol-2-ylidene (17)

Yield: 215 mg (65%). ¹H NMR (THF, 400 MHz, 298 K): δ (ppm) 7.03-6.31 (12H, m, C₆H₅, NCHCHN), 4.12 (1H, sept, NCH(CH₃)₂, ³J_{HH} = 6.71 Hz), 1.62 (6H, d, NCH(CH₃)₂, ³J_{HH} = 6.71 Hz), 1.38 (6H, s, NC(CH₃)₂). ¹³C {¹H} NMR (THF, 101 MHz, 298 K): δ (ppm) 215.1 (NCN), 173.4 (C=N), 147.6, 136.6, 131.7, 128.3, 127.8, 126.9, 123.1, 121.7 (C₆H₅),

117.8, 117.1 (NCHCHN), 67.8 (s, NC(CH₃)₂), 50.8 (s, NCH(CH₃)₂), 25.2 NCH(CH₃)₂), 25.1 (s, NC(CH₃)₂).

1-Isopropyl-3-(2-methoxy-5-methylphenyl)imidazole-2-ylidene (18)

Yield: 167 mg (73%). ¹H NMR (THF, 500 MHz, 298 K): δ (ppm) 7.89 (2H, d, NCHCHN, ³J_{HH} = 7.42 Hz), 7.45 (1H, s, *ortho*-CH), 7.31 (2H, m, *meta*- and *para*-CH), 4.65 (1H, sept, NCH(CH₃)₂ ³J_{HH} = 6.74 Hz), 3.79 (3H, s, O-CH₃), 2.18 (3H, s, *meta*-CH₃), 1.69 (6H, d, CH(CH₃)₂, ³J_{HH} = 6.79 Hz). ¹³C {¹H} NMR (THF, 125 MHz, 298 K): δ (ppm) 212.8 (NCN), 150.2 (C-OMe), 133.1, 131.7, 128.4, 123.2, 122.0 (C₆H₃), 120.8, 119.5 (NCCN), 55.7 (s, O-CH₃), 52.3 (s, NCH(CH₃)₂), 21.3 (s, *meta*-CCH₃), 15.9 (s, CH(CH₃)₂).

General procedure for the formation of silver(I) complexes. Dichloromethane (20 ml) was added to a round bottom flask containing Ag₂O (1 mmol) and the imidazolium salt (1.5 mmol). The mixture was stirred for 16 hours, followed by filtration (through celite) and removal of the solvent. The residue was washed, diethyl ether (2 × 10 ml), recrystallised from a dichloromethane/diethyl ether mixture and dried *in vacuo*.

[Ag(NHC)₂] (NHC=1-Methyl-3-(2-isobutyrophenone)imidazol-2-ylidene) (19)

Yield: 390 mg (69%). ¹H NMR (d⁶ DMSO, 400 MHz, 298 K): δ (ppm) 7.94 (4H, d, NCHCHN, ³J_{HH} = 7.48 Hz), 7.67 (2H, m, *para*-CH), 7.42-7.28 (8H, m, *ortho*- and *meta*-CH), 3.75 (6H, s, N-CH₃), 1.89 (12H, s, NC(CH₃)₂). ¹³C {¹H} NMR (d⁶ DMSO, 101 MHz, 298 K): δ (ppm) 197.9 (C=O), 133.0, 129.2, 128.7, 126.8 (C₆H₅), 122.9, 119.7 (NCCN), 67.1 (NC(CH₃)₂), 54.9 (N-CH₃), 28.0 (NC(CH₃)₂). HRMS (ES) (MeCN): found 563.1212 (C₂₈H₃₄N₄O₂Ag⁺ requires 563.1209 dev: 5.3 ppm).

[Ag(NHC)Br] (NHC=1-Isopropyl-3-(2-isobutyrophenone)imidazol-2-ylidene) (20)

Yield: 300 mg (67%). ¹H NMR (d⁶ DMSO, 400 MHz, 298 K): δ (ppm) 8.15-7.41 (7H, m, C₆H₅, NCHCHN), 4.41 (1H, sept, NCH(CH₃)₂, ³J_{HH} = 6.71 Hz), 1.93 (6H, s, NC(CH₃)₂), 1.36 (6H, d, NCH(CH₃)₂, ³J_{HH} = 6.67 Hz). ¹³C {¹H} NMR (d⁶ DMSO, 101 MHz, 298 K): δ (ppm) 198.5 (C=O), 130.2, 128.6, 128.2, 120.2 (C₆H₅), 119.4, 118.3 (NCCN), 67.5 (NC(CH₃)₂), 54.7 (NCH(CH₃)₂), 27.9 (NCH(CH₃)₂), 22.7 (NC(CH₃)₂). HRMS (ES) (MeCN): found 404.0872 (C₁₈H₂₄N₃OAg⁺ requires 404.0870 dev: 4.95 ppm).

[Ag(NHC)Br] (NHC=1-Tertiarybutyl-3-(2-isobutyrophenone)imidazol-2-ylidene) (21)

Yield: 325 mg (71%). ^1H NMR (d^6 DMSO, 400 MHz, 298 K): δ (ppm) 8.18-8.07 (7H, m, C_6H_5 , NCHCHN), 2.00 (6H, s, $\text{NC}(\text{CH}_3)_2$), 1.64 (9H, s, $\text{NC}(\text{CH}_3)_3$). ^{13}C $\{^1\text{H}\}$ NMR (d^6 DMSO, 101 MHz, 298 K): δ (ppm) 198.9 (C=O), 134.9, 132.8, 128.9, 127.9 (C_6H_5), 119.4, 118.2 (NCCN), 69.4 ($\text{NC}(\text{CH}_3)_2$), 67.8 ($\text{NC}(\text{CH}_3)_3$), 28.2 ($\text{NC}(\text{CH}_3)_3$), 25.6 ($\text{NC}(\text{CH}_3)_2$). HRMS (ES) (MeCN): found 418.0825 ($\text{C}_{19}\text{H}_{26}\text{N}_3\text{OAg}^+$ requires 418.0823 dev: 4.78 ppm).

[Ag(NHC)Br] (NHC=1,3-Di-(2-isobutyrophenone)imidazol-2-ylidene) (22)

Yield: 360 mg (66%). ^1H NMR (d^6 DMSO, 400 MHz, 298 K): δ (ppm) 7.92 (2H, s, NCHCHN), 7.38 (10H, m, C_6H_5), 1.86 (12H, s, $\text{NC}(\text{CH}_3)_2$). ^{13}C $\{^1\text{H}\}$ NMR (d^6 DMSO, 101 MHz, 298 K): δ (ppm) 199.2 (C=O), 135.6, 132.2, 129.1, 128.4 (C_6H_5), 118.9 (NCCN), 64.9 ($\text{NC}(\text{CH}_3)_2$), 26.6 ($\text{NC}(\text{CH}_3)_2$). HRMS (ES) (MeCN): found 508.0621 ($\text{C}_{25}\text{H}_{28}\text{N}_3\text{O}_2\text{Ag}^+$ requires 508.0624 dev: -5.9 ppm).

[Ag(NHC)Br] (NHC=1-Mesityl-3-(2-isobutyrophenone)imidazol-2-ylidene) (23)

Yield: 300 mg (58%). ^1H NMR (CD_2Cl_2 , 400 MHz, 298 K): δ (ppm) 8.28 (2H, m, NCHCHN), 7.73-7.24 (7H, m, C_6H_5 , C_6H_2), 2.54 (3H, s, *para*- CH_3), 2.15 (6H, s, *ortho*- CH_3), 1.94 (6H, s, $\text{NC}(\text{CH}_3)_2$). ^{13}C $\{^1\text{H}\}$ NMR (CD_2Cl_2 , 101 MHz, 298 K): δ (ppm) 198.0 (C=O), 140.2, 135.7, 133.1, 132.8, 130.9, 129.6, 129.3, 128.5 (C_6H_5 , C_6H_2), 120.4, 119.7 (s, NCCN), 69.1 (s, $\text{NC}(\text{CH}_3)_2$), 26.8 (s, $\text{NC}(\text{CH}_3)_2$), 21.4 (s, *para*- CH_3), 19.4 (s, *ortho*- CH_3). HRMS (ES) (MeCN): found 480.1279 ($\text{C}_{24}\text{H}_{28}\text{N}_3\text{OAg}^+$ requires 480.1281 dev: -4.2 ppm).

[Ag(NHC)Br] (NHC=1-(Diisopropylphenyl)-3-(2-isobutyrophenone)imidazol-2-ylidene) (24)

Yield: 365 mg (65%). ^1H NMR (CD_2Cl_2 , 400 MHz, 298 K): δ (ppm) 7.82 (2H, d, NCHCHN, $^3J_{\text{HH}} = 7.31$ Hz), 7.73-7.28 (8H, m, C_6H_5 , C_6H_3), 2.35 (2H, sept, $\text{CH}(\text{CH}_3)_2$, $^3J_{\text{HH}} = 6.72$ Hz), 1.67 (6H, d, $\text{CH}(\text{CH}_3)_2$, $^3J_{\text{HH}} = 6.73$ Hz), 1.50 (6H, d, $\text{CH}(\text{CH}_3)_2$, $^3J_{\text{HH}} = 6.75$ Hz), 1.42 (6H, s, $\text{NC}(\text{CH}_3)_2$). ^{13}C $\{^1\text{H}\}$ NMR (CD_2Cl_2 , 101 MHz, 298 K): δ (ppm) 195.4 (C=O), 138.3, 136.6, 134.2, 133.9, 132.1, 130.7, 129.6, 129.1 (C_6H_5 , C_6H_3), 123.7, 122.1 (NCHCHN), 69.6 (s, $\text{NC}(\text{CH}_3)_2$), 30.3 (s, $\text{CH}(\text{CH}_3)_2$), 27.7 (s, $\text{NC}(\text{CH}_3)_2$), 24.1 (s, $\text{CH}(\text{CH}_3)_2$). HRMS (ES) (MeCN): found 522.1760 ($\text{C}_{27}\text{H}_{34}\text{N}_3\text{OAg}^+$ requires 522.1758 dev: 3.8 ppm).

[Ag(NHC)₂] (NHC=1-Methyl-3-(phenylpropylidenebenzenamine)imidazol-2-ylidene) (25)

Yield: 520 mg (73%). ¹H NMR (CD₂Cl₂, 400 MHz, 298 K): δ (ppm) 7.08-6.63 (24H, m, C₆H₅, NCHCHN), 3.84 (6H, s, N-CH₃), 1.95 (12H, s, NC(CH₃)₂). ¹³C {¹H} NMR (CD₂Cl₂, 101 MHz, 298 K): δ (ppm) 176.2 (C=N), 152.6, 140.50, 139.8, 133.9, 132.4, 131.9, 131.6, 130.3 (C₆H₅), 121.9, 120.3 (NCHCHN), 67.6 (NC(CH₃)₂), 41.3 (N-CH₃), 29.2 (NC(CH₃)₂). HRMS (ES) (MeCN): found 713.2489 (C₄₄H₅₂N₆Ag⁺ requires 713.2522 dev: -4.6 ppm).

[Ag(NHC)Br]**(NHC=1-Isopropyl-3-(phenylpropylidenebenzenamine)imidazole-2-ylidene) (26)**

Yield: 360 mg (68%). ¹H NMR (CD₂Cl₂, 400 MHz, 298 K): δ (ppm) 7.56-6.93 (12H, m, C₆H₅, NCHCHN), 4.43 (1H, sept, NCH(CH₃)₂, ³J_{HH} = 6.72 Hz), 1.89 (6H, d, NCH(CH₃)₂, ³J_{HH} = 6.69 Hz), 1.63 (6H, s, NC(CH₃)₂). ¹³C {¹H} NMR (CD₂Cl₂, 101 MHz, 298 K): δ (ppm) 175.9 (C=N), 149.8, 138.2, 136.5, 133.9, 133.1, 131.7, 130.3, 128.8 (C₆H₅), 120.9, 120.1 (NCHCHN), 69.2 (s, NC(CH₃)₂), 53.6 (s, NCH(CH₃)₂), 29.5 (NCH(CH₃)₂), 27.8 (s, NC(CH₃)₂). HRMS (ES) (MeCN): found 479.1342 (C₂₄H₂₉N₄Ag⁺ requires 479.1343 dev: -2.1 ppm).

[Ag(NHC)Br] (NHC=1-Isopropyl-3-(2-methoxy-5-methylphenyl)imidazole-2-ylidene) (27)

Yield: 270 mg (64%). ¹H NMR (CD₂Cl₂, 400 MHz, 298 K): δ (ppm) 7.92 (2H, d, NCHCHN, ³J_{HH} = 7.40 Hz), 7.45 (1H, d, *meta*-CH, ³J_{HH} = 8.31 Hz), 7.37 (1H, s, *ortho*-CH), 7.18 (1H, d, *para*-CH, ³J_{HH} = 8.23 Hz), 4.87 (1H, sept, NCH(CH₃)₂, ³J_{HH} = 6.71 Hz), 3.72 (3H, s, O-CH₃), 2.26 (3H, s, CH₃), 1.48 (6H, d, NCH(CH₃)₂, ³J_{HH} = 6.70 Hz). ¹³C {¹H} NMR (CD₂Cl₂, 101 MHz, 298 K): δ (ppm) 151.8 (C-OMe), 131.1, 129.1, 128.9, 128.4, 124.1 (C₆H₃) 122.9, 122.7 (NCCN), 56.3 (O-CH₃), 54.5 (NCH(CH₃)₂), 24.0 (CCH₃), 20.4 (NCH(CH₃)₂). HRMS (ES) (MeCN): found 377.1621 (C₁₆H₂₂N₃OAg⁺ requires 377.1619 dev: 3.5 ppm)

[Pd(NHC)₂Cl₂] (NHC=1-Isopropyl-3-(2-isobutyrophenone)imidazol-2-ylidene) (28)

To a suspension of **20** (300 mg, 0.675 mmol) in dichloromethane (10 ml), a solution of Pd(MeCN)₂Cl₂ (90 mg, 0.337 mmol) in dichloromethane (10 ml) was added, and the mixture heated to reflux for 16 h. After cooling to room temperature, the mixture was filtered through celite and the solvent removed *in vacuo*. Recrystallisation from dichloromethane/hexane, followed by washing with ethanol afforded a yellow solid. Yield (150 mg, 65%). ¹H NMR

(CD₂Cl₂, 500 MHz, 298 K): δ (ppm) 7.83 (2H, d, NCHCHN, $^3J_{\text{HH}} = 7.23$ Hz), 7.38-7.23 (5H, m, C₆H₅), 3.55 (1H, sept, NCH(CH₃)₂, $^3J_{\text{HH}} = 6.63$ Hz), 2.42 (6H, d, NCH(CH₃)₂, $^3J_{\text{HH}} = 6.65$ Hz), 1.48 (6H, s, NC(CH₃)₂). ¹³C {¹H} NMR (d⁶ DMSO, 101 MHz, 298 K): δ (ppm) 153.7 (NCN), 194.9 (C=O), 133.1, 130.3, 128.8, 128.2 (C₆H₅), 120.7, 119.5 (NCCN), 68.9 (NC(CH₃)₂), 39.1 (NCH(CH₃)₂), 29.0 (NCH(CH₃)₂), 23.5 (NC(CH₃)₂). HRMS (ES) (MeCN): found 361.1764 (C₁₆H₂₁N₂OPd⁺ requires 361.1766 dev: -5.5 ppm) [L-Pd]⁺.

2.5 References

- [1] Wang, H. M. J.; Lin, I. J. B. *Organometallics* **1998**, *17*, 972.
- [2] Arduengo, A. J.; Dias, H. V. R.; Calabrese, J. C.; Davidson, F. *Organometallics* **1993**, *12*, 3405.
- [3] Tulloch, A. A. D.; Danopoulos, A. A.; Winston, S.; Kleinhenz, S.; Eastham, G. *J. Chem. Soc. Dalton Trans.* **2000**, 4499.
- [4] (a) Guerret, O.; Solé, S.; Gornitzka, H.; Trinquier, G.; Bertrand, G.; *J. Organomet. Chem.* **2000**, *600*, 112. (b) Guerret, O.; Solé, S.; Gornitzka, H.; Teichert, M.; Trinquier, G.; Bertrand, G. *J. Am. Chem. Soc.* **1997**, *119*, 6668.
- [5] Lin, I. J. B.; Vasam, C. S. *Coord. Chem. Rev.* **2007**, *251*, 642.
- [6] Lee, K. M.; Wang, H. M. J.; Lin, I. J. B. *J. Chem. Soc. Dalton Trans.* **2002**, 2852.
- [7] Catalano, V. J.; Malwitz, M. A. *Inorg. Chem.* **2003**, *42*, 5483.
- [8] Nielsen, D. J.; Cavell, K. J.; Viciu, M. S.; Nolan, S. P.; Skelton, B. W.; White, A. H. *J. Organomet. Chem.* **2005**, *690*, 6133.
- [9] (a) Arduengo, A. J., III; Dias, H. V. R.; Calabrese, J. C.; Davidson, F. *Organometallics* **1993**, *12*, 3405. (b) Fox, M. A.; Mahon, M. F.; Patmore, N. J.; Weller, A. S. *Inorg. Chem.* **2002**, *41*, 4567. (c) Hu, X.; Tang, Y.; Gantzel, P.; Meyer, K. *Organometallics* **2003**, *22*, 612. (d) Kascatan-Nebioglu, A.; Panzner, M. J.; Garrison, J. C.; Tessier, C. A.; Youngs, W. J. *Organometallics* **2004**, *23*, 1928.
- [10] Wang, J.-W.; Song, H.-B.; Li, Q.-S.; Xu, F.-B.; Zhang, Z.-Z. *Inorg. Chim. Acta* **2005**, *358*, 3653.

- [11] Cotton, F. A.; Wilkinson, G.; Murillo, C. A.; Bochmann, M. *Advanced Inorganic Chemistry*, 6th ed., Wiley, New York, **1999**.
- [12] Nielsen, D. J.; Cavell, K. J.; Skelton, B. W.; White, A. H. *Inorg. Chim. Acta* **2002**, *327*, 116.
- [13] César, V.; Bellemin-Lapponnaz, S.; Gade, L. H. *Organometallics* **2002**, *21*, 5204.
- [14] Simons, R. S.; Custer, P.; Tessier, C. A.; Youngs, W. J. *Organometallics* **2003**, *22*, 1979.
- [15] Garrison, J. C.; Simons, R. S.; Talley, J. M.; Wesdemiotis, C.; Tessier, C. A.; Youngs, W. J. *Organometallics* **2001**, *20*, 1276.
- [16] Caballero, A.; Diez-Barra, E.; Jalon, F. A.; Merino, S.; Rodriguez, A. M.; Tejada, J. J. *Organomet. Chem.* **2001**, *627*, 263.
- [17] Lansdown, A. B. G. *Br. J. Nurs.* **2004**, *13*, S6.
- [18] (a) Melaiye, A.; Simons, R. S.; Milsted, A.; Pingitore, F.; Wesdemiotis, C.; Tessier, C. A.; Youngs, W. J. *J. Med. Chem.* **2004**, *47*, 973. (b) Kascatan-Nebioglu, A.; Melaiye, A.; Hindi, K.; Durmus, S.; Panzner, M.; Milsted, A.; Ely, D.; Tessier, C. A.; Hogue, L. A.; Mallett, R. J.; Hovis, C. E.; Coughenour, M.; Crosby, S. D.; Cannon, C. L.; Youngs, W. J. *J. Med. Chem.* **2006**, *49*, 6811. (c) Garrison, J. C.; Tessier, C. A.; Youngs, W. J. *J. Organomet. Chem.* **2005**, *690*, 6008.
- [19] Kascatan-Nebioglu, A.; Panzner, M. J.; Tessier, C. A.; Cannon, C. L.; Youngs, W. J. *Coord. Chem. Rev.* **2007**, *251*, 884.
- [20] Herrmann, W. A.; Köcher, C.; Gooßen, L. J.; Artus, G. R. J. *Chem. Eur. J.* **1996**, *2*, 1627.
- [21] Normand, A.; Cavell, K. J. *Eur. J. Inorg. Chem.* **2008**, 2781.

- [22] (a) Herrmann, W. A. *Angew. Chem. Int. Ed.* **2002**, *41*, 1290. (b) Whitcombe, N. J.; Hii, K. K.; Gibson, S. E. *Tetrahedron* **2001**, *57*, 7449. (c) Littke, A. F.; Fu, G. C. *Angew. Chem. Int. Ed.* **2002**, *41*, 4176.
- [23] Hahn, F. E.; Jahnke, M. C. *Angew. Chem. Int. Ed.* **2008**, *47*, 3122 and references therein.
- [24] (a) Enders, D.; Gielen, H. J. *J. Organomet. Chem.* **2001**, *617*, 70. (b) McGuinness, D. S.; Cavell, K. J. *Organometallics* **2000**, *19*, 741. (c) Herrmann, W. A.; Elison, M.; Fischer, J.; Köcher, C.; Artus, G. R. J. *Angew. Chem. Int. Ed. Engl.* **1995**, *34*, 2371. (d) Tulloch, A. A. D.; Danopoulos, A. A.; Tooze, R. P.; Cafferkey, S. M.; Kleinhenz, S.; Hursthouse, M. B. *Chem. Commun.* **2000**, 1247. (e) Magill, A. M.; McGuinness, D. S.; Cavell, K. J.; Britovsek, G. J. P.; Gibson, V. C.; White, A. J. P.; Williams, D. J.; White A. H.; Skelton, B. W. *J. Organomet. Chem.* **2001**, *617*, 546. (f) Chen, J. C. C.; Lin, I. J. B. *Organometallics* **2000**, *19*, 5113. (g) Tulloch, A. A. D.; Danopoulos, A. A.; Kleinhenz, S.; Light, M. E.; Hursthouse, M. B.; Eastham, G. *Organometallics* **2001**, *20*, 2027. (h) Herrmann, W. A.; Gooßen, L. J.; Spiegler, M. *J. Organomet. Chem.* **1997**, *547*, 357. (i) Herrmann, W. A.; Gooßen, L. J.; Spiegler, M. *Organometallics* **1998**, *17*, 2162.
- [25] Steiner, G.; Kopacka, H.; Ongania, K. H.; Wurst, K.; Preishuber-Pflügl, P.; Bildstein, B. *Eur. J. Inorg. Chem.* **2005**, 1325.
- [26] Liu, S. T.; Lee, C. I.; Fu, C. F.; Chen, C. H.; Lui, Y. H.; Elsevier, C. J.; Peng, S. M.; Chen, J. T. *Organometallics* **2009**, *28*, 6957.
- [27] (a) Froseth, M.; Dhindsa, A.; Roise, H.; Tilset, M. *Dalton Trans.* **2003**, 4516. (b) Coleman, K. S.; Chamberlayne, H. T.; Turberville, S.; Green, M. L. H.; Cowley, A. R. *Dalton Trans.* **2003**, 2917.
- [28] Arduengo, A. J. III; Gamper, S. F.; Tamm, M.; Calabrese, J. C.; Davidson, F.; Craig, H. A. *J. Am. Chem. Soc.* **1995**, *117*, 572.
- [29] Füstner, A.; Alcarazo, M.; César, V.; Lehmann, C. W. *Chem. Commun.* **2006**, 2176.

- [30] Lui, J.; Chen, J.; Zhao, Y.; Li, L.; Zhang, H. *Synthesis* **2003**, *17*, 2661.
- [31] (a) Tang, B. X.; Guo, S. M.; Zhang, M. B. *Synthesis* **2008**, *11*, 1707. (b) Altman, R. A.; Koval, E. D.; Buchwald, S. L. *J. Organic Chemistry* **2007**, *16*, 6190. (c) Alcalde, E.; Dinares, I.; Rodriguez, S.; Garcia de Miguel, C. *European Journal of Organic Chemistry* **2005**, *8*, 1637.
- [32] Froseth, M.; Netland, K. A.; Törnroos, K. W.; Dhindsa, A.; Tilset, M. *Dalton Trans.* **2005**, 1664.
- [33] Tilset, M.; Andell, O.; Dhindsa, A.; Froseth, M. WO 0249758A1, **2002**.
- [34] Andersh, B.; Murphy, D. L.; Olson, R. J. *Synth. Commun.* **2000**, *30*, 2091.
- [35] Pratt, D. A.; Pesavento, R. P.; van der Donk, W. A. *Organic Letters* **2005**, *13*, 2735.
- [36] (a) Garisson, J. C.; Youngs, W. J. *Chem. Rev.* **2005**, *105*, 3978. (b) de Fremont, P.; Scott, N. M.; Stevens, E. D.; Ramnial, T.; Lightbody, O. C.; Macdonald, C. L. B.; Clyburne, J. A. C.; Abernethy, C. D.; Nolan, S. P. *Organometallics* **2005**, *24*, 6301.
- [37] Lee, C. K.; Lee, K. M.; Lin, I. J. B. *Organometallics* **2002**, *21*, 10.
- [38] Newman, C. P.; Clarkson, G. J.; Rourke, J. P. *J. Organomet. Chem.* **2007**, *692*, 4962.
- [39] Compounds **20** and **28** were prepared as part of Jay Dusford's BSc project.

Chapter Three

Preparation and EPR Analysis of Chromium(I) bis(phosphine) Complexes

Chapter Three

Preparation and EPR Analysis of Cr(I) bis(phosphine) Complexes

3.1 Introduction

Complexes of chromium in oxidation state +1 are relatively rare due to the instability of the systems. However, interest in these types of complexes, particularly those containing bis(phosphine) ligands, has been sparked due to their postulated role in catalysis, specifically the selective oligomerisation of ethylene.

In this chapter the role of chromium(I) compounds in catalysis is discussed. The crucial use of EPR spectroscopy in analysing such paramagnetic systems is reported, and the preparation and EPR analysis of a series of new Cr(I) complexes will also be described.

The work described in this chapter was carried out in order to gain valuable experience in the synthesis, characterisation and EPR analysis of sensitive chromium(I) complexes. The ligands were provided by Sasol Technology, the sponsor of this work.

3.1.1 Role of Chromium(I) in the Ethylene Trimerisation Process

Given the interest in the selective oligomerisation of ethylene to produce 1-hexene and 1-octene, many catalyst systems¹⁻⁴ have been developed and tested over recent years as discussed in chapter 1. Much of the catalytic testing is carried out under *in situ* conditions in the presence of a co-catalyst, usually MAO, and therefore the identity of the active species is somewhat unclear. A significant proportion of the work carried out in this area has focussed on modifying ligand design to obtain catalysts capable of high activities as well as selectivities.⁵

Chromium complexes with a variety of ligands, including SNS,^{6,7} PNP,⁸ ONN,⁹ CNC¹⁰ and NNN^{11,12} donors have all been reported to show great potential in the selective trimerisation and/or tetramerisation of ethylene. A brief selection of these systems is shown in figure 3.1.

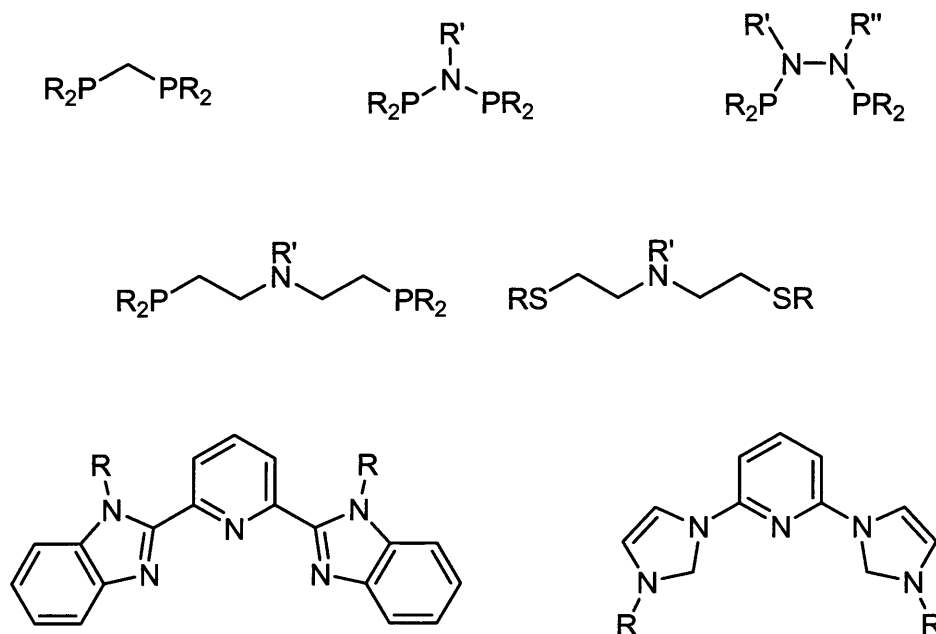


Figure 3.1 Various ligands used in ethylene trimerisation and tetramerisation.

The majority of catalytic systems studied in the literature are based on chelating bis(phosphine) ligands of the type shown in figure 3.1. This is due to the many proven advantages¹³ of phosphine ligands in catalysis, such as the ease of preparation and the ability to ‘fine-tune’ the ligands in order to modify the properties and produce a wide range of catalytic systems fairly quickly. As shown in figure 3.1, there is a large scope for modifying these ligands. For example the inclusion of electron withdrawing or donating groups, the presence of one or two linking nitrogen atoms in the backbone, as well as the differences arising from the use of alkyl, aryl or silyl substituents all result in there being a large number of reported systems with very different catalytic activities. It has been shown that subtle differences within the ligand system can cause very significant differences in catalytic performance, even changing the selectivity from trimerisation toward tetramerisation.^{4,5} Variations, such as the inclusion of a nitrogen atom in the backbone, the presence of pendant coordinating groups such as an *ortho* methoxy group acting as a hemi-labile donor, as well as increased steric bulk in the immediate vicinity of the metal centre, have all been shown to affect catalytic results, particularly selectivity.⁵

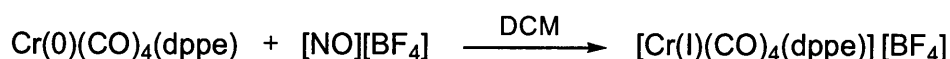
A number of mechanistic investigations have been carried out in order to gain more information about the precise nature of the active species responsible for the catalysis, and in particular the oxidation state of that species. Work carried out by Bercaw *et. al.*⁷ in 2004

provides significant evidence for a Cr(I)-Cr(III) metallocyclic mechanism. They carried out trimerisation experiments with a mixture of C₂H₄ and C₂D₄. Analysis of the products showed that no H/D scrambling had taken place, therefore ruling out a Cossee-Arlman type mechanism and providing support for the metallocyclic route. Work carried out by Sasol¹⁴ in 2005 provides further support for the metallocyclic mechanism for such PNP type ligand systems; the co-catalyst MAO is said to act upon the precursor to generate a cationic species as the catalytically active complex. This cationic species is generally believed to be the Cr(I) species.¹⁵

Cr(III) catalyst systems are generally inexpensive and more convenient in terms of preparation, which explains why a significant amount of research has focussed on the investigation of these systems and their catalytic activity. There is relatively little information available about Cr(I) compounds. This oxidation state is however, likely to be more important in terms of identifying and analysing the active species. Hence this chapter focuses on the synthesis and analysis of a series of Cr(I) compounds.

3.1.2 Background and Previous Work

As discussed in section 3.1, the number of existing publications on the synthesis of these types of cationic chromium(I) complexes is low, the majority of which contain carbonyl ligands for stabilisation. Carbonyl ligands are good π -acceptors, containing high energy antibonding orbitals which are able to stabilise the d_{π} orbital set on the metal centre, allowing the excess electron density on the metal centre to be distributed among the ligands. The incorporation of carbonyl ligands therefore allows low-valent metals to form more stable complexes. The extent of backbonding to the metal centre exhibited by carbonyls is lower in a 17-electron system when compared to a standard 18-electron complex.



Scheme 3.1 Preparation of chromium(I) phosphine system by Connelly.¹⁶

Some early work on the preparation of such cationic chromium(I) complexes was carried out by Connelly¹⁶ and co-workers in 1982, where an oxidising agent was used to prepare the cationic complex from neutral chromium(0) analogues (scheme 3.1). This is the standard method used for preparing these complexes, with differences only in the oxidising agent used. Common oxidising agents are shown in figure 3.2.

More recently, Wass *et. al.*¹⁷ and Sasol¹⁵ have prepared chromium(I) complexes for catalytic testing. It was concluded in both cases that the use of weakly coordinating anions is crucial for catalysis. Use of acetyl ferrocinium tetrafluoroborate (figure 3.2) as the oxidising agent resulted in inactive catalysts, whereas use of silver tetrakis(perfluoro-*tert*-butoxy)aluminate ($\text{Ag}[\text{Al}(\text{OC}(\text{CF}_3)_3)_4]$) gave the activities and selectivities expected from the PNP systems. The reasoning for this was that the tetrafluoroborate anion in the former case coordinates too strongly to the chromium centre.¹⁷

Of the oxidising agents described in figure 2, only $\text{Ag}[\text{Al}(\text{OC}(\text{CF}_3)_3)_4]$ and $[\text{NAr}_3][\text{B}(\text{C}_6\text{F}_5)_4]$ can be described as yielding very weakly coordinating anions. From a synthetic point of view, this is not a great consideration but given the catalytic implications, something that should be taken into account.

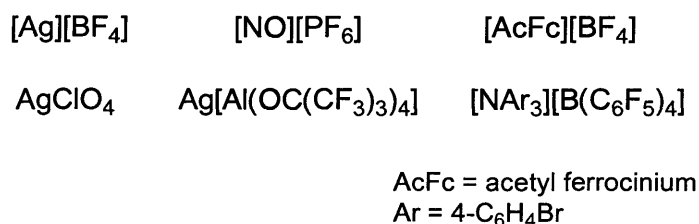
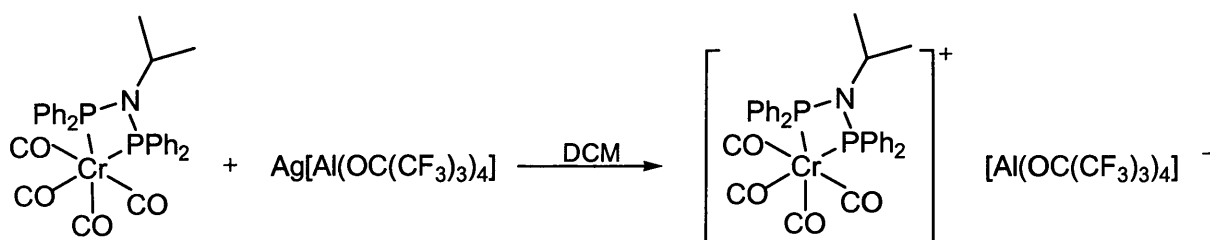


Figure 3.2 Oxidising agents.

In the tetramerisation process, a high MAO to chromium ratio is required. This is undesirable due to the high cost of MAO, so considerable research has taken place to find alternative co-catalysts that display similar catalytic selectivity and productivity. Triethylaluminium, AlEt_3 has been reported as a cheaper replacement for MAO when combined with an alkyl abstracting agent.¹⁸ Fluorinated borane co-catalysts such as $[\text{NAr}_3][\text{B}(\text{C}_6\text{F}_5)_4]$ in combination with AlEt_3 gives rise to active trimerisation and tetramerisation catalysts showing similar selectivities to when MAO is used. However, these catalysts have very short lifetimes due to fast exchange reactions between the borate anion and excess trialkylaluminium, resulting in rapid anion degradation.¹⁸

For this reason, the aluminate species reported by Krossing¹⁹ and used by Sasol¹⁵ is perhaps the best system for this purpose, as it is thought to be one of the most weakly coordinating anions known.²⁰ Much stronger interactions were reported between the chromium(I) cationic species with anions BF_4^- and PF_6^- than with $\text{Al}(\text{OC}(\text{CF}_3)_3)_4^-$.¹⁵ Additionally, studies have shown that catalysis with this aluminate along with AlEt_3 gives productivities and selectivities equivalent to those obtained when MAO is used, with no obvious shortening of catalyst lifetime.¹⁵



Scheme 3.2 Reported synthesis¹⁵ of $[\text{Cr}(\text{CO})_4(\text{Ph}_2\text{PN}(\text{iPr})\text{PPh}_2)]^+$.

During the oxidation from the Cr(0) precursor, one electron is abstracted by the silver resulting in a 17-electron chromium(I) system (scheme 3.2). A shift in the carbonyl stretching frequencies in the infra-red spectrum is observed on oxidation, with the cationic compound showing CO stretches at a higher wavenumber. The reduction in electron density available at the metal centre for backbonding to the carbonyl ligands results in a stronger C-O bond, as less electron density is taken into the antibonding CO orbitals. X-ray structures of both the chromium(0) and chromium(I) compounds have been reported^{15, 17} and are shown in figures 3.3 and 3.4.

The structure reported for the Cr(0) compound (figure 3) shows that, as expected, the Cr-CO bonds trans to the phosphine are slightly shorter than when trans to other carbonyl ligands, confirming the weaker trans-influence of the P-donor.¹⁷

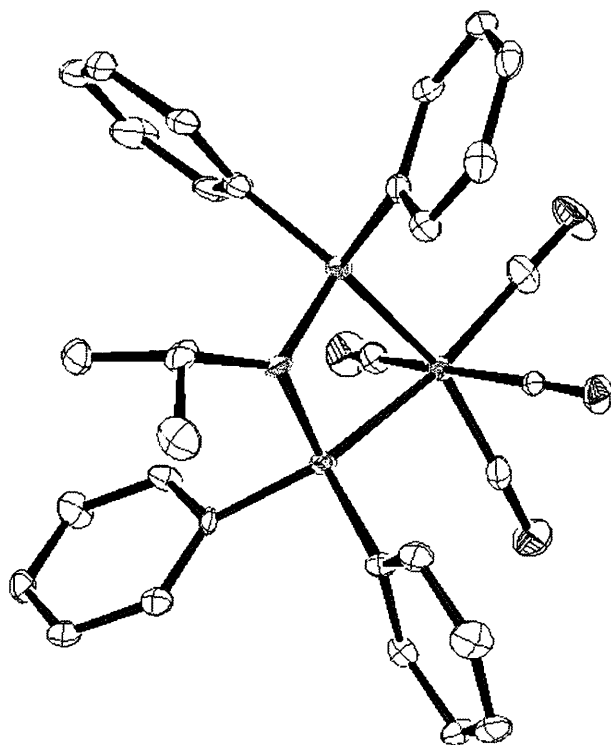


Figure 3.3 X-ray structure of $[\text{Cr}(0)(\text{CO})_4(\text{Ph}_2\text{PN}(\text{iPr})\text{PPh}_2)]$.¹⁷

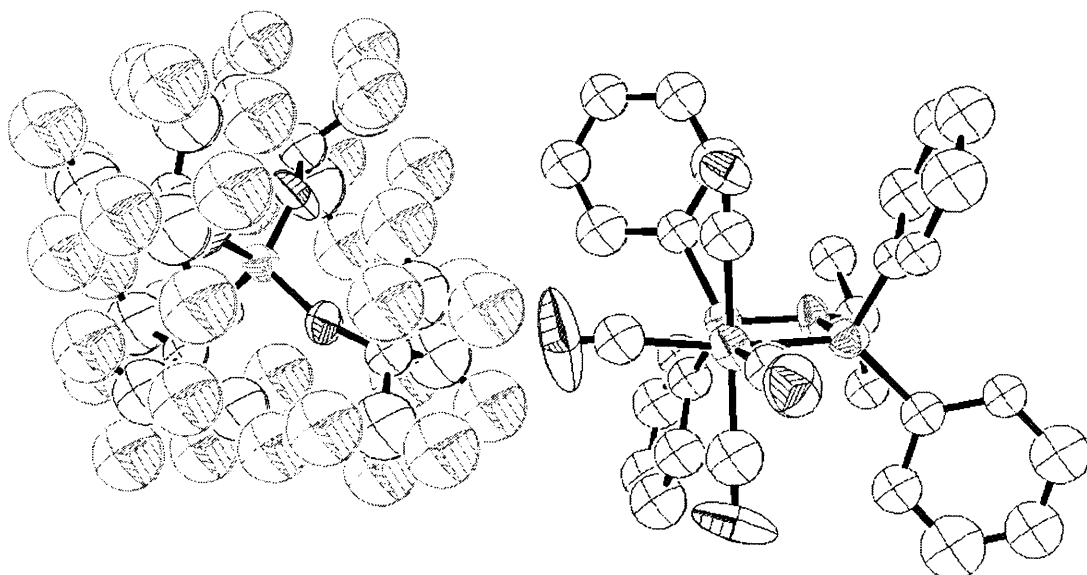


Figure 3.4 X-ray structure of $[\text{Cr}(\text{I})(\text{CO})_4(\text{Ph}_2\text{PN}(\text{iPr})\text{PPh}_2)][\text{Al}(\text{OC}(\text{CF}_3)_3)_4]$.¹⁵

To obtain a crystal structure of a chromium(I) species such as this is very difficult, due to the instability of the complex (particularly in solution) and to our knowledge the only example of this type is shown in figure 3.4. When both structures are compared, we see that upon oxidation, the coordination geometry is retained while a difference in bond lengths is observed. The cationic Cr(I) complex shows shorter C-O bonds as expected. This is also confirmed in the infra-red spectrum. The Cr-P bonds are no longer equivalent in length in the 17-electron complex. This is due to an intramolecular interaction between a fluorine atom on the counterion and a carbonyl oxygen atom, causing the Cr-P bond *trans* to lengthen as electron density is pulled toward the electronegative fluorine. A difference of 0.4 Å between both Cr-P bonds is observed,¹⁷ which is a relatively large difference.

3.1.3 Use of EPR for d⁵ Complexes of Chromium

Magnetic resonance techniques, particularly NMR, are the most versatile and important analytical tools for the characterisation of metal complexes. However, the systems we are interested in, i.e. d⁵ low-spin, contain one unpaired electron, and such paramagnetic species are unsuitable for analysis by NMR. They are however ideal for EPR studies, which can readily provide information not only on the principle oxidation states involved, but also the electronic properties of the metal centre.

A major contribution of EPR spectroscopy is to our understanding of electronic structure. In particular, the components of the g matrix can provide information on the ligand field splitting of the d-orbitals and nuclear hyperfine coupling matrices can be deconvoluted to provide a map of the Singly Occupied Molecular Orbital (SOMO).

The symmetry of transition metal complexes and therefore electronic structure is particularly important in EPR. The splitting of d-orbitals (as a result of the symmetry of the system) affects the EPR spectra due to the differences in separation energy, Δ_o , which affect spin lattice relaxation mechanisms. If spin-lattice relaxation mechanisms are very efficient, spectra can only be recorded at liquid helium temperatures. Such is the case for octahedral systems; when Δ_o is large compared to the pairing energy, the five electrons (in the case of d⁵ systems of the type we are interested in) occupy the t_{2g} set, giving a nominal ²T_{2g} ground state, the low spin configuration (see figure 3.5). As the symmetry of the system is lowered to C_{4v}, in the case of monosubstitution, the t_{2g} orbitals are split into b_{2g} (d_{xy}) and e_g (d_{xz}, d_{yz}).

The ground state is now determined by the π accepting ability of the ligand; for example if the ligand is a stronger π acceptor than the metal centre, then the e_g orbitals will be more bonding than the b_{2g} and therefore lower in energy, resulting in b_{2g} as the SOMO and a ground state of 2B_2 . If the ligand is a weaker π -acceptor than the metal centre, then the opposite case occurs and the ground state of 2E is expected. (figure 3.5)

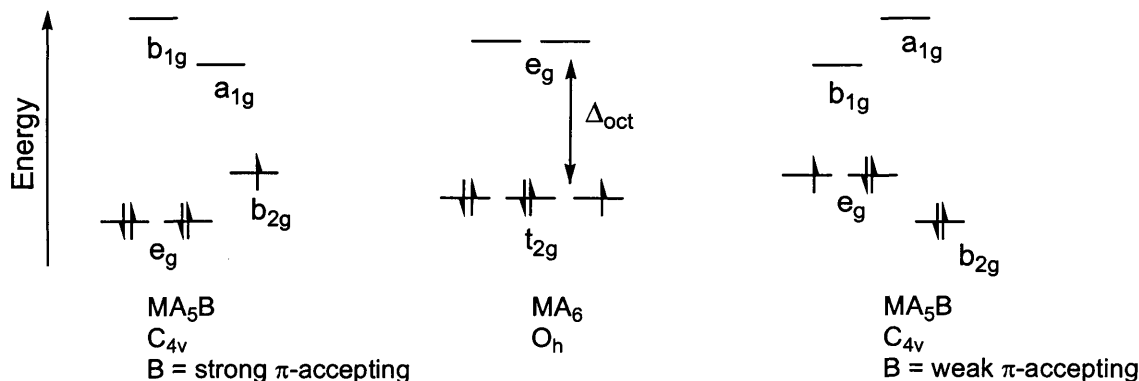


Figure 3.5 Schematic representation of the effect of symmetry distortions on the orbital energies of an octahedral complex MA_6 .

In complexes of symmetry C_{2v} such as the complexes we are interested in $[Cr(CO)_4(PP)]$, the symmetry is lowered again compared to the system described above, and the degeneracy of the t_{2g} orbitals is completely removed. The identity of the SOMO depends on the nature of the ligands, but regardless of the ligand system, a non-degenerate ground state is expected, and therefore liquid helium temperatures are not required.

To date, most of the available EPR literature on chromium complexes has focussed on Cr(III) and Cr(V) compounds,²¹⁻²³ with very little reported on low-spin Cr(I). Some of the earliest reports of Cr(I) EPR spectra²⁴ were by Bond²⁵⁻³⁰ and co workers, who reported isotropic EPR spectra for a series of phosphine and phosphite derivatives of $[Cr(CO)_6]^+$. Lappert³¹ and co workers carried out the oxidation of Cr(0) carbene complexes inside the EPR cavity due to the thermal instability of these systems. More recently, EPR studies carried out by Rieger³² showed the first quantitative photochemical transformation for a Cr(I) complex.

3.2 Results and Discussion

As discussed in 3.1, it is extremely valuable to gain a better insight into this type of Cr(I) species as little is known about these air-sensitive, paramagnetic systems.

Ligands **29-35** shown in figure 3.6, were used to prepare a series of chromium(0) and chromium(I) compounds in order to gain more information on this family of catalyst systems. It is known that PNP-type ligands are prevalent within trimerisation studies due to their high selectivity and catalytic ability^{33, 34} PCP-type donor systems have been shown to be quite inactive in both trimerisation and tetramerisation,² and are included to give a complete picture of this family of complexes with a view to provide further information about the catalytic process.

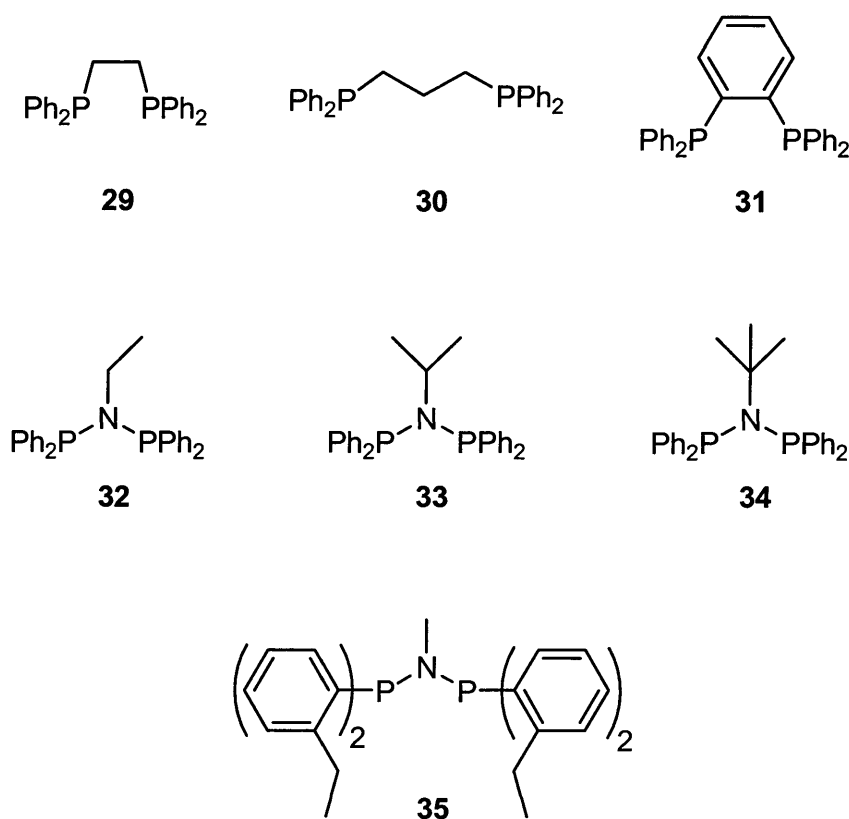
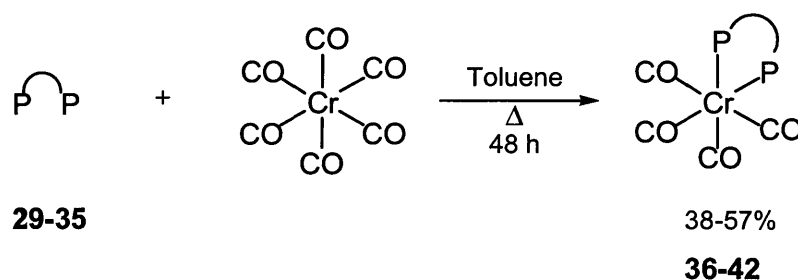


Figure 3.6 Ligands **29-35**.

3.2.1 Synthesis and Characterisation of Chromium(0) Compounds

There have been several reported synthetic procedures for the preparation of chromium tetracarbonyl bis(phosphine) systems, however the best method was found to be a simple reflux in toluene¹⁷ (Scheme 3.3), followed by recrystallisation of the crude product from dichloromethane and methanol.



Scheme 3.3 Reaction of ligands **29-35** to produce chromium(0) complexes **36-42**.¹⁷

Chromium(0) complexes **36-42** were characterised by ³¹P, ¹H and ¹³C NMR spectroscopy, and spectra consistent with the proposed structures were obtained. Infra-red spectra were recorded for the slightly air sensitive compounds and compared to existing data on similar complexes. The spectra were typical for Cr(CO)₄(L)₂ compounds, with carbonyl stretching frequencies differing slightly as expected, due to the differences in electronegativity and basicity of the coordinated ligands. Compounds **36-42** all have the same symmetry, i.e. C_{2v}, and we therefore expect to see the same number of stretches in each IR spectrum. Theoretically we should see four carbonyl stretches, however due to overlap of peaks we see three distinct bands in each case. IR provides information about the ligand system but perhaps more importantly, will act as a point of comparison to use when the spectra of the analogous chromium(I) species are analysed.

As shown in table 3.1, the basicity of the ligand (i.e. the extent to which electron density is donated to the metal centre) affects the carbonyl stretching frequency. As the electron density available at the metal centre increases, the degree of backbonding to the carbonyl groups will increase resulting in a weaker CO bond, displayed by a stretch at lower frequency. Differences in the backbones of ligands **29-35** will of course result in different chelate 'bites'. This can also influence the extent of ligand donation; for example complexes **39-42**, essentially containing 4-membered rings, will have much smaller bite angles than complex **37**.


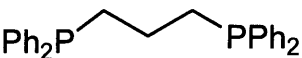
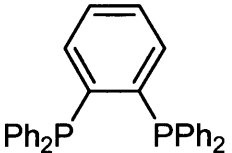
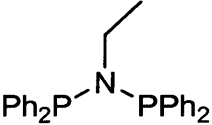
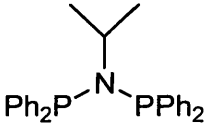
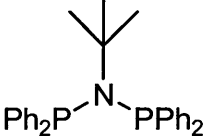
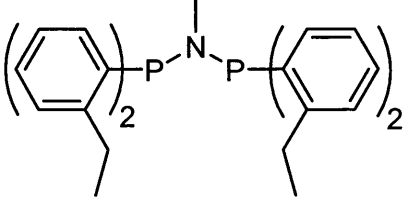
Cr(CO) ₄ (L)	Ligand	ν (CO)/cm ⁻¹			Av ν (CO)/ cm ⁻¹
36		1870	1902	2005	1926
37		1885	1913	2005	1934
38		1893	1916	2012	1940
39		1891	1915	2007	1938
40		1887	1923	2006	1939
41		1890	1919	2006	1938
42		1864	1895	2006	1922

Table 3.1 Carbonyl Stretches for Cr(CO)₄(L) Compounds 36-42

One expects that the carbonyl stretches of compounds 39-42 will be higher than those of compounds 36-38, and this is the general trend observed if the average stretching frequencies are compared. This is due to the inclusion of an electronegative nitrogen atom, which will reduce the electron donating ability and therefore the overall basicity of the ligand. Ligands used in compounds 39-42 are less basic, resulting in less electron density

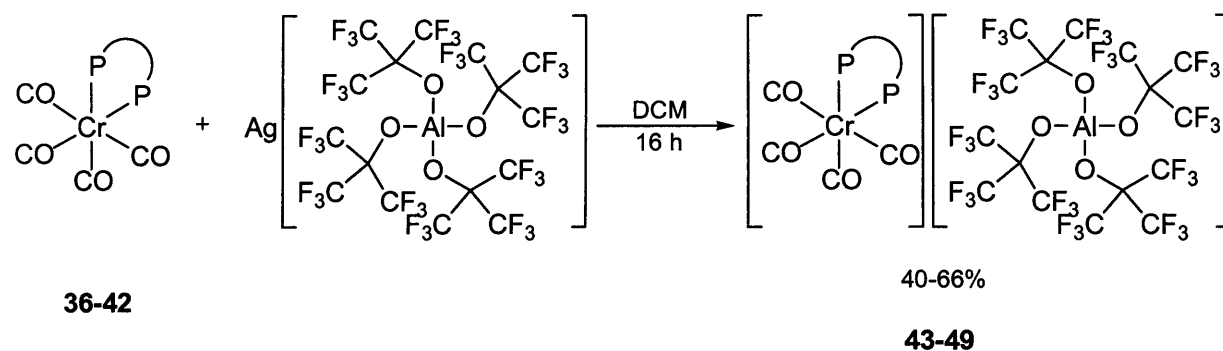
being donated to the metal centre. When the metal centre is less electron-rich, there is less electron density available for backbonding to the carbonyl ligands. This results in a stronger C-O bond and a slight increase in the observed wavenumbers at which we see stretches relative to the non-nitrogen containing systems.

An exception to this pattern is observed with compound **38**, where the presence of a conjugated benzene ring reduces the basicity of the ligand, resulting in higher wavenumbers than the other PCP systems. The presence of ethyl groups on the phenyl rings in compound **42** appears to lower the stretching frequency; the electron donating nature of these ethyl groups results in a more basic ligand. Clearly the presence of electron donating groups overrides the electronegative effect of the presence of the nitrogen in the bridge (i.e. significantly lower stretching frequencies for compound **42**).

3.2.2 Synthesis and Characterisation of Chromium(I) Compounds

In order to prepare and isolate a series of 17-electron chromium(I) species from chromium(0) compounds **36-42**, a suitable oxidising agent is required to remove one electron from the stable 18-electron precursor compounds. For reasons discussed in 3.1.2, the aluminate ($\text{Ag}[\text{Al}(\text{OC}(\text{CF}_3)_3)_4]$) was the best candidate for our purposes. Furthermore, since these compounds were to be used in ENDOR studies, a further consideration was the fact that ^{19}F has a spin of $1/2$ so will be visible. This can result in coupling or overlapping of ENDOR signals, so from this point of view the most weakly coordinating anion is required to lessen the effects described.

The cationic chromium complexes **43-49** were prepared according to scheme 3.4. An excess of aluminate was used to ensure full conversion of the chromium(0) starting material. With exclusion of light, the mixture was stirred in dichloromethane for 16 hours. An immediate colour change from yellow to dark purple/blue was observed upon addition of the solvent, and a silver mirror was formed inside the Schlenk tube as the silver counterion is reduced.



Scheme 3.4 Synthesis of Chromium(I) Complexes **43-49**.

Characterisation of the resulting complexes **43-49** was somewhat limited due to their paramagnetic nature. EPR analysis was carried out and is discussed in section 3.2.3. Infra-red data and mass spectrometric analysis were also used to confirm the presence of the complex. Positive and negative ion mass spectra were obtained, to confirm the presence of the aluminate counterion as well as the chromium species. Despite the sensitive nature of these compounds, high resolution spectra were obtained when a solution of each complex in dry solvent was injected directly into the machine, to limit decomposition of the air/moisture-sensitive compounds.

In order to obtain IR data, solutions of each compound were made up in dichloromethane inside the glove box and the spectra obtained immediately. As shown in table 3.2, significant shifts in the carbonyl stretching frequency were observed for the chromium(I) compounds when compared to the analogous neutral systems. This is a result of the change in oxidation state of the central chromium atom. The amount of electron density available for backbonding to the carbonyl ligands is much less than in the 18-electron complexes (**36-42**). The CO bonds are therefore stronger and shorter as less electron density is present in the antibonding orbitals (π^*) of the carbonyl ligands; one therefore observes stretches at higher wavenumbers.



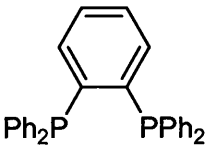
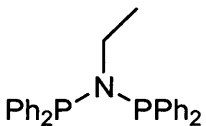
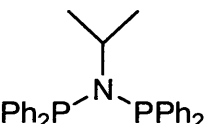
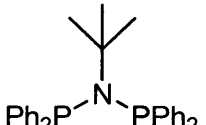
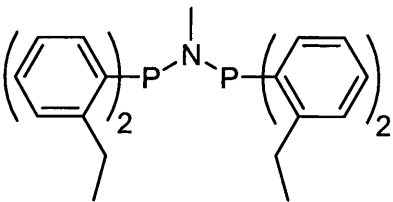
[Cr(CO) ₄ L] ⁺	Ligand	ν(CO) /cm ⁻¹	
		Cr(0)	Cr(I)
43		1870	1971
		1902	2034
		2005	2085
44		1885	1954
		1913	2046
		2005	2086
45		1893	1969
		1916	2032
		2012	2086
46		1891	1968
		1915	2036
		2007	2089
47		1887	1964
		1923	2032
		2006	2086
48		1890	1965
		1919	2031
		2006	2084
49		1864	1975
		1895	2022
		2006	2082

Table 3.2 Comparison of carbonyl stretches in neutral and cationic complexes.

3.2.3 EPR Studies

The cationic compounds **43-49** are all low spin d^5 systems. They were prepared under an atmosphere of argon and analysed by cw-EPR (continuous wave-EPR) as frozen solutions.

The cw-EPR spectrum for **43** along with the corresponding EPR simulation are shown in figure 3.7, and can be described as possessing an axial g tensor. A well resolved superhyperfine structure in both the perpendicular and parallel components can be easily observed and each component of the g tensor is split into a 1:2:1 triplet pattern due to the superhyperfine interaction of the unpaired electron on the chromium centre with two equivalent ^{31}P nuclei ($I = 1/2$). In some cases, broadening of one or both of these components is observed. This broadening is a result of fast spin-lattice relaxation mechanisms. The resulting spin Hamiltonian parameters (extracted by simulation of the EPR spectra) are listed in Table 3. Since the natural abundance of ^{53}Cr ($I = 3/2$) is only 9.5%, coupled with the large linewidths associated with the ^{31}P hyperfine pattern, no anisotropic hyperfine interaction associated with ^{53}Cr was detected in the frozen solution spectrum.

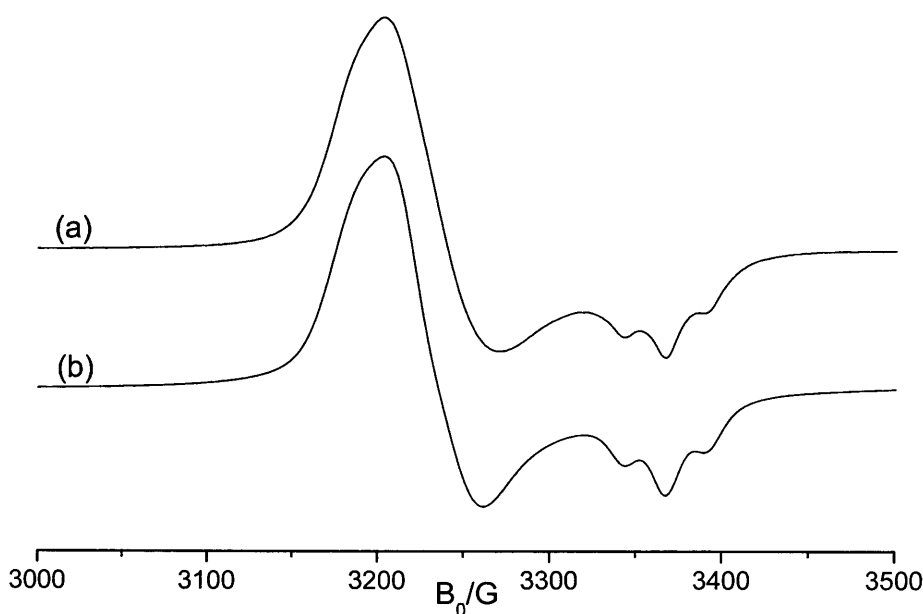


Figure 3.7 Experimental (a) and simulated (b) cw-EPR spectra (130K) of **43** recorded in dichloromethane/toluene.

The EPR spin Hamiltonian parameters (g and A) for any paramagnetic complex will depend on the coordination state and symmetry of the metal centre. The g_{xx} and g_{yy} values

were expected to be significantly higher than g_e ($g_e = 2.023$) while g_{zz} was expected to be slightly less than g_e . These trends are indeed observed experimentally, with g_{\perp} ($g_{xx} = g_{yy}$) = 2.063 and g_{\parallel} (g_{zz}) = 1.987 (Table 3.3), confirming a d_{xy} ground state for all complexes.³⁵

Cr(I) complex	g_{\perp}	g_{\parallel}	${}^P A_{\perp} / G^*$	${}^P A_{\parallel} / G^*$	a_{iso} / G	% S□
49	2.089	1.983	29.0	24.0	27.3	0.573
45	2.084	1.989	25.5	25.0	25.3	0.532
43	2.083	1.989	24.8	24.5	24.8	0.518
46	2.077	1.985	27.7	25.5	27.0	0.534
47	2.072	1.988	27.0	25.5	26.5	0.556
48	2.068	1.988	27.0	25.5	26.5	0.556
44	2.063	1.987	24.9	24.5	24.7	0.520

* A values $\pm 0.2G$

□ Percentage spin density in the ${}^{31}P$ s-orbital (Fermi contact term)

Table 3.3 Spin Hamiltonian parameters obtained by simulation for $[Cr(CO)_4L]^+$ compounds **43-49**.

The cw-EPR spectra for all the complexes **43-49** are shown in figure 3.8. In all cases, axial g tensors ($g_{\perp} > g_e > g_{\parallel}$) are observed and the corresponding spin Hamiltonian parameters for each complex are listed in Table 3.3 (the individual spectra and simulations are in appendix B figures 1-6). Similar to the above discussion for complex **43**, it appears that the ground state in all the complexes can therefore be described as d_{xy} . It should be noted however, that the resolution of the spectra, and indeed the spin Hamiltonian values, are found to be highly dependent on the ligand type (Table 3.3). The difference in g values (defined as $\Delta g = g_{\perp} - g_{\parallel}$), for example, is greatest for **49** and smallest for **44** (see figure 3.8 and Table 3.3). Despite these clear differences in the Δg shift, caused by the extent of tetragonal distortion in the complexes, no obvious correlation emerges between the observed spectral shifts and the ligand type. Further detailed analysis has been carried out using ENDOR which was reported elsewhere.³⁵

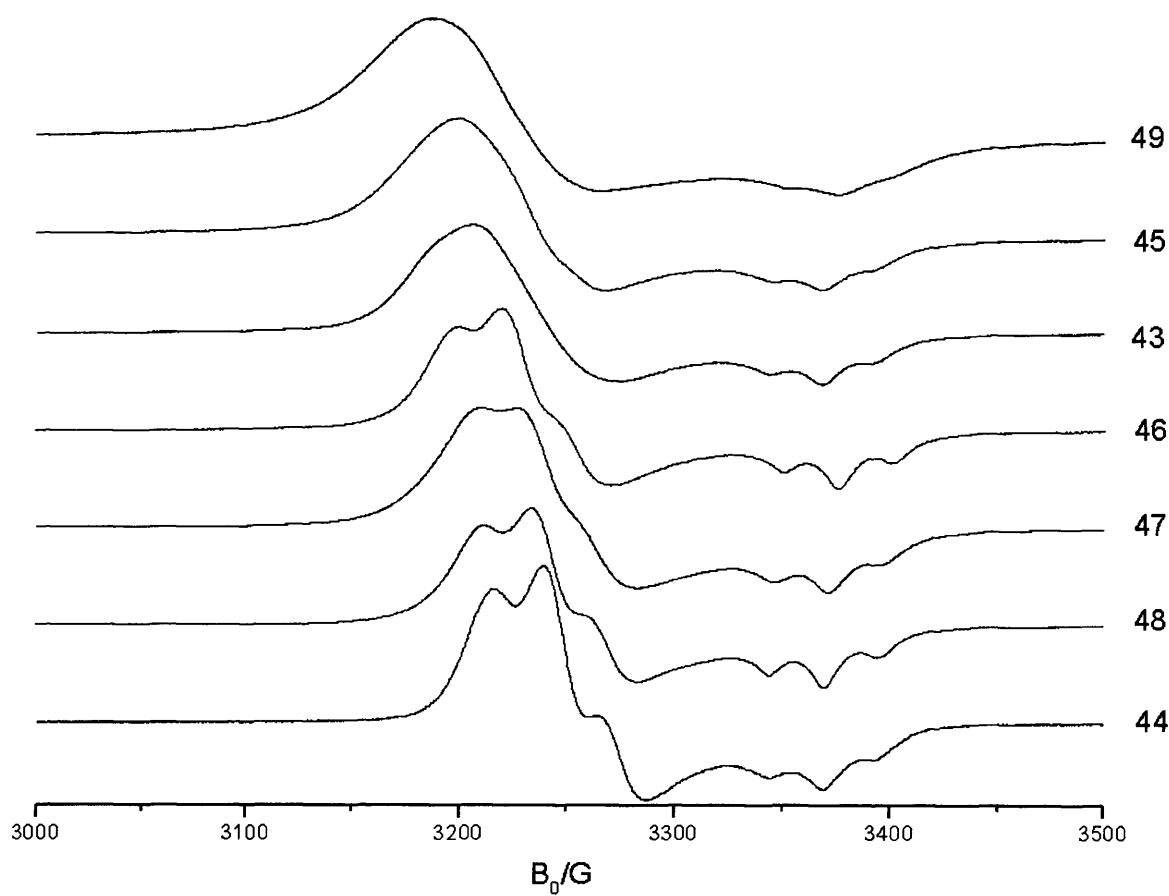


Figure 3.8 cw-EPR spectra (130K) of 43-49 recorded in dichloromethane/toluene.

3.3 Conclusion

A series of chromium(0) and chromium(I) complexes containing various bis(phosphine) ligands have been prepared and characterised via NMR, infra red and cw-EPR spectroscopies.

Subtle differences have been identified between the chromium(I) complexes in terms of the g components. The spin Hamiltonian parameters were found to be consistent with low-spin d^5 systems of C_{2v} symmetry, possessing a SOMO where the metal contribution is primarily d_{xy} .

The isotropic Fermi contact term (P_{iso}^P) was found to be largest for complexes containing ligands 32 - 35, indicating that the ^{31}P 3s character in the SOMO is higher for the P-N-P type ligands than the P-C-P types. Observed changes in the g matrix did not however follow the same trends of ligand type, indicating that g is dependent not just on the energy of

the SOMO but also on the structural differences in ligand which influence the extent of tetragonal distortion in the complexes.

Structural differences in the $[\text{Cr}(\text{CO})_4\text{L}_2]^+$ complexes were also revealed through ^1H , ^{14}N and ^{31}P ENDOR (data not reported here), where the observed spectral changes were attributed to variations in the phenyl ring conformations as a function of ligand type. These EPR and ENDOR results reveal that the ligands **29** - **35** impart very subtle electronic and structural alterations to this class of complex, but that these parameters do not correlate with any trend in catalytic data at least for the parent pre-catalyst prior to activation.³⁵

Nevertheless, despite a lack of correlation emerging between the EPR data and the known catalytic activities of these systems, it should be stressed that the nature of the activated complexes may be very different compared to the pre-catalyst complexes reported in this chapter. In any case, the results presented here offer some insight into the electronic properties of these air-sensitive Cr(I) complexes where few EPR studies have been reported to date.

3.4 Experimental Section

General Procedures. All manipulations were performed using standard Schlenk techniques under an argon atmosphere, or in a nitrogen atmosphere MBraun UNILAB glovebox with less than 0.1ppm water and O₂. Solvents were dried using a Braun Solvent Purification System, and degassed prior to use. Ligands **29**, **30** and **31** were purchased from Aldrich, ligands **32**, **34**, and **35** were prepared and supplied by Sasol Technology. Ligand **33**,³⁶ chromium compounds **36-49**^{15,17} and silver aluminate¹⁹ were prepared according to literature procedures.

NMR spectra were recorded at 298 K on Bruker Avance AMX 400 or Jeol Eclipse 300 spectrometers. Chemical shift values are given relative to residual solvent peak. ESI-MS were performed on a Waters LCT Premier XE instrument. Infra-red spectra were recorded using a JASCO FT/IR-660 *Plus* spectrometer and analysed in solution (dichloromethane). EPR spectra and computer simulations were carried out with Lucia McDyre, a PhD student at Cardiff University. EPR spectra were recorded at 130K on an X-band Bruker EMX spectrometer operating at 100 kHz field modulation, 10mW microwave power and equipped with a high sensitivity cavity (ER 4119HS). EPR computer simulations were performed using the SimEPR32 program.³⁷ *g* Values were determined using a DPPH standard. Complexes were dissolved in 200µl DCM/toluene and a frozen solution produced by placing the EPR tube in liquid nitrogen.

[Cr(CO)₄(Ph₂PCH₂CH₂PPh₂)] (**36**)

Toluene (40 ml) was added to a mixture of chromium hexacarbonyl (372 mg, 1.69 mmol) and **29** (505 mg, 1.27 mmol) and the mixture was heated to reflux for 48 h, ensuring that the sublimed hexacarbonyl was periodically washed back into the stirred mixture. The solution was then cooled to 0°C and filtered to remove excess chromium hexacarbonyl. Solvent was removed *in vacuo* and the product extracted into dichloromethane (10 ml). Methanol (20 ml) was added to precipitate the product which was isolated by filtration and dried *in vacuo* yielding a yellow microcrystalline solid (300 mg, 42%). ¹H NMR (CD₂Cl₂, 400 MHz, 298 K): δ (ppm) 2.00 (t, 4H, CH₂CH₂ ³J_{HH} = 4.1 Hz), 7.20-7.35 (m, 16H, *ortho*- and *meta*-C₆H₅), 7.50 (m, 4H, *para*-C₆H₅). ³¹P {¹H} NMR (CD₂Cl₂, 121 MHz, 298 K): δ (ppm) 80.35 (s). ¹³C {¹H} NMR (CD₂Cl₂, 125 MHz, 298 K): δ (ppm) 27.3 (CH₂CH₂), 127.7 (*meta*-C₆H₅),

130.4 (*para*-C₆H₅), 131.9 (*ortho*-C₆H₅), 137.6 (*ipso*-C₆H₅), 219.6 (*cis*-CO), 228.3 (*trans*-CO). High Resolution ESI_{pos}-MS (MeCN): found 562.0542 (C₃₀H₂₄O₄P₂Cr⁺ requires 562.0555 dev: -2.3 ppm). IR (CH₂Cl₂): $\nu = 1870$ (s) (CO), 1902 (s) (CO), 2005 (s) (CO) cm⁻¹.

[Cr(CO)₄(Ph₂P(CH₂)₃PPh₂)] (37)

An analogous method to that of **36** was followed, using chromium hexacarbonyl (355 mg, 1.61 mmol) and **30** (502 mg, 1.22 mmol). The product was obtained as a yellow solid (400 mg, 57%). ¹H NMR (CDCl₃, 400 MHz, 298 K): δ (ppm) 1.88 (m, 2H, CH₂), 2.34 (m, 4H, CH₂), 7.32 (m, 20H, C₆H₅). ³¹P {¹H} NMR (CDCl₃, 121 MHz, 298 K): δ (ppm) 42.38 (s). ¹³C {¹H} NMR (CDCl₃, 125 MHz, 298 K): δ (ppm) 18.6 (CH₂), 29.6 (CH₂), 127.3 (*meta*-C₆H₅), 128.4 (*para*-C₆H₅), 130.8 (*ortho*-C₆H₅), 136.7 (*ipso*-C₆H₅), 220.7 (*cis*-CO), 225.1 (*trans*-CO). High Resolution ESI_{pos}-MS (MeCN): found 576.0717 (C₃₁H₂₆O₄P₂Cr⁺ requires 576.0711 dev: 1.0 ppm). IR (CH₂Cl₂): $\nu = 1885$ (s) (CO), 1913 (s) (CO), 2005 (s) (CO) cm⁻¹.

[Cr(CO)₄(Ph₂PBzPPh₂)] (38)

An analogous method to that of **36** was followed, using chromium hexacarbonyl (325 mg, 1.48 mmol) and **31** (498 mg, 1.11 mmol). The product was obtained as a yellow solid (320 mg, 47%). ¹H NMR (CD₂Cl₂, 400 MHz, 298 K): δ (ppm) 7.30 (m, 20H, *ortho*-, *meta*-C₆H₅, C₆H₄), 7.45 (m, 4H, *para*-C₆H₅). ³¹P {¹H} NMR (CD₂Cl₂, 121 MHz, 298 K): δ (ppm) 83.33 (s). ¹³C {¹H} NMR (CD₂Cl₂, 125 MHz, 298 K): δ (ppm) 127.4 (*meta*-C₆H₅), 127.6 (*para*-C₆H₅), 128.9, 129.7, 131.3 (C₆H₄), 131.4 (*ortho*-C₆H₅), 135.6 (*ipso*-C₆H₅). High Resolution ESI_{pos}-MS (MeCN): found 610.0564 (C₃₄H₂₄O₄P₂Cr⁺ requires 610.0555 dev: 1.4 ppm). IR (CH₂Cl₂): $\nu = 1893$ (s) (CO), 1916 (s) (CO), 2012 (s) (CO) cm⁻¹.

[Cr(CO)₄(Ph₂PN(Et)PPh₂)] (39)

An analogous method to that of **36** was followed, using chromium hexacarbonyl (355 mg, 1.61 mmol) and **32** (500 mg, 1.21 mmol). The product was obtained as a yellow solid (350 mg, 50%). ¹H NMR (CDCl₃, 400 MHz, 298 K): δ (ppm) 0.75 (t, 3H, CH₃, ³J_{HH} = 7.3 Hz), 3.00 (m, 2H, CH₂), 7.41 (m, 20H, C₆H₅). ³¹P {¹H} NMR (CDCl₃, 121 MHz, 298 K): δ (ppm) 114.36 (s). ¹³C {¹H} NMR (CDCl₃, 125 MHz, 298 K): δ (ppm) 15.1 (CH₃), 44.0 (CH₂), 127.5 (*meta*-C₆H₅), 129.6 (*para*-C₆H₅), 130.9 (*ortho*-C₆H₅), 135.6 (*ipso*-C₆H₅), 221.2 (*cis*-CO), 227.2 (*trans*-CO). High Resolution ESI_{pos}-MS (MeCN): found 577.0656}

(C₃₀H₂₅O₄P₂CrN⁺ requires 577.0664 dev: -1.4 ppm). IR (CH₂Cl₂): ν = 1891 (s) (CO), 1915 (s) (CO), 2007 (s) (CO) cm⁻¹.

[Cr(CO)₄(Ph₂PN(ⁱPr)PPh₂)] (40)

An analogous method to that of **36** was followed, using chromium hexacarbonyl (340 mg, 1.55 mmol) and **33** (494 mg, 1.16 mmol). The product was obtained as a yellow solid (260 mg, 38%). ¹H NMR (CDCl₃, 400 MHz, 298 K): δ (ppm) 0.62 (d, 6H, CH₃, ³J_{HH} = 6.8 Hz), 3.52 (sept, 1H, CH, ³J_{HH} = 7.0 Hz), 7.41 (m, 12H, *meta*-, *para*-C₆H₅), 7.69 (m, 8H, *ortho*-C₆H₅). ³¹P {¹H} NMR (CDCl₃, 121 MHz, 298 K): δ (ppm) 112.70 (s). ¹³C {¹H} NMR (CDCl₃, 125 MHz, 298 K): δ (ppm) 22.5 (CH₃), 54.8 (CH), 127.4 (*meta*-C₆H₅), 129.5 (*para*-C₆H₅), 130.9 (*ortho*-C₆H₅), 136.1 (*ipso*-C₆H₅), 221.9 (*cis*-CO), 227.4 (*trans*-CO). High Resolution ESI_{pos}-MS (MeCN): found 591.0796 (C₃₁H₂₇O₄P₂CrN⁺ requires 591.0820 dev: -4.1 ppm). IR (CH₂Cl₂): ν = 1887 (s) (CO), 1923 (s) (CO), 2006 (s) (CO) cm⁻¹.

[Cr(CO)₄(Ph₂PN(^tBu)PPh₂)] (41)

An analogous method to that of **36** was followed, using chromium hexacarbonyl (340 mg, 1.55 mmol) and **34** (510 mg, 1.16 mmol). The product was obtained as a yellow solid (350 mg, 50%). ¹H NMR (CDCl₃, 400 MHz, 298 K): δ (ppm) 0.49 (s, 9H, C(CH₃)₃), 7.48 (m, 20H, C₆H₅). ³¹P {¹H} NMR (CDCl₃, 121 MHz, 298 K): δ (ppm) 115.86 (s). ¹³C {¹H} NMR (CDCl₃, 125 MHz, 298 K): δ (ppm) 30.6 (CH₃), 61.6 (C(CH₃)₃), 127.3 (*meta*-C₆H₅), 129.5 (*para*-C₆H₅), 130.8 (*ortho*-C₆H₅), 135.9 (*ipso*-C₆H₅), 222.5 (*cis*-CO), 227.7 (*trans*-CO). High Resolution ESI_{pos}-MS (MeCN): found 605.0962 (C₃₂H₂₉O₄P₂CrN⁺ requires 605.0976 dev: -2.3 ppm). IR (CH₂Cl₂): ν = 1890 (s) (CO), 1919 (s) (CO), 2006 (s) (CO) cm⁻¹.

[Cr(CO)₄(Ar₂PN(Me)PAr₂)] (Ar=2-C₆H₄(Et)) (42)

An analogous method to that of **36** was followed, using chromium hexacarbonyl (293 mg, 1.33 mmol) and **35** (511 mg, 1.0 mmol). The product was obtained as a yellow solid (350 mg, 53%). ¹H NMR (CD₂Cl₂, 400 MHz, 298 K): δ (ppm) 0.85 (br s, 12H, CH₃), 2.46 (s, 3H, CH₃), 2.61 (br s, 8H, CH₂), 7.32 (m, 16H, *Ar*-H). ³¹P {¹H} NMR (CD₂Cl₂, 121 MHz, 298 K): δ (ppm) 103.4 (br s). ¹³C {¹H} NMR (CD₂Cl₂, 125 MHz, 298 K): δ (ppm) 13.3 (CH₃), 26.0 (CH₂), 33.5 (N-CH₃), 124.9 (*meta*-C₆H₅), 129.1 (*para*-C₆H₅), 134.5 (*ortho*-C₆H₅), 144.6 (*ipso*-C₆H₅), 219.8 (*cis*-CO), 227.7 (*trans*-CO). High Resolution ESI_{pos}-MS (MeCN): found

675.1746 ($C_{37}H_{43}O_4P_2CrN^+$ requires 675.1759 dev: -1.9 ppm). IR (CH_2Cl_2): $\nu = 1864$ (s) (CO), 1895 (s) (CO), 2006 (s) (CO) cm^{-1} .

[Cr(CO)₄(Ph₂PCH₂CH₂PPh₂)] [Al(OC(CF₃)₃)₄] (43)

Complex **36** (50 mg, 0.089 mmol) and the silver aluminate (143 mg, 0.13 mmol) were combined in a Schlenk tube and dichloromethane (5 ml) added, the mixture, which immediately changed colour, was left to stir for 16 h at room temperature under the exclusion of light. After filtration, the solvent was removed *in vacuo* leaving a dark purple residue which was washed with hexane (2 × 5 ml) and dried *in vacuo* to yield the product as a deep purple powder (90 mg, 66%). High Resolution ESI_{pos}-MS (MeCN): found 562.0562 ($C_{30}H_{24}O_4P_2Cr^+$ requires 562.0555 dev: 1.2 ppm). High Resolution ESI_{neg}-MS (MeCN): found 966.9030 ($C_{16}H_{36}O_4Al^+$ requires 966.9037 dev: -0.7 ppm). IR (CH_2Cl_2): $\nu = 1971$ (s) (CO), 2034 (s) (CO), 2085 (s) (CO) cm^{-1} .

[Cr(CO)₄(Ph₂P(CH₂)₃PPh₂)] [Al(OC(CF₃)₃)₄] (44)

An analogous method to that of **43** was followed, using chromium compound **37** (100 mg, 0.17 mmol) and silver aluminate (275 mg, 0.255 mmol). The product was obtained as a dark blue powder (145 mg, 54%). High Resolution ESI_{pos}-MS (MeCN): found 576.0706 ($C_{31}H_{26}O_4P_2Cr^+$ requires 576.0711 dev: -0.8 ppm). High Resolution ESI_{neg}-MS (MeCN): found 966.9084 ($C_{16}H_{36}O_4Al^+$ requires 966.9037 dev: 4.8 ppm). IR (CH_2Cl_2): $\nu = 1954$ (s) (CO), 2046 (s) (CO), 2086 (s) (CO) cm^{-1} .

[Cr(CO)₄(Ph₂PBzPPh₂)] [Al(OC(CF₃)₃)₄] (45)

An analogous method to that of **43** was followed, using chromium compound **38** (50 mg, 0.081 mmol) and silver aluminate (130 mg, 0.121 mmol). The product was obtained as a dark blue powder (65 mg, 50%). High Resolution ESI_{pos}-MS (MeCN): found 610.0540 ($C_{34}H_{24}O_4P_2Cr^+$ requires 610.0555 dev: -2.4 ppm). IR (CH_2Cl_2): $\nu = 1969$ (s) (CO), 2032 (s) (CO), 2086 (s) (CO) cm^{-1} .

[Cr(CO)₄(Ph₂PN(Et)PPh₂)] [Al(OC(CF₃)₃)₄] (46)

An analogous method to that of **43** was followed, using chromium compound **39** (100 mg, 0.17 mmol) and silver aluminate (278 mg, 0.26 mmol). The product was obtained as a dark

blue powder (120 mg, 45%). High Resolution ESI_{pos}-MS (MeCN): found 577.0648 (C₃₀H₂₅O₄P₂CrN⁺ requires 577.0664 dev: -2.7 ppm). IR (CH₂Cl₂): ν = 1968 (s) (CO), 2036 (s) (CO), 2089 (s) (CO) cm⁻¹.

[Cr(CO)₄(Ph₂PN(iPr)PPh₂)] [Al(OC(CF₃)₃)₄] (47)

An analogous method to that of **43** was followed, using chromium compound **40** (100 mg, 0.17 mmol) and silver aluminate (271 mg, 0.25 mmol). The product was obtained as a dark blue powder (105 mg, 40%). High Resolution ESI_{pos}-MS (MeCN): found 591.0824 (C₃₁H₂₇O₄P₂CrN⁺ requires 591.0820 dev: 0.6 ppm). IR (CH₂Cl₂): ν = 1964 (s) (CO), 2032 (s) (CO), 2086 (s) (CO) cm⁻¹.

[Cr(CO)₄(Ph₂PN(^tBu)PPh₂)] [Al(OC(CF₃)₃)₄] (48)

An analogous method to that of **43** was followed, using chromium compound **41** (50 mg, 0.083 mmol) and silver aluminate (133 mg, 0.124 mmol). The product was obtained as a dark blue powder (62 mg, 48%). High Resolution ESI_{pos}-MS (MeCN): found 605.0993 (C₃₂H₂₉O₄P₂CrN⁺ requires 605.0976 dev: 2.8 ppm). IR (CH₂Cl₂): ν = 1965 (s) (CO), 2031 (s) (CO), 2084 (s) (CO) cm⁻¹.

[Cr(CO)₄(Ar₂PN(Me)PAr₂)] [Al(OC(CF₃)₃)₄] (Ar=2-C₆H₄(Et)) (49)

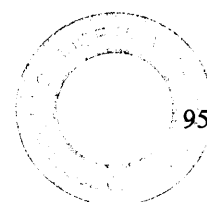
An analogous method to that of **43** was followed, using chromium compound **42** (100 mg, 0.15 mmol) and silver aluminate (238 mg, 0.22 mmol). The product was obtained as a dark blue powder (150 mg, 62%). High Resolution ESI_{pos}-MS (MeCN): found 675.1773 (C₃₇H₄₃O₄P₂CrN⁺ requires 675.1759 dev: 2.0 ppm). IR (CH₂Cl₂): ν = 1975 (s) (CO), 2022 (s) (CO), 2082 (s) (CO) cm⁻¹.

3.5 References

- [1] McGuinness, D. S.; Wasserscheid, P.; Keim, W.; Morgan, D.; Dixon, J. T.; Bollmann, A.; Maumela, H.; Hess, F.; Englert, U. *J. Am. Chem. Soc.* **2003**, *125*, 5272.
- [2] Carter, A.; Cohen, S. A.; Cooley, N. A.; Murphy Scutt, A. J.; Wass, D. F. *Chem. Commun.* **2002**, 858.
- [3] Blann, K.; Bollmann, A.; Dixon, J. T.; Hess, F. M.; Killian, E.; Maumela, H.; Morgan, D. H.; Neveling, A.; Otto, S.; Overett, M. *Chem. Commun.* **2005**, 620.
- [4] Bollmann, A.; Blann, K.; Dixon, J. T.; Hess, F. M.; Killian, E.; Maumela, H.; McGuinness, D. S.; Morgan, D. H.; Neveling, A.; Otto, S.; Overett, M.; Slawin, A. M. Z.; Wasserscheid, P.; Kuhlmann, S. *J. Am. Chem. Soc.* **2004**, *126*, 14712.
- [5] Overett, M. J.; Blann, K.; Bollmann, A.; Dixon, J. T.; Hess, F.; Killian, E.; Maumela, H.; Morgan, D. H.; Neveling, A.; Otto, S. *Chem. Commun.* **2005**, 622.
- [6] McGuinness, D. S.; Wasserscheid, P.; Keim, W.; Hu, C.; Englert, U.; Dixon, J. T.; Grove, C. *Chem. Commun.* **2003**, 334.
- [7] Agapie, T.; Schofer, S. J.; Labinger, J. A.; Bercaw, J. E. *J. Am. Chem. Soc.* **2004**, *126*, 1304.
- [8] McGuinness, D. S.; Wasserscheid, P.; Morgan, D. H.; Dixon, J. T. *Organometallics* **2005**, *24*, 552.
- [9] Jones, D. J.; Gibson, V. C.; Green, S. M.; Maddox, P. J. *Chem. Commun.* **2002**, 1038.
- [10] Kreisel, K. A.; Yap, G. P. A.; Theopold, K. H. *Organometallics* **2006**, *25*, 4670.
- [11] Köhn, R. D.; Haufe, M.; Kociok-Köhn, G.; Grimm, S.; Wasserscheid, P.; Keim, W. *Angew. Chem. Int. Ed.* **2000**, *39*, 4337.

- [12] (a) Wills, A. R.; Edwards, P. G. *J. Chem. Soc., Dalton Trans.* **1989**, 1253. (b) Wasserscheid, P.; Grimm, S.; Köhn, R. D.; Haufe, M. *Adv. Synth. Catal.* **2001**, *343*, 814. (c) Rüther, T.; Cavell, K. J.; Braussaud, N. C.; Skelton, B. W.; White, A. H. *Dalton Trans.* **2002**, 4684.
- [13] Ittel, S.; Parshall, G. *Homogeneous Catalysis: The Applications and Chemistry of Catalysis by Soluble Transition Metal Complexes*, Wiley, New York, **1992**.
- [14] Overett, M. J.; Blann, K.; Bollmann, A.; Dixon, J. T.; Haasbroek, D.; Killian, E.; Maumela, H.; McGuinness, D. S.; Morgan, D. H. *J. Am. Chem. Soc.* **2005**, *127*, 10723.
- [15] Rucklidge, A. J.; McGuinness, D. S.; Tooze, R. P.; Slawin, A. M. Z.; Pelletier, J. D. A.; Hanton, M. J.; Webb, P. B. *Organometallics* **2007**, *26*, 2782.
- [16] Ashford, P. K.; Baker, P. K.; Connelly, N. G.; Kelly, R. L.; Woodley, V. A. *J. Chem. Soc. Dalton Trans.* **1982**, 477.
- [17] Bowen, L. E.; Haddow, M. F.; Orpen, A. G.; Wass, D. F. *J. Chem. Soc. Dalton Trans.* **2007**, 1160.
- [18] McGuinness, D. S.; Overett, M.; Tooze, R. P.; Blann, K.; Dixon, J. T.; Slawin, A. M. Z. *Organometallics* **2007**, *26*, 1108.
- [19] Krossing, I. *Chem. Eur. J.* **2001**, *7*, 490.
- [20] McGuinness, D. S.; Rucklidge, A. J.; Tooze, R. P.; Slawin, A. M. Z. *Organometallics* **2007**, *26*, 2561.
- [21] Weyhermüller, T.; Paine, T. K.; Bothe, E.; Bill, E.; Chaudhuri, P. *Inorg. Chimica Acta* **2002**, *337*, 344.
- [22] Bruckner, A.; Jabor, J. K.; McConnell, A. E. C.; Webb, P. B. *Organometallics* **2008**, *27*, 3849.

- [23] (a) Branca, M.; Fruianu, M.; Sau, S.; Zoroddu, M. A.; *J. Inorg. Biochem.* **1996**, *62*, 223. (b) Branca, M.; Micera, G.; Sanna, D. *Inorg. Chem.* **1993**, *32*, 578.
- [24] (a) Rieger, P. H. *Coord. Chem. Rev.* **1994**, *135*, 203. b) Rieger, A. L.; Rieger, P. H. *Organometallics* **2002**, *21*, 5868. (b) Cummings, D. A.; McMaster, J.; Rieger, A. L.; Rieger, P. H. *Organometallics* **1997**, *16*, 4362.
- [25] Bagchi, R. N.; Bond, A. M.; Colton, R. *J. Electroanal. Chem.* **1986**, *199*, 297.
- [26] Bagchi, R. N.; Bond, A. M.; Brain, G.; Colton, R.; Henderson, T. L. E.; Kevekordes, J. E. *Organometallics* **1984**, *3*, 4.
- [27] Bond, A. M.; Carr, S. W.; Colton, R. *Inorg. Chem.* **1984**, *23*, 2343.
- [28] Bond, A. M.; Colton, R.; Kevekordes, J. E.; Panagiotidou, P. *Inorg. Chem.* **1987**, *26*, 1430.
- [29] Bond, A. M.; Colton, R.; Jackowski, J. J. *Inorg. Chem.* **1975**, *14*, 2526.
- [30] (a) Bagchi, R. N.; Bond, A. M.; Colton, R.; Greece, I.; McGregor, K.; Whyte, T. *Organometallics* **1991**, *10*, 2611. (b) Connor, J. A.; Riley, P. I.; Rix, C. J. *J. Chem. Soc. Dalton Trans.* **1977**, 1317. (c) Connor, J. A.; Riley, P. I. *J. Chem. Soc. Dalton Trans.* **1979**, 1231.
- [31] Lappert, M. F.; McCabe, R. W.; MacQuitty, J. J.; Pye, P. L.; Riley, P. I. *J. Chem. Soc. Dalton Trans.* **1980**, *1*, 90.
- [32] Rieger, A. L.; Rieger, P. H. *Organometallics* **2002**, *21*, 5868.
- [33] Walsh, R.; Morgan, D. H.; Bollmann, A.; Dixon, J. T. *Appl. Catal. A* **2006**, *306*, 184.
- [34] Kuhlmann, S.; Dixon, J. T.; Haumann, M.; Morgan, D. H.; Ofili, J.; Spuhl, O.; Taccardi, N.; Wasserscheid, P. *Adv. Synth. Catal.* **2006**, *348*, 1200.



- [35] McDyre, L. E.; Hamilton, T.; Murphy, D. M.; Cavell, K. J.; Gabrielli, W. F.; Hanton, M. J.; Smith, D. M. *Dalton Trans.*, **2010**, 39, 7792.
- [36] Balakrishna, M. S.; Prakasha, T. K.; Krishnamurthy, S. S.; Siriwardane, U.; Hosmane, N. S. *J. Organomet. Chem.* **1990**, 390, 203.
- [37] Spalek, T. P. P.; Sojka, Z. *J. Chem. Inf. Model* **2005**, 45, 18.

Chapter Four

Low Oxidation State Chromium Complexes

Chapter Four

Low Oxidation State Chromium Complexes

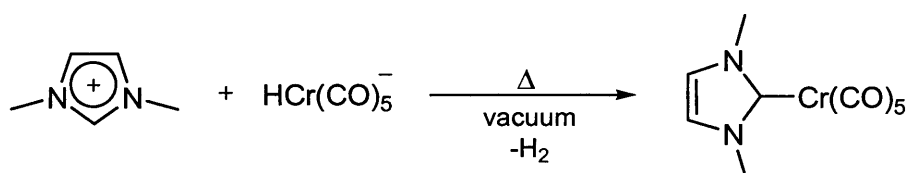
4.1 Introduction

Chromium complexes in oxidation states +I and +II containing N-heterocyclic carbenes are extremely rare despite the relevance of these oxidation states in selective oligomerisation.¹⁻⁴ A series of chromium(0)-NHC complexes has been prepared, including several novel compounds containing expanded six- and seven-membered NHC ligands. One electron oxidation of these compounds, as described in chapter 3, has been carried out and a series of new Cr(I)-NHC complexes have been isolated and analysed by EPR spectroscopy.

The possible role of Cr(II) in the selective oligomerisation of ethylene is discussed, and a series of novel functionalised and non-functionalised Cr(II)-NHC complexes are reported and characterised in this chapter.

4.1.1 Cr(0)-NHC Complexes

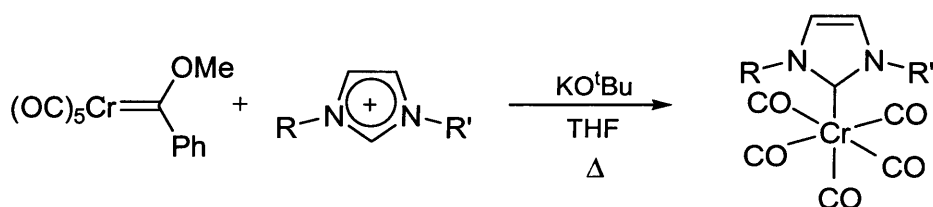
In 1968, more than 20 years before the first free-NHC was isolated, Öfele⁵ and co-workers utilised the acidic nature of imidazolium salts to synthesise the first chromium NHC complex (scheme 4.1). The chromium hydride precursor acts as a base in the same way as Ag₂O in the formation of silver(I)-NHC complexes described by Lin.⁶ Like Ag(I)-NHC complexes, Cr(0)-NHC complexes have also been applied in transmetallation reactions.⁷



Scheme 4.1 Synthesis of first Cr(0)-NHC complex.

Since the first chromium(0)-NHC complex, different synthetic methods have been reported using different sources of chromium; $\text{Cr}(\text{CO})_6$, $\text{Cr}(\text{CO})_3(\text{MeCN})_3$, $\text{Cr}(\text{CO})_5\text{THF}$ and $\text{Na}_2\text{Cr}_2(\text{CO})_{10}$, but isolating the complexes in reasonable yields can be difficult.⁸⁻¹² Chromium(0)-NHC complexes are well known, but not as widely studied as one may think, and this has been attributed to the lack of generally applicable synthetic procedures.¹³

More recently a template synthesis developed by Hahn and co-workers has successfully produced chromium(0)-benzanulated NHC complexes from isocyanides,^{12a} and a series of chromium(0)-NHC complexes have been isolated by Chung and co-workers,¹³ using Fischer carbene complexes as transfer agents (scheme 4.2). Yields of 40-60% were reported, which is preferable to the yields of less than 20% generally reported for some of the other methods.¹³



Scheme 4.2 Use of chromium Fischer carbene complex as chromium source.

4.1.2 Cr(I) and Cr(II)-NHC Complexes

N-heterocyclic carbene complexes of chromium(I) are extremely rare. Good donor ligands are required to stabilise Cr(I) complexes. NHC ligands are strong donors and in this sense should help stabilise Cr(I) d^5 complexes.

The first reported examples of NHC-containing Cr(I) complexes were described by Lappert and co-workers¹ in 1980 (figure 4.1). Interestingly, no Cr(I)-NHC pentacarbonyl complexes were reported by Lappert. Only complexes containing both phosphine and carbene ligands, or those with two NHCs, were prepared and characterised by EPR spectroscopy. The complexes with more donor ligands were reported to be more stable, with bulkier ligands imparting a greater stability. More recently Hirao and co-workers² reported the oxidation of a benzanulated NHC-Cr(0) complex and the resulting cationic complex was characterised by

EPR spectroscopy. They proposed that the delocalisation of the system resulted in the presence of the single electron within the benzimidazolylidene ring.²

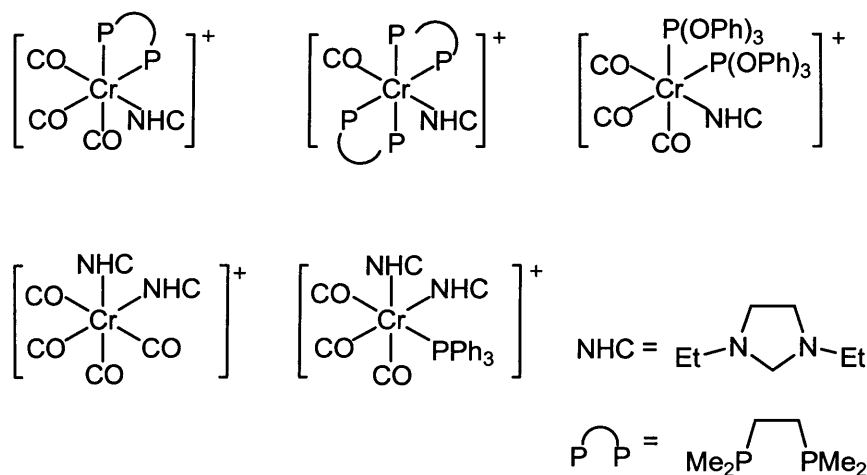


Figure 4.1 Cr(I)-NHC complexes prepared by Lappert *et al.*

NHC-Cr bonds are reported to be much stronger than phosphine-Cr bonds in Cr(0) complexes.¹⁴ This has been attributed to the fact that NHCs are more nucleophilic ligands than phosphines. This suggests that Cr(I)-NHC complexes should be stabilised to a greater extent than the phosphine-containing complexes. Another major difference is that NHC ligands bind to metals via σ -bonding while π -backbonding is negligible.¹⁵ This will result in stronger π -backdonation to the carbonyl ligands than in phosphine complexes.

The +II (d^4) oxidation state is a strongly reducing one for chromium and complexes require careful handling and storage to prevent oxidation. As a result Cr(II) complexes are not widely known, and represent a gap in our knowledge of chromium chemistry.

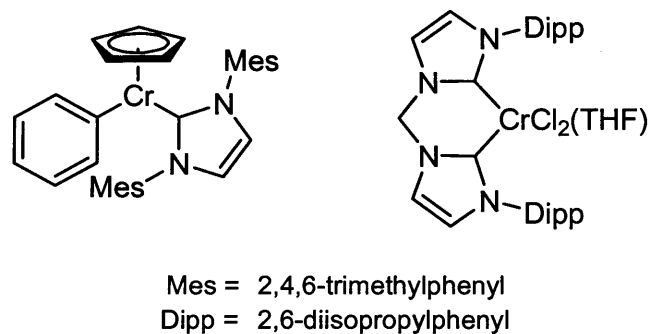


Figure 4.2 Examples of Cr(II)-NHC complexes.

The majority of early Cr(II) complexes reported were stabilised by a cyclopentadienyl ligand.¹⁶⁻¹⁹ More recently mono- and dimeric complexes have been reported with a variety of ligands.^{20,21,22} The complexes shown in figure 4.2 represent some of the only examples of Cr(II)-NHC complexes.^{3,4}

4.1.3 Role of Chromium(II) in the Ethylene Trimerisation Process

In terms of catalysis and the trimerisation of ethylene, significant evidence points toward a Cr(I)-Cr(III) redox process.²³⁻²⁵ However a Cr(II) catalytic system has been reported to show comparable activities and selectivities to the Cr(III) analogue.²⁰ Very few of the reported systems are based on isolated Cr(II) complexes, perhaps because of their sensitive nature, but a mechanism involving the initial reduction of trivalent systems to active Cr(II) species has been discussed in the literature.^{24,26-35} This active species is then proposed to undergo 2-electron oxidation as part of the metallocyclic mechanism, resulting in a Cr(II)-Cr(IV) redox couple.²⁰

4.2 Results and Discussion

4.2.1 Cr(0)-NHC Complexes

Chromium(0) complexes are relatively air stable, and as a result these d^6 systems have been widely reported. N-heterocyclic carbene complexes of Cr(0) were some of the first reported carbene-containing complexes⁵ and a lot of the early NHC work was carried out on group 6 metal complexes. As described in 4.1.1, there are several different synthetic procedures to these compounds.

A selection of Cr(0)-NHC complexes (figure 4.3) have been prepared from simple imidazolium salt precursors (**50-56**) in order to form a novel series of Cr(I)-NHC complexes via one electron oxidation as described with phosphine complexes in chapter 3. Compounds **65**, **66**, **69** and **70** are new, and **64**, **67** and **68** have been previously reported.^{12b, 13} As discussed in 4.1.2, Cr(I)-NHC compounds are extremely rare, with only 2 reported examples in the literature to date.^{1,2}

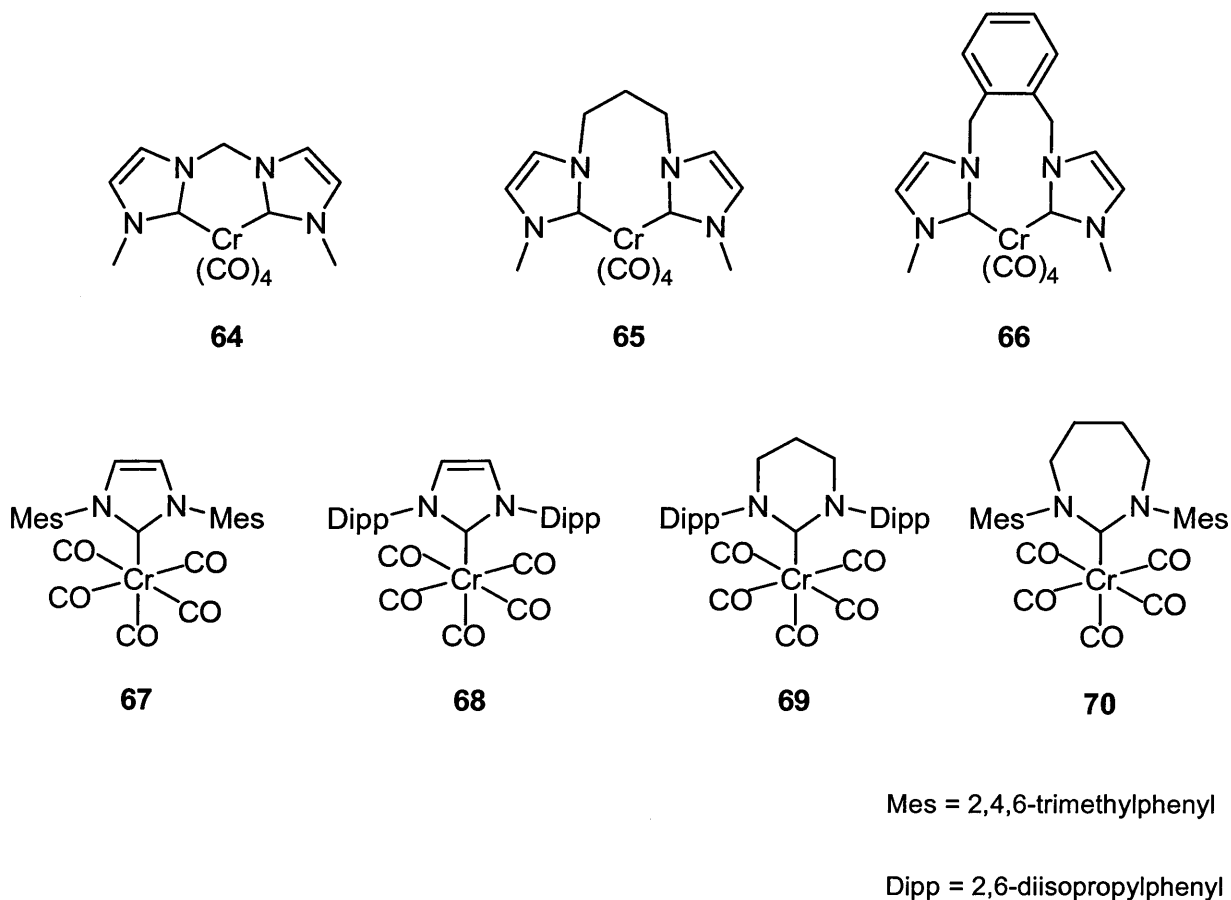
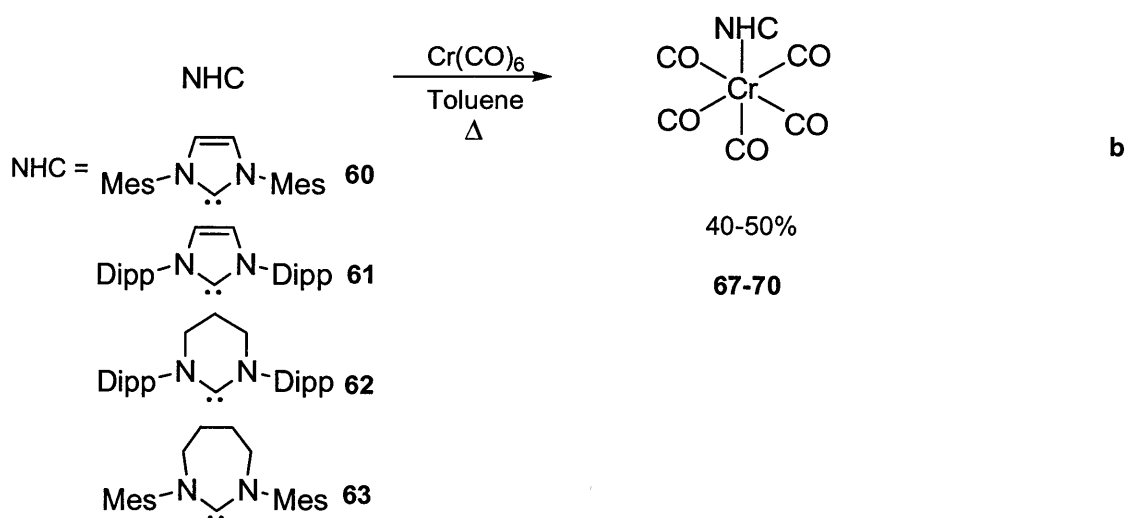
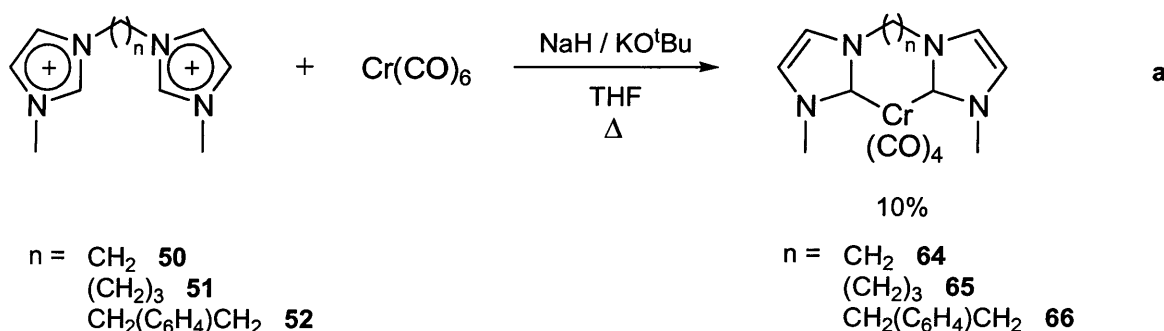


Figure 4.3 Cr(0)-NHC complexes prepared in this study (**64**, **67** and **68** are known compounds^{12b, 13}).

Complexes **64-66** containing bis(carbene) ligands were synthesised according to literature procedures¹² (scheme 4.3a). The imidazolium salts (**50-52**) were deprotonated *in situ* using sodium hydride as a base, with a catalytic amount of KO^tBu, forming free carbenes **57-59**. A method analogous to that used to prepare bis(phosphine)-Cr(0) complexes in chapter 3 was used for NHC complexes **67-70**.³⁶ The free carbenes (**60-63**) were formed first and then added to chromium hexacarbonyl in toluene, and then the mixture was heated for 48 h (scheme 4.3b).

A significant energy barrier needs to be overcome in order to remove a carbonyl ligand from the metal centre due to the thermodynamic stability of the complex. Free carbenes generally exhibit poor stability to heat, so it was considered that the high temperatures required may also result in decomposition of the free carbene. Products were however isolated in yields of around 45%. These yields are comparable to some of the better literature results, which often involve more steps.¹³



Scheme 4.3 Synthesis of Cr(0)-NHC complexes **64-70**.

While the monodentate NHC complexes were isolated in good yields, the bis(carbene) complexes were obtained in poor yields (~10%), and attempts to prepare these complexes in higher yield via different methods were unsuccessful. The consistently low yields obtained could be attributed to the presence of acidic protons α - to the nitrogen atoms, as discussed in chapter 2.

All chromium (0) complexes (figure 4.3) were characterised by ^1H and ^{13}C NMR spectroscopy. The characteristic absence of the imidazolium proton resonance at around 9 ppm in the ^1H NMR spectra was noted, as well as the large downfield shift in the position of the NCN signal in the ^{13}C NMR spectra. Two resonances between 200 and 220 ppm corresponding to the *cis*- and *trans*- carbonyl ligands were also observed, confirming the proposed structures.

Infra-red spectra were recorded for the bright yellow compounds **64-70** and were typical for complexes of the type $\text{Cr}(\text{CO})_4(\text{L})_2$ and $\text{Cr}(\text{CO})_5\text{L}$ with C_{2v} and C_{4v} symmetry respectively. As described in chapter 3, infra-red spectroscopy is a very important analytical tool for the purpose of confirming oxidation to Cr(I).

The carbonyl stretching frequencies for complexes **64-70** are shown in table 4.1. The significant increase in basicity of expanded NHCs, i.e. six- and seven-membered, has been previously noted,³⁷ and this is observed in the infra red spectra where we see lower wavenumbers, particularly for the seven-membered NHC complex **70**, than for the analogous five-membered pentacarbonyl systems. Lower wavenumbers are also observed for the chelating NHC complexes **64-66**, as a result of the extra electron density being donated to the metal centre by a second strongly electron donating carbene ligand.

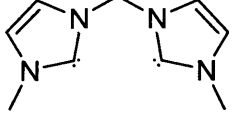
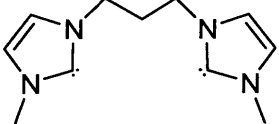
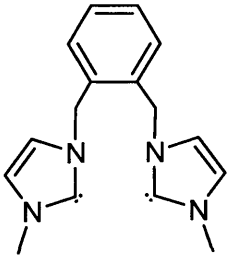


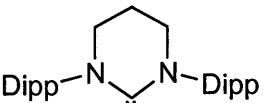
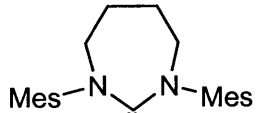
Cr(0) complex	Ligand	$\nu(\text{CO})/\text{cm}^{-1}$			Av
					$\nu(\text{CO})/\text{cm}^{-1}$
64		1870	1920	1951	1913
65		1861	1874	1980	1905
66		1823	1922	1976	1907
67		1922	2059	1990	
68		1923	2053	1988	
69		1927	2044	1985	
70		1925	2043	1984	

Table 4.1 Carbonyl stretching frequencies for Cr(0) complexes 64-70.

Interestingly, upon comparison of the tetracarbonyl complexes (**64-66**) with the bis(phosphine) complexes discussed in the previous chapter, we see much lower wavenumbers for the NHC complexes. From what we know about phosphines and carbenes as ligands, we would expect that phosphines, as weaker donors and with their ability to backbond to the metal centre, will lead to less electron density at the chromium resulting in lower M-CO backdonation, stronger C-O bonds and therefore higher wavenumbers. Carbenes on the other hand are strong σ -donors that do not generally undergo π -backbonding, so the extra electron density at the metal centre is donated to the carbonyl ligands, resulting in weaker C-O bonds and stretches at lower wavenumbers in the infra-red spectra.

Complex **64** and the propylene bridged bis(phosphine) complex **36** in the previous chapter are analogous, i.e. CNCNC and PCCCP. They both form six-membered metallacycles with chromium and when directly compared, one observes lower wavenumbers for the NHC containing complex **64**.

Crystals suitable for structure determination by single crystal X-ray methods were grown from a dichloromethane/methanol solution of **69**. The structure is shown in figure 4.4 and is, the first reported example of an expanded NHC-Cr(0) complex.

One can see from the structure shown in figure 4.4 that two of the equatorial carbonyl ligands are bent away from the NHC ligand. The average Cr-C-O angle reported¹³ for this type of complex is 176.4° and in complex **69** this angle is much smaller (166.3°) i.e. the bend is much greater, presumably due to the steric repulsions from such a sterically demanding ligand. A similar bend is observed, but to a lesser extent with the equivalent five-membered NHC-Cr(0) complex where an angle of 169.4° is reported.¹³ The difference between the five- and six-membered NHC complexes can be attributed to the larger NCN angle in expanded carbenes, which have been reported to force the N-substituents closer to the metal centre,⁴⁶ therefore having more impact on the carbonyl ligands. This impact of the N-substituents can be clearly seen in figure 4.4. The other two carbonyl ligands lie very close to the reported average, and appear to be unaffected by the extra bulk of the expanded carbene.

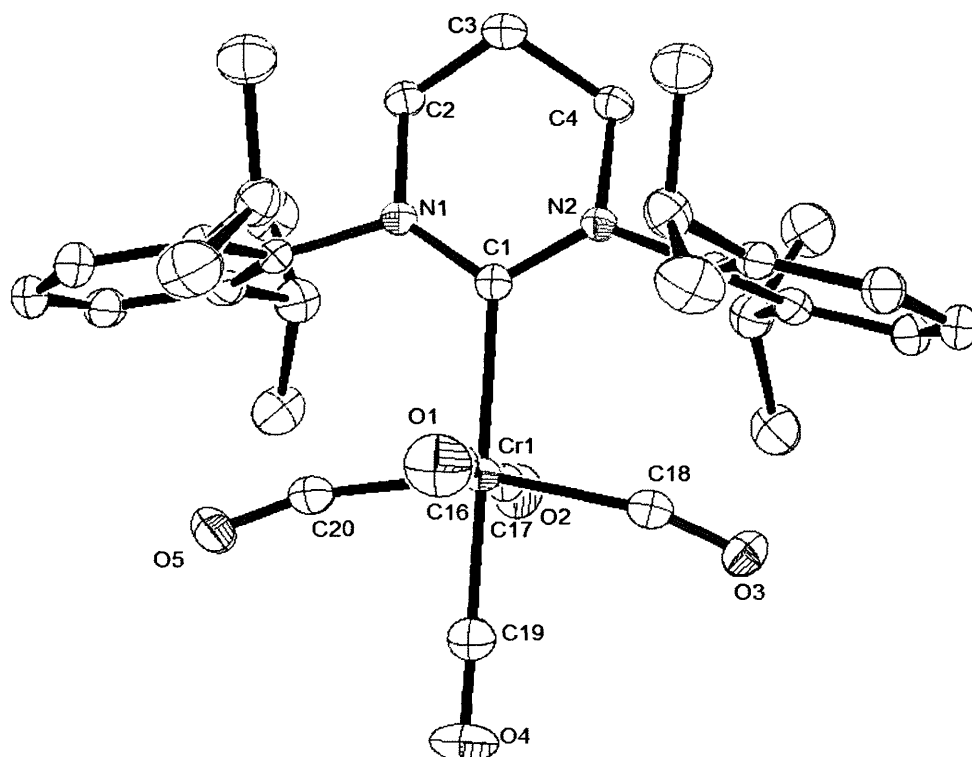


Figure 4.4 ORTEP plot at 50% probability of the molecular structure of **69**.

Lengths (Å)		Angles (°)	
C(1)-Cr(1)	2.210(2)	N(1)-C(1)-N(1)	114.24(19)
Cr(1)-C(16)	1.887(3)	C(1)-Cr(1)-C(16)	93.24(9)
Cr(1)-C(17)	1.905(3)	C(1)-Cr(1)-C(17)	85.71(9)
Cr(1)-C(18)	1.9056(18)	C(1)-Cr(1)-C(18)	99.41(5)
Cr(1)-C(19)	1.850(3)	C(1)-Cr(1)-C(19)	178.59(10)
Cr(1)-C(20)	1.9056(18)	C(1)-Cr(1)-C(20)	99.41(5)
C(16)-O(1)	1.150(3)	Cr(1)-C(16)-O(1)	174.3(2)
C(17)-O(2)	1.145(3)	Cr(1)-C(17)-O(2)	177.4(2)
C(18)-O(3)	1.149(2)	Cr(1)-C(18)-O(3)	166.38(15)
C(19)-O(4)	1.153(3)	Cr(1)-C(19)-O(4)	177.7(2)
C(20)-O(5)	1.149(2)	Cr(1)-C(20)-O(5)	166.38(15)
		C(18)-Cr(1)-C(19)	80.59(5)
		C(17)-Cr(1)-C(19)	92.89(11)

Table 4.2 Selected bond lengths (Å) and angles (°) for compound **69**.

4.2.2 Functionalised NHC-Cr(0) Complexes

Synthesis of Cr(0) complexes containing the functionalised NHC ligands shown in figure 4.5 was found to be much more problematic than the systems described above. Different procedures were attempted to obtain the complexes, but no functionalised NHC-Cr(0) complexes were isolated. However, a very interesting side reaction was observed (*vide infra*).

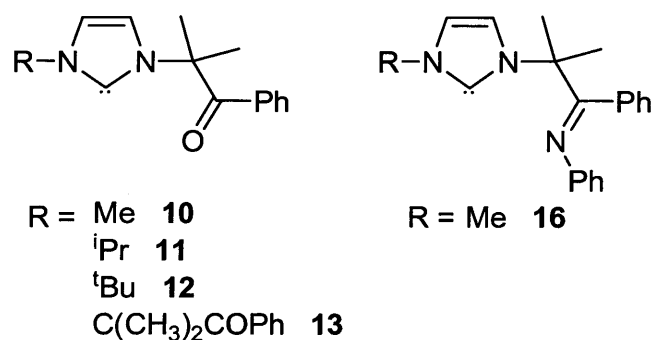
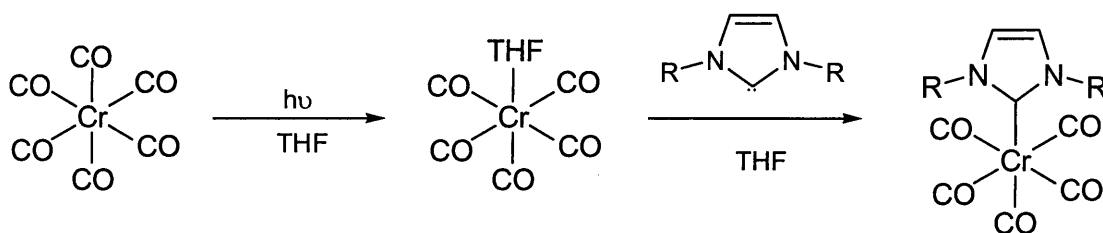


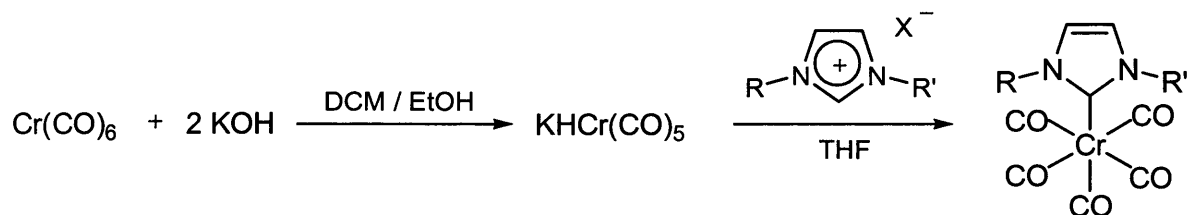
Figure 4.5 Functionalised free carbenes **10-13**, and **16**.

One standard method involves the use of $\text{Cr}(\text{CO})_5\text{THF}$ as a chromium source, prepared by photolysis of chromium hexacarbonyl in THF. This was carried out, as shown in scheme 4.4, followed by addition of the pre-formed free carbene. THF is much more labile than a carbonyl ligand, so should be easily displaced by the free carbene. After removal of the solvent, analysis of the crude product by NMR spectroscopy showed no resonances corresponding to the NHC. After repeating the reaction unsuccessfully with a non-functionalised NHC, it was concluded that this is not a particularly suitable method, as the monodentate non-functionalised NHC-Cr(0) is a known complex.



Scheme 4.4 Preparation of Cr(0)-NHC complex using photolysis.

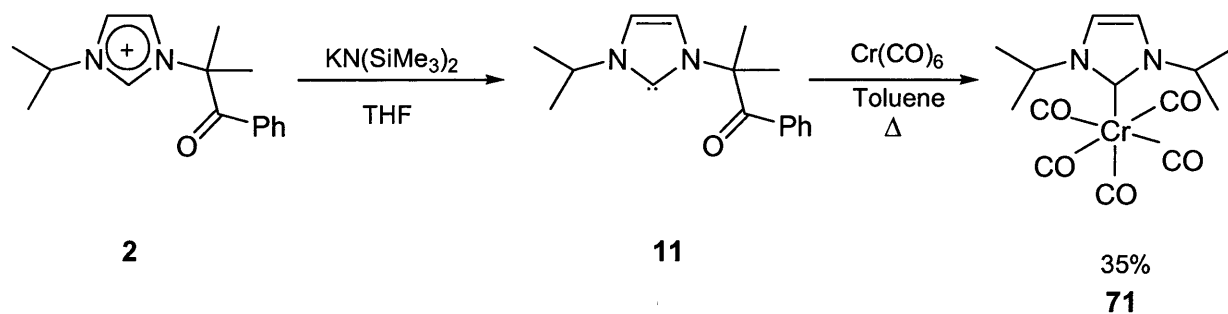
While the stability of the free carbenes were found to be relatively good (as discussed in chapter 2), a more recent report by Chauvin *et. al.*³⁸ describes a new route to a source of chromium complex suitable for reaction with imidazolium salts, similar to Öfele's original method.⁵ Unfortunately, no isolable product containing the functionalised NHC was obtained using this method (Scheme 4.5).



Scheme 4.5 Use of imidazolium salt to prepare Cr(0)-NHC complex.

The use of other chromium sources, including a Fischer carbene chromium(0) complex, $\text{Cr}(\text{CO})_3(\text{MeCN})_3$, as well as the *in situ* method successfully used for the bis-carbenes all proved unsuccessful, with no identifiable product being recovered. While many Cr(0)-NHC complexes have been reported in good yields using the chromium Fischer carbene complex as a transfer agent, none contained functionalised NHCs.

However, a very interesting result was observed when the free carbene **11** was heated with chromium hexacarbonyl in toluene (scheme 4.6) using the method described for the monodentate, non-functionalised complexes **67-70**. Analysis by NMR spectroscopy of the yellow crystalline solid showed that the ligand had decomposed to give the 1,3-diisopropyl NHC complex **71** shown in scheme 4.6.



Scheme 4.6 Unexpected reaction of functionalised NHC with $\text{Cr}(\text{CO})_6$.

Crystals suitable for X-ray were grown from a dichloromethane/methanol solution and the structure confirms the product as **71**. Selected bond lengths and angles are shown in Table 4.3, and lie within the range reported for Cr(0)-NHC complexes.⁸

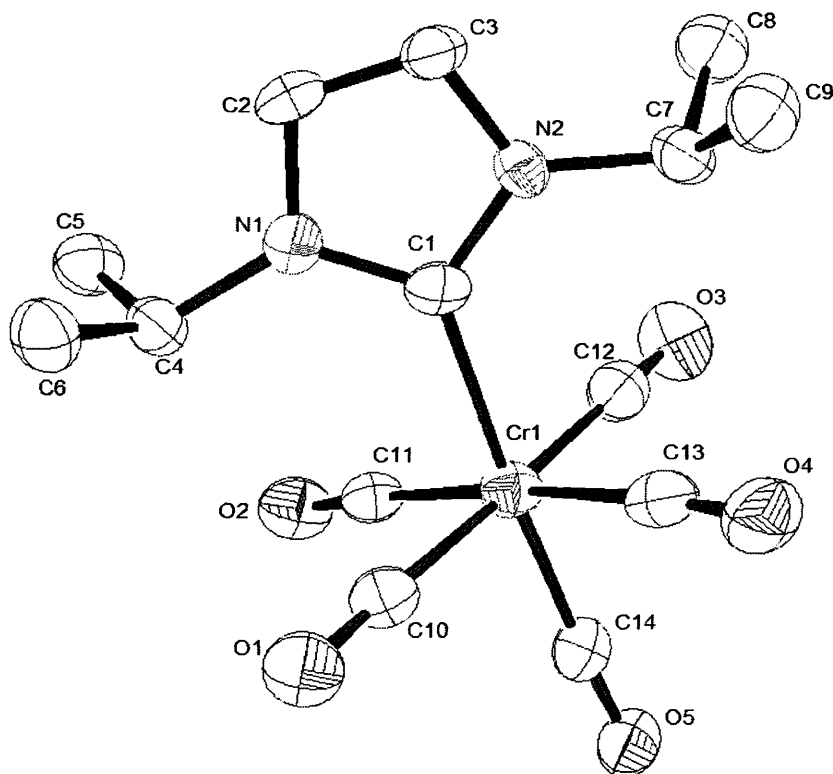


Figure 4.6 ORTEP plot at 50% probability of the molecular structure of **71**.

Lengths (Å)		Angles (°)	
C(1)-Cr(1)	2.154(7)	C(1)-Cr(1)-C(14)	176.2(3)
Cr(1)-C(14)	1.852(8)	C(1)-Cr(1)-C(10)	91.7(3)
C(14)-O(5)	1.152(7)	C(10)-Cr(1)-C(14)	91.3(3)
Cr(1)-C(10)	1.903(7)	N(1)-C(1)-N(2)	103.6(5)
C(10)-O(1)	1.138(7)		

Table 4.3 Selected bond lengths (Å) and angles (°) for compound **71**.

This reaction was repeated with the symmetrical di-ketone free carbene **13**, and the same product (**71**) was confirmed by NMR spectroscopy as well as mass spectrometry. When the reaction was carried out with the N-methyl free carbene **10** the resulting 1-methyl-3-isopropyl NHC complex **72** shown in figure 4.7 is isolated. The reaction was also repeated with the N-methyl imine-functionalised free carbene **16** and the same result was again observed. It is known that imines are readily hydrolysed back to ketones, even in the presence of traces of moisture, as discussed in chapter 2, so it is perhaps unsurprising that under these forcing conditions one observes the same result.

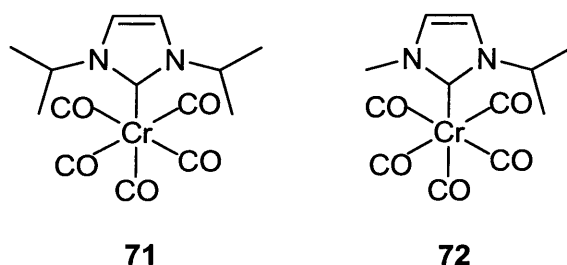


Figure 4.7 Structures of dialkyl NHC-Cr(0) complexes.

In order to obtain information about the mechanism of this unexpected reaction, experiments were repeated using deuterated solvents (toluene and methanol) to see if and where deuterium uptake was taking place. At least one proton was required in the case of **11**, whereas two were required when the symmetrical NHC **13** was used. No deuterium uptake was observed, suggesting that the source of the hydrogen(s) was the ligand itself and not the solvent.

The salt was heated in toluene with no chromium source and was found to remain intact. Heating the free carbene in toluene caused decomposition, but not to the di-isopropyl NHC, as might be expected, just to an unidentifiable residue.

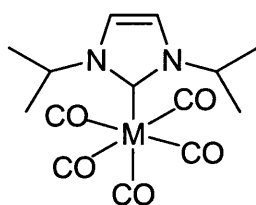
Benzaldehyde was assumed to be lost during the reaction, but is generally not classed as a good leaving group, and analysis of all reaction components did not reveal the presence of PhC(H)O. A mass spectrum of the methanol washings did however, show a small amount of the functionalised NHC-Cr(0) pentacarbonyl complex, which could not be isolated, leading us to believe that it was present only in very small quantities. This suggests that

coordination of the intact ligand initially takes place, but does not chelate. NHCs are noted for the robustness of the complexes they form, with excellent thermal stabilities at temperatures up to 290 °C reported.^{3,39} It is therefore surprising that the complex seems to form and then break down, as suggested by these results.

Based on the assumption that coordination of the NHC takes place before degradation of the ligand, reactions were carried out at different temperatures and reaction times in an attempt to find the point at which this degradation occurs. When lower temperatures and shorter timeframes were used, chromium hexacarbonyl was recovered and decomposition of the free carbene is observed to material that could not be identified.

Consistent isolated yields of around 35% of complex **71** led us to believe that since the reactions were carried out under anhydrous conditions, the extra protons were being abstracted from the ligand itself, suggesting an intermolecular mechanism is taking place. As far as we are aware, no reports of this type of metal-mediated ligand degradation are present in the literature.

Since this ligand degradation only occurred in the presence of the metal source, the reaction was repeated with the other group 6 metals, molybdenum and tungsten hexacarbonyl, under the same reaction conditions. Interestingly, the isolated products, which are shown in figure 4.8, show that this unusual reaction is not exclusive to chromium.



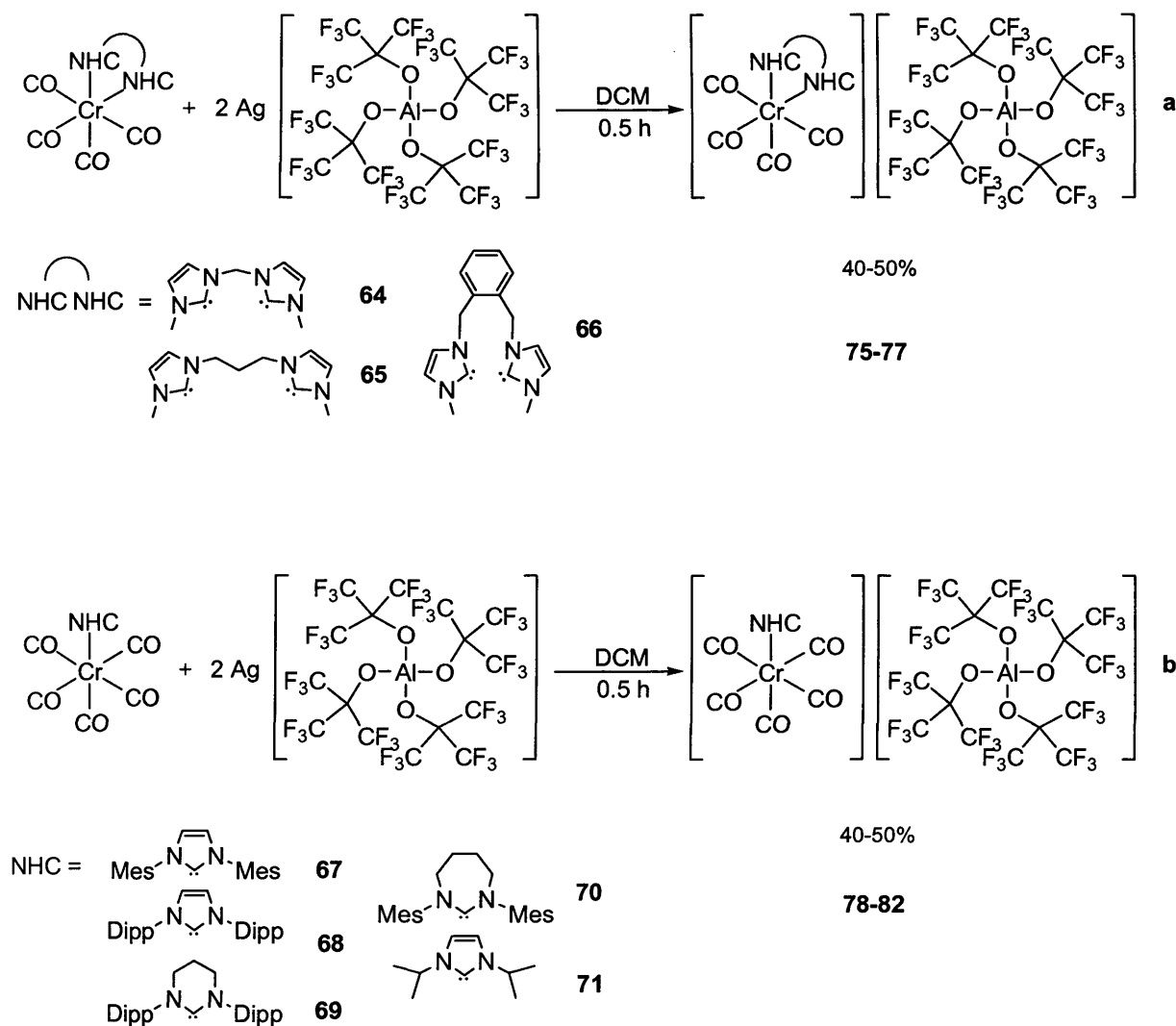
M = Mo **73**
W **74**

Figure 4.8 Molybdenum and Tungsten complexes isolated.

4.2.3 Synthesis and Characterisation of Chromium(I)-NHC Complexes

Synthesis of cationic chromium(I)-NHC complexes **75-82** was carried out by one-electron oxidation (scheme 4.8) using $\text{Ag}[\text{Al}(\text{OC}(\text{CF}_3)_3)_4]$ as described in chapter 3. However the resulting complexes are significantly less stable than those of the phosphines, so the reaction time was reduced to just 30 minutes.

An immediate colour change was observed upon addition of the solvent, from bright yellow to red-purple, but if the reaction mixture was left to stir for 16 hours, a further colour change to pale yellow was observed, and infra-red analysis of this product suggested decomposition of the complex to the chromium(0) precursor. This has been reported by Wass and co-workers³⁶ with similar diphosphine Cr(I) systems, with half-lives between 4 and 24 h at room temperature. Complexes **81** and **82** were found to be particularly sensitive, and began to lose their intense colour during removal of the solvent after 30 min. Infra red data were collected, but EPR data could not be obtained for **81** and only a very poor EPR spectrum was obtained in the case of **82**.



Scheme 4.7 Synthesis of Cr(I) complexes 75-82.

The fact that the Cr(I)-NHC complexes **75-82** were found to be even more unstable than the Cr(I)-phosphine systems described in the previous chapter was expected for the monodentate NHC complexes, due to the lack of additional stability as a result of the chelate effect. The lack of large substituent groups on the chelating bis(carbene) complexes **75-77** could result in lower steric protection than the analogous bis(phosphines), which contain large phenyl group substituents, this has been shown to affect metal-donor bond strength,¹⁴ and therefore could partially contribute to the lower stability.

Unfortunately, attempts to obtain mass spectra failed for all of these complexes. This was attributed to their extremely sensitive nature, and crystals suitable for X-ray analysis could not be grown due to the instability of these complexes in solution.

Analysis by infra-red and EPR spectroscopies confirms the formation of chromium(I) complexes **75-82**. Carbonyl stretching frequencies are displayed in table 4.4, and it can be seen that significant shifts in the carbonyl stretching frequencies are observed upon oxidation. One sees these higher wavenumbers due to the reduced electron density available at the metal centre in the 17-electron complex. Upon comparison with the chelating phosphine complexes **43-49** in the previous chapter, it is clear that there is more electron density available at the metal centre in the chelating NHC complexes, possibly due to the lack of backbonding occurring in the carbene systems.

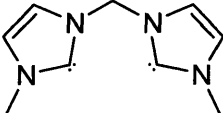
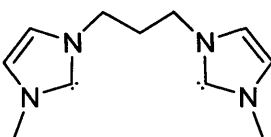
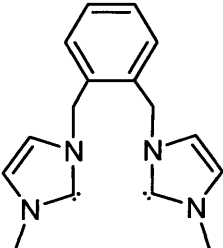
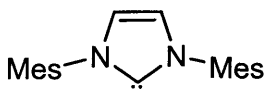
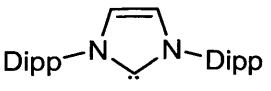
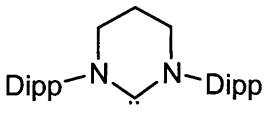
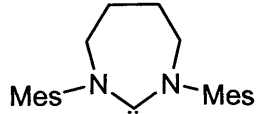
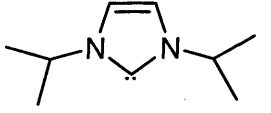
Cr(I) complex	Ligand	$\nu(\text{CO})/\text{cm}^{-1}$	
		Cr(0)	Cr(I)
75		1870	1986
		1920	2015
		1951	2047
76		1861	1982
		1874	2019
		1980	2043
77		1823	1980
		1922	2021
		1976	2054
78		1922	2011
		2059	2129
79		1923	2013
		2053	2119
80		1927	2056
		2044	2143
81		1925	2044
		2043	2128
82		1921	2030
		2054	2132

Table 4.4 Carbonyl stretching frequencies for Cr(I) complexes 75-82.

4.2.4 EPR Studies

The X-band *cw*-EPR spectra were recorded for complexes **75** – **80**, and the resulting spectra are shown below in figures 4.9 - 4.14. The EPR spectra of **81** and **82** were also recorded, but their quality was very poor, suggesting the cell may have leaked (leading to sample decomposition).

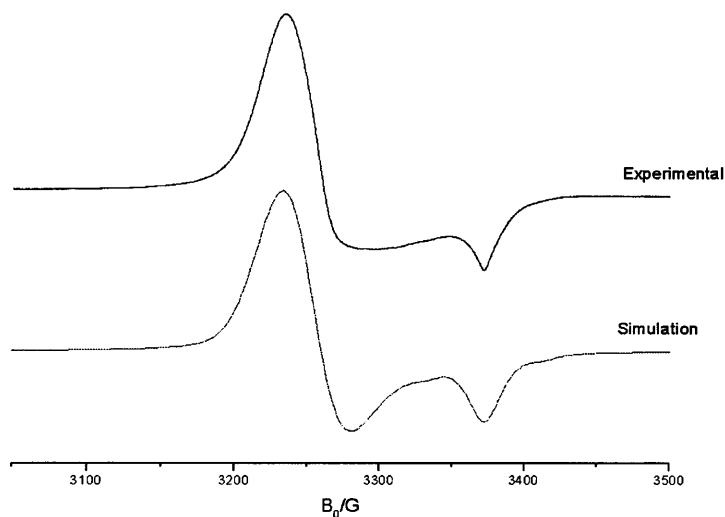


Figure 4.9 Experimental and simulated *cw*-EPR spectra (130K) of complex **75**.

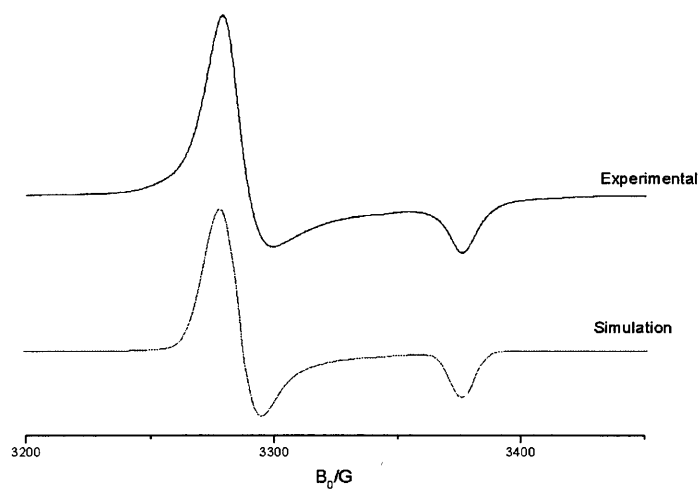


Figure 4.9 Experimental and simulated *cw*-EPR spectra (130K) of complex **76**.

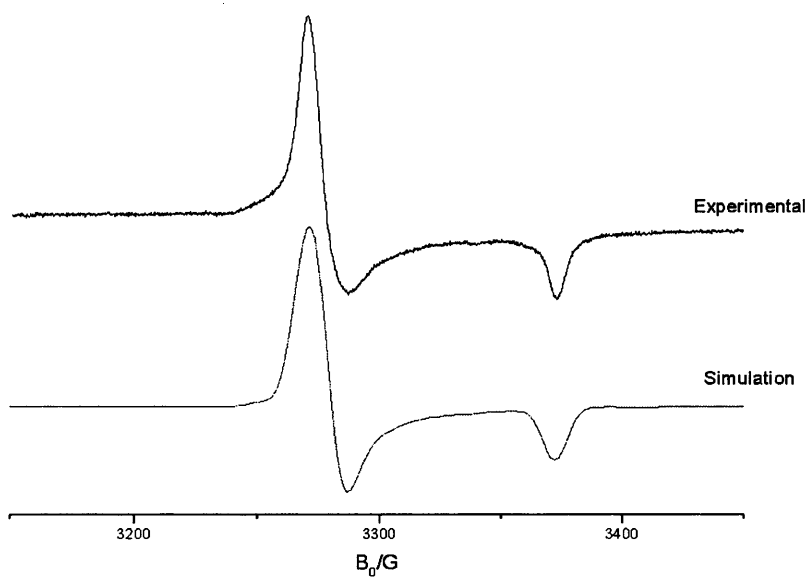


Figure 4.9 Experimental and simulated cw-EPR spectra (130K) of complex 77.

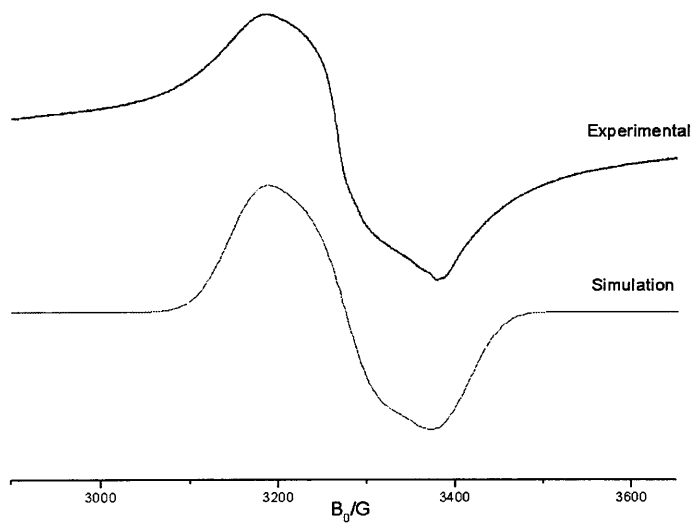


Figure 4.9 Experimental and simulated cw-EPR spectra (130K) of complex 78.

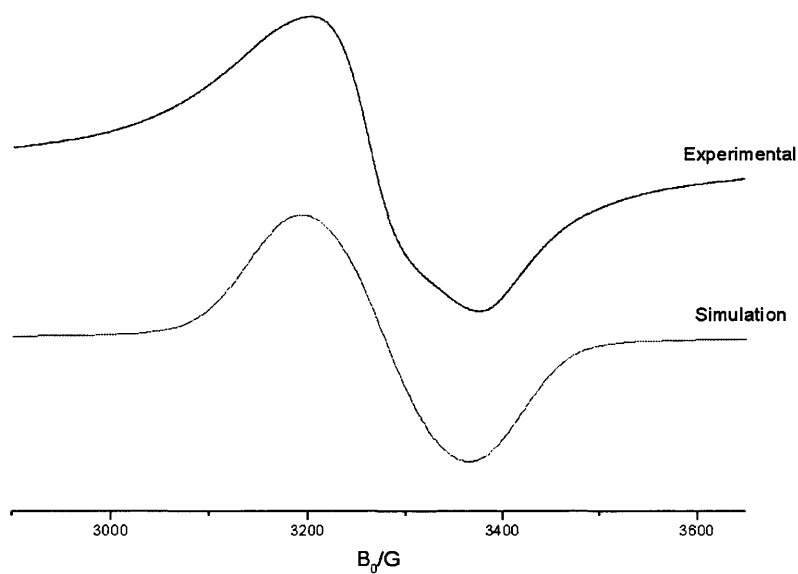


Figure 4.9 Experimental and simulated cw-EPR spectra (130K) of complex 79.

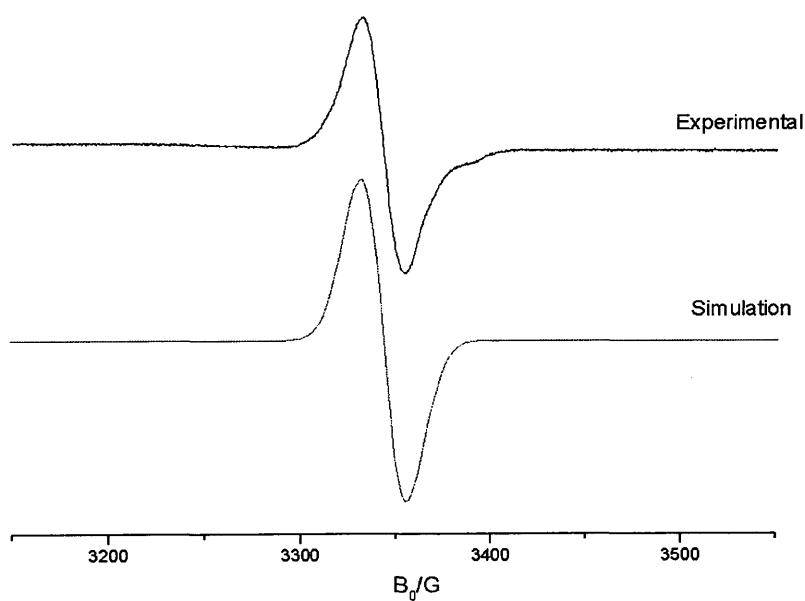


Figure 4.9 Experimental and simulated cw-EPR spectra (130K) of complex 80.

Complex	g and A values
76	$g_{\perp} = 2.045, g_{\parallel} = 1.988$ $^{53}\text{Cr}: A_{\perp} = 15\text{G}, A_{\parallel} = 23\text{G}$
77	$g_{\perp} = 2.047, g_{\parallel} = 1.988.$ $^{53}\text{Cr}: A_{\perp} = 15\text{G}, A_{\parallel} = 23\text{G}$
78	$g_{zz} = 1.979, g_{yy} = 2.045, g_{xx} = 2.11$
79	$g_{zz} = 1.982, g_{yy} = 2.045, g_{zz} = 2.1$

Table 4.5 g and A values for complexes 76-79.

Monosubstitution or disubstitution is equivalent to a tetragonal distortion from octahedral symmetry. In the case of MA_5B (C_{4v} symmetry), *trans*- MA_4B_2 (D_{4h} symmetry) or *cis*- MA_4B_2 (C_{2v} symmetry) complexes, the t_{2g} orbitals split into b_2 or $b_{2g}(d_{xy})$ and e or $e_g(d_{xz}, d_{yz})$ (figure 4.15). As was already described in the chapter three, the g tensor for the $[\text{Cr}(\text{CO})_4\text{PNP}]^+$ complexes was consistent with a SOMO based primarily on a d_{xy} ground state. In that case, the z -axis of the ‘disubstituted’ (bidentate) complex (defined as the CO-Cr-CO direction) was unique. In the current situation, the monodentate and bidentate carbenes complexes of Cr(I) will lead to different extents of tetragonal distortion away from octahedral symmetry. According to the EPR spectra of the bidentate complexes 75, 76 and 77 shown above, they all had a pronounced axial symmetry with $g_{\perp} > g_e > g_{\parallel}$ and the resulting g tensor was in fact very similar to that observed in chapter three for the $[\text{Cr}(\text{CO})_4\text{PNP}]^+$ complexes. This indicates that the Cr carbene complexes 75, 76 and 77 must possess a SOMO where the metal contribution is primarily d_{xy} .

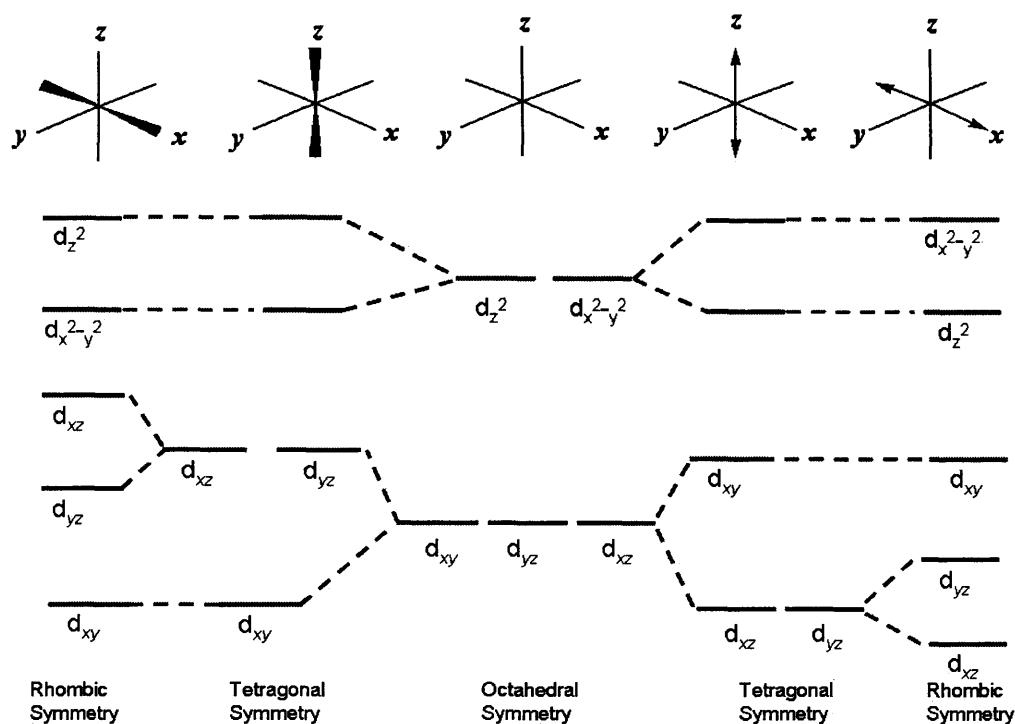


Figure 4.15 Effects of symmetry on electronic structure.

However, in the case of the monodentate complexes **78** and **79**, the profile of the EPR spectra changes to rhombic symmetry. The g values extracted by simulation were approximately 2.11, 2.045 and 1.979 for both complexes (Table 4.5). These EPR spectra indicate that a further rhombic distortion must be occurring to the t_{2g} set. Two situations can account for this, as illustrated in figure 4.15. The left hand side of the figure represents the common $(d_{xy})^2(d_{xz}, d_{yz})^3$ electronic ground state whereas the right hand side corresponds to the less common $(d_{xz}, d_{yz})^4(d_{xy})^1$ ground state. The unique x -axis in the monodentate complex lifts the degeneracy of the d_{xz} , d_{yz} orbitals, so the resulting EPR spectrum would be expected to possess a rhombic profile. In this case two components of the tensor (g_{xx} and g_{yy}) would be expected to be greater than g_e , whilst one component (g_{zz}) should be lower than g_e . This is indeed observed experimentally ($2.11, 2.045 > g_e$; $1.979 < g_e$) and suggests that the Cr(I) monodentate carbene complex also possess the d_{xy} ground state.

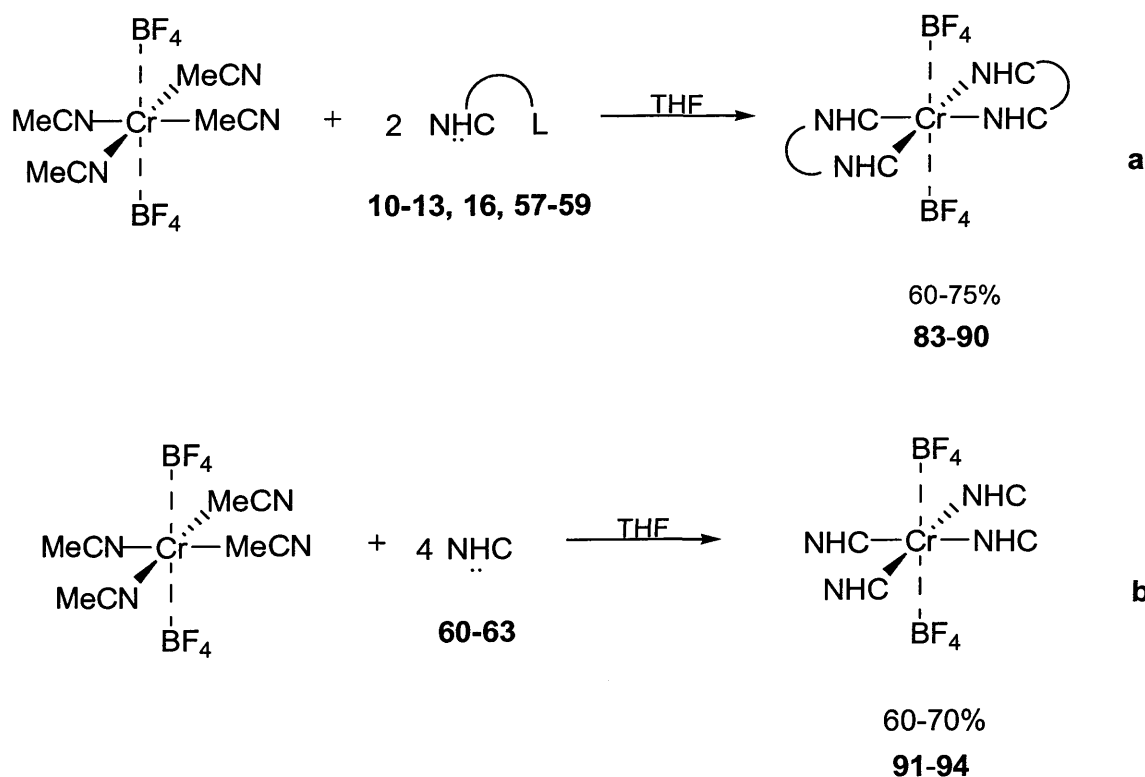
It should be mentioned that one cannot rule out the possibility of a complex possessing a d_{yz} ground state, with the $(d_{xy})^2(d_{xz}, d_{yz})^3$ electronic ground. In that case, two EPR situations can arise; one is characterised by a single feature EPR signal with $g_{\max} > 3$, while the other has a rhombic profile with $g_{\max} < 3$. Nevertheless, owing to the similarity in the

bonding features of the monodentate pentacarbonyl and bidentate tetracarbonyl Cr(I) complexes, it is most likely that this SOMO based on d_{yz} does not occur.

A final peculiarity arises with the complex **80**, that appears to produce an isotropic signal = 2.004. There is no obvious explanation why this occurs, and indeed what symmetry of complex would give rise to non-degenerate states. For the moment, one must assume this result is anomalous, and further experiments are required to better understand the EPR features of this complex (**80**) along with complexes **81** and **82** (which, as stated earlier, did not produce resolved spectra).

4.2.5 Cr(II)-NHC Complexes

Most reported Cr(II) complexes rely on carbonyl, or other strongly π -accepting ligands to impart stability to the low oxidation state, such as cyclopentadienyl,⁴⁰ complexes containing NHCs are extremely rare. We have prepared a series of Cr(II)-NHC complexes in good yield as shown in scheme 4.8, using tetrakis(acetonitrile)Cr(II)bis(tetrafluoroborate), which was prepared according to a literature procedure.⁴¹ Complexes containing functionalised and non-functionalised carbenes have been included.



Scheme 4.8 Preparation of Cr(II)-NHC complexes containing chelating and monodentate ligands.

The substitution reaction is much easier than in the case of chromium hexacarbonyl; forcing conditions were not required, and functionalised carbene ligands remain unchanged. The pre-formed free carbene is added to a blue suspension of $\text{Cr}(\text{MeCN})_4(\text{BF}_4)_2$ in THF. An immediate colour change was observed, and the mixture stirred at room temperature for 16 h, after which the THF solution was concentrated and diethyl ether added to precipitate the complexes shown in figure 4.16.

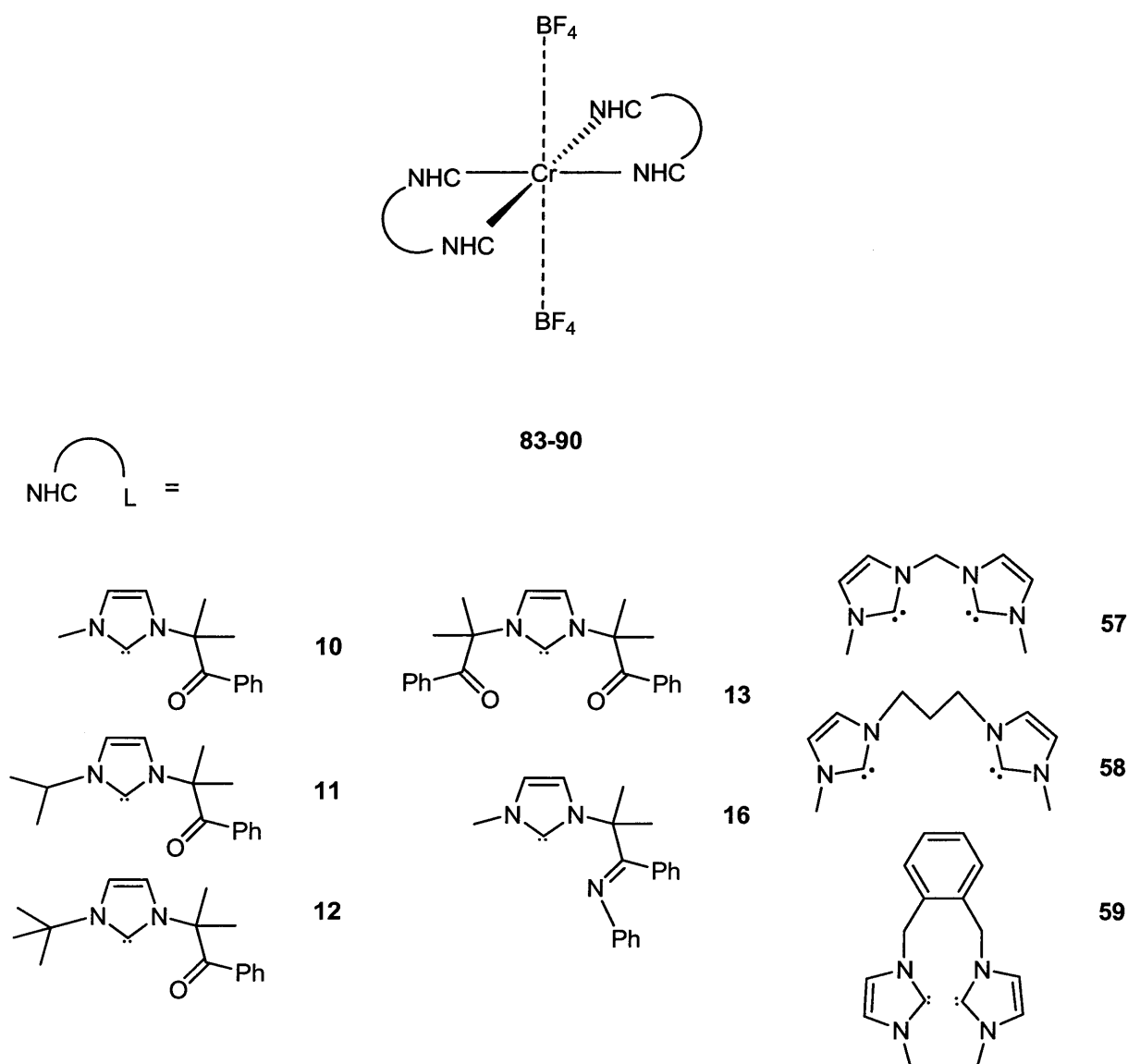


Figure 4.16 Cr(II) complexes with chelating NHC ligands.

Complexes **83-94** were isolated as brightly coloured solids for which characterisation techniques were limited due to the very sensitive nature toward air and moisture. Cr(II) complexes are paramagnetic and therefore broad, uninformative NMR spectra were obtained,

however, NMR data was used to determine magnetic susceptibilities (*vide infra*). The complexes are also EPR silent. This observation is consistent with those reported for other paramagnetic Cr(II) complexes,¹⁹ and is due to the very short spin-lattice relaxation times associated with these high spin d^4 systems.

Complexes **83-90** were characterised by elemental analysis which suggests the equatorial arrangement of the chelating NHCs as shown in figure 4.16. Complex **86** contains a potentially tridentate NHC, but the elemental analysis data shows the presence of two NHCs and two BF_4 ligands. Compounds **91-94**, however, showed ambiguous results, this could be due to the fact that these monodentate species are significantly less stable than complexes **83-90**, which have added stability due to the chelate effect. The proposed structures in figure 4.17 seem likely given the lability of the acetonitrile ligands, and the presence of four equivalents of free carbene in the reaction mixture. Analysis by mass spectroscopy provided no meaningful information about the structure of the complexes, this was also reported in the literature for one of the first Cr(II)-NHC complexes.⁴²

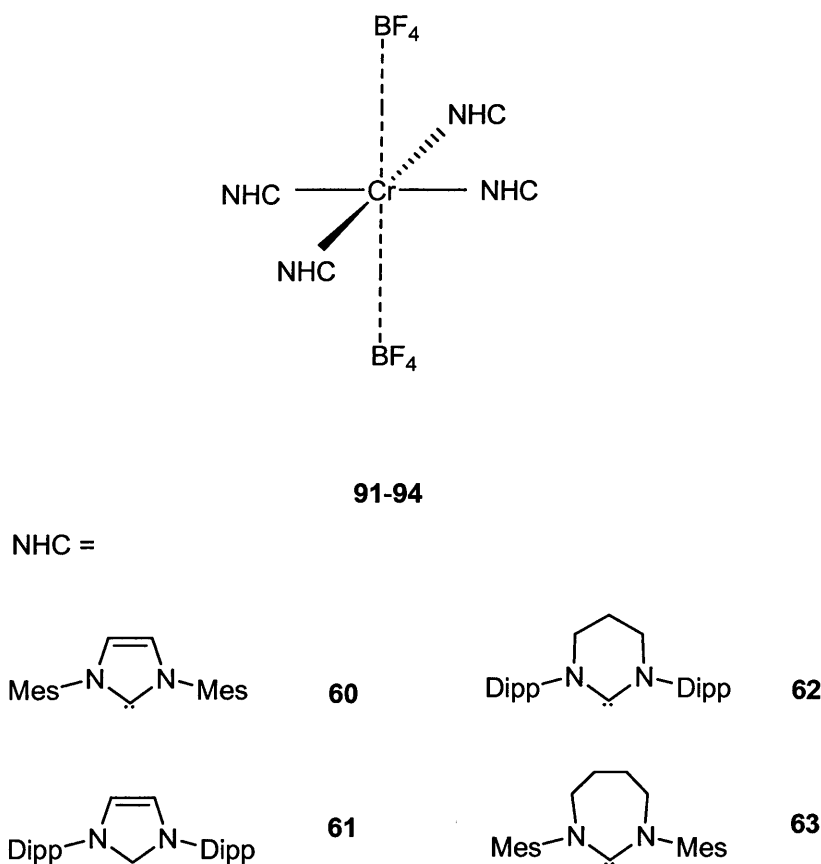


Figure 4.17 Cr(II) complexes with monodentate NHC ligands.

Magnetic susceptibilities were measured for Cr(II) complexes **83-94**, following Evans' method,⁴³ the most convenient method given the sensitive nature of the compounds. A sealed capillary tube containing 2% TMS in CDCl_3 was placed in a known concentration of the complex in CDCl_3 and the NMR spectra obtained, the paramagnetic solution was then spiked with the same concentration of TMS and a second NMR acquired. The resulting shift in the TMS resonance (figure 4.17) as a result of the paramagnetic complex in solution can be used to determine the magnetic susceptibility, and therefore the effective magnetic moment of the complex. The solution magnetic susceptibilities of these complexes was found to be between 4.66 and 5.14 μ_B , indicating high-spin d^4 ions, as reported for similar systems.⁴¹

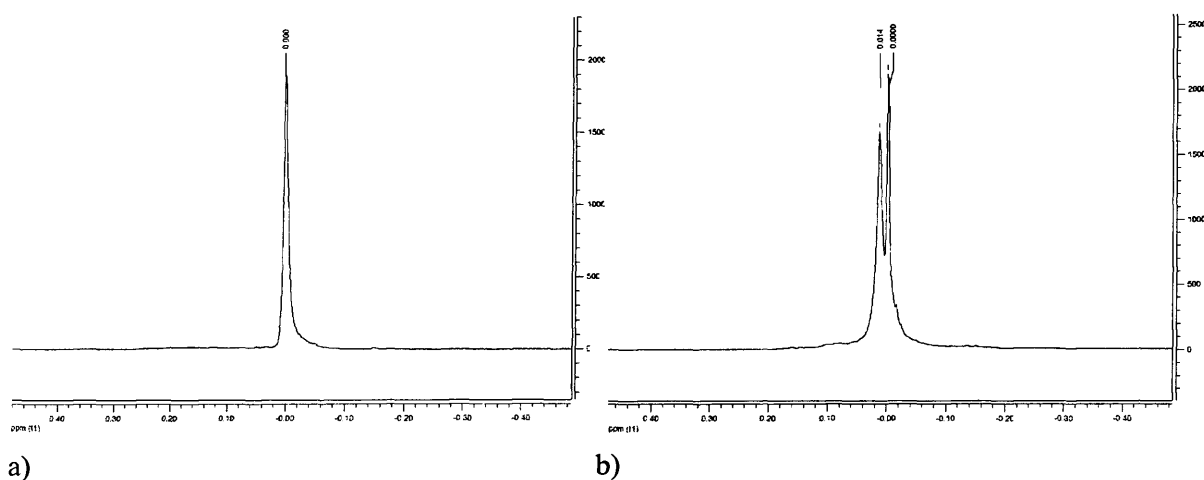


Figure 4.18 a) TMS in sealed capillary b) TMS in paramagnetic solution of **83**.

Electronic spectra were obtained by sealing a known concentration of the complex in dichloromethane in a glass cuvette inside the glovebox. There is very little data in the literature with which to compare these spectra, as electronic spectra of chromium(II) complexes are notoriously difficult to obtain⁴⁴ presumably due to their ease of oxidation to Cr(III). Theoretically, high-spin d^4 systems in pure octahedral complexes should show two absorptions, corresponding to two transitions. The effect of Jahn-Teller distortions, however, causes one of the transitions to split, resulting in three absorptions.

Complexes of the type we are interested in have D_{4h} symmetry, and are expected to result in the same splitting as observed in the Jahn-Teller distorted octahedral complexes. In practice, unless low temperatures are used this splitting is not observed, and two absorptions broaden into one. The spectra obtained for complexes **83-94** show one clear absorption at

around 500-600 nm, which is comparable to reported data⁴⁴ and corresponds to the $^5A_{1g} \leftarrow ^5B_{1g}$ transition, the lower energy transitions were not observed (figure 4.19).

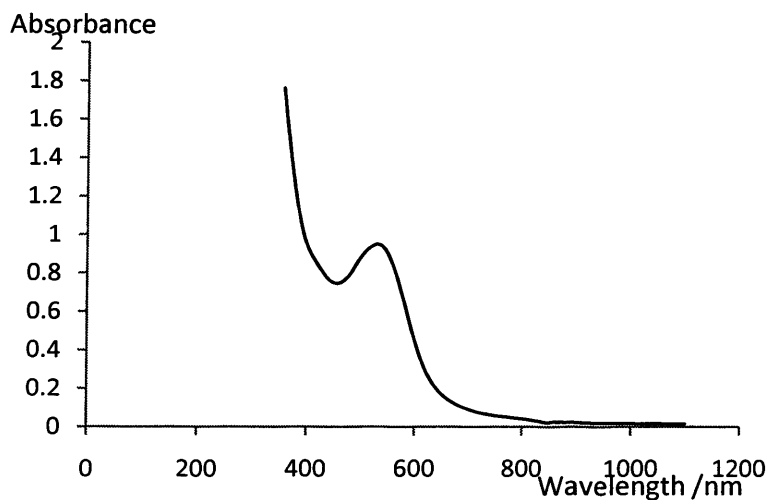


Figure 4.19 UV spectrum of 83.

For monodentate complexes **91-94**, UV data and magnetic susceptibilities seem to be in line with the other complexes of this type, however the lack of any further data means that they cannot be unambiguously characterised.

4.3 Conclusion

A series of chromium(0)-NHC complexes has been prepared, and the first example of an expanded NHC-Cr(0) complex structurally characterised. Oxidation of these compounds led to the characterisation of Cr(I)-NHC complexes of the type not previously reported. These complexes have been analysed by EPR spectroscopy, where they compare to the analogous Cr(I)-bis(phosphine) complexes previously reported. In particular, they appear to possess similar electronic properties with a SOMO based on a metal contribution of d_{xy} .

An unusual reaction has been described when attempting to prepare chromium(0) complexes containing functionalised NHC ligands, in which the ligand appears to break down under the reaction conditions employed. We have also reported a series of characterised Cr(II) complexes containing chelating NHC ligands in a square planar geometry, which are the first of their type to be reported as far as we are aware.

4.4 Experimental Section

General Procedures. All manipulations were performed using standard Schlenk techniques under an argon atmosphere, or in a nitrogen atmosphere MBraun UNILAB glovebox with less than 0.1ppm water and O₂. Solvents were dried using a Braun Solvent Purification System, and degassed prior to use. Free carbenes **10-13**, **16**, **57-63** were prepared according to literature procedures⁴⁶ or as described in 2.4, Cr(0) complexes **64-70**,^{12,36,45,46} silver aluminate [Ag[Al(OC(CF₃)₃)₄]]⁴⁷ and chromium(II) precursor [Cr(MeCN)₄(BF₄)₂]⁴¹ were prepared according to literature procedures.

NMR spectra were recorded at 298 K on Bruker Avance AMX 400 or Bruker-ACS 60 spectrometers. Chemical shift values are given relative to residual solvent peak. ESI-MS were performed on a Waters LCT Premier XE instrument. Infra-red spectra were recorded using a JASCO FT/IR-660 *Plus* spectrometer and analysed in solution (dichloromethane). Electronic spectra were recorded in dichloromethane on a Perkin Elmer Lambda 900 UV/VIS/NIR spectrometer. EPR spectra and computer simulations were carried out with the assistance of Lucia McDyre, a PhD student at Cardiff University. EPR spectra were recorded at 130K on an X-band Bruker EMX spectrometer operating at 100 kHz field modulation, 10mW microwave power and equipped with a high sensitivity cavity (ER 4119HS). EPR computer simulations were performed using the SimEPR32 program.⁴⁸ g Values were determined using a DPPH standard. Complexes were dissolved in 200µl DCM/toluene and a frozen solution produced by placing the EPR tube in liquid nitrogen.

cis-Tetracarbonyl-[1,1'-methylene-3,3'-dimethylimidazole-2,2'-diylidene]chromium (64)

Di-imidazolium salt **50** (1.5 g, 4.44 mmol) and chromium hexacarbonyl (980 mg, 4.44 mmol) were suspended in THF (30 ml). NaH (213 mg, 8.88 mmol) and KO^tBu (50 mg, 0.44 mmol) were added, and the yellow mixture heated to reflux for 6 h. After cooling to room temperature, the solvent was removed *in vacuo* and the residue washed with methanol (2 × 20 ml). Extraction with THF (3 × 20 ml) and filtration through silica, followed by removal of the solvent *in vacuo* resulted in isolation of a yellow microcrystalline solid (150 mg, 9.9 %). ¹H NMR (acetone-d₆, 400 MHz, 298 K): δ (ppm) 7.29 (d, 2H, NCHCHN, ³J_{HH} = 1.6 Hz), 7.07 (d, 2H, NCHCHN, ³J_{HH} = 2.0 Hz), 5.98 (s, 2H, NCH₂N), 3.80 (s, 6H, NCH₃). ¹³C {¹H} NMR (acetone-d₆, 125 MHz, 298 K): δ (ppm) 221.5 (CO), 211.3 (CO), 201.5 (NCN), 121.9 (NCHCHN), 120.2 (NCHCHN), 61.8 (NCH₂), 36.7 (NCH₃). High

Resolution ESI_{pos}-MS (MeCN): found 340.0430 (C₁₃H₁₂N₄O₄Cr⁺ requires 340.0421 dev: 2.6 ppm). IR (CH₂Cl₂): $\nu = 1951$ (s) (CO), 1920 (s), 1870 (s) (CO) cm⁻¹.

cis-Tetracarbonyl-[1,1'-propylene-3,3'-dimethylimidazole-2,2'-diylidene]chromium (65)

An analogous method to that of **64** was followed, using salt **51** (2.0 g, 5.47 mmol), chromium hexacarbonyl (1.2 g, 5.47 mmol), NaH (262 mg, 10.9 mmol) and KO^tBu (60 mg, 0.54 mmol). The product was obtained as a yellow microcrystalline solid (200 mg, 9.95 %). ¹H NMR (acetone-d₆, 400 MHz, 298 K): δ (ppm) 7.19 (d, 2H, NCHCHN, ³J_{HH} = 1.7 Hz), 7.05 (d, 2H, NCHCHN, ³J_{HH} = 1.8 Hz), 3.97 (s, 6H, NCH₃), 3.78 (m, 2H, NCH₂), 3.66 (m, 2H, NCH₂), 1.62 (m, 2H, NCH₂CH₂). ¹³C {¹H} NMR (acetone-d₆, 125 MHz, 298 K): δ (ppm) 225.9 (CO), 211.5 (CO), 202.5 (NCN), 124.6 (NCHCHN), 120.2 (NCHCHN), 45.6 (NCH₂), 40.1 (NCH₃), 34.5 (CH₂). High Resolution ESI_{pos}-MS (MeCN): found 368.0593 (C₁₅H₁₆N₄O₄Cr⁺ requires 368.0577 dev: 4.3 ppm). IR (CH₂Cl₂): $\nu = 1861$ (s) (CO), 1874 (s) (CO), 1980 (s) (CO) cm⁻¹.

cis-Tetracarbonyl-[1,1'-xylylene-3,3'-dimethylimidazole-2,2'-diylidene]chromium 66

An analogous method to that of **64** was followed, using salt **52** (1.5 g, 3.5 mmol), chromium hexacarbonyl (771 mg, 3.5 mmol), NaH (168 mg, 7.0 mmol) and KO^tBu (40 mg, 0.35 mmol). The product was obtained as a yellow microcrystalline solid (130 mg, 8.6 %). ¹H NMR (acetone-d₆, 400 MHz, 298 K): δ (ppm) 7.37 (m, 2H, NCHCHN), 7.24 (m, 2H, NCHCHN), 7.10 (d, 2H, C₆H₄, ³J_{HH} = 1.6 Hz), 6.75 (m, 2H, C₆H₄), 5.31 (d, 2H, NCH₂, ²J_{HH} = 14 Hz), 4.58 (d, 2H, NCH₂, ²J_{HH} = 14 Hz), 3.99 (s, 6H, NCH₃). ¹³C {¹H} NMR (acetone-d₆, 125 MHz, 298 K): δ (ppm) 226.9 (CO), 217.5 (CO), 201.3 (NCN), 129.0 (C₆H₄), 134.1 (C₆H₄), 126.7 (C₆H₄), 121.7 (NCHCHN), 53.1 (N-CH₂), 41.2 (N-CH₃). High Resolution ESI_{pos}-MS (MeCN): found 431.0816 (C₂₀H₁₈N₄O₄Cr⁺ requires 431.0811 dev: 1.2 ppm); IR (CH₂Cl₂): $\nu = 1823$ (s) (CO), 1922 (s) (CO), 1976 (s) (CO) cm⁻¹.

Pentacarbonyl-[1,3-bis-(2,4,6-trimethylphenyl)imidazole-2-ylidene]chromium (67)

A solution of free carbene **60** (500 mg, 1.65 mmol) in toluene (40 ml) was added to a Schlenk containing chromium hexacarbonyl (480 mg, 2.18 mmol), and the mixture heated to reflux for 48 h. The sublimed hexacarbonyl was periodically washed back into the stirred mixture. The solution was cooled to 0°C and filtered to remove excess chromium hexacarbonyl.

Solvent was removed *in vacuo* and the product extracted into dichloromethane (10 ml). Methanol (20 ml) was added to precipitate the product which was isolated by filtration and dried *in vacuo* yielding a yellow microcrystalline solid (350 mg, 43 %). ^1H NMR (acetone- d_6 , 400 MHz, 298 K): δ (ppm) 6.99 (s, 2H, NCHCHN), 6.95 (s, 4H, C_6H_2), 2.29 (s, 6H, *para*- CH_3), 2.02 (s, 12H, *ortho*- CH_3). ^{13}C $\{^1\text{H}\}$ NMR (acetone- d_6 , 125 MHz, 298 K): δ (ppm) 220.9 (CO), 215.4 (CO), 197.3 (NCN), 138.7, 136.6, 134.8, 128.4 (C_6H_2), 123.3 (NCHCHN), 20.1 (*para*- CH_3), 16.6 (*ortho*- CH_3). High Resolution ESI_{pos}-MS (MeCN): found 496.1073 ($C_{26}H_{24}N_2O_5Cr^+$ requires 496.1078 dev: -1.0 ppm). IR (CH_2Cl_2): $\nu = 1922$ (s) (CO), 2059 (s) (CO) cm^{-1} .

Pentacarbonyl-[1,3-bis-(2,6-diisopropylphenyl)imidazole-2-ylidene]chromium (68)

An analogous method to that of **67** was followed, using free carbene **61** (500 mg, 1.28 mmol) and chromium hexacarbonyl (370 mg, 1.68 mmol). The product was obtained as a yellow microcrystalline solid (300 mg, 40 %). ^1H NMR (acetone- d_6 , 400 MHz, 298 K): δ (ppm) 7.44 (m, 2H, C_6H_3), 7.25 (m, 4H, C_6H_3), 7.00 (s, 2H, NCHCHN), 2.62 (*sept*, 4H, $CH(CH_3)_2$, $^3J_{HH} = 6.80$ Hz), 1.30 (d, 12H, $CH(CH_3)_2$, $^3J_{HH} = 6.81$ Hz), 1.05 (d, 12H, $CH(CH_3)_2$, $^3J_{HH} = 6.82$ Hz). ^{13}C $\{^1\text{H}\}$ NMR (acetone- d_6 , 125 MHz, 298 K): δ (ppm) 219.9 (CO), 214.9 (CO), 198.6 (NCN), 145.3, 136.5, 129.6, 124.4 (C_6H_3), 123.2 (NCHCHN), 28.0 ($CH(CH_3)_2$), 24.9 ($CH(CH_3)_2$), 22.8 ($CH(CH_3)_2$). High Resolution ESI_{pos}-MS (MeCN): found 580.1125 ($C_{32}H_{36}N_2O_5Cr^+$ requires 580.1114 dev: 1.9 ppm). IR (CH_2Cl_2): $\nu = 1923$ (s) (CO), 2053 (s) (CO) cm^{-1} .

Pentacarbonyl-[1,3-bis(2,6-diisopropylphenyl)-4,5,6-trihydropyrimidin-2-ylid]chromium (69)

An analogous method to that of **67** was followed, using free carbene **62** (500 mg, 1.23 mmol) and chromium hexacarbonyl (363 mg, 1.61 mmol). The product was obtained as a yellow microcrystalline solid (280 mg, 46%). ^1H NMR (acetone- d_6 , 400 MHz, 298 K): δ (ppm) 7.28 (m, 2H, C_6H_3), 7.17 (m, 4H, C_6H_3), 3.45 (m, 4H, $NCH(CH_3)_2$), 3.07 (m, 4H, NCH_2), 1.48 (m, 2H, NCH_2CH_2), 1.19 (d, 12H, $CH(CH_3)_2$, $^3J_{HH} = 6.7$ Hz), 1.07 (d, 12H, $CH(CH_3)_2$, $^3J_{HH} = 6.7$ Hz). ^{13}C $\{^1\text{H}\}$ NMR (acetone- d_6 , 125 MHz, 298 K): δ (ppm) 219.8 (CO), 214.5 (CO), 201.2 (NCN), 144.6 (C_6H_3), 128.3 (C_6H_3), 124.5 (C_6H_3), 123.3 (C_6H_3), 27.7 (NCH_2), 26.8, 25.3 ($NCH(CH_3)_2$), 22.9 (NCH_2CH_2). High Resolution ESI_{pos}-MS (MeCN): found 596.1435

($C_{28}H_{40}N_2O_5Cr^+$ requires 596.1425 dev: 1.7 ppm). IR (CH_2Cl_2): $\nu = 1927$ (s) (CO), 2044 (s) (CO) cm^{-1} .

Pentacarbonyl-[1,3-bis-(2,4,6-trimethylphenyl)-4,5,6,7-tetrahydro-[1,3]-diazepin-2-ylidene]chromium (70)

An analogous method to that of **67** was followed, using free carbene **63** (500 mg, 1.5 mmol) and chromium hexacarbonyl (428 mg, 1.95 mmol). The product was obtained as a yellow microcrystalline solid (290 mg, 37 %). 1H NMR (acetone- d_6 , 400 MHz, 298 K): δ (ppm) 6.72 (m, 4H, C_6H_2), 3.17 (m, 4H, NCH_2), 2.51 (s, 6H, *para*- CH_3), 2.38 (m, 4H, NCH_2CH_2), 2.12 (s, 12H, *ortho*- CH_3). ^{13}C $\{^1H\}$ NMR (acetone- d_6 , 125 MHz, 298 K): δ (ppm) 223.9 (CO), 218.1 (CO), 220.9 (NCN), 139.5 (C_6H_2), 136.4 (C_6H_2), 133.7 (C_6H_2), 129.8 (C_6H_2), 53.7 (NCH_2), 27.6 (NCH_2CH_2), 20.6 (*para*- CH_3), 17.5 (*ortho*- CH_3). High Resolution ESI_{pos}-MS (MeCN): found 526.1519 ($C_{28}H_{30}N_2O_5Cr^+$ requires 526.1504 dev: 2.8 ppm). IR (CH_2Cl_2): $\nu = 1925$ (s) (CO), 2043 (s) (CO) cm^{-1} .

Pentacarbonyl-[1,3-bis-(diisopropyl)imidazole-2-ylidene]chromium (71)

An analogous method to that of **67** was followed, using free carbene **11** (500 mg, 1.95 mmol) and chromium hexacarbonyl (559 mg, 2.54 mmol). The product was obtained as a yellow microcrystalline solid (250 mg, 37 %). 1H NMR ($CDCl_3$, 400 MHz, 298 K): δ (ppm) 6.99 (s, 2H, $NCHCHN$), 5.13 (sept, 2H, $NCH(CH_3)_2$, $^3J_{HH} = 6.67$ Hz), 1.38 (d, 12H, $NCH(CH_3)_2$, $^3J_{HH} = 6.67$ Hz). ^{13}C $\{^1H\}$ NMR (acetone- d_6 , 125 MHz, 298 K): δ (ppm) 223.1 (CO), 218.6 (CO), 193.1 (NCN), 120.7 ($NCHCHN$), 53.3 ($NCH(CH_3)_2$), 23.7 ($NCH(CH_3)_2$). High Resolution ESI_{pos}-MS (MeCN): found 344.0521 ($C_{14}H_{16}N_2O_4Cr^+$ requires 344.0534 dev: -3.8 ppm). IR (CH_2Cl_2): $\nu = 1921$ (s) (CO), 2054 (s) (CO) cm^{-1} .

Pentacarbonyl-[1,3-bis-(diisopropyl)imidazole-2-ylidene]molybdenum (73)

An analogous method to that of **67** was followed, using free carbene **11** (500 mg, 1.95 mmol) and molybdenum hexacarbonyl (670 mg, 2.54 mmol). The product was obtained as a yellow microcrystalline solid (300 mg, 39 %). 1H NMR (acetone- d_6 , 400 MHz, 298 K): δ (ppm) 7.42 (s, 2H, $NCHCHN$), 5.06 (sept, 2H, $NCH(CH_3)_2$, $^3J_{HH} = 6.7$ Hz), 1.35 (d, 12H, $NCH(CH_3)_2$, $^3J_{HH} = 6.7$ Hz). ^{13}C $\{^1H\}$ NMR (acetone- d_6 , 125 MHz, 298 K): δ (ppm) 211.9 (CO), 205.7

(CO), 192.6 (NCN), 118.5 (NCHCHN), 52.7 (CH(CH₃)₂), 22.3 (CH(CH₃)₂). High Resolution ESI_{pos}-MS (MeCN): found 390.0114 (C₁₄H₁₆N₂O₄Mo⁺ requires 390.0092 dev: 5.6 ppm).

Pentacarbonyl-[1,3-bis-(diisopropyl)imidazole-2-ylidene]tungsten (74)

An analogous method to that of **67** was followed, using free carbene **11** (500 mg, 1.95 mmol) and tungsten hexacarbonyl (894 mg, 2.54 mmol). The product was obtained as a yellow microcrystalline solid (350 mg, 37 %). ¹H NMR (acetone-d₆, 400 MHz, 298 K): δ (ppm) 7.45 (s, 2H, NCHCHN), 5.07 (sept, 2H, NCH(CH₃)₂ ³J_{HH} = 6.71 Hz), 1.37 (d, 12H, NCH(CH₃)₂ ³J_{HH} = 6.71 Hz). ¹³C {¹H} NMR (acetone-d₆, 125 MHz, 298 K): δ (ppm) 203.5 (CO), 198.4 (CO), 185.3 (NCN), 119.8 (NCHCHN), 53.4 (CH(CH₃)₂), 21.9 (CH(CH₃)₂). High Resolution ESI_{pos}-MS (MeCN): found 476.0573 (C₁₄H₁₆N₂O₄W⁺ requires 476.0561 dev: 2.5 ppm).

[cis-Tetracarbonyl-[1,1'-methylene-3,3'-dimethylimidazole-2,2'-diylidene]chromium][aluminate] (75)

Complex **64** (50 mg, 0.14 mmol) and the silver aluminate (317 mg, 0.29 mmol) were combined in a Schlenk tube and dichloromethane (10 ml) added. The mixture, which immediately changed colour, was left to stir for 30 min at room temperature with the exclusion of light. After filtration, the solvent was removed *in vacuo* leaving a red-purple residue which was washed with hexane (2 × 5 ml) and dried *in vacuo* to yield the product as a red-purple solid (80 mg, 41 %). IR (CH₂Cl₂): ν = 1986 (s) (CO), 2015 (s) (CO), 2047 (s) (CO) cm⁻¹.

[cis-Tetracarbonyl-[1,1'-propylene-3,3'-dimethylimidazole-2,2'-diylidene]chromium][aluminate] (76)

An analogous method to that of **75** was followed, using chromium compound **65** (50 mg, 0.14 mmol) and silver aluminate (290 mg, 0.27 mmol). The product was obtained as a dark red solid (75 mg, 40 %). IR (CH₂Cl₂): ν = 1982 (s) (CO), 2019 (s) (CO), 2043 (s) (CO) cm⁻¹.

[cis-Tetracarbonyl-[1,1'-xylylene-3,3'-dimethylimidazole-2,2'-diylidene]chromium][aluminate] (77)

An analogous method to that of **75** was followed, using chromium compound **66** (50 mg, 0.12 mmol) and silver aluminate (250 mg, 0.23 mmol). The product was obtained as a dark purple solid (70 mg, 43 %). IR (CH₂Cl₂): $\nu = 1980$ (s) (CO), 2021 (s), 2054 (CO) cm⁻¹.

[Pentacarbonyl-[1,3-bis-(2,4,6-trimethylphenyl)imidazole-2-ylidene]chromium][aluminate] (78)

An analogous method to that of **75** was followed, using chromium compound **67** (50 mg, 0.10 mmol) and silver aluminate (210 mg, 0.20 mmol). The product was obtained as a dark red solid (60 mg, 40 %). IR (CH₂Cl₂): $\nu = 2011$ (s) (CO), 2129 (s) (CO) cm⁻¹.

[Pentacarbonyl-[1,3-bis-(2,6-diisopropylphenyl)imidazole-2-ylidene]chromium][aluminate] (79)

An analogous method to that of **75** was followed, using chromium compound **68** (50 mg, 0.08 mmol) and silver aluminate (184 mg, 0.17 mmol). The product was obtained as a dark red solid (60 mg, 45 %). IR (CH₂Cl₂): $\nu = 2012$ (s) (CO), 2119 (s) (CO) cm⁻¹.

[Pentacarbonyl-[1,3-bis(2,6-diisopropylphenyl)-4,5,6-trihydropyridin-2-ylid]chromium][aluminate] (80)

An analogous method to that of **75** was followed, using chromium compound **69** (50 mg, 0.08 mmol) and silver aluminate (181 mg, 0.17 mmol). The product was obtained as a red solid (65 mg, 49 %). IR (CH₂Cl₂): $\nu = 2056$ (s) (CO), 2143 (s) (CO) cm⁻¹.

[Pentacarbonyl-[1,3-bis-(2,4,6-trimethylphenyl)-4,5,6,7-tetrahydro-[1,3]-diazepin-2-ylid]chromium][aluminate] (81)

An analogous method to that of **75** was followed, using chromium compound **70** (50 mg, 0.09 mmol) and silver aluminate (200 mg, 0.19 mmol). The product was obtained as a dark red solid (60 mg, 42 %). IR (CH₂Cl₂): $\nu = 2044$ (s) (CO), 2127 (s) (CO) cm⁻¹.

[Pentacarbonyl-[1,3-bis-(diisopropyl)imidazole-2-ylidene]chromium][aluminate] (82)

An analogous method to that of **75** was followed, using chromium compound **71** (50 mg, 0.15 mmol) and silver aluminate (313 mg, 0.29 mmol). The product was obtained as a red-purple solid (90 mg, 47 %). IR (CH₂Cl₂): $\nu = 2030$ (s), 2132 (CO) cm⁻¹.

[1-methyl-3-isobutyrophenoneimidazole-2-ylidene]chromium(II) tetrafluoroborate (83)

A solution of free carbene **10** (291 mg, 1.28 mmol) in THF (10 ml) was added dropwise to a slurry of Cr(MeCN)₄(BF₄)₂ (250 mg, 0.64 mmol) in THF (10 ml), and the mixture stirred for 16 h at room temperature. Concentration of the THF solution, followed by addition of diethyl ether resulted in precipitation of the product. The resulting solid was washed with diethyl ether (3 × 5 ml) and dried *in vacuo* to yield a dark pink solid (300 mg, 69 %). Anal. Calcd for C₂₈H₃₂O₂N₄CrB₂F₈ (found): C, 49.30 (49.54); H, 4.73 (5.28); N, 8.21 (8.56). $\lambda_{\max}(\text{dcm})/\text{nm}$ 530. Magnetic moment $\mu_{\text{eff}} = 4.66 \mu_{\text{B}}$.

[1-isopropyl-3-isobutyrophenoneimidazole-2-ylidene]chromium(II) tetrafluoroborate (84)

An analogous method to that of **83** was followed, using Cr(MeCN)₄(BF₄)₂ (250 mg, 0.64 mmol) and free carbene **11** (330 mg, 1.28 mmol). The product was isolated as a red-brown solid (320 mg, 67 %). Anal. Calcd for C₃₂H₄₀O₂N₄CrB₂F₈ (found): C, 52.06 (51.30); H, 5.46 (4.91); N, 7.59 (7.53). $\lambda_{\max}(\text{dcm})/\text{nm}$ 510. Magnetic moment $\mu_{\text{eff}} = 4.81 \mu_{\text{B}}$.

[1-^tButyl-3-isobutyrophenoneimidazole-2-ylidene]chromium(II) tetrafluoroborate (85)

An analogous method to that of **83** was followed, using Cr(MeCN)₄(BF₄)₂ (250 mg, 0.64 mmol) and free carbene **12** (345 mg, 1.28 mmol). The product was isolated as a pale green solid (320 mg, 65 %). Anal. Calcd for C₃₄H₄₄O₂N₄CrB₂F₈ (found): C, 53.29 (51.51); H, 5.79 (5.33); N, 7.31 (7.63). $\lambda_{\max}(\text{dcm})/\text{nm}$ 630. Magnetic moment $\mu_{\text{eff}} = 4.66 \mu_{\text{B}}$.

[1,3-diisobutyrophenoneimidazole-2-ylidene]chromium(II) tetrafluoroborate (86)

An analogous method to that of **83** was followed, using Cr(MeCN)₄(BF₄)₂ (250 mg, 0.64 mmol) and free carbene **13** (460 mg, 1.28 mmol). The product was isolated as a pale green solid (440 mg, 70 %). Anal. Calcd for C₄₆H₄₈O₄N₄CrB₂F₈ (found): C, 58.35 (60.08); H, 5.07 (4.95); N, 5.92 (6.22). $\lambda_{\max}(\text{dcm})/\text{nm}$ 620. Magnetic moment $\mu_{\text{eff}} = 5.08 \mu_{\text{B}}$.

**[1-methyl-3-phenylpropylidenebenzenamineimidazole-2-ylidene]chromium(II)
tetrafluoroborate (87)**

An analogous method to that of **83** was followed, using $\text{Cr}(\text{MeCN})_4(\text{BF}_4)_2$ (250 mg, 0.64 mmol) and free carbene **16** (390 mg, 1.28 mmol). The product was isolated as a green solid (320 mg, 60 %). Anal. Calcd for $\text{C}_{40}\text{H}_{42}\text{N}_6\text{CrB}_2\text{F}_8$ (found): C, 57.69 (59.08); H, 5.05 (5.15); N, 10.10 (9.22). $\lambda_{\text{max}}(\text{dcm})/\text{nm}$ 590. Magnetic moment $\mu_{\text{eff}} = 5.14 \mu_{\text{B}}$.

**bis-[1,1'-methylene-3,3'-dimethylimidazole-2,2'-diylidene]-chromium(II)
tetrafluoroborate (88)**

An analogous method to that of **83** was followed, using $\text{Cr}(\text{MeCN})_4(\text{BF}_4)_2$ (250 mg, 0.64 mmol) and free carbene **57** (225 mg, 1.28 mmol). The product was isolated as a red solid (280 mg, 75 %). Anal. Calcd for $\text{C}_{18}\text{H}_{24}\text{N}_8\text{CrB}_2\text{F}_8$ (found): C, 37.40 (38.58); H, 4.18 (3.94); N, 19.38 (19.09). $\lambda_{\text{max}}(\text{dcm})/\text{nm}$ 530. Magnetic moment $\mu_{\text{eff}} = 4.76 \mu_{\text{B}}$.

**bis-[1,1'-propylene-3,3'-dimethylimidazole-2,2'-diylidene]chromium(II)
tetrafluoroborate (89)**

An analogous method to that of **83** was followed, using $\text{Cr}(\text{MeCN})_4(\text{BF}_4)_2$ (250 mg, 0.64 mmol) and free carbene **58** (260 mg, 1.28 mmol). The product was isolated as a red-brown solid (300 mg, 74 %). Anal. Calcd for $\text{C}_{22}\text{H}_{32}\text{N}_8\text{CrB}_2\text{F}_8$ (found): C, 41.67 (38.32); H, 5.09 (5.14); N, 17.66 (16.83). $\lambda_{\text{max}}(\text{dcm})/\text{nm}$ 510. Magnetic moment $\mu_{\text{eff}} = 5.02 \mu_{\text{B}}$.

**bis-[1,1'-xylylene-3,3'-dimethylimidazole-2,2'-diylidene]chromium(II) tetrafluoroborate
(90)**

An analogous method to that of **83** was followed, using $\text{Cr}(\text{MeCN})_4(\text{BF}_4)_2$ (250 mg, 0.64 mmol) and free carbene **59** (340 mg, 1.28 mmol). The product was isolated as a dark pink solid (340 mg, 70 %). Anal. Calcd for $\text{C}_{32}\text{H}_{36}\text{N}_8\text{CrB}_2\text{F}_8$ (found): C, 50.69 (49.48); H, 4.79 (4.32); N, 14.77 (14.02). $\lambda_{\text{max}}(\text{dcm})/\text{nm}$ 520. Magnetic moment $\mu_{\text{eff}} = 4.87 \mu_{\text{B}}$.

4.5 References

- [1] Lappert, M. F.; McCabe, R. W.; MacQuitty, J. J.; Pye, P. L.; Riley, P. I. *J.C.S. Dalton Trans.* **1980**, 90.
- [2] Sakurai, H.; Sugitani, K.; Moriuchi, T.; Hirao, T. *J. Organomet. Chem.* **2005**, *690*, 1750.
- [3] Voges, M. H.; Rømming, C.; Tilset, M. *Organometallics* **1999**, *18*, 529.
- [4] Kreisel, K. A.; Yap, G. P. A.; Theopold, K. H. *Organometallics*, **2006**, *25*, 4670.
- [5] Öfele, K. *J. Organomet. Chem.* **1968**, *12*, 42.
- [6] Wang, H. M. J.; Lin, I. J. B. *Organometallics* **1998**, *17*, 972.
- [7] Dötz, K. H. *Angew. Chem. Int. Ed. Engl.* **1984**, *23*, 587.
- [8] Nonnenmacher, M.; Kunz, D.; Rominger, F.; Oeser, T. *J. Organomet. Chem.* **2005**, *690*, 5647.
- [9] Bolm, C.; Kesselgruber, M.; Raabe, G. *Organometallics* **2002**, *21*, 707.
- [10] Tafipolsky, M.; Schere, W.; Öfele, K.; Artus, G.; Pedersen, B.; Herrmann, W. A.; McGrady, G. S. *J. Am. Chem. Soc.* **2002**, *124*, 5865.
- [11] Raubenheimer, H. G.; Stander, Y.; Marais, E. K.; Thompson, C.; Kruger, G. J.; Cronje, S.; Deetlefs, M. *J. Organomet. Chem.* **1999**, *590*, 158.
- [12] (a) Hahn, F. E.; Langenhahn, V.; Meier, N.; Lügger, T.; Fehlhammer, W. P. *Chem. Eur. J.* **2003**, *9*, 704. (b) Öfele, K.; Herrmann, W. A.; Mihalios, D.; Elison, M.; Herdtweck, E.; Schere, W.; Mink, J. *J. Organomet. Chem.* **1993**, *459*, 177.

- [13] Kim, S.; Choi, S. Y.; Lee, Y. T.; Park, K. H.; Sitzmann, H.; Chung, Y. K. *J. Organomet. Chem.* **2007**, *692*, 5390.
- [14] Lee, M. T.; Hu, C. H. *Organometallics* **2004**, *23*, 976.
- [15] Herrmann, W. A.; Kocher, C. *Angew. Chem. Int. Ed.* **1997**, *36*, 2162.
- [16] Thomas, B. J.; Noh, S. K.; Schulte, G. K.; Sendlinger, S. C.; Theopold, K. H. *J. Am. Chem. Soc.* **1991**, *113*, 893.
- [17] Heintz, R. A.; Ostrander, R. L.; Rheingold, A. L.; Theopold, K. H. *J. Am. Chem. Soc.* **1994**, *116*, 11387.
- [18] Bhandari, G.; Kim, Y.; McFarland, J. M.; Rheingold, A. L.; Theopold, K. H. *Organometallics* **1996**, *14*, 738.
- [19] Fryzuk, M. D.; Leznoff, D. B.; Rettigt, S. J. *Organometallics* **1996**, *14*, 5193.
- [20] Jabri, A.; Crewdson, P.; Gambarotta, S.; Korobkov, I.; Duchateau, R. *Organometallics* **2006**, *25*, 715.
- [21] Haftbaradaran, F.; Mund, G.; Batchelor, R. J.; Britten, J. F.; Leznoff, D. B. *Dalton Trans.* **2005**, 2343.
- [22] Filippou, A. C.; Schneider, S.; Schnakenburg, G. *Inorg. Chem.* **2003**, *42*, 6974.
- [23] Agapie, T.; Schofer, S. J.; Labinger, J. A.; Bercaw, J. E. *J. Am. Chem. Soc.* **2004**, *126*, 1304.
- [24] Overett, M. J.; Blann, K.; Bollmann, A.; Dixon, J. T.; Häsbrök, D.; Killian, E.; Maumela, H.; McGuinness, D. S.; Morgan, D. H. *J. Am. Chem. Soc.* **2005**, *127*, 10723.

- [25] Rucklidge, A. J.; McGuinness, D. S.; Tooze, R. P.; Slawin, A. M. Z.; Pelletier, J. D. A.; Hanton, M. J.; Webb, P. B. *Organometallics* **2007**, *26*, 2782.
- [26] Carter, A.; Cohen, S. A.; Cooley, N. A.; Murphy, A.; Scott, J.; Wass, D. F. *Chem. Commun.* **2002**, 858.
- [27] Blann, K.; Bollmann, A.; Dixon, J. T.; Hess, F. M.; Killian, E.; Maumela, H.; Morgan, D. H.; Neveling, A.; Otto, S.; Overett, M. J. *Chem. Commun.* **2005**, 620.
- [28] McGuinness, D. S.; Gibson, V. C.; Wass, D. F.; Steed, J. W. *J. Am. Chem. Soc.* **2003**, *125*, 12716.
- [29] McGuinness, D. S.; Wasserscheid, P.; Morgan, D. H.; Dixon, J. T. *Organometallics* **2005**, *24*, 552.
- [30] Ruther, T. H.; Braussaud, N.; Cavell, K. J. *Organometallics* **2001**, *20*, 1247.
- [31] Jolly, P. W. *Acc. Chem. Res.* **1996**, *29*, 544.
- [32] Morgan, D. H.; Schwikkard, S. L.; Dixon, J. T.; Nair, J. J.; Hunter, R. *Adv. Synth. Catal.* **2003**, 939.
- [33] Yang, Y.; Kim, H.; Lee, J.; Paik, H.; Jang, H. G. *Appl. Catal. A* **2000**, *193*, 29.
- [34] Theopold, K. H. *Eur. J. Inorg. Chem.* **1998**, 15.
- [35] Temple, C.; Jabri, A.; Crewdson, P.; Gambarotta, S.; Korobkov, I.; Duchateau, R. *Angew. Chem. Int. Ed.* **2006**, *45*, 7050.
- [36] Bowen, L. E.; Haddow, M. F.; Orpen, A. G.; Wass, D. F. *J. Chem. Soc., Dalton Trans.* **2007**, 1160.

- [37] (a) Iglesias, M.; Beetstra, D. J.; Stasch, A.; Horton, P. N.; Hursthouse, M. B.; Coles, S. J.; Cavell, K. J.; Dervisi, A.; Fallis, I. A. *Organometallics* **2007**, *26*, 4800. (b) Alder, R. W.; Blake, M. E.; Oliva, J. M. *J. Phys. Chem.* **1999**, *103*, 11200. (c) Magill, A. M.; Cavell, K. J.; Yates, B. F. *J. Am. Chem. Soc.* **2004**, *126*, 8717 and references therein.
- [38] Brunet, J. J.; Chauvin, R.; Donnadieu, B.; Leglaye, P.; Neibecker, D. *J. Organomet. Chem.* **1998**, *571*, 7.
- [39] Herrmann, W. A.; Elison, M.; Fischer, J.; Köcher, C.; Artus, G. R. *J. Angew. Chem., Int. Ed. Engl.* **1995**, *34*, 2371.
- [40] Theopold, K. H. *Encyclopedia of Inorganic Chemistry* Wiley, New York, **1994**, *2*, 666.
- [41] Henriques, R. T.; Herdtweck, E.; Kühn, F. E.; Lopes, A. D.; Mink, J.; Romão, C. C. *J. Chem. Soc. Dalton Trans.* **1998**, 1293.
- [42] Danopoulos, A. A.; Hankin, D. M.; Wilkinson, G.; Cafferkey, S. M.; Sweet, T. K. N.; Hursthouse, M. B. *Polyhedron* **1997**, *16*, 3879.
- [43] (a) Evans, J. *J. Chem. Soc.* **2003**, 1960. (b) Evans, D. F. *J. Chem. Soc.* **1959**, 2003. (c) Sur, S. K. *J. Magn. Reson.* **1989**, 169. (d) Grant, D. H. *J. Chem. Educ.* **1995**, 39.
- [44] Lever, A. B. P. *Inorganic Electronic Spectroscopy*, 2nd edition, Elsevier, **1986**.
- [45] Scherg, T.; Schneider, S. K.; Frey, G. D.; Schwarz, J.; Herdtweck, E.; Herrmann, W. *A. Synlett* **2006**, *18*, 2894.
- [46] Iglesias, M.; Beetstra, D. J.; Knight, J. C.; Ooi, L.; Stasch, A.; Coles, S.; Male, L.; Hursthouse, M. B.; Cavell, K. J.; Dervisi, A.; Fallis, I. A. *Organometallics* **2008**, *27*, 3279.
- [47] Krossing, I. *Chem. Eur. J.* **2001**, *7*, 490.

- [48] Spalek, T. P. P.; Sojka, Z. *J. Chem. Inf. Model.* **2005**, *45*, 18.

Chapter Five

**Synthesis, Characterisation and Catalytic
Testing of Some Novel Chromium(III) and
Titanium(III)-NHC Complexes**

Chapter Five

Synthesis, Characterisation and Catalytic Testing of Some Novel Chromium(III) and Titanium(III)-NHC Complexes

5.1 Introduction

Cr(III) complexes are much more widely reported than other oxidation states of chromium, and represent a series of complexes of significant interest in terms of catalytic activity, particularly in ethylene oligomerisation and polymerisation.

While well established in the field of late-transition metals,¹ the use of NHCs in early transition metal chemistry is much less common^{2,3} and this has been attributed to the ease of dissociation of the metal-carbene bond in such complexes.⁴ Cr(III) however represents one of the more stable (kinetically inert) oxidation states, and a number of complexes containing NHC ligands have been reported.⁵⁻¹⁶ Ti(III)-NHC complexes are less well known than their chromium analogues, with only a few being recently reported.¹⁷⁻¹⁹

In this chapter we discuss the role of Cr(III) as well as other metal complexes in selective ethylene oligomerisation catalysis, and report the synthesis and EPR analysis of a series of novel chromium(III) and titanium(III)-NHC complexes. The catalytic behaviour of a selection of these complexes is also reported.

5.1.1 Role of Cr(III) in Ethylene Oligomerisation

The use of chromium in ethylene oligomerisation is well established in both homogeneous and heterogeneous catalytic systems. As described in 1.1, conventional ethylene oligomerisation processes generally produce a statistical (Schultz-Flory) distribution of linear alpha olefins (LAOs),²⁰ which is undesirable from an industrial point of view.²¹

In 1977 Manyik and co-workers reported the selective trimerisation of ethylene to produce 1-hexene,²² a reaction which has since received much attention with a significant amount of research focussing on the development of catalysts capable of high selectivity.

Other metal complexes have been investigated in this process, and are discussed in section 5.1.2, but chromium remains the preferred metal to catalyse this reaction, since it appears to result in the best activity as well as selectivity.²³ As described in 1.2.2, a metallocyclic mechanism involving a 2-electron redox couple is generally thought to be in place; the formal oxidation state(s) of the active species is yet to be confirmed. The active catalyst is usually generated *in-situ* from a Cr(III) compound, added ligand, and a co-catalyst (commonly MAO). Cr(I)-Cr(III),²⁴ Cr(II)-Cr(IV)²⁵ and Cr(III)-Cr(V)²⁶ couples have been suggested as the principle oxidation states involved. Cr(V) and Cr(I) complexes are rare and generally unstable; Cr(V) complexes typically have oxygen or halide ligands, whereas Cr(I) complexes with isocyanides and bipy ligands are known.²⁶ Cr(III) complexes are the most widely studied, possibly due to their increased stability relative to the other oxidation states of chromium postulated to be involved in the mechanism, and at present, a Cr(I)-Cr(III) couple is favoured. However, this is by no means certain, and it may be that different couples operate within different catalyst systems or operating conditions.

There are a large number of Cr(III) complexes which, when activated with MAO or similar co-catalyst, are reported to display excellent activities and selectivities for ethylene trimerisation.^{21,28-30} More recently, similar complexes have been reported as effective tetramerisation catalysts³⁰ producing 1-octene, another valuable industrial reagent, with high selectivity. This is extremely new, however, and a creditable mechanism has only recently been published, and is able to explain the observed side-products.²⁷

Some of the most active catalysts reported generally include bidentate heteroatomic ligands containing mixed phosphorus and nitrogen atoms (PNP type ligands), as described in 3.1.1. Catalytic conditions can involve activation of the preformed Cr(III) complex with a co-catalyst, or in the case of *in situ* systems; addition of the co-catalyst to a mixture of ligand and Cr(III) source. The co-catalyst MAO,³¹ is generally thought to facilitate alkyl abstraction from the catalyst precursor to yield a cationic metal fragment.³¹⁻³³ Since MAO is relatively poorly defined and used in large excess, the identity of the active metal species generally remains unknown.³¹

The PNP type ligand systems generally show good catalytic activity and selectivity, and as a result a number have been studied, allowing detailed comparisons to be made and conclusions drawn about the effect of ligand properties on catalyst capability. Distinct ligand effects on activity have been observed, where increased steric bulk on the nitrogen atom has been demonstrated to result in the switch from predominantly 1-octene to 1-hexene production.³⁰

Additionally, studies by Sasol Technology have shown that selectivity can be shifted from trimerisation to tetramerisation by the reducing the number of *ortho*-alkyl substituents from four to zero as shown in figure 5.1,^{30a} providing further evidence that the steric effects of the ligand clearly influences the selectivity.

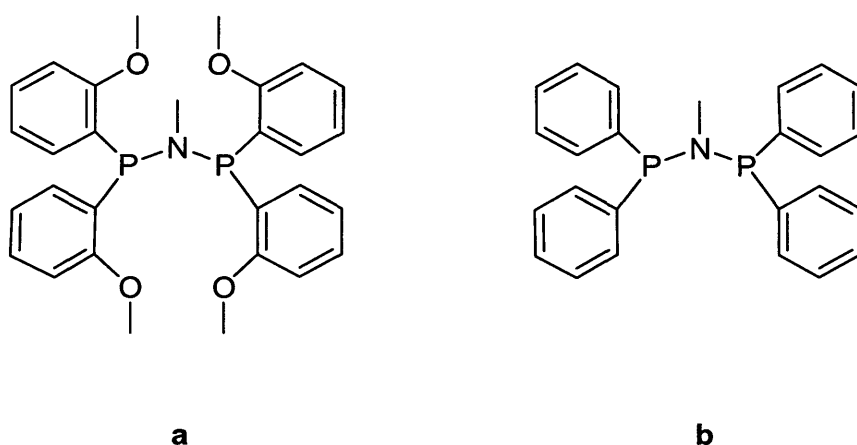


Figure 5.1 (a) Selective toward 1-hexene (b) Selective toward 1-octene.

5.1.2 Role of Other Metals in Ethylene Oligomerisation

Although most reported trimerisation catalysts are based on chromium, some systems based on other early transition metals have also been described.³⁴⁻³⁸

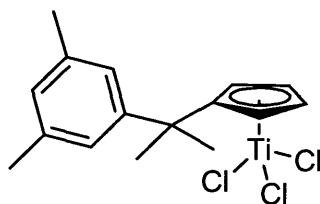


Figure 5.2 Titanium catalyst reported by Hessen.³⁵

The first titanium complex capable of high selectivity in ethylene trimerisation was reported by Hessen and co-workers³⁵ in 2001 (figure 5.2) where, upon activation with MAO, the pendant aromatic group is reported to coordinate to the metal centre. This hemilabile coordination was reported to be responsible for the observed high selectivity toward 1-hexene. Similar to the postulated chromium-based trimerisation mechanism,^{27, 29} the

titanium catalysed systems are thought to be based on a metallacyclic mechanism, where chain growth terminates at the metallacycloheptane intermediate, resulting in good selectivity toward 1-hexene.^{34,35} Despite good selectivity and activity reported for titanium-based trimerisation systems, the major disadvantage is the large excess of MAO required.²¹

Zirconium complexes have been reported as good dimerisation catalysts, but with respect to 1-hexene; activity and selectivity is low and the production of large quantities of polyethylene means that zirconium complexes are not considered viable alternatives to chromium catalysts.

Vanadium catalytic systems have proven to be active catalysts²¹ in the ethylene trimerisation process, and interestingly, the addition of a co-catalyst was reported as not essential, which is an attractive attribute. Nevertheless, overall catalyst performance does not compare to chromium systems.²¹

More recently, tantalum compounds have also been reported to efficiently trimerise ethylene, producing 1-hexene in excellent selectivities.^{36, 38} Interestingly, no ligand is involved; TaCl₅ is treated with an alkylating agent to form an intermediate precursor to the active catalyst, which is proposed to be 'naked'.²¹ These catalysts are again reported to carry out the trimerisation via a metallacyclic mechanism, but crucially do not require the use of an expensive co-catalyst necessary in other chromium systems.

Most known ethylene trimerisation catalysts are based on early transition metals, but some nickel based systems and uranium based systems have also been evaluated in the patent literature.²¹ Very few other systems compare to the more established chromium catalysts, and the fact that investigation continues can be partially attributed to intellectual property considerations, as well as potential catalyst improvements, and the environmental concerns associated with chromium. Also, from a mechanistic point of view, it is interesting to see how the catalyst capabilities are affected with different systems.

The development of catalyst systems based on other transition metals rather than chromium has resulted in more information being gained about the general mechanism, suggesting that similar processes are occurring in each case. Although activities reported thus far are generally much lower than with the more established chromium catalysts,³⁹ the potential to provide valuable mechanistic insight means that the continuing study of other early transition metal complexes remains an exciting area of research.

5.1.3 Cr(III)-NHC Complexes

As described in 1.1.2, NHC complexes have shown excellent results in many different types of catalysis with late transition metals,^{15,16} including Heck coupling reactions, hydroformylation, hydrogenation and olefin metathesis.¹ As a result, NHC ligands have become popular alternatives to the much used phosphines, partially due to their lower toxicity.^{5-14,16} NHCs benefit from strong σ -donating but poor π -accepting character, and allow steric and electronic properties to be easily altered; they therefore have the potential to be excellent ancillary ligands in many different types of catalysis, including the ethylene oligomerisation reactions we are interested in.

By comparison to the large amount of work carried out in the area, relatively few ethylene oligomerisation catalysts containing NHC ligands have been reported.^{15,16,40-43} This has been partially attributed to the decomposition of alkyl-metal carbene complexes via alkyl imidazolium reductive elimination. This can result in decomposition of the complex before effective catalysis can take place, and has been observed for several late transition metal complexes.⁴⁴ Chelating carbene ligands impart extra stability due to the chelate effect, and therefore represent a ligand set that can stabilise the alkyl-metal intermediates thought to be part of the oligomerisation mechanism, thus limiting the decomposition pathway.⁴⁴

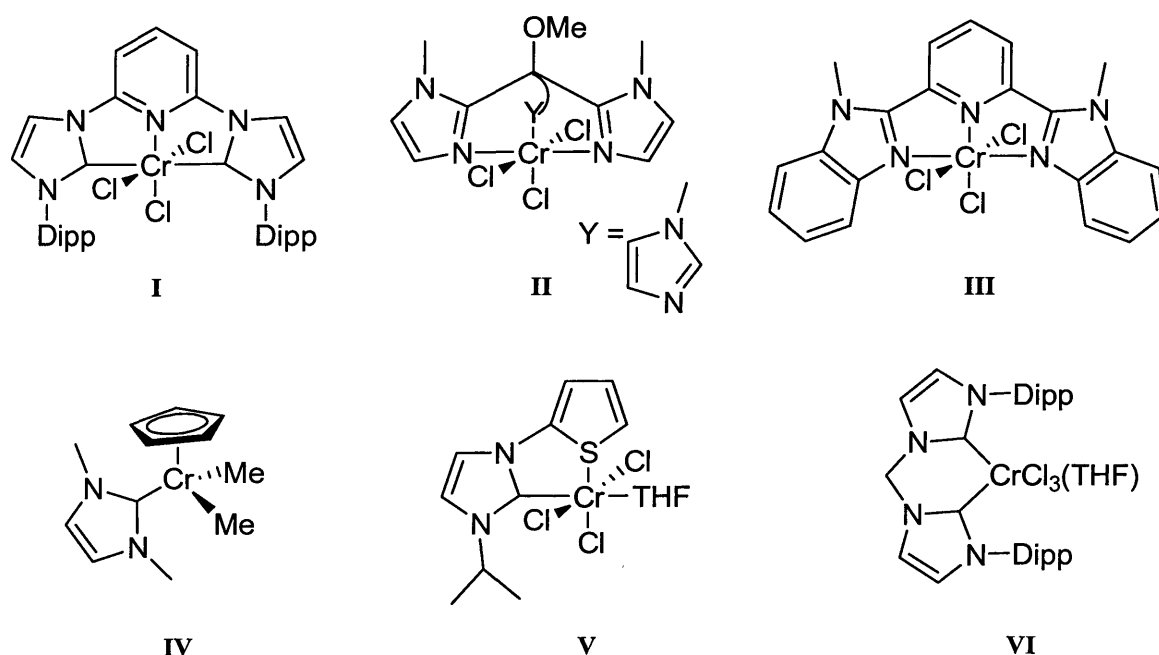


Figure 5.3 Selection of reported Cr(III)-NHC and related complexes.

Gibson and co-workers⁴² reported a tridentate bis(carbene) complex of chromium (III) containing a pyridine donor group (I, figure 5.3) which was the first Cr(III)-NHC complex to be structurally characterised. This was also the first Cr(III)-NHC complex to show excellent catalytic results in ethylene oligomerisation in the presence of MAO.

McGuinness and co-workers⁴³ went on to report NHC complexes incorporating a thiophene donor group (V, figure 5.3), which were found to be significantly less active than the pyridine analogues. A series of related complexes bearing imidazole-based chelate ligands (II, III, figure 5.3) were first reported by Cavell and co-workers⁴⁰ and were found to be active catalysts upon activation with MAO, and Theopold reported a bidentate bis(carbene) complex (VI, figure 5.3) which displayed only low ethylene polymerisation activity.¹⁶ This variation in catalytic activity demonstrates that while NHC ligands have the potential to produce catalysts with excellent oligomerisation capabilities, further work in this relatively poorly explored area of chemistry is required to develop the knowledge of ligand influence, and ‘fine-tune’ NHC ligands accordingly.

5.1.4 Ti(III)-NHC Complexes

Of the titanium complexes reported to contain NHC ligands,^{18, 44, 45} only a small number are complexes in the +III oxidation state,^{4,18,19,46} with EPR data reported only for a few.^{18,46}

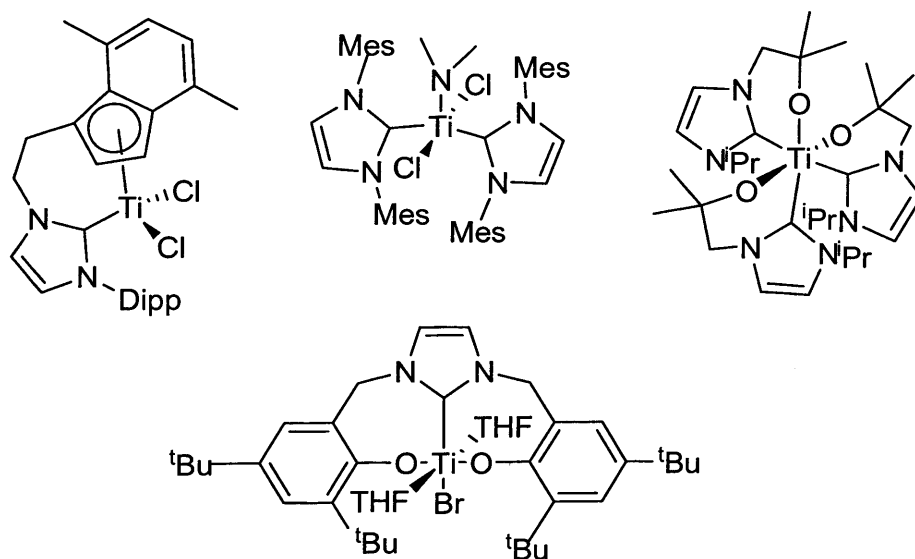


Figure 5.4 Examples of Ti(III)-NHC complexes.

Some examples are shown in figure 5.4, and show that generally an ancillary donor group is required to help stabilise the highly reducing Ti(III) oxidation state.

These Ti(III) complexes are particularly suited to analysis by EPR spectroscopy as they are d^1 paramagnetic ions, and the presence of only one unpaired electron should result in relatively simple interpretable spectra.

The homoleptic alkoxy-N-heterocyclic carbene complex (figure 5.4) reported by Arnold and co-workers¹⁸ was the first titanium(III)-NHC complex synthesised from a Ti(III) metal precursor. Arnold reported an efficient synthetic procedure to the metal precursor $TiCl_3(THF)_3$, previously deemed a very useful but expensive starting material. The method allows high purity and yields of $TiCl_3(THF)_3$ to be isolated from commercially available, inexpensive starting materials and provides a more accessible route to Ti(III) complexes.

The first highly active Ti(III) ethylene polymerisation catalyst to contain an NHC ligand was reported by Kawaguchi and co-workers, and a number of ethylene polymerisation catalysts based on functionalised carbene ligands with Ti(III) have since been reported.

Given the increasing application of NHCs in early transition metal chemistry, and in particular, the increased momentum in the use of the complexes as catalysts for alkene oligomerisation and polymerisation, we were interested in developing the fundamental understanding of these compounds by preparing a series of Cr(III) and Ti(III)-NHC complexes for catalytic testing as well as EPR analysis.

5.2 Results and Discussion

A series of N-heterocyclic carbene ligands shown in figure 5.5 were used to prepare chromium(III) and titanium(III) complexes. A variety of ligands, including chelating bis(carbenes), functionalised carbenes, and simple monodentate carbenes were chosen in order to obtain a wide selection of complexes for EPR analysis and catalytic testing. Free carbenes **10-13**, **16**, **18**, **57-60**, **62**, **63** and **96** were prepared *in situ* by reaction of the corresponding imidazolium salts (**1-4**, **7**, **9**, **50-56** and **95**) with potassium bis(trimethylsilyl)amide (KHMDs) as described in 2.2.2.

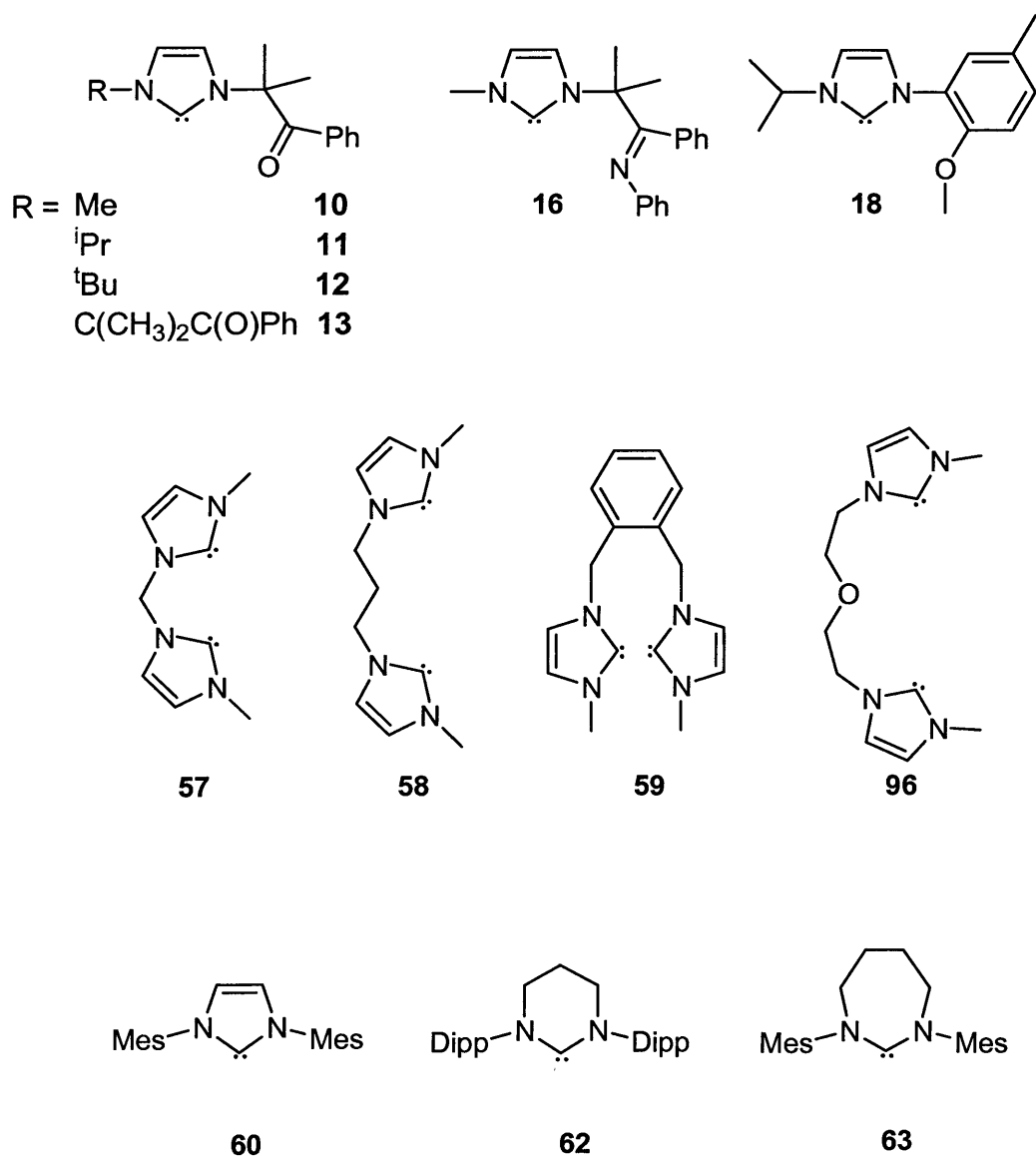
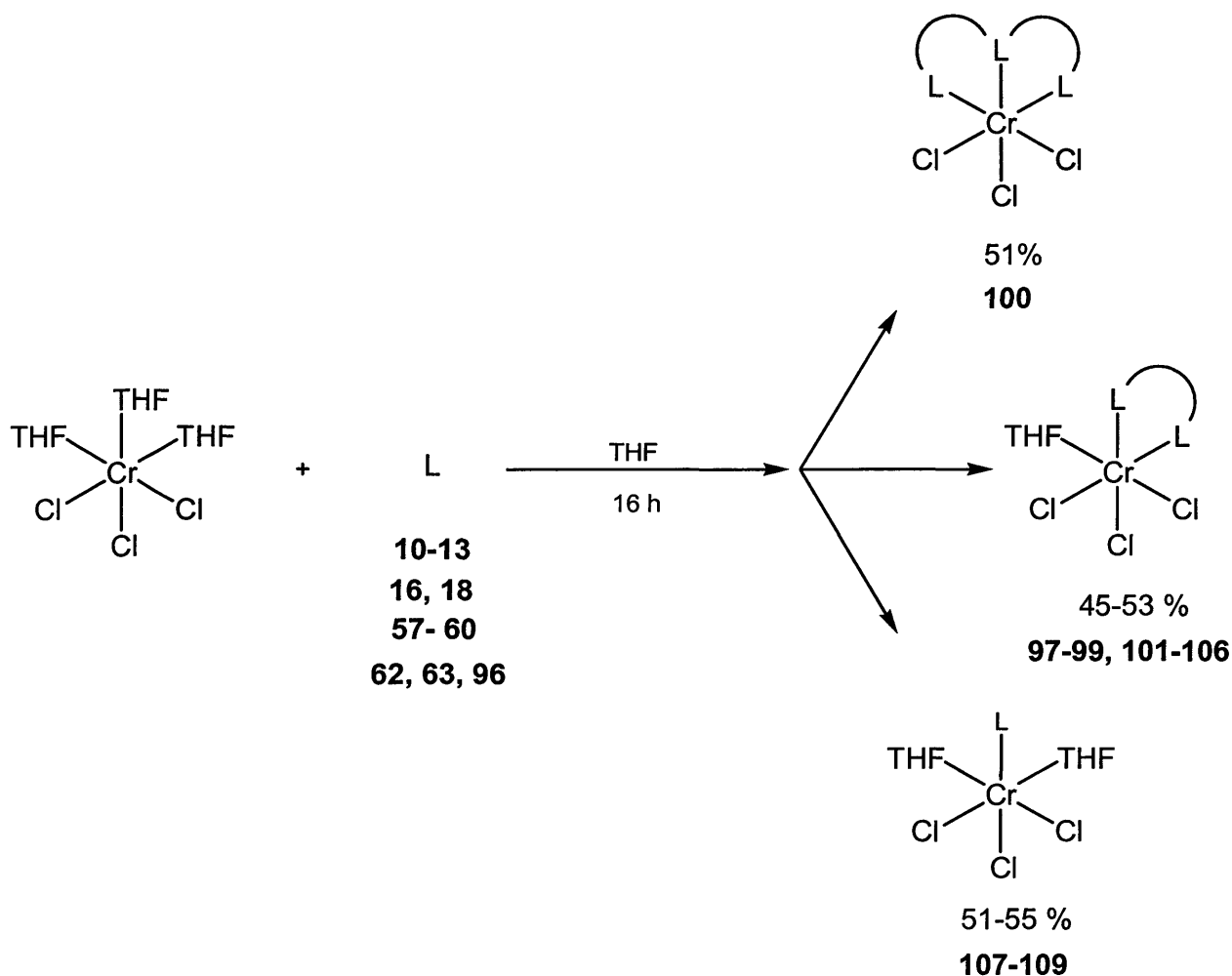


Figure 5.5 ligands used to prepare M(III) complexes (M = Cr, Ti).

5.2.1 Synthesis of Cr(III)-NHC Complexes

A solution of free carbene in THF at -10°C was added dropwise to a solution of the chromium precursor in THF at -10°C (scheme 5.1). Low temperatures were used in order to prevent the formation of polymeric material, which is not uncommon for this type of reaction.



Scheme 5.1 Synthesis of Cr(III)-NHC complexes **97-109**.

McGuinness⁴³ has reported that if addition of the free carbene is carried out too fast, a disproportionation reaction can occur, forming the dichloride complex (Figure 5.6a) with a chromium counterion rather than the expected trichloride complex (Figure 5.6b).

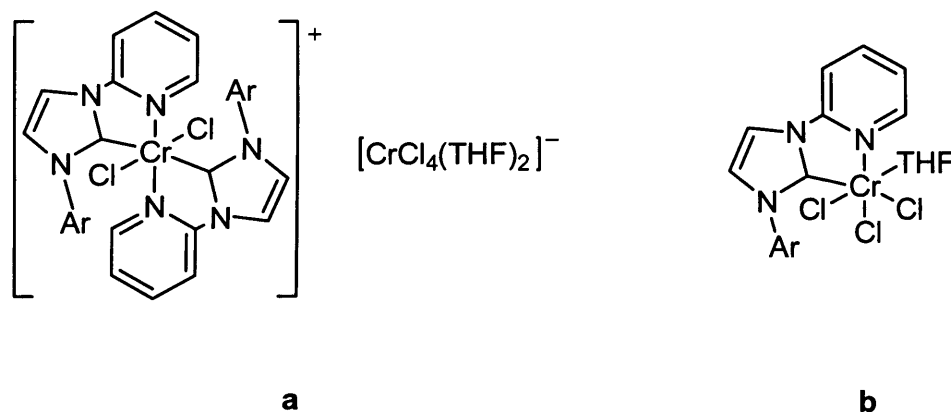
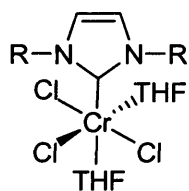


Figure 5.6 Complexes formed when NHC is added (a) quickly and (b) slowly.

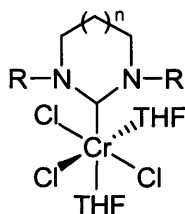
A colour change was usually observed during the addition of the free carbene, along with the disappearance of the insoluble purple chromium precursor. The mixture was left to stir for 16 h (after slowly allowing to reach room temperature) and the resulting precipitate collected by filtration. Complexes **97-109** were isolated as brightly coloured free flowing solids which quickly change colour upon exposure to air and/or moisture. Based on the stoichiometry of reagents, the structures of the complexes were expected to be as displayed in figure 5.7. Similar octahedral structures are reported for related complexes in the literature.^{16, 40-42, 47}

Free carbenes are very strong sigma donor ligands, which easily displace labile THF ligands in the $\text{CrCl}_3(\text{THF})_3$ metal precursor. Carbenes **10-12**, **16**, **18**, and **57-59** (i.e. donor-functionalised NHC ligands) were expected to form chelate complexes of the type $\text{Cr}(\text{NHC})(\text{THF})\text{Cl}_3$ (Type 2, figure 5.7), whereas the monodentate carbenes **60**, **62** and **63** were expected to result in complexes containing one NHC and two THF ligands. The potentially tridentate NHC ligands **13** and **96** were expected to form complexes of the type $\text{Cr}(\text{NHC})\text{Cl}_3$ (Type 3, figure 5.7). Cr(III) complexes have been known to form dinuclear (bridging) complexes, particularly with chloride ligands present,^{16, 48} and is reported to be due to the desire to form octahedral complexes in the absence of sufficient ligands.¹⁶ This is relatively rare however, so complexes **97-109** were expected to be mononuclear, as shown in figure 5.7.

Type 1



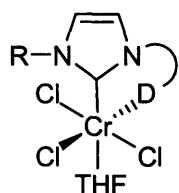
R = Mes 107



R = Dipp, n = 1 108

R = Mes, n = 2 109

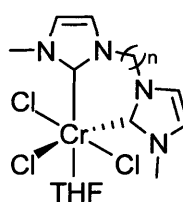
Type 2



R = Me, D = O 97

R = ⁱPr, D = O 98R = ^tBu, D = O 99

R = Me, D = N-Ph 101

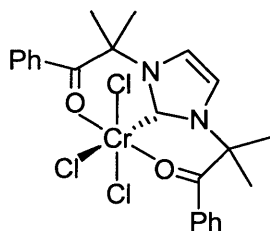
R = ⁱPr, D = O-Me 102

n = 1 103

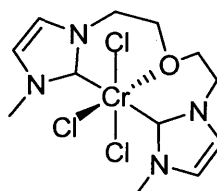
n = 2 104

n = CH₂(C₆H₄)CH₂ 105

Type 3



100



106

Figure 5.7 Probable structures of Cr(III) complexes 97-109.

Crystals suitable for X-ray analysis were obtained by slow diffusion of diethyl ether into a dichloromethane solution of complex **100**. The structure is shown in figure 5.8 and selected bond lengths and angles are displayed in table 5.1. An octahedral geometry in which

the tridentate ligand is arranged equatorially is observed, confirming the coordination of the ketone functional groups of the ligand. The geometry around the Cr is distorted from perfectly octahedral, with the O(2)-Cr(1)-O(1) angle forced from the expected linear geometry to $172.4(3)^\circ$ by the constraints of the ligand. The Cl(1)-Cr(1)-Cl(2) angle is also significantly removed from linearity at $172.9(11)^\circ$; interestingly the apical chlorides are slightly bent toward the more sterically hindered NHC rather than toward the chloride *trans* to the carbene.

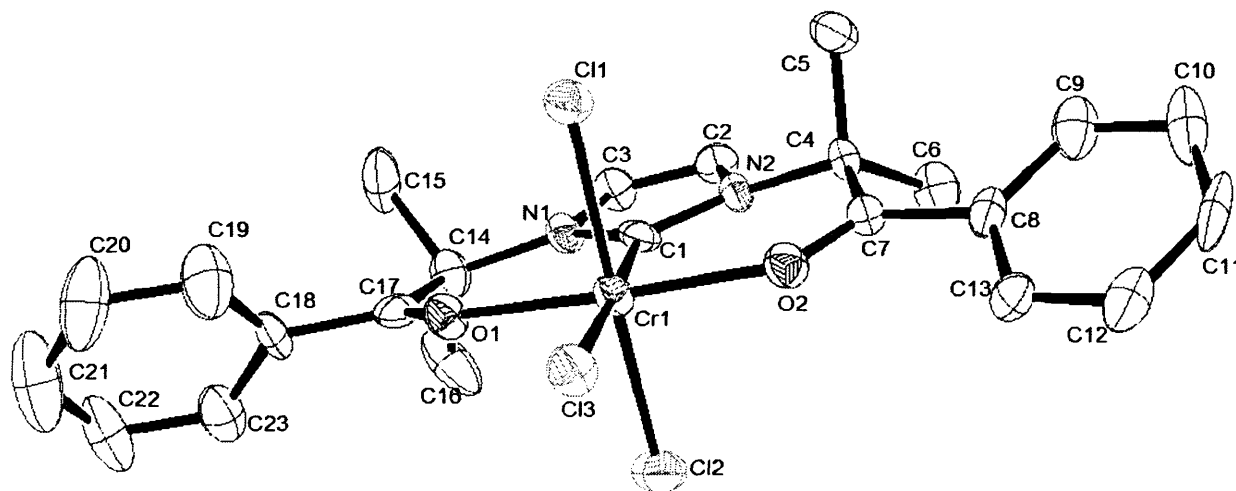


Figure 5.8 ORTEP plot at 50% probability of the molecular structure of **100**.

Bond length (Å)		Bond angle (°)	
Cr(1)-C(1)	1.997(9)	N(1)-C(1)-N(2)	106.0(7)
Cr(1)-Cl(3)	2.369(3)	C(1)-Cr(1)-Cl(3)	177.9(3)
Cr(1)-O(1)	1.987(6)	O(2)-Cr(1)-O(1)	172.4(3)
Cr(1)-O(2)	1.958(6)	C(1)-Cr(1)-O(2)	86.3(3)
C(7)-O(2)	1.236(10)	C(1)-Cr(1)-O(1)	86.1(3)
C(17)-O(1)	1.233(11)	Cl(1)-Cr(1)-Cl(2)	172.9(11)
Cr(1)-Cl(1)	2.327(3)		
Cr(1)-Cl(2)	2.317(3)		

Table 5.1 Selected bond lengths and angles for **100**.

The C(1)-Cr(1) bond length (1.997(9) Å) is on the shorter end of reported Cr-NHC complexes (average 2.158 Å).^{16, 42} However, the chloride ligand *trans* to the NHC shows no significant *trans* influence exerted by the strongly σ -donating carbene ligand, and all three Cr-Cl bonds lie in the range expected for these complexes.^{11, 42, 49}

The chelate bite angles (86.3(3) °, 86.1(3) °) are significantly larger than for the similar tridentate NHC-Pyridine-NHC-Cr(III) complex reported by Gibson and co-workers⁴² (76.3(2) °, 75.68(9) °) and demonstrate the symmetry of the coordinated ligand.

Comparison with the imidazolium salt precursor **4** shows there is no significant change in bond lengths in the imidazole ring upon coordination, as might be expected due to loss of π -electron delocalisation, we do however see a slight elongation of the carbonyl bonds C(17)-O(1) and C(7)-O(2) (1.233(11) Å, 1.236(10) Å) relative to the salt (1.211(5) Å, 1.215(5) Å) as coordination to the chromium centre takes place.

Full characterisation of complexes **97-109** proved difficult due to their sensitive and paramagnetic nature. Attempts at elemental analysis often resulted in diminished carbon and nitrogen values. A recent study on similar complexes showed that although the complexes did not appear to change, microanalytical data showed up to six molecules of water absorbed after only a short time exposed to air.⁴⁷ Our complexes showed low values for carbon and nitrogen, even with crystalline samples of **100** that were found suitable for X-ray analysis, so it was concluded that absorption of water was taking place.

Complexes **97-102** and **106** were analysed by infra-red spectroscopy, where a low frequency shift of $\sim 130\text{ cm}^{-1}$ upon coordination, relative to the free ligand is generally observed for the donor-functional groups, and has been reported for similar complexes.⁴⁷ This shift in observed frequency is due to coordination; in the case of the ketone-functionalised NHC ligands, the coordination of the oxygen to the chromium centre will result in a slightly longer and weaker C=O bond (as observed in the X-ray data for **100**). This bond will therefore absorb at a lower frequency than in the uncoordinated salts previously reported. The IR data thus confirms the bidentate coordination structure described in figure 5.7. Complex **106** was expected to coordinate to the metal centre through the linking oxygen atom as well as the two NHC moieties, forming a Cr(NHC)Cl₃ complex similar to **100**, however analysis of the IR spectra suggests that the oxygen does not coordinate. We would expect a shift relative to the free ligand upon coordination as described above, however we do not see any significant change in the stretching frequency, suggesting that no (or very weak) coordination takes place, and complex **106** therefore contains a bidentate ligand and has a structure of Type 2 (figure 5.7).

Electronic spectra for octahedral complexes of chromium(III) are expected to display three absorptions. The spectra for complexes **97-109** were recorded, and we generally see two of these absorptions, corresponding to the transition ${}^4T_{2g} \leftarrow {}^4A_{2g}$ at around 600 nm and the transition ${}^4T_{1g} \leftarrow {}^4A_{2g}$ at around 450 nm, which is comparable to reported data for similar complexes.⁴⁷ The third expected transition ${}^4T_{1g} \leftarrow {}^4A_{2g}$ was not observed, and is generally reported to be obscured by charge transfer bands.⁴⁴ The magnetic moments of complexes **97-109** were determined using the method of Evans, as described in 4.2.5, and lie in the range $3.63 \mu_B - 3.92 \mu_B$ confirming three unpaired electrons, and providing further evidence that these complexes are mononuclear as described in figure 5.6; dinuclear structures are reported to have lower magnetic moments ($\sim 3.0 \mu_B$).^{40, 50}

Characterisation of these complexes by mass spectrometry proved consistently unsuccessful, despite several attempts to limit exposure to moisture by direct injection. Characterisation difficulties due to high sensitivity has been reported many times in the literature for this type of complex.^{47, 51-54} However, in light of the evidence provided, and the data obtained from the EPR studies (see EPR analyses below; section 5.2.2), complexes **97-109** are confidently assigned as mononuclear octahedral chromium complexes of the type proposed in figure 5.7. These complexes were also tested as pre-catalysts for chain-growth reactions (ethylene oligomerisation/polymerisation). Reaction conditions and catalytic results are described below (section 5.2.3).

5.2.2 EPR Studies

The *cw*-EPR spectra for the Cr(III)-NHC complexes are shown below in figures 5.9 and 5.10. At this frequency (9 GHz) the spectra are broad and poorly resolved owing to the $S = 3/2$ spin state of the system.

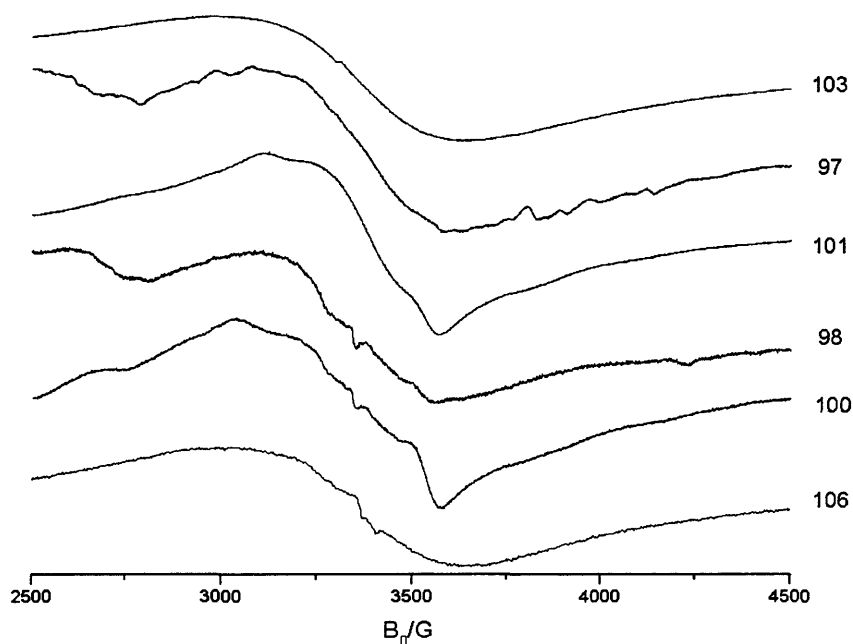


Figure 5.9 Experimental spectra of Cr(III) complexes.

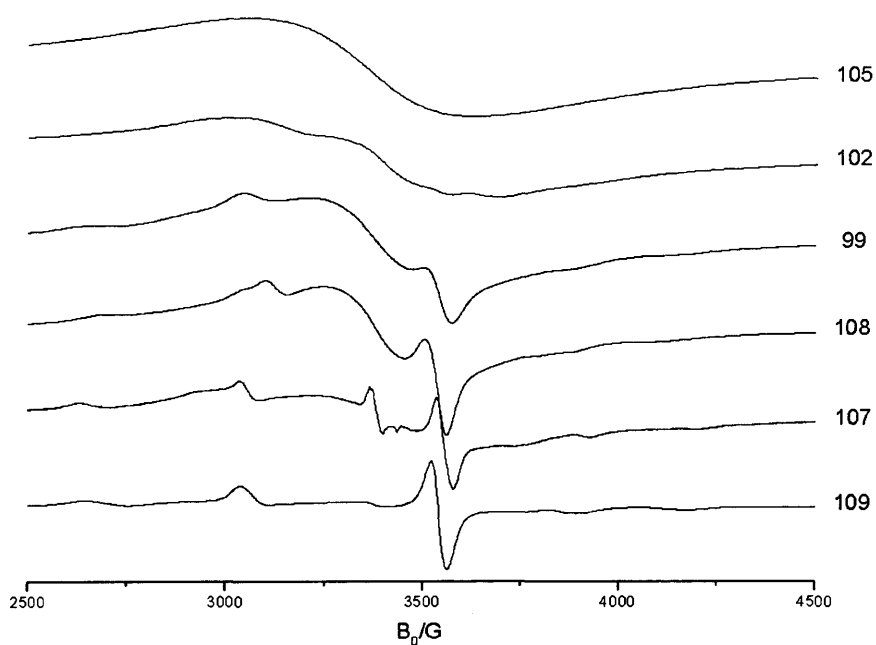


Figure 5.10 Experimental spectra of Cr(III) complexes.

Cr(III) has the electronic configuration s^0d^3 and ground state 4F as a free ion. Numerous studies have been conducted on Cr(III), as it has been demonstrated to yield room temperature EPR spectra with well defined lines. The energy gain from a low spin configuration is usually offset by the electron pairing energy, and complexes are usually encountered with high spin $S = 3/2$. As such Cr(III) spectra are significantly influenced by the values for zero field splitting (zfs), and the spectra must be considered in terms of the two Kramer's doublets $|^3/2, \pm 1/2\rangle$ and $|^3/2, \pm 3/2\rangle$, separated by $|2D|$.

Zero field splitting is frequently large in the case of transition metal species, with the result that the spin states are so widely separated that the microwave energy in conventional EPR spectrometers (X-band ~ 9 GHz (0.3cm^{-1}), Q-band ~ 35 GHz (1.2cm^{-1})) is insufficient to cause a transition. Consequently integer spin transitional metal species appear to be "EPR-silent" – no signal can be observed with these instruments. High frequency EPR is then required.

Three distinct cases can be considered for Cr(III) species in both rhombic and axial environments; these are i) $|D| \ll h\nu$, ii) $|D| \gg h\nu$ and iii) $|D| \approx h\nu$:

- i) $|D| \ll h\nu$; All three spin allowed transitions are observed around $g \approx 2$, in both rhombic and axial environments; however the superposition generating the glass spectrum together with line broadening effects will commonly result in an unresolved broad feature around free spin.
- ii) $|D| \gg h\nu$; Within an axial environment the $|^3/2, \pm 3/2\rangle$ Kramers doublet is essentially EPR silent resulting in only the transitions within the $|^3/2, \pm 1/2\rangle$ manifold being observed. The applied field strengths for these resonances is given by:

$$g^2(\theta) = g_{\parallel}^2 \cos^2 \theta + 4g_{\perp}^2 \sin^2 \theta$$

Turning points in the absorption spectrum (i.e., features in the EPR spectrum) are therefore observed at $\theta = 0^\circ$ and 90° to the z axis – corresponding to g_{\parallel} at $g_{\text{eff}} \approx 2$ and $2g_{\perp}$ at $g_{\text{eff}} \approx 4$.

For a rhombic environment, the E term must also be considered, which has the effect of intermixing the $|^3/2, \pm 1/2\rangle$ and $|^3/2, \pm 3/2\rangle$ states. The structure of a spectrum arising from such a system is best considered in terms of rotation of a crystalline sample in the cases $\lambda \approx 1/3$ and $\lambda \rightarrow 0$ (where $\lambda = E/D$).

With the external field parallel to z, two equally intense transitions occur asymmetrically about free spin, with the high field resonance originating from the

lower Kramers doublet, and the lower resonance from the higher energy doublet. Glass spectra from the systems are, as discussed superpositions of all these orientations, potentially with quite broad lines. Such spectra can therefore appear complex and highly variable.

- iii) $|D| \approx h\nu$; Transitions between doublets are possible in this scenario in both symmetry environments. Furthermore, off-axis turning points - “looping” transitions - become significant, and in cases of high λ the E term intermixes the Kramers doublets to the extent that a fourth transition maybe observed. Powder spectra in the case $|D| \approx h\nu$ rhombic symmetry can therefore be more complicated than either of the other $|D|$ regimes considered.

As a result the detailed interpretation of the EPR spin Hamiltonian parameters can only be extracted by performing measurements at multiple frequencies (which we did not have access to in this project), particularly higher frequencies. Therefore the current spectra shown in Figure 5.9 and 5.10 at this stage can only be used to confirm the high spin nature of the $S = 3/2$ spin system with significant ZFS and to confirm that the coordination mode is a distorted octahedral system.

5.2.3 Catalysis

Catalytic testing was largely carried out by Dr David McGuinness and James Sutil at the University of Tasmania. This was done to provide consistency and to allow comparisons with other Sasol catalyst systems.

The complexes were activated with 300 equivalents of co-catalyst MAO, and reacted under 10 bar ethylene in toluene.

The catalysis results are displayed in table 5.2, and show that the complexes tested give mostly polymer (69.35%-98.87%), with small amounts of linear alpha olefins (LAOs), and generally show no pattern in selectivity toward the LAOs. The activities of the complexes vary significantly, and if comparisons are made between the turnover numbers (TON), it can be seen that particularly low activities are observed for complexes containing chelating bis(carbene) ligands (**104** and **106**), while complex **105** shows one of the highest TONs, suggesting that the added steric bulk present due to the bridging xylyl group is a factor in catalyst activity.

Catalyst	% C-4	% C-6	% C-8	% C-10	% > C-10 and Branched C10*	% PE	Total TON
97	0.02	0.05	0.23	0.03	0.58	98.36	5017
98	0.48	0.16	0.43	0.05	0.88	97.52	2442
99	0.29	0.15	0.19	0.04	0.21	98.87	3697
100	1.65	3.06	2.38	1.16	1.71	87.57	2647
102	8.41	8.27	4.65	2.22	2.50	69.35	1447
104	5.87	0.68	0.96	0.12	0.40	90.16	499
105	0.38	0.99	0.94	0.50	2.28	92.85	3623
106	6.78	3.49	2.39	0.87	1.10	80.48	758
108	1.95	3.77	2.51	1.24	2.02	86.83	3030
109	6.58	4.17	2.76	1.09	1.26	79.26	933

* Describes LAOs

Table 5.2 Catalysis results for a selection of Cr(III)-NHC complexes.

Interestingly, the two monodentate, expanded NHC complexes **108** and **109** show very different activities; the complex containing the 6-membered NHC has a TON more than three times that of the 7-membered NHC complex. This could be due to the different ring size, which has been previously reported to affect catalytic capability, but the difference in steric bulk of the N-substituents (Dipp and Mes respectively) could also be partially responsible for the different observed TON.

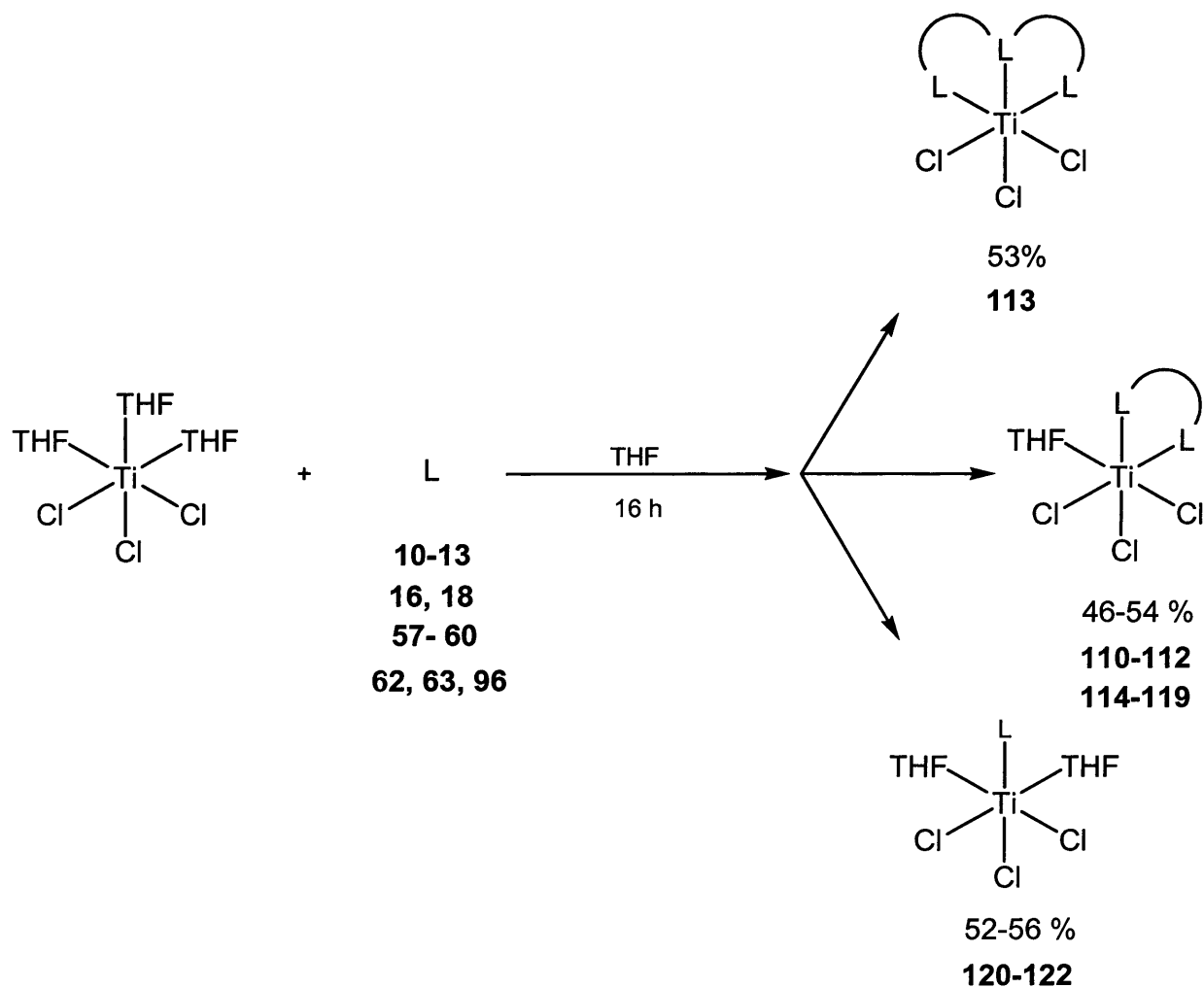
Compound **103** was previously studied by Theopold and co-workers,¹⁶ and showed production of polymer with little branching. Our results obtained for the related bis(carbene) compounds **104** and **105** showed similar selectivities.

The results reported in table 5.2 show lower selectivity toward LAOs than similar reported systems,⁴¹ however, given the interest in carbene-based polymerisation catalysis, this work represents an interesting survey of chromium(III)-NHC complexes, contributing to this growing area of homogeneous catalysis as well as the development of NHC-containing catalysts.

5.2.4 Synthesis of Ti(III)-NHC Complexes

Given the suitability of Ti(III) complexes for EPR studies and their potential catalytic application, we were interested in preparing a series of Ti(III)-NHC model compounds analogous to the chromium complexes **97-109** described in 5.2.1.

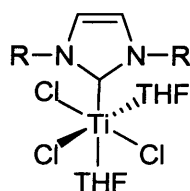
NHC ligands **10-13**, **16**, **18**, **57-60**, **62**, **63** and **96** were prepared as previously described, and slowly added to a solution of $\text{TiCl}_3(\text{THF})_3$ in THF at $-10\text{ }^\circ\text{C}$. Again, a colour change was generally observed, along with the formation of a precipitate, which was isolated by filtration after stirring for 16 h at room temperature (scheme 5.2).



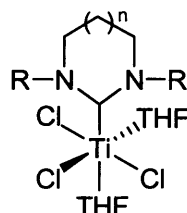
Scheme 5.2 Synthesis of Ti(III)-NHC complexes **110-122**.

The use of $\text{TiCl}_3(\text{THF})_3$ ¹⁸ as a metal precursor, the same ligands, and similar reaction conditions to those already described meant that the resulting complexes (110-122) could be expected to be isostructural to the chromium complexes 97-109 (Figure 5.11).

Type 1



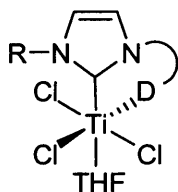
R = Mes 120



R = Dipp, n = 1 121

R = Mes, n = 2 122

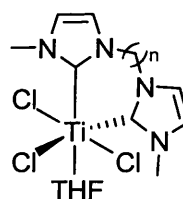
Type 2



R = Me, D = O 110

R = ⁱPr, D = O 111R = ^tBu, D = O 112

R = Me, D = N-Ph 114

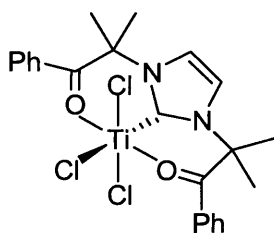
R = ⁱPr, D = O-Me 115

n = 1 116

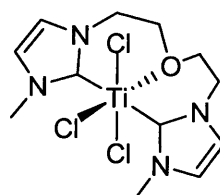
n = 2 117

n = CH₂(C₆H₄)CH₂ 118

Type 3



113



119

Figure 5.11 Probable structures of Ti(III) complexes 110-122.

As discussed in 5.1, the use of NHC ligands for coordination to early transition metals is much less common than for late transition metals, and this has been attributed to the ease of dissociation of the metal-carbene bond.^{19, 46, 55-58} A Ti(III)-NHC complex recently reported by Lorber⁴⁶ and co-worker was found to be extremely air and moisture sensitive, decomposing within minutes of exposure, making characterisation difficult.

Unfortunately, no crystals suitable for X-ray analysis were obtained for these brightly coloured complexes **110-122**. Elemental analysis gave poor results, consistently low in carbon and nitrogen, suggesting that similar to chromium complexes **97-109**, moisture absorption and/or decomposition was taking place, a reasonable assumption based on previously reported complexes described in the literature.^{4, 46}

Infra-red analysis of complexes **110-115** confirmed coordination of the functional groups, characterised by a shift in the stretching frequency relative to the free ligands as described for chromium complexes **97-102**. This evidence supports the proposed structures described in figure 5.8. Again we see no evidence of coordination of the bridging oxygen in **119**, suggesting a similar structure to **106**, i.e. bidentate ligand coordination.

Electronic spectra were recorded for titanium complexes **110-122**, and show a single absorption around 500-600 nm, corresponding to the transition ${}^2E_g \leftarrow {}^2T_{2g}$. This single transition is reported for such octahedral Ti(III) complexes⁵⁹ and confirms the d^1 electronic configuration. This was corroborated by the determination of magnetic moments, which lie in the range $1.65 \mu_B - 1.98 \mu_B$, consistent with a d^1 ion containing one unpaired electron. Bridging dinuclear structures are generally not observed with titanium complexes of this type, so the confirmation of a mononuclear structure was expected.

Again, analysis by mass spectroscopy proved unsuccessful due to the sensitive nature of the complexes. Given the lack of X-ray and elemental analysis data, the complexes **110-122** cannot be unambiguously characterised. However, analysis by EPR spectroscopy in collaboration with infra-red and electronic spectroscopy provides strong evidence for the proposed structures, and comparison with reported data also provides significant support for the proposed complexes described in figure 5.8.^{18, 19, 46, 60}

5.2.5 EPR Studies

The low temperature EPR spectra (X-band) for the mono- and bi-dentate Ti(III)-NHC complexes are shown below in figures 5.12 and 5.13 respectively:

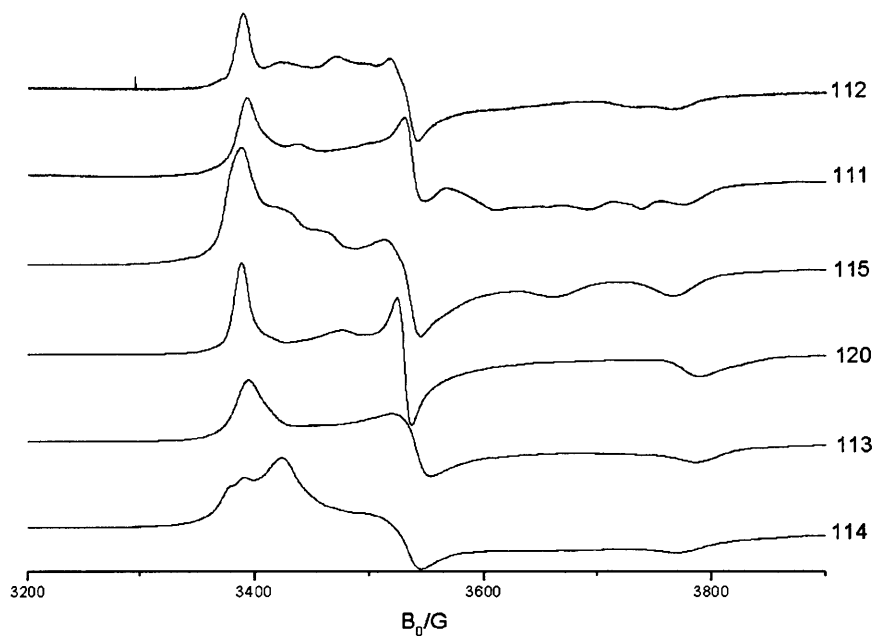


Figure 5.12 Experimental spectra of Ti(III) complexes.

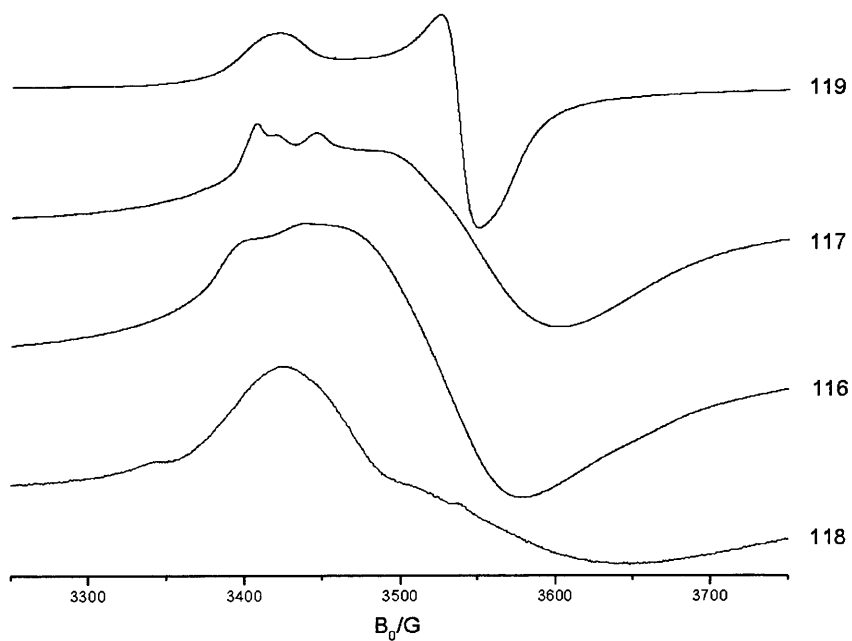


Figure 5.13 Experimental spectra of Ti(III) complexes.

The mono-dentate complexes possess a pronounced rhombic EPR symmetry (Figure A). The g values were all less than free spin (as expected for a d^1 transition metal ion) with approximate values of $g_1 \approx 1.978$, $g_2 \approx 1.985$, and $g_3 \approx 1.775$. For paramagnetic metal complexes of the type $[MA_xB_y]$ the relationship between the point symmetry and the EPR parameters is straightforward. For example, in $[MA_5B]$ -type complexes possessing C_{4v} symmetry, then $g_x = g_y \neq g_z$ while in $[MA_4B_2]$, the *trans* complex possesses D_{4h} symmetry with $g_x = g_y \neq g_z$ whilst the *cis* complex of C_{2v} symmetry produces $g_x \neq g_y \neq g_z$ (in theory, although in practice it often appears as axial since $g_x \approx g_y$). Hence a simple analysis of the EPR data was possible for the $[Cr(I)(CO)_4\text{-bis(phosphine)}]$ complexes discussed in Chapter 3 and the $[Cr(I)(CO)_4\text{-NHC}]$ complexes discussed in Chapter 4. In the present case, the mono-dentate $[Ti(III)(Cl)_3(THF)_2\text{-carbene}]$ complexes and the bi-dentate $[Ti(III)(Cl)_3(THF)\text{-carbene}]$ complexes are less straightforward to analyse simply.

The orbital splitting pattern for an octahedral complex with tetragonal distortion (either elongation or compression) was shown previously in figure 4.15 in chapter 4. As shown in this diagram, compression of the M-L bonds along the z -axis produces the expected terms ${}^2A_{1g}$ and ${}^2B_{1g}$ (in the upper 2E_g state) and 2E_g and ${}^2B_{2g}$ (in the lower ${}^2T_{2g}$ state). Such a splitting pattern produces a paramagnetic state for a low spin d^5 system (such as Cr(I)) but would lead to an EPR silent ground state for a d^1 system in the absence of additional rhombic distortion. In other words, the single unpaired electron in the degenerate d_{xz} and d_{yz} orbitals would be EPR silent. If this degeneracy was lifted by rhombic distortion (eg., d_{xz} lowest level as shown in figure 4.15 in chapter 4) then an EPR spectrum would be seen. Alternatively, with compression of the M-L bonds along the z -axis, the single d_{xy} orbital now has lowest energy and this will lead to an EPR signal both in a tetragonal distortion and subsequent rhombic distortion. The observation of the EPR spectra from the mono- and bi-dentate carbene complexes suggests that this situation must be occurring. The axial g values for complex **119** ($g_{\perp} = 1.895$, $g_{\parallel} = 1.965$) and the rhombic g values for complexes **111** - **115** and **120** ($g_1 \approx 1.978$, $g_2 \approx 1.985$, and $g_3 \approx 1.775$) are both consistent with this view and the predicted structures given in figure 5.11 above.

5.2.6 Catalysis

Catalytic testing was carried out for titanium complexes **110-113**, **115** and **117-122** in the same way as the analogous chromium complexes discussed in section 5.2.3. The results are displayed in table 5.3 and generally show lower TONs than the analogous chromium catalysts, an observation that has been previously demonstrated in the literature.^{44a}

One notable exception observed in our systems is complex **122** which shows a significantly higher TON and lower selectivity towards the linear alpha olefins than the chromium analogue **109**. The result of this is that the two monodentate, expanded NHC complexes **121** and **122** show more similar results in the titanium catalysts than in the previously discussed chromium systems

Catalyst	% C-4	% C-6	% C-8	% C-10	% > C-10 and Branched C10*	% PE	Total TON
110	1.89	1.72	0.44	0.11	1.61	92.95	2556
111	1.26	1.30	0.34	0.09	1.28	94.73	2657
112	2.10	1.09	0.49	0.42	2.27	92.87	1734
113	1.50	0.96	0.46	0.21	2.35	93.87	1717
115	1.09	0.88	0.53	0.38	3.96	92.52	3397
117	3.80	0.69	0.35	0.09	1.17	92.53	389
118	3.42	1.07	0.48	0.19	2.29	91.40	1804
119	1.74	1.69	1.15	0.88	10.09	83.29	1659
121	1.03	0.74	0.46	0.32	2.94	93.95	2735
122	0.99	0.97	0.31	0.14	1.41	95.30	3230

* Describes LAOs

Table 5.3 Catalysis results for a selection of Ti(III)-NHC complexes.

Again, we see no pattern in selectivity toward the LAOs in respect of the nature of the ligand present, but interestingly, while the titanium catalysts also gave mostly polymer we observe a narrower range than the chromium systems (83.29% - 95.30%) compared to (69.35% - 98.87%).

5.3 Conclusion

A series of new NHC containing chromium(III) and titanium(III) complexes have been prepared. Characterisation using EPR spectroscopy confirms the oxidation state and symmetry described for the complexes, and an X-ray structure in addition to other analytical data provides significant evidence for the proposed chromium structures. The paramagnetic character, and extreme sensitivity of many of the complexes made the common methods of complex characterisation (NMR, mass spectrometry, elemental analysis) unsuitable or unreliable. However, based on the data provided above, the structures of the complexes can be assigned with some confidence.

Given the application of these types of complexes, a number have been tested as catalysts. The results show very little selectivity toward LAOs, with no apparent correlation between structure and selectivity.

5.4 Experimental Section

General Remarks. All manipulations were performed using standard Schlenk techniques under an argon atmosphere, or in a nitrogen atmosphere MBraun UNILAB glovebox with less than 0.1ppm water and O₂. Solvents were dried using a Braun Solvent Purification System, and degassed prior to use. CrCl₃(thf)₃ was purchased from Aldrich, Carbenes **10-13**, **16**, **18**, **57-60**, **62**, **63** and **96** were prepared as previously described (2.4) or according to literature procedures^{61, 62} and TiCl₃(THF)₃¹⁸ was prepared according to a literature procedure.

NMR spectra were recorded at 298 K on Bruker Avance AMX 400 or Bruker-ACS 60 spectrometers. Chemical shift values are given relative to residual solvent peak. ESI-MS were performed on a Waters LCT Premier XE instrument. Electronic spectra were recorded in dichloromethane on a Perkin Elmer Lambda 900 UV/VIS/NIR spectrometer. EPR spectra and computer simulations were carried out with the assistance of Lucia McDyre, a PhD student at Cardiff University. EPR spectra were recorded at 130K on an X-band Bruker EMX spectrometer operating at 100 kHz field modulation, 10mW microwave power and equipped with a high sensitivity cavity (ER 4119HS). EPR computer simulations were performed using the SimEPR32 program.⁶³ g Values were determined using a DPPH standard. Complexes were dissolved in 200μl DCM/toluene and a frozen solution produced by placing the EPR tube in liquid nitrogen.

CrCl₃(NHC)(THF) (NHC = 1-methyl-3-isobutyrophenoneimidazole-2-ylidene) (**97**)

To a slurry of CrCl₃(THF)₃ (535 mg, 1.43 mmol) in THF (10 ml) at -10 °C a solution of free carbene **10** (1.49 mmol) in THF (10 ml) was added dropwise over 30 min. The resulting mixture was allowed to slowly warm to room temperature, and left to stir for 16 h. The solution was concentrated and diethyl ether (10 ml) added to precipitate the complex. The product was isolated by filtration, washed with diethyl ether (3 × 10 ml) and dried *in vacuo* to give the product as a green solid (350 mg, 53%). IR (CH₂Cl₂): $\nu = 1551$ (s) (CO) cm⁻¹. λ_{max} (CH₂Cl₂)/nm 620, 450. Magnetic moment $\mu_{\text{eff}} = 3.87 \mu_{\text{B}}$.

CrCl₃(NHC)(THF) (NHC = 1-isopropyl-3-isobutyrophenoneimidazole-2-ylidene) (98)

An analogous method to that of **97** was followed, using CrCl₃(THF)₃ (530 mg, 1.41 mmol) and free carbene **11** (1.47 mmol). The product was obtained as a green powder (360 mg, 52%). IR (CH₂Cl₂): $\nu = 1551$ (s) (CO) cm⁻¹. $\lambda_{\max}(\text{CH}_2\text{Cl}_2)/\text{nm}$ 620, 440. Magnetic moment $\mu_{\text{eff}} = 3.85 \mu_{\text{B}}$.

CrCl₃(NHC)(THF) (NHC = 1-^tButyl-3-isobutyrophenoneimidazole-2-ylidene) (99)

An analogous method to that of **97** was followed, using CrCl₃(THF)₃ (515 mg, 1.37 mmol) and free carbene **12** (1.43 mmol). The product was obtained as a purple powder (340 mg, 49%). IR (CH₂Cl₂): $\nu = 1550$ (s) (CO) cm⁻¹. $\lambda_{\max}(\text{CH}_2\text{Cl}_2)/\text{nm}$ 570, 470. Magnetic moment $\mu_{\text{eff}} = 3.88 \mu_{\text{B}}$.

CrCl₃(NHC) (NHC = 1,3-diisobutyrophenoneimidazole-2-ylidene) (100)

An analogous method to that of **97** was followed, using CrCl₃(THF)₃ (530 mg, 1.42 mmol) and free carbene **13** (1.48 mmol). The product was obtained as a pale blue powder (370 mg, 51%). IR (CH₂Cl₂): $\nu = 1549$ (s) (CO) cm⁻¹. $\lambda_{\max}(\text{CH}_2\text{Cl}_2)/\text{nm}$ 590, 460. Magnetic moment $\mu_{\text{eff}} = 3.79 \mu_{\text{B}}$.

CrCl₃(NHC)(THF)**(NHC = 1-methyl-3-phenylpropylidenebenzenamineimidazole-2-ylidene) (101)**

An analogous method to that of **97** was followed, using CrCl₃(THF)₃ (535 mg, 1.43 mmol) and free carbene **16** (1.49 mmol). The product was obtained as a red powder (370 mg, 48%). IR (CH₂Cl₂): $\nu = 1484$ (s) (CO) cm⁻¹. $\lambda_{\max}(\text{CH}_2\text{Cl}_2)/\text{nm}$ 560, 420. Magnetic moment $\mu_{\text{eff}} = 3.81 \mu_{\text{B}}$.

CrCl₃(NHC)(THF)**(NHC = 1-Isopropyl-3-(2-methoxy-5-methylphenyl)imidazole-2-ylidene) (102)**

An analogous method to that of **97** was followed, using CrCl₃(THF)₃ (540 mg, 1.44 mmol) and free carbene **18** (1.50 mmol). The product was obtained as a green powder (300 mg, 45%). IR (CH₂Cl₂): $\nu = 1156$ (s) (COC) cm⁻¹; $\lambda_{\max}(\text{CH}_2\text{Cl}_2)/\text{nm}$ 640, 410. Magnetic moment $\mu_{\text{eff}} = 3.80 \mu_{\text{B}}$.

CrCl₃(NHC)(THF) (NHC=1,1'-methylene-3,3'-dimethylimidazole-2,2'-diylidene) (103)

An analogous method to that of **97** was followed, using CrCl₃(THF)₃ (530 mg, 1.42 mmol) and free carbene **57** (1.48 mmol). The product was obtained as a yellow powder (300 mg, 52%). $\lambda_{\max}(\text{CH}_2\text{Cl}_2)/\text{nm}$ 610, 430; Magnetic moment $\mu_{\text{eff}} = 3.67 \mu_{\text{B}}$.

CrCl₃(NHC)(THF) (NHC = 1,1'-propylene-3,3'-dimethylimidazole-2,2'-diylidene) (104)

An analogous method to that of **97** was followed, using CrCl₃(THF)₃ (540 mg, 1.44 mmol) and free carbene **58** (1.50 mmol). The product was obtained as a lilac powder (310 mg, 49%). $\lambda_{\max}(\text{CH}_2\text{Cl}_2)/\text{nm}$ 590, 420. Magnetic moment $\mu_{\text{eff}} = 3.82 \mu_{\text{B}}$.

CrCl₃(NHC)(THF) (NHC = 1,1'-xylylene-3,3'-dimethylimidazole-2,2'-diylidene) (105)

An analogous method to that of **97** was followed, using CrCl₃(THF)₃ (520 mg, 1.40 mmol) and free carbene **59** (1.45 mmol). The product was obtained as a green powder (350 mg, 50%). $\lambda_{\max}(\text{CH}_2\text{Cl}_2)/\text{nm}$ 630, 450. Magnetic moment $\mu_{\text{eff}} = 3.74 \mu_{\text{B}}$.

CrCl₃(NHC)(THF) (NHC = 1,1'-bis(2-(3-methylimidazolin-2-yliden-1-yl)ethyl)ether) (106)

An analogous method to that of **97** was followed, using CrCl₃(THF)₃ (525 mg, 1.40 mmol) and free carbene **96** (1.45 mmol). The product was obtained as a lilac powder (260 mg, 47%). IR (CH₂Cl₂): $\nu = 1259$ (s) (COC) cm⁻¹. $\lambda_{\max}(\text{CH}_2\text{Cl}_2)/\text{nm}$ 570, 450. Magnetic moment $\mu_{\text{eff}} = 3.72 \mu_{\text{B}}$.

CrCl₃(NHC)(THF)₂ (NHC = 1,3-bis-(2,4,6-trimethylphenyl)imidazole-2-ylidene) (107)

An analogous method to that of **97** was followed, using CrCl₃(THF)₃ (530 mg, 1.42 mmol) and free carbene **60** (1.48 mmol). The product was obtained as a green powder (470 mg, 55%). $\lambda_{\max}(\text{CH}_2\text{Cl}_2)/\text{nm}$ 640, 470. Magnetic moment $\mu_{\text{eff}} = 3.92 \mu_{\text{B}}$.

CrCl₃(NHC)(THF)₂**(NHC = 1,3-bis(2,6-diisopropylphenyl)-4,5,6-trihydropyridin-2-ylid) (108)**

An analogous method to that of **97** was followed, using CrCl₃(THF)₃ (520 mg, 1.40 mmol) and free carbene **62** (1.45 mmol). The product was obtained as a lilac powder (500 mg, 51%). $\lambda_{\max}(\text{CH}_2\text{Cl}_2)/\text{nm}$ 590, 440. Magnetic moment $\mu_{\text{eff}} = 3.63 \mu_{\text{B}}$.

CrCl₃(NHC)(THF)₂**(NHC = 1,3-bis-(2,4,6-trimethylphenyl)-4,5,6,7-tetrahydro-[1,3]-diazepin-2-ylid) (109)**

An analogous method to that of **97** was followed, using CrCl₃(THF)₃ (500 mg, 1.34 mmol) and free carbene **63** (1.40 mmol). The product was obtained as a lilac powder (450 mg, 53%). $\lambda_{\max}(\text{CH}_2\text{Cl}_2)/\text{nm}$ 580, 450. Magnetic moment $\mu_{\text{eff}} = 3.70 \mu_{\text{B}}$.

TiCl₃(NHC)(THF) (NHC = 1-methyl-3-isobutyrophenoneimidazole-2-ylidene) (110)

An analogous method to that of **97** was followed, using TiCl₃(THF)₃ (495 mg, 1.33 mmol) and free carbene **10** (1.39 mmol). The product was obtained as a yellow powder (290 mg, 48%). IR (CH₂Cl₂): $\nu = 1552$ (s) (CO) cm⁻¹. $\lambda_{\max}(\text{CH}_2\text{Cl}_2)/\text{nm}$ 480. Magnetic moment $\mu_{\text{eff}} = 1.87 \mu_{\text{B}}$.

TiCl₃(NHC)(THF) (NHC = 1-isopropyl-3-isobutyrophenoneimidazole-2-ylidene) (111)

An analogous method to that of **97** was followed, using TiCl₃(THF)₃ (525 mg, 1.42 mmol) and free carbene **11** (1.48 mmol). The product was obtained as a green powder (350 mg, 51%). IR (CH₂Cl₂): $\nu = 1551$ (s) (CO) cm⁻¹. $\lambda_{\max}(\text{CH}_2\text{Cl}_2)/\text{nm}$ 630. Magnetic moment $\mu_{\text{eff}} = 1.65 \mu_{\text{B}}$.

TiCl₃(NHC)(THF) (NHC = 1^t-Butyl-3-isobutyrophenoneimidazole-2-ylidene) (112)

An analogous method to that of **97** was followed, using TiCl₃(THF)₃ (545 mg, 1.46 mmol) and free carbene **12** (1.53 mmol). The product was obtained as a green powder (360 mg, 50%). IR (CH₂Cl₂): $\nu = 1548$ (s) (CO) cm⁻¹. $\lambda_{\max}(\text{CH}_2\text{Cl}_2)/\text{nm}$ 630. Magnetic moment $\mu_{\text{eff}} = 1.86 \mu_{\text{B}}$.

TiCl₃(NHC) (NHC = 1,3-diisobutyrophenoneimidazole-2-ylidene) (113)

An analogous method to that of **97** was followed, using TiCl₃(THF)₃ (515 mg, 1.39 mmol) and free carbene **13** (1.45 mmol). The product was obtained as a brown powder (380 mg, 53%). IR (CH₂Cl₂): $\nu = 1546$ (s) (CO) cm⁻¹. $\lambda_{\max}(\text{CH}_2\text{Cl}_2)/\text{nm}$ 580. Magnetic moment $\mu_{\text{eff}} = 1.98 \mu_{\text{B}}$.

TiCl₃(NHC)(THF)**(NHC = 1-methyl-3-phenylpropylidenebenzenamineimidazole-2-ylidene) (114)**

An analogous method to that of **97** was followed, using TiCl₃(THF)₃ (500 mg, 1.36 mmol) and free carbene **16** (1.42 mmol). The product was obtained as a green powder (380 mg, 52%). IR (CH₂Cl₂): $\nu = 1463$ (s) (CO) cm⁻¹. $\lambda_{\max}(\text{CH}_2\text{Cl}_2)/\text{nm}$ 600. Magnetic moment $\mu_{\text{eff}} = 1.77 \mu_{\text{B}}$.

TiCl₃(NHC)(THF)**(NHC = 1-Isopropyl-3-(2-methoxy-5-methylphenyl)imidazole-2-ylidene) (115)**

An analogous method to that of **97** was followed, using TiCl₃(THF)₃ (530 mg, 1.43 mmol) and free carbene **18** (1.49 mmol). The product was obtained as a green powder (350 mg, 54%). IR (CH₂Cl₂): $\nu = 1159$ (s) (COC) cm⁻¹. $\lambda_{\max}(\text{CH}_2\text{Cl}_2)/\text{nm}$ 610. Magnetic moment $\mu_{\text{eff}} = 1.80 \mu_{\text{B}}$.

TiCl₃(NHC)(THF) (NHC=1,1'-methylene-3,3'-dimethylimidazole-2,2'-diylidene) (116)

An analogous method to that of **97** was followed, using TiCl₃(THF)₃ (530 mg, 1.44 mmol) and free carbene **57** (1.50 mmol). The product was obtained as a purple powder (290 mg, 50%). $\lambda_{\max}(\text{CH}_2\text{Cl}_2)/\text{nm}$ 590. Magnetic moment $\mu_{\text{eff}} = 1.83 \mu_{\text{B}}$.

TiCl₃(NHC)(THF) (NHC = 1,1'-propylene-3,3'-dimethylimidazole-2,2'-diylidene) (117)

An analogous method to that of **97** was followed, using TiCl₃(THF)₃ (508 mg, 1.37 mmol) and free carbene **58** (1.43 mmol). The product was obtained as a brown powder (300 mg, 51%). $\lambda_{\max}(\text{CH}_2\text{Cl}_2)/\text{nm}$ 560. Magnetic moment $\mu_{\text{eff}} = 1.92 \mu_{\text{B}}$.

TiCl₃(NHC)(THF) (NHC = 1,1'-xylylene-3,3'-dimethylimidazole-2,2'-diylidene) (118)

An analogous method to that of **97** was followed, using TiCl₃(THF)₃ (500 mg, 1.34 mmol) and free carbene **59** (1.40 mmol). The product was obtained as a green powder (350 mg, 53%). $\lambda_{\max}(\text{CH}_2\text{Cl}_2)/\text{nm}$ 610. Magnetic moment $\mu_{\text{eff}} = 1.84 \mu_{\text{B}}$.

TiCl₃(NHC)(THF) (NHC = 1,1'-bis(2-(3-methylimidazolin-2-yliden-1-yl)ethyl)ether) (119)

An analogous method to that of **97** was followed, using TiCl₃(THF)₃ (520 mg, 1.40 mmol) and free carbene **96** (1.46 mmol). The product was obtained as a lilac powder (250 mg, 46%). IR (CH₂Cl₂): $\nu = 1258$ (s) (COC) cm⁻¹. $\lambda_{\max}(\text{CH}_2\text{Cl}_2)/\text{nm}$ 590. Magnetic moment $\mu_{\text{eff}} = 1.90 \mu_{\text{B}}$.

TiCl₃(NHC)(THF)₂ (NHC = 1,3-bis-(2,4,6-trimethylphenyl)imidazole-2-ylidene) (120)

An analogous method to that of **97** was followed, using TiCl₃(THF)₃ (500 mg, 1.34 mmol) and free carbene **60** (1.40 mmol). The product was obtained as a brown powder (450 mg, 56%). $\lambda_{\max}(\text{CH}_2\text{Cl}_2)/\text{nm}$ 510. Magnetic moment $\mu_{\text{eff}} = 1.83 \mu_{\text{B}}$.

TiCl₃(NHC)(THF)₂**(NHC = 1,3-bis(2,6-diisopropylphenyl)-4,5,6-trihydropyridin-2-ylid) (121)**

An analogous method to that of **97** was followed, using TiCl₃(THF)₃ (545 mg, 1.47 mmol) and free carbene **62** (1.53 mmol). The product was obtained as a yellow powder (570 mg, 55%). $\lambda_{\max}(\text{CH}_2\text{Cl}_2)/\text{nm}$ 450. Magnetic moment $\mu_{\text{eff}} = 1.98 \mu_{\text{B}}$.

TiCl₃(NHC)(THF)₂**(NHC = 1,3-bis-(2,4,6-trimethylphenyl)-4,5,6,7-tetrahydro-[1,3]-diazepin-2-ylid) (122)**

An analogous method to that of **97** was followed, using TiCl₃(THF)₃ (510 mg, 1.37 mmol) and free carbene **63** (1.43 mmol). The product was obtained as a red-brown powder (450 mg, 52%). $\lambda_{\max}(\text{CH}_2\text{Cl}_2)/\text{nm}$ 490. Magnetic moment $\mu_{\text{eff}} = 1.63 \mu_{\text{B}}$.

5.5 References

- [1] Herrmann, W. A. *Angew. Chem. Int. Ed.* **2002**, *41*, 1291 and references therein.
- [2] Kreisel, K. A.; Yap, G. P. A.; Theopold, K. H. *Chem. Commun.* **2007**, 1510.
- [3] Oefele, K.; Herrmann, W. A.; Mihalios, D.; Elison, M.; Herdtweck, E.; Priermeier, T.; Kiprof, P. *J. Organomet. Chem.* **1995**, *498*, 1.
- [4] Zhang, D.; Liu, N. *Organometallics* **2009**, *28*, 499.
- [5] Waltman, A. W.; Grubbs, R. H. *Organometallics* **2004**, *23*, 3105.
- [6] Dharmasena, U. L.; Foucault, H. M.; dos Santos, E. N.; Fogg, D. E.; Nolan, S. P. *Organometallics* **2005**, *24*, 1056.
- [7] Hu, X.; Castro-Rodriguez, I.; Olsen, K.; Meyer, K. *Organometallics* **2004**, *23*, 755.
- [8] Dorta, R.; Stevens, E. D.; Hoff, C. D.; Nolan, S. P. *J. Am. Chem. Soc.* **2003**, *125*, 10490.
- [9] Caddick, S.; Cloke, F.G. N.; Hitchcock, P. B.; Lewis, A. K. D. *Angew. Chem. Int. Ed.* **2004**, *43*, 5824.
- [10] Buchgraber, P.; Toupet, L.; Guerchais, V. *Organometallics* **2003**, *22*, 5144.
- [11] Voges, M. H.; Rømming, C.; Tilset, M. *Organometallics* **1999**, *18*, 529.
- [12] Danopoulos, A. A.; Hankin, D. M.; Wilkinson, G.; Cafferkey, S. M.; Sweet, T. K. N.; Hursthouse, M. B. *Polyhedron* **1997**, *16*, 3879.
- [13] Castarlenas, R.; Esteruelas, M. A.; Onate, E. *Organometallics* **2005**, *24*, 4343.

- [14] Nakai, H.; Hu, X.; Zakharov, L. N.; Rheingold, A. L.; Meyer, K. *Inorg. Chem.* **2004**, *43*, 855.
- [15] (a) Döhring, A.; Göhre, J.; Jolly, P. W.; Kryger, B.; Rust, J.; Verhovnik, G. P. *J. Organometallics* **2000**, *19*, 388. (b) Jens, K.-J.; Tilset, M.; Voges, H.; Blom, R.; Froseth, M. (Borealis) WO 0001739, **2000**. (c) Tilset, M.; Andell, O.; Dhindsa, A.; Froseth, M. (Borealis) WO 0249758, **2002**. (d) Niehues, M.; Kehr, G.; Erker, G.; Wibbeling, B.; Fröhlich, R.; Blacque, O.; Berke, H. *J. Organomet. Chem.* **2002**, *663*, 192. (e) Bielawski, C. W.; Grubbs, R. H. *Angew. Chem. Int. Ed.* **2000**, *39*, 2903. (f) Frenzel, U.; Weskamp, T.; Kohl, F. J.; Schattenmann, O. N.; Herrmann, W. A. *J. Organomet. Chem.* **1999**, *586*, 263. (g) Frey, G. D.; Schutz, J.; Herdtweck, E.; Herrmann, W. A. *Organometallics* **2005**, *24*, 4416. (h) Gstottmayr, C. W. K.; Bohm, V. P. W.; Herdtweck, E.; Grosche M.; Herrmann, W. A. *Angew. Chem. Int. Ed.* **2002**, *41*, 1363.
- [16] Kreisel, K. A.; Yap, G. P. A.; Theopold, K. H. *Organometallics* **2006**, *25*, 4670.
- [17] Downing, S. P.; Danopoulos, A. A. *Organometallics* **2006**, *25*, 1337.
- [18] Jones, N. A.; Liddle, S. T.; Wilson, C.; Arnold, P. L. *Organometallics* **2007**, *26*, 755.
- [19] Downing, S. P.; Guadanõ, S. C.; Pugh, D.; Danopoulos, A. A.; Bellabarba, R. M.; Hanton, M.; Smith, D.; Tooze, R. P. *Organometallics* **2007**, *26*, 3762.
- [20] (a) Schulz, G. V. *Z. Phys. Chem. B* **1935**, *30*, 379. (b) Flory, P. J. *J. Am. Chem. Soc.* **1936**, *58*, 1877. (c) Skupinska, J. *Chem. Rev.* **1991**, *91*, 613.
- [21] Dixon, J. T.; Green, M. J.; Hess, F. M.; Morgan, D. H. *J. Organomet. Chem.* **2004**, *689*, 3641.
- [22] (a) Manyik, R. M.; Walker, W. E.; Wilson, T. P. (Union Carbide Corporation) US 3300458, **1967**. (b) Briggs, J. R. *J. Chem. Soc. Chem. Commun.* **1989**, 674.

- [23] Temple, C.; Jabri, A.; Crewdson, P.; Gambarotta, S.; Korobkov, I.; Duchateau, R. *Angew. Chem. Int. Ed.* **2006**, *45*, 7050.
- [24] (a) Manyik, R. M.; Walker, W. E.; Wilson, T. P. *J. Catal.*, **1977**, *47*, 197. (b) Köhn, R. D.; Haufe, M.; Mihan, S.; Lilje, D. *Chem. Commun.*, **2000**, 1927.
- [25] (a) Morgan, D. H.; Schwikkard, S. L.; Dixon, J. T.; Nair, J. J.; Hunter, R. *Adv. Synth. Catal.*, **2003**, *345*, 939. (b) van Rensburg, W. J.; Grove, C.; Steynberg, J. P.; Stark, K. B.; Huysen, J. J.; Steynberg, P. J. *Organometallics*, **2004**, *23*, 1207.
- [26] (a) Meijboom, N.; Schaverien, C. J.; Orpen, A. G. *Organometallics*, **1990**, *9*, 774. (b) Cotton, F. A.; Wilkinson, G.; Murillo, C. A.; Bochmann, M. *Advanced Inorganic Chemistry*, Wiley, **1999**, 1355.
- [27] Overett, M. J.; Blann, K.; Bollmann, A.; Dixon, J. T.; Haasbroek, D.; Killian, E.; Maumela, H.; McGuinness, D. S.; Morgan, D. H. *J. Am. Chem. Soc.* **2005**, *127*, 10723.
- [28] Carter, A.; Cohen, S. A.; Cooley, N. A.; Murphy, A.; Scutt, J.; Wass, D. F. *Chem. Commun.* **2002**, 858.
- [29] Agapie, T.; Schofer, S. J.; Labinger, J. A.; Bercaw, J. E. *J. Am. Chem. Soc.* **2004**, *126*, 1304.
- [30] (a) Blann, K.; Bollmann, A.; Dixon, J. T.; Hess, F. M.; Killian, E.; Maumela, H.; Morgan, D. H.; Neveling, A.; Otto, S.; Overett, M. *Chem. Commun.* **2005**, 620. (b) Blann, K.; Bollmann, A.; Dixon, J. T.; Neveling, A.; Morgan, D. H.; Maumela, H.; Killian, E.; Hess, F. M.; Otto, S.; Pepler, L.; Mahomed, H. A.; Overett, M. J.; Green, M. J. (Sasol Technology) WO 04056478A1, **2004**.
- [31] McGuinness, D. S.; Rucklidge, A. J.; Tooze, R. P.; Slawin, A. M. Z. *Organometallics* **2007**, *26*, 2561.
- [32] Marks, T. J.; Chen, E. Y.-X. *Chem. Rev.* **2000**, *100*, 1391.

- [33] van Rensburg, W. J.; van den Berg, J. A.; Steynberg, P. J. *Organometallics* **2007**, *26*, 1000.
- [34] Deckers, P. J. W.; Hessen, B.; Teuben, J. H. *Organometallics* **2002**, *21*, 5122.
- [35] Deckers, P. J. W.; Hessen, B.; Teuben, J. H. *Angew. Chem., Int. Ed.* **2001**, *40*, 2516.
- [36] Andes, C.; Harkins, S. B.; Murtuza, S.; Oyler, K.; Sen, A. *J. Am. Chem. Soc.* **2001**, *123*, 7423.
- [37] Tobisch, S.; Ziegler, T. *J. Am. Chem. Soc.* **2004**, *126*, 9059.
- [38] Arteaga-Müller, R.; Tsurugi, H.; Saito, T.; Yanagawa, M.; Oda, S.; Mashima, K. *J. Am. Chem. Soc.* **2009**, *131*, 5370.
- [39] Agapie, T.; Day, M. W.; Henling, L. M.; Labinger, J. A.; Bercaw, J. A. *Organometallics* **2006**, *25*, 2733 and references therein.
- [40] Rüther, T.; Braussaud, N.; Cavell, K. J. *Organometallics* **2001**, *20*, 1247.
- [41] Zhang, W.; Sun, W. H.; Zhang, S.; Hou, J.; Wedeking, K.; Schultz, S.; Fröhlich, R.; Song, H. *Organometallics* **2006**, *25*, 1961.
- [42] McGuinness, D. S.; Gibson, V. C.; Wass, D. F.; Steed, J. W. *J. Am. Chem. Soc.* **2003**, *125*, 12716.
- [43] McGuinness, D. S.; Suttill, J. A.; Gardiner, M. G.; Davies, N. W. *Organometallics* **2008**, *27*, 4238.
- [44] (a) McGuinness, D. S.; Gibson, V. C.; Steed, J. W. *Organometallics* **2004**, *23*, 6288. (b) McGuinness, D. S.; Saendig, N.; Yates, B. F.; Cavell, K. J. *J. Am. Chem. Soc.* **2001**, *123*, 4029. (c) Shukla, P.; Johnson, J. A.; Vidovic, D.; Cowley, A. H.; Abernethy, C. D. *Chem. Commun.* **2004**, 360. (d) Alder, R. W.; Blake, M. E.; Chaker,

- L.; Harvey, J. N.; Paolini, F.; Schutz, J. *Angew. Chem. Int. Ed.* **2004**, *43*, 5896. (e) Alder, R. W.; Blake, M. E.; Bortolotti, C.; Bufalli, S.; Butts, C. P.; Linehan, E.; Oliva, J. M.; Orpen, A. G.; Quayle, M. J. *Chem. Commun.* **1999**, 241. (f) Patel, D.; Liddle, S. T.; Mungur, S. A.; Rodden, M.; Blake, A. J.; Arnold, P. L. *Chem. Commun.* **2006**, 1124. (g) Pugh, D.; Wright, J. A.; Freeman, S.; Danopoulos, A. A. *Dalton Trans.* **2006**, 775. (h) Arnold, P. L.; Scarisbrick, A. C.; Blake, A. J.; Wilson, C. *Chem. Commun.* **2001**, 2340. (i) Aihara, H.; Matsuo, T.; Kawaguchi, H. *Chem. Commun.* **2003**, 2204. (j) Arnold, P. L.; Mungur, S. A.; Blake, A. J.; Wilson, C. *Angew. Chem. Int. Ed.* **2003**, *42*, 5981. (k) Arnold, P. L.; Rodden, M.; Davis, K. M.; Scarisbrick, A. C.; Blake, A. J.; Wilson, C. *Chem. Commun.* **2004**, 1612.
- [45] Niehues, M.; Erker, G.; Kehr, G.; Schwab, P.; Frohlich, R.; Blacque, O.; Berke, H. *Organometallics* **2002**, *21*, 2905.
- [46] Lorber, C.; Vendier, L. *Dalton Trans.* **2009**, 6972.
- [47] Rüther, T.; Cavell, K. J.; Braussaud, N. C.; Skelton, B. W.; White, A. H. *J. Chem. Soc. Dalton Trans.* **2002**, 4684.
- [48] Dyer, P. W.; Gibson, V. C.; Jeffery, J. C. *Polyhedron* **1995**, *14*, 3095.
- [49] Abernethy, C. D.; Clyburne, J. A. C.; Cowley, A. H.; Jones, R. A. *J. Am. Chem. Soc.* **1999**, *121*, 2329.
- [50] (a) Bhandari, G.; Kim, Y.; McFarland, J. M.; Rheingold, A. L.; Theopold, K. H. *Organometallics* **1995**, *14*, 738. (b) Richeson, D. S.; Mitchell, J. F.; Theopold, K. H. *Organometallics* **1989**, *8*, 2570.
- [51] Hagen, H.; Boersma, J.; Lutz, M.; Spek, A. L.; Van Koten, G. *Eur. J. Inorg. Chem.* **2001**, 117 and references therein.
- [52] Budzelaar, P. H. M.; Van Oort, A. B.; Orpen, A. G. *Eur. J. Inorg. Chem.* **1998**, 1485.
- [53] Al-Benna, S.; Sarsfield, M. J.; Thornton-Pett, M.; Ormsby, D. L.; Maddox, P. J.; Brès, P.; Bochmann, M. *J. Chem. Soc. Dalton Trans.* **2000**, 4247.

- [54] Kotov, V. V.; Avtomonov, E. V.; Sundermeyer, J.; Aitola, E.; Repo, T.; Lemenovskii, D. A. *J. Organomet. Chem.* **2001**, *640*, 21.
- [55] Liddle, S. T.; Edworthy, I. S.; Arnold, P. L. *Chem. Soc. Rev.*, **2007**, *36*, 1732.
- [56] Edworthy, I. S.; Blake, A. J.; Wilson, C.; Arnold, P. L. *Organometallics*, **2007**, *26*, 3684.
- [57] Pugh, D.; Wright, J. A.; Freeman, S.; Danopoulos, A. A. *Dalton Trans.* **2006**, 775.
- [58] Spencer, L. P.; Beddie, C.; Hall, M. B.; Fryzuk, M. D. *J. Am. Chem. Soc.* **2006**, *128*, 12531.
- [59] Lever, A. B. P. *Inorganic Electronic Spectroscopy*, 2nd edition, Elsevier, **1986**.
- [60] Aihara, H.; Matsuo, T.; Kawaguchi, H. *Chem. Commun.* **2003**, 2204.
- [61] Iglesias, M.; Beetstra, D. J.; Knight, J. C.; Ooi, L. L.; Stasch, A.; Coles, S.; Male, L.; Hursthouse, M. B.; Cavell, K. J.; Dervisi, A.; Fallis, I. A. *Organometallics* **2008**, *27*, 3279.
- [62] Nielsen, D. J.; Cavell, K. J.; Viciu, M. S.; Nolan, S. P.; Skelton, B. W.; White, A. H. *Journal of Organometallic Chemistry*, **2005**, *690*, 6133.
- [63] Spalek, T. P. P.; Sojka, Z. *J. Chem. Inf. Model*, **2005**, *45*, 18.

Appendix A

EPR Spectra

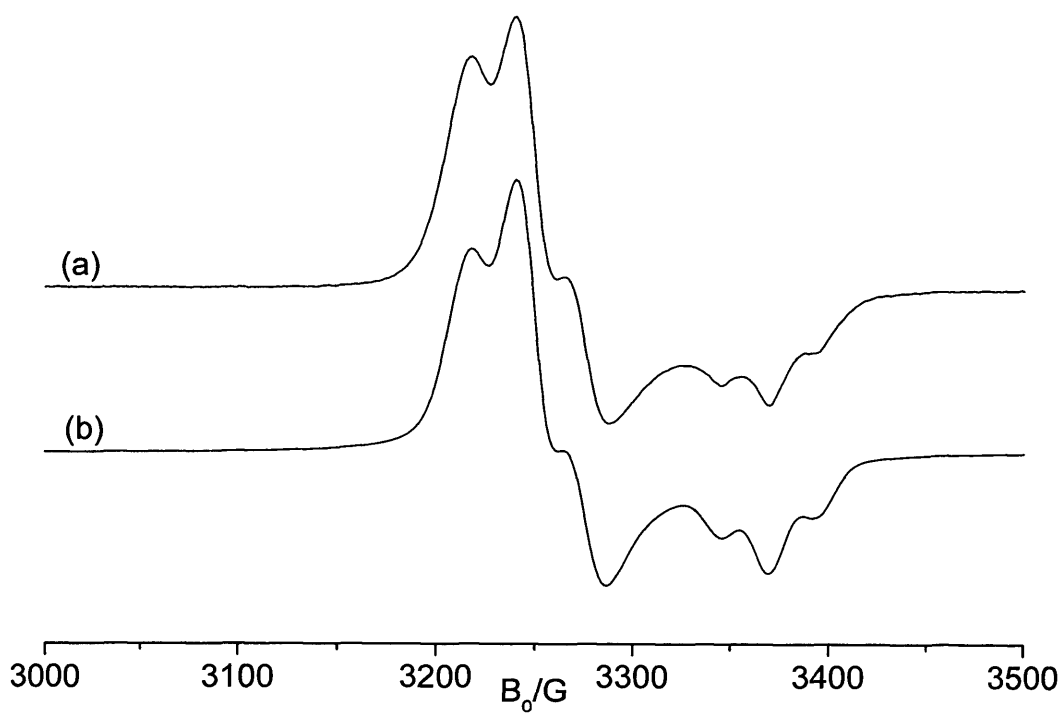


Figure 1 Experimental (a) and simulated (b) cw-EPR spectra (130K) of **44**

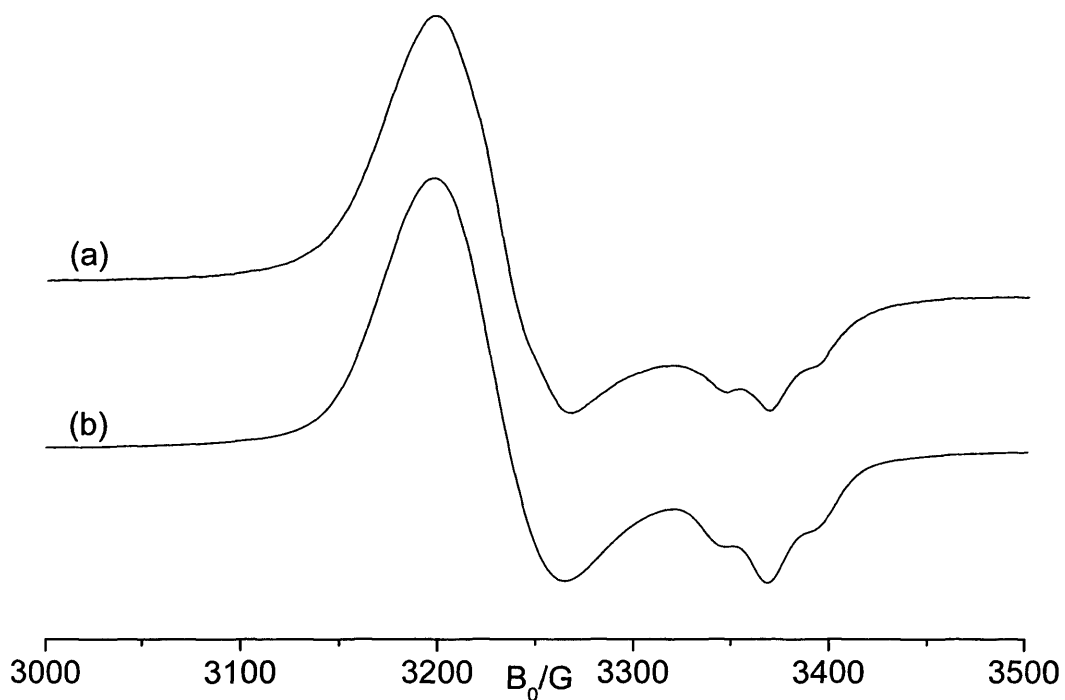


Figure 2 Experimental (a) and simulated (b) cw-EPR spectra (130K) of **45**

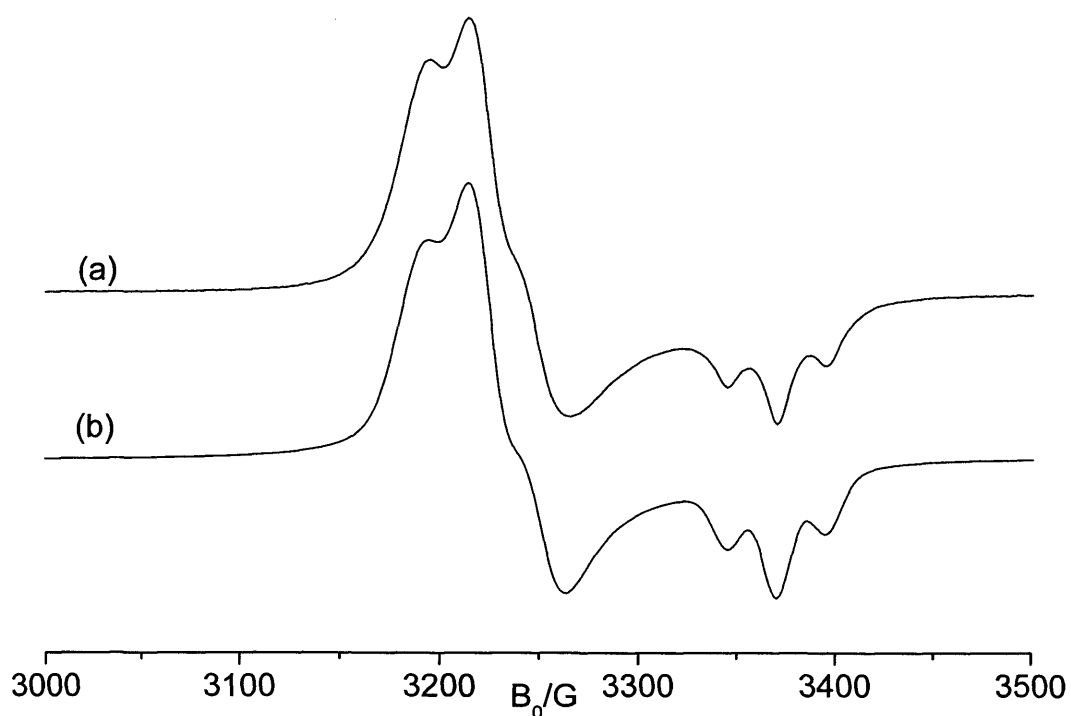


Figure 3 Experimental (a) and simulated (b) cw-EPR spectra (130K) of 46

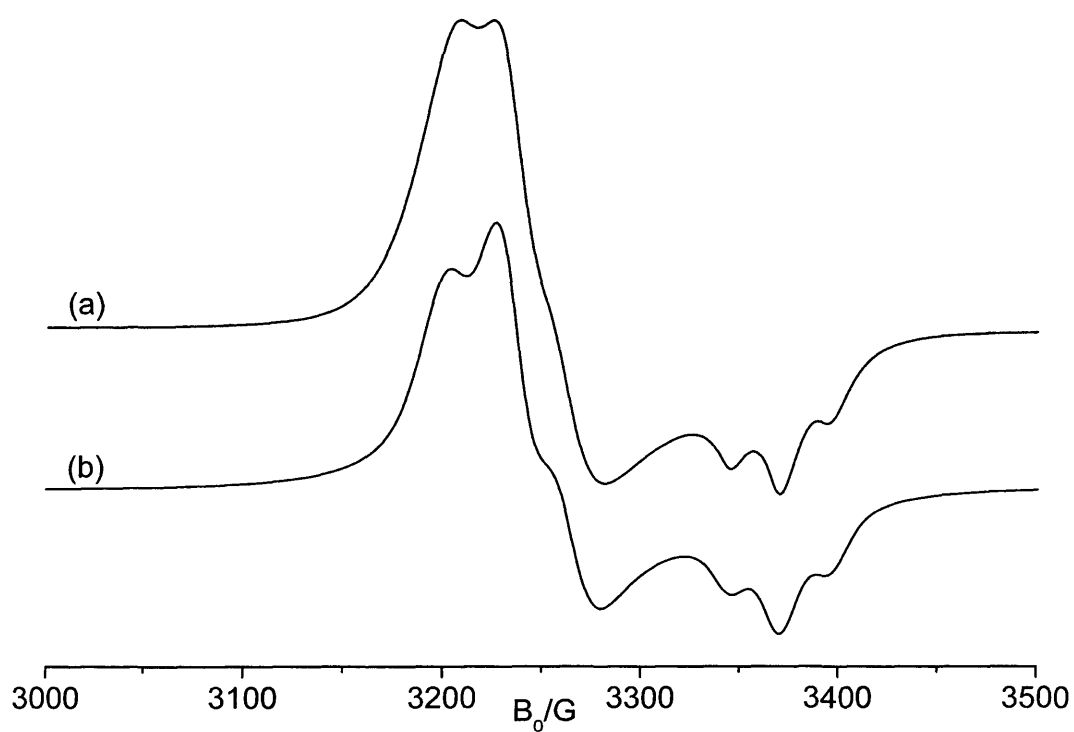


Figure 4 Experimental (a) and simulated (b) cw-EPR spectra (130K) of 47

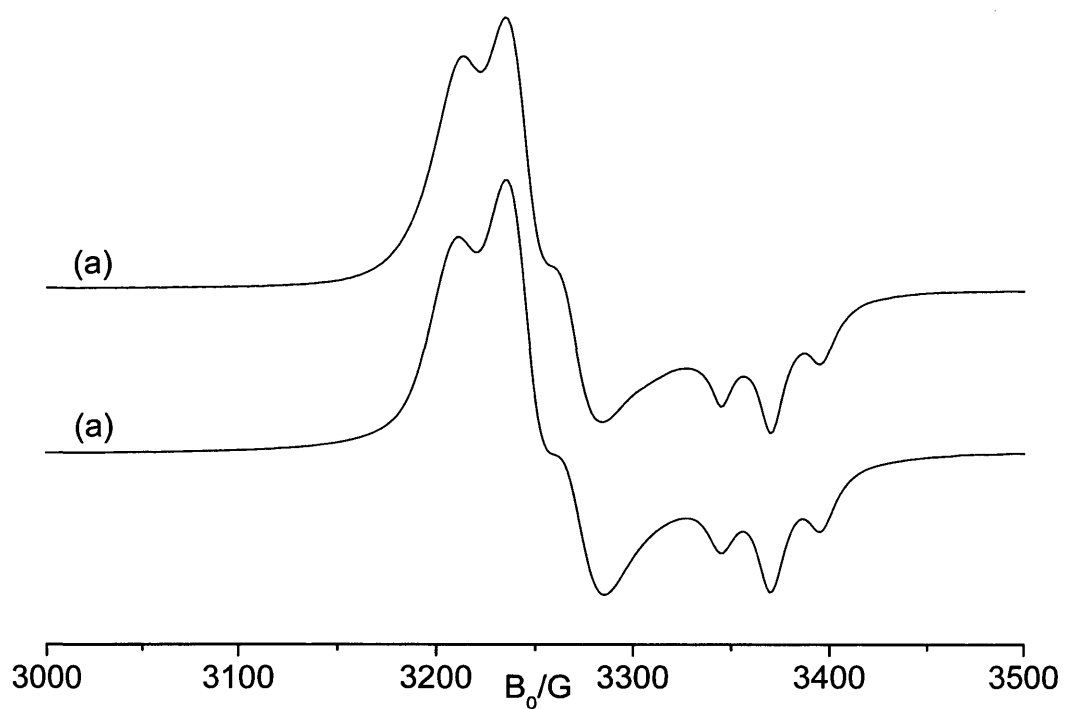


Figure 5 Experimental (a) and simulated (b) cw-EPR spectra (130K) of **48**

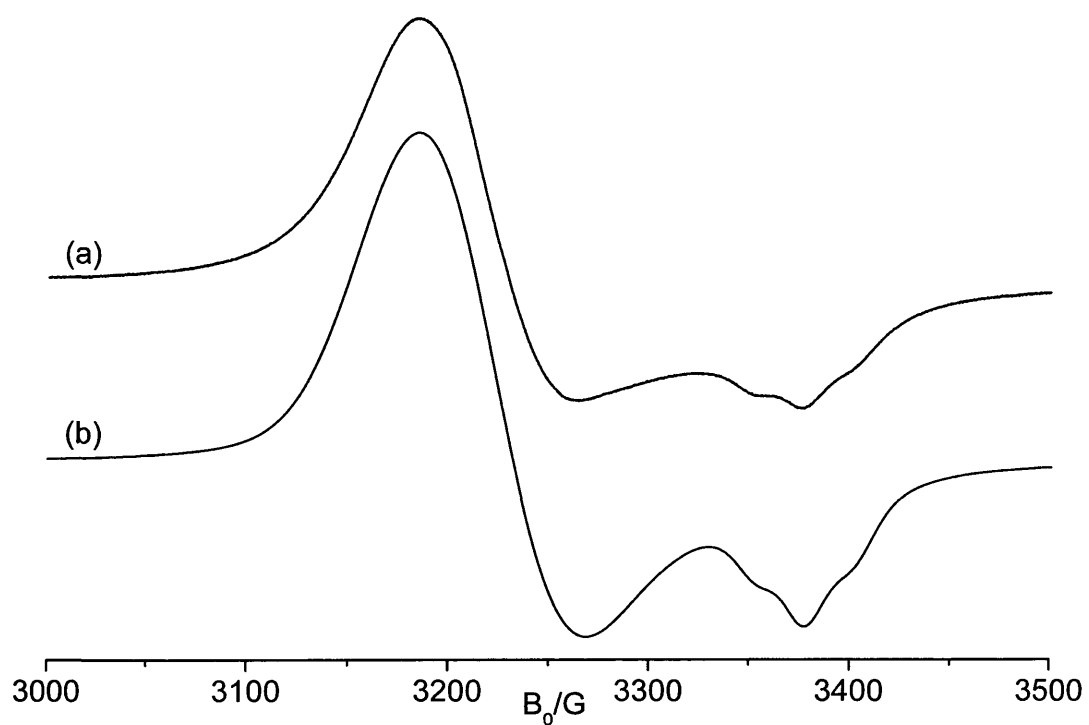
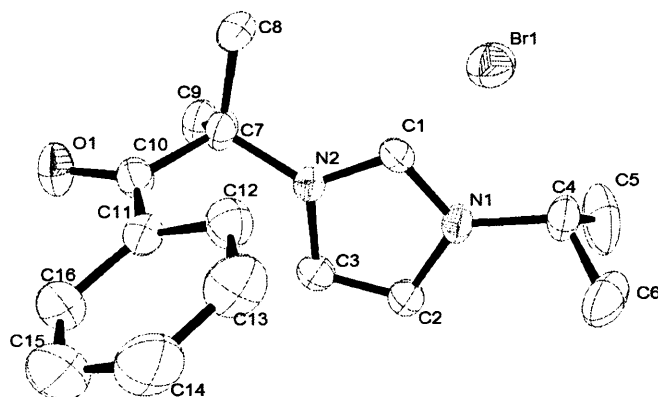


Figure 6 Experimental (a) and simulated (b) cw-EPR spectra (130K) of **49**

Appendix B

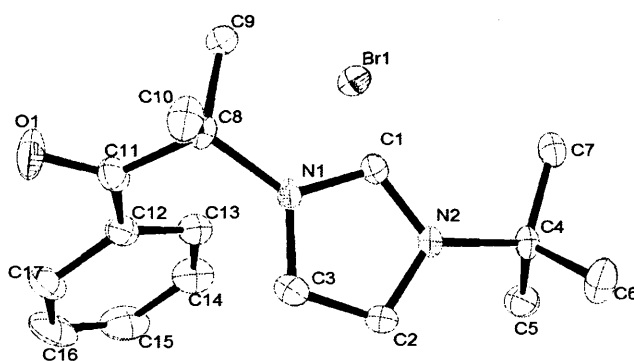
X-Ray data

Table 1. Crystal data and structure refinement for **2**

Identification code	kjc0837	
Empirical formula	C ₁₆ H ₂₁ Br N ₂ O	
Formula weight	337.26	
Temperature	150(2) K	
Wavelength	0.71073 Å	
Crystal system	Orthorhombic	
Space group	Pna21	
Unit cell dimensions	a = 7.6170(2) Å	α = 90°.
	b = 21.6820(3) Å	β = 90°.
	c = 10.3540(7) Å	γ = 90°.
Volume	1709.98(13) Å ³	
Z	4	
Density (calculated)	1.310 Mg/m ³	
Absorption coefficient	2.402 mm ⁻¹	
F(000)	696	
Crystal size	0.30 x 0.22 x 0.15 mm ³	
Theta range for data collection	2.83 to 27.47°.	
Index ranges	-9 ≤ h ≤ 9, -28 ≤ k ≤ 27, -13 ≤ l ≤ 13	
Reflections collected	3633	
Independent reflections	3633 [R(int) = 0.0000]	
Completeness to theta = 27.47°	99.8 %	
Max. and min. transmission	0.7146 and 0.5327	
Refinement method	Full-matrix least-squares on F ²	
Data / restraints / parameters	3633 / 1 / 186	
Goodness-of-fit on F ²	1.040	
Final R indices [I > 2σ(I)]	R1 = 0.0458, wR2 = 0.0856	
R indices (all data)	R1 = 0.0643, wR2 = 0.0935	
Absolute structure parameter	0.515(14)	
Largest diff. peak and hole	0.296 and -0.515 e.Å ⁻³	

Table 2. Atomic coordinates ($\times 10^4$) and equivalent isotropic displacement parameters ($\text{\AA}^2 \times 10^3$) for kjc0837. $U(\text{eq})$ is defined as one third of the trace of the orthogonalized U^{ij} tensor.

	x	y	z	U(eq)
C(1)	7834(5)	467(2)	7592(4)	30(1)
C(2)	5114(5)	524(2)	8288(5)	36(1)
C(3)	5667(5)	1097(2)	8034(4)	34(1)
C(4)	6523(6)	-545(2)	8148(6)	46(1)
C(5)	5342(9)	-824(2)	7118(8)	80(2)
C(6)	6045(6)	-722(2)	9526(9)	64(2)
C(7)	8459(6)	1587(2)	7173(5)	33(1)
C(8)	10355(6)	1375(2)	6898(5)	42(1)
C(9)	7614(7)	1840(2)	5938(5)	44(1)
C(10)	8511(5)	2090(2)	8216(5)	35(1)
C(11)	8589(5)	1950(2)	9626(5)	33(1)
C(12)	9140(6)	1384(2)	10124(5)	40(1)
C(13)	9229(7)	1296(3)	11442(5)	53(1)
C(14)	8737(8)	1750(3)	12270(6)	63(2)
C(15)	8169(8)	2321(3)	11781(6)	66(2)
C(16)	8102(7)	2417(2)	10479(6)	45(1)
O(1)	8548(4)	2626(1)	7847(4)	46(1)
N(1)	6502(4)	133(1)	8011(4)	31(1)
N(2)	7381(4)	1059(1)	7606(3)	27(1)
Br(1)	11066(1)	-177(1)	9413(1)	37(1)

Table 1. Crystal data and structure refinement for **3**

Identification code	kjc0835t	
Empirical formula	C ₁₇ H ₂₃ Br N ₂ O	
Formula weight	351.28	
Temperature	150(2) K	
Wavelength	0.71073 Å	
Crystal system	Orthorhombic	
Space group	Pna21	
Unit cell dimensions	a = 8.0820(2) Å	α = 90°.
	b = 21.1830(3) Å	β = 90°.
	c = 10.3590(5) Å	γ = 90°.
Volume	1773.47(10) Å ³	
Z	4	
Density (calculated)	1.316 Mg/m ³	
Absorption coefficient	2.319 mm ⁻¹	
F(000)	728	
Crystal size	0.35 x 0.25 x 0.20 mm ³	
Theta range for data collection	2.70 to 27.43°.	
Index ranges	-10 ≤ h ≤ 9, -21 ≤ k ≤ 27, -13 ≤ l ≤ 8	
Reflections collected	8748	
Independent reflections	3329 [R(int) = 0.0386]	
Completeness to theta = 27.43°	99.5 %	
Max. and min. transmission	0.6541 and 0.4974	
Refinement method	Full-matrix least-squares on F ²	
Data / restraints / parameters	3329 / 1 / 195	
Goodness-of-fit on F ²	1.027	
Final R indices [I > 2σ(I)]	R ₁ = 0.0331, wR ₂ = 0.0679	
R indices (all data)	R ₁ = 0.0422, wR ₂ = 0.0717	
Absolute structure parameter	0.004(10)	
Largest diff. peak and hole	0.248 and -0.522 e.Å ⁻³	

Table 2. Atomic coordinates ($\times 10^4$) and equivalent isotropic displacement parameters ($\text{\AA}^2 \times 10^3$) for kjc0835t. $U(\text{eq})$ is defined as one third of the trace of the orthogonalized U^{ij} tensor.

	x	y	z	U(eq)
C(1)	2124(4)	-4574(1)	6640(3)	18(1)
C(2)	4704(4)	-4401(1)	7252(3)	22(1)
C(3)	4085(4)	-3854(1)	6781(3)	23(1)
C(4)	3621(4)	-5527(1)	7529(3)	21(1)
C(5)	4034(4)	-5543(1)	8966(3)	29(1)
C(6)	5024(4)	-5808(2)	6716(4)	34(1)
C(7)	1993(4)	-5864(1)	7262(3)	25(1)
C(8)	1370(4)	-3495(1)	5793(3)	19(1)
C(9)	-403(4)	-3747(1)	5739(3)	24(1)
C(10)	2039(5)	-3372(2)	4438(3)	30(1)
C(11)	1348(4)	-2876(2)	6580(4)	25(1)
C(12)	1587(4)	-2851(1)	8002(3)	25(1)
C(13)	1314(3)	-3358(1)	8836(5)	27(1)
C(14)	1544(4)	-3288(2)	10146(4)	37(1)
C(15)	2061(5)	-2711(2)	10645(4)	46(1)
C(16)	2343(5)	-2209(2)	9839(4)	46(1)
C(17)	2095(4)	-2271(2)	8511(4)	31(1)
N(1)	2475(3)	-3966(1)	6412(2)	18(1)
N(2)	3454(3)	-4847(1)	7146(3)	18(1)
O(1)	1081(3)	-2393(1)	5965(3)	39(1)
Br(1)	-1351(1)	-4784(1)	8728(1)	27(1)

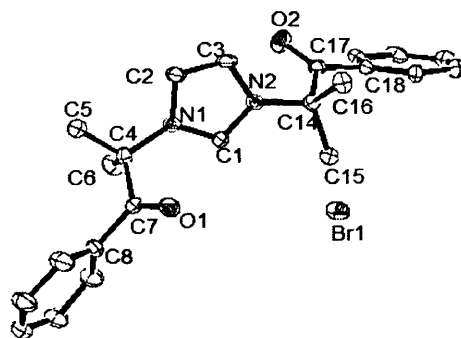


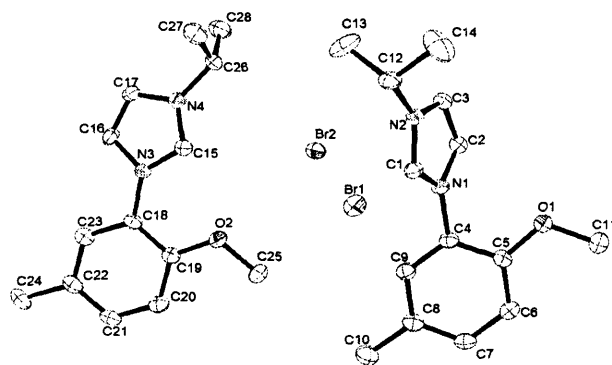
Table 1. Crystal data and structure refinement for 4

Identification code	kjc0834	
Empirical formula	C ₂₃ H ₂₅ Br N ₂ O ₂	
Formula weight	441.36	
Temperature	150(2) K	
Wavelength	0.71073 Å	
Crystal system	Triclinic	
Space group	P-1	
Unit cell dimensions	a = 5.94800(10) Å	α = 101.1190(10)°.
	b = 12.9300(2) Å	β = 90.0260(10)°.
	c = 27.7910(7) Å	γ = 94.1910(10)°.
Volume	2091.38(7) Å ³	
Z	4	
Density (calculated)	1.402 Mg/m ³	
Absorption coefficient	1.986 mm ⁻¹	
F(000)	912	
Crystal size	0.20 x 0.05 x 0.05 mm ³	
Theta range for data collection	3.11 to 27.51°.	
Index ranges	-6 ≤ h ≤ 7, -16 ≤ k ≤ 16, -36 ≤ l ≤ 36	
Reflections collected	14699	
Independent reflections	9453 [R(int) = 0.0453]	
Completeness to theta = 27.51°	98.4 %	
Max. and min. transmission	0.9072 and 0.6921	
Refinement method	Full-matrix least-squares on F ²	
Data / restraints / parameters	9453 / 0 / 526	
Goodness-of-fit on F ²	1.043	
Final R indices [I > 2σ(I)]	R1 = 0.0661, wR2 = 0.1643	
R indices (all data)	R1 = 0.1142, wR2 = 0.1902	
Largest diff. peak and hole	1.224 and -0.892 e.Å ⁻³	

Table 2. Atomic coordinates ($\times 10^4$) and equivalent isotropic displacement parameters ($\text{\AA}^2 \times 10^3$) for kjc0834. $U(\text{eq})$ is defined as one third of the trace of the orthogonalized U^{ij} tensor.

	x	y	z	U(eq)
C(1)	7734(8)	3413(3)	3456(2)	23(1)
C(2)	6594(9)	2690(4)	3086(2)	32(1)
C(3)	7463(10)	1743(4)	2890(2)	40(1)
C(4)	9488(10)	1498(4)	3075(2)	39(1)
C(5)	10567(9)	2186(4)	3463(2)	34(1)
C(6)	9723(8)	3156(4)	3649(2)	30(1)
C(7)	6641(8)	4415(3)	3654(2)	20(1)
C(8)	7781(7)	5470(3)	3559(2)	22(1)
C(9)	7318(9)	5470(4)	3016(2)	31(1)
C(10)	10310(8)	5638(4)	3673(2)	29(1)
C(11)	6470(7)	6475(3)	4355(2)	18(1)
C(12)	5538(8)	7131(3)	3711(2)	23(1)
C(13)	4747(8)	7736(3)	4113(2)	24(1)
C(14)	4794(7)	7776(3)	5031(2)	19(1)
C(15)	5369(8)	7005(3)	5360(2)	23(1)
C(16)	2246(7)	7940(4)	5048(2)	26(1)
C(17)	6250(7)	8838(3)	5164(2)	20(1)
C(18)	6574(7)	9405(3)	5687(2)	20(1)
C(19)	4965(8)	9452(3)	6051(2)	22(1)
C(20)	5416(9)	10084(4)	6511(2)	29(1)
C(21)	7506(8)	10629(3)	6617(2)	29(1)
C(22)	9142(8)	10568(3)	6261(2)	26(1)
C(23)	8665(8)	9976(3)	5796(2)	23(1)
C(24)	3426(7)	5593(3)	-691(2)	18(1)
C(25)	5070(8)	5559(3)	-1051(2)	23(1)
C(26)	4663(8)	4932(3)	-1512(2)	27(1)
C(27)	2586(8)	4372(3)	-1629(2)	28(1)
C(28)	921(8)	4429(3)	-1279(2)	26(1)
C(29)	1362(7)	5017(3)	-807(2)	20(1)
C(30)	3724(7)	6156(3)	-167(2)	19(1)
C(31)	5198(7)	7219(3)	-27(2)	18(1)
C(32)	4646(8)	7990(3)	-359(2)	23(1)
C(33)	7732(7)	7052(4)	-34(2)	25(1)

C(34)	3490(7)	8522(3)	648(2)	20(1)
C(35)	5101(8)	7227(3)	888(2)	23(1)
C(36)	4261(8)	7828(3)	1290(2)	21(1)
C(37)	2095(7)	9510(3)	1439(2)	20(1)
C(38)	-421(8)	9339(4)	1322(2)	31(1)
C(39)	2576(9)	9518(4)	1980(2)	32(1)
C(40)	3238(8)	10566(3)	1339(2)	20(1)
C(41)	2160(7)	11574(3)	1540(2)	21(1)
C(42)	170(8)	11836(4)	1354(2)	29(1)
C(43)	-665(9)	12802(4)	1541(2)	35(1)
C(44)	460(10)	13497(4)	1921(2)	37(1)
C(45)	2449(10)	13247(4)	2107(2)	38(1)
C(46)	3311(9)	12294(4)	1910(2)	32(1)
O(1)	4807(5)	4389(2)	3843(1)	28(1)
O(2)	7212(6)	9195(3)	4840(1)	31(1)
O(3)	2734(6)	5798(3)	152(1)	29(1)
O(4)	5078(6)	10593(2)	1154(1)	30(1)
N(1)	6640(6)	6343(3)	3864(1)	19(1)
N(2)	5318(6)	7319(3)	4513(1)	19(1)
N(3)	4619(6)	7667(3)	489(1)	17(1)
N(4)	3240(6)	8637(3)	1131(1)	20(1)
Br(1)	0	0	0	28(1)
Br(2)	0	5000	5000	27(1)
Br(3)	2441(1)	6880(1)	2465(1)	19(1)
Br(4)	7537(3)	8187(2)	2545(1)	34(1)

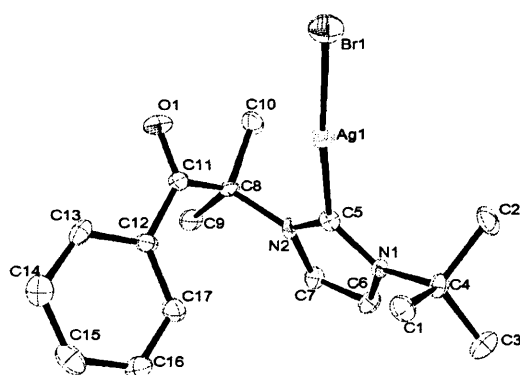
Table 1. Crystal data and structure refinement for **9**

Identification code	kjc0830	
Empirical formula	C ₁₄ H ₁₉ Br N ₂ O	
Formula weight	311.22	
Temperature	150(2) K	
Wavelength	0.71073 Å	
Crystal system	Triclinic	
Space group	P-1	
Unit cell dimensions	a = 10.3150(2) Å	α = 64.4450(10)°.
	b = 12.1050(3) Å	β = 70.5430(10)°.
	c = 13.6140(3) Å	γ = 76.5140(10)°.
Volume	1437.98(6) Å ³	
Z	4	
Density (calculated)	1.438 Mg/m ³	
Absorption coefficient	2.850 mm ⁻¹	
F(000)	640	
Crystal size	0.41 x 0.22 x 0.15 mm ³	
Theta range for data collection	2.67 to 27.50°.	
Index ranges	-13 ≤ h ≤ 12, -15 ≤ k ≤ 13, -17 ≤ l ≤ 17	
Reflections collected	9732	
Independent reflections	6550 [R(int) = 0.0281]	
Completeness to theta = 27.50°	99.1 %	
Max. and min. transmission	0.6745 and 0.3879	
Refinement method	Full-matrix least-squares on F ²	
Data / restraints / parameters	6550 / 0 / 333	
Goodness-of-fit on F ²	1.014	
Final R indices [I > 2σ(I)]	R1 = 0.0425, wR2 = 0.0820	
R indices (all data)	R1 = 0.0641, wR2 = 0.0908	
Largest diff. peak and hole	0.420 and -0.524 e.Å ⁻³	

Table 2. Atomic coordinates ($\times 10^4$) and equivalent isotropic displacement parameters ($\text{\AA}^2 \times 10^3$) for *kjc0830*. $U(\text{eq})$ is defined as one third of the trace of the orthogonalized U^{ij} tensor.

	x	y	z	$U(\text{eq})$
C(1)	8586(3)	2683(3)	7757(2)	21(1)
C(2)	10737(3)	2999(3)	6763(2)	23(1)
C(3)	9988(3)	4106(3)	6586(2)	23(1)
C(4)	10210(3)	803(3)	7940(2)	20(1)
C(5)	11158(3)	321(3)	8600(2)	20(1)
C(6)	11422(3)	-951(3)	9086(2)	23(1)
C(7)	10765(3)	-1695(3)	8895(2)	24(1)
C(8)	9865(3)	-1219(3)	8210(2)	24(1)
C(9)	9600(3)	58(3)	7731(2)	23(1)
C(10)	9205(4)	-2041(3)	7984(3)	35(1)
C(11)	12663(3)	669(3)	9416(3)	27(1)
C(12)	7460(3)	4838(3)	7337(3)	26(1)
C(13)	7185(4)	5608(3)	6189(3)	43(1)
C(14)	7781(4)	5591(4)	7855(4)	54(1)
C(15)	6911(3)	2945(3)	3071(2)	24(1)
C(16)	5990(3)	3210(3)	1716(2)	24(1)
C(17)	6350(3)	4301(3)	1518(3)	26(1)
C(18)	6113(3)	1072(3)	3188(2)	20(1)
C(19)	6752(3)	200(3)	4011(2)	21(1)
C(20)	6501(3)	-1029(3)	4426(3)	25(1)
C(21)	5664(3)	-1371(3)	4025(3)	26(1)
C(22)	5035(3)	-515(3)	3190(2)	25(1)
C(23)	5267(3)	710(3)	2790(2)	24(1)
C(24)	4121(4)	-886(3)	2743(3)	34(1)
C(25)	8245(3)	-284(3)	5192(3)	30(1)
C(26)	7489(4)	5080(3)	2476(3)	30(1)
C(27)	6296(4)	5871(3)	2941(3)	40(1)
C(28)	8407(4)	5818(3)	1340(3)	38(1)
N(1)	9847(2)	2118(2)	7496(2)	20(1)
N(2)	8644(3)	3891(2)	7224(2)	21(1)
N(3)	6343(2)	2355(2)	2700(2)	19(1)
N(4)	6930(3)	4120(2)	2365(2)	25(1)
O(1)	11736(2)	1153(2)	8704(2)	25(1)

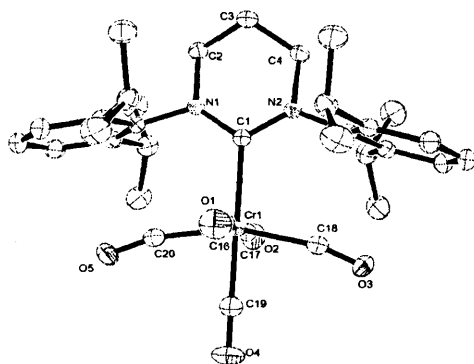
O(2)	7559(2)	607(2)	4369(2)	26(1)
Br(1)	5104(1)	2491(1)	9749(1)	29(1)
Br(2)	8789(1)	2862(1)	4954(1)	30(1)

Table 1. Crystal data and structure refinement for **20**

Identification code	kjc0822	
Empirical formula	C ₁₇ H ₂₂ Ag Br N ₂ O	
Formula weight	458.15	
Temperature	150(2) K	
Wavelength	0.71073 Å	
Crystal system	Monoclinic	
Space group	P2 ₁ /n	
Unit cell dimensions	a = 7.3336(2) Å	α = 90°.
	b = 15.5160(4) Å	β = 98.7770(10)°.
	c = 15.4923(6) Å	γ = 90°.
Volume	1742.20(9) Å ³	
Z	4	
Density (calculated)	1.747 Mg/m ³	
Absorption coefficient	3.453 mm ⁻¹	
F(000)	912	
Crystal size	0.35 x 0.35 x 0.2 mm ³	
Theta range for data collection	2.92 to 27.46°.	
Index ranges	-9 ≤ h ≤ 9, -20 ≤ k ≤ 20, -13 ≤ l ≤ 20	
Reflections collected	11008	
Independent reflections	3961 [R(int) = 0.0783]	
Completeness to theta = 27.46°	99.3 %	
Absorption correction	Semi-empirical from equivalents	
Max. and min. transmission	0.503 and 0.310	
Refinement method	Full-matrix least-squares on F ²	
Data / restraints / parameters	3961 / 0 / 204	
Goodness-of-fit on F ²	1.052	
Final R indices [I > 2σ(I)]	R ₁ = 0.0500, wR ₂ = 0.1248	
R indices (all data)	R ₁ = 0.0720, wR ₂ = 0.1366	
Largest diff. peak and hole	0.596 and -1.675 e.Å ⁻³	

Table 2. Atomic coordinates ($\times 10^4$) and equivalent isotropic displacement parameters ($\text{\AA}^2 \times 10^3$) for kjc0822. $U(\text{eq})$ is defined as one third of the trace of the orthogonalized U^{ij} tensor.

	x	y	z	U(eq)
C(1)	3430(7)	-1231(3)	1018(4)	22(1)
C(2)	5225(8)	-2580(3)	825(4)	28(1)
C(3)	5060(8)	-1397(4)	-265(3)	26(1)
C(4)	5123(7)	-1606(3)	698(3)	18(1)
C(5)	7245(7)	-1239(3)	2096(3)	16(1)
C(6)	8054(7)	-689(3)	868(3)	19(1)
C(7)	9274(7)	-389(3)	1533(3)	18(1)
C(8)	9698(7)	-565(3)	3193(3)	18(1)
C(9)	11035(7)	199(3)	3216(4)	24(1)
C(10)	10781(8)	-1372(3)	3533(4)	25(1)
C(11)	8263(7)	-345(3)	3792(3)	20(1)
C(12)	6931(7)	398(3)	3590(3)	18(1)
C(13)	6095(7)	697(3)	4283(3)	20(1)
C(14)	4911(7)	1407(4)	4181(4)	26(1)
C(15)	4516(8)	1791(4)	3366(4)	29(1)
C(16)	5297(8)	1485(3)	2668(4)	27(1)
C(17)	6522(8)	807(3)	2778(4)	24(1)
N(1)	6806(6)	-1200(2)	1215(3)	15(1)
N(2)	8770(6)	-731(2)	2290(3)	15(1)
O(1)	8313(6)	-729(2)	4469(3)	33(1)
Br(1)	4725(1)	-3047(1)	3874(1)	32(1)
Ag(1)	6068(1)	-2026(1)	2964(1)	19(1)

Table 1. Crystal data and structure refinement for **69**

Identification code	kjc0927t	
Empirical formula	C ₃₃ H ₄₀ Cr N ₂ O ₅	
Formula weight	596.67	
Temperature	150(2) K	
Wavelength	0.71073 Å	
Crystal system	Orthorhombic	
Space group	Pnma	
Unit cell dimensions	a = 18.2203(4) Å	α = 90°.
	b = 19.3328(5) Å	β = 90°.
	c = 8.7582(2) Å	γ = 90°.
Volume	3085.07(13) Å ³	
Z	4	
Density (calculated)	1.285 Mg/m ³	
Absorption coefficient	0.413 mm ⁻¹	
F(000)	1264	
Crystal size	0.40 x 0.30 x 0.30 mm ³	
Theta range for data collection	3.33 to 27.48°.	
Index ranges	-23 ≤ h ≤ 23, -25 ≤ k ≤ 24, -11 ≤ l ≤ 11	
Reflections collected	6660	
Independent reflections	3623 [R(int) = 0.0327]	
Completeness to theta = 27.48°	99.3 %	
Absorption correction	Empirical	
Max. and min. transmission	0.8861 and 0.8522	
Refinement method	Full-matrix least-squares on F ²	
Data / restraints / parameters	3623 / 0 / 204	
Goodness-of-fit on F ²	1.022	
Final R indices [I > 2σ(I)]	R1 = 0.0412, wR2 = 0.0970	
R indices (all data)	R1 = 0.0550, wR2 = 0.1042	
Extinction coefficient	0.0141(14)	
Largest diff. peak and hole	0.342 and -0.408 e.Å ⁻³	

Table 2. Atomic coordinates ($\times 10^4$) and equivalent isotropic displacement parameters ($\text{\AA}^2 \times 10^3$) for kjc0927t. $U(\text{eq})$ is defined as one third of the trace of the orthogonalized U^{ij} tensor.

	x	y	z	U(eq)
C(1)	5980(1)	2500	5993(2)	16(1)
C(2)	5281(1)	1875(1)	3911(2)	23(1)
C(3)	4791(1)	2500	3781(3)	25(1)
C(4)	5869(1)	1217(1)	5888(2)	20(1)
C(5)	5395(1)	948(1)	7009(2)	22(1)
C(6)	5461(1)	248(1)	7370(2)	30(1)
C(7)	5973(1)	-168(1)	6651(2)	33(1)
C(8)	6436(1)	107(1)	5565(2)	29(1)
C(9)	6393(1)	803(1)	5148(2)	24(1)
C(10)	4813(1)	1387(1)	7798(2)	26(1)
C(11)	4071(1)	1327(1)	6995(2)	33(1)
C(12)	4716(1)	1203(1)	9492(2)	38(1)
C(13)	6910(1)	1084(1)	3941(2)	28(1)
C(14)	7714(1)	932(1)	4347(3)	37(1)
C(15)	6742(1)	784(1)	2353(2)	41(1)
C(16)	6097(1)	2500	9393(3)	24(1)
C(17)	7517(1)	2500	6228(3)	23(1)
C(18)	6930(1)	3472(1)	8086(2)	24(1)
C(19)	7523(1)	2500	9336(3)	27(1)
N(1)	5736(1)	1911(1)	5323(2)	18(1)
O(1)	5709(1)	2500	10431(2)	39(1)
O(2)	7962(1)	2500	5305(2)	35(1)
O(3)	7100(1)	4020(1)	8459(2)	33(1)
O(4)	7949(1)	2500	10310(2)	42(1)
Cr(1)	6810(1)	2500	7832(1)	18(1)

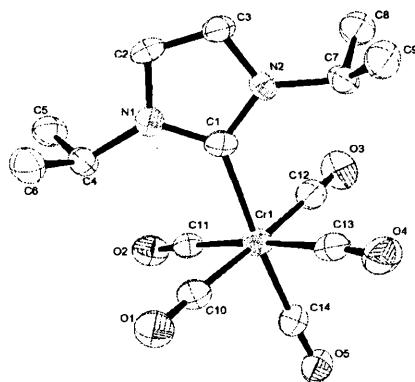


Table 1. Crystal data and structure refinement for 71

Identification code	kjc0919	
Empirical formula	C ₁₄ H ₁₆ Cr N ₂ O ₅	
Formula weight	344.29	
Temperature	150(2) K	
Wavelength	0.71073 Å	
Crystal system	Orthorhombic	
Space group	Pbca	
Unit cell dimensions	a = 12.7330(9) Å	α = 90°.
	b = 18.3060(14) Å	β = 90°.
	c = 13.6620(12) Å	γ = 90°.
Volume	3184.5(4) Å ³	
Z	8	
Density (calculated)	1.436 Mg/m ³	
Absorption coefficient	0.742 mm ⁻¹	
F(000)	1424	
Crystal size	0.40 x 0.30 x 0.02 mm ³	
Theta range for data collection	2.45 to 20.72°.	
Index ranges	-12 ≤ h ≤ 12, -18 ≤ k ≤ 18, -13 ≤ l ≤ 13	
Reflections collected	3012	
Independent reflections	1633 [R(int) = 0.0489]	
Completeness to theta = 20.72°	99.0 %	
Absorption correction	Empirical	
Max. and min. transmission	0.9853 and 0.7557	
Refinement method	Full-matrix least-squares on F ²	
Data / restraints / parameters	1633 / 0 / 203	
Goodness-of-fit on F ²	1.197	
Final R indices [I > 2σ(I)]	R ₁ = 0.0643, wR ₂ = 0.1271	
R indices (all data)	R ₁ = 0.0873, wR ₂ = 0.1358	
Largest diff. peak and hole	0.238 and -0.303 e.Å ⁻³	

Table 2. Atomic coordinates ($\times 10^4$) and equivalent isotropic displacement parameters ($\text{\AA}^2 \times 10^3$) for kjc0919. $U(\text{eq})$ is defined as one third of the trace of the orthogonalized U^{ij} tensor.

	x	y	z	U(eq)
C(1)	710(5)	7137(4)	885(4)	29(2)
C(2)	-148(6)	8020(4)	1738(4)	33(2)
C(3)	-614(5)	7387(4)	1935(5)	33(2)
C(4)	1390(5)	8442(3)	741(4)	33(2)
C(5)	2085(6)	8710(4)	1585(5)	41(2)
C(6)	796(6)	9054(4)	246(5)	46(2)
C(7)	-394(6)	6073(3)	1505(4)	37(2)
C(8)	-229(6)	5809(4)	2555(5)	48(2)
C(9)	-1522(5)	5976(4)	1151(5)	46(2)
C(10)	1598(5)	7283(4)	-1072(5)	34(2)
C(11)	2971(6)	7072(4)	365(5)	33(2)
C(12)	1999(6)	5882(4)	944(5)	38(2)
C(13)	615(6)	6063(4)	-632(5)	38(2)
C(14)	2645(6)	6019(4)	-872(5)	33(2)
N(1)	665(4)	7876(3)	1090(4)	29(1)
N(2)	-92(4)	6849(3)	1431(4)	28(1)
Cr(1)	1771(1)	6567(1)	-76(1)	33(1)
O(1)	1514(4)	7703(3)	-1681(3)	46(1)
O(2)	3743(4)	7357(3)	602(3)	46(1)
O(3)	2208(4)	5470(3)	1545(4)	54(2)
O(4)	-43(4)	5745(3)	-1024(4)	52(2)
O(5)	3175(4)	5653(2)	-1349(3)	43(1)

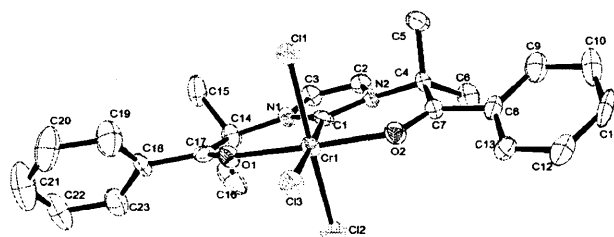


Table 1. Crystal data and structure refinement for **100**

Identification code	kjc0913	
Empirical formula	C ₂₄ H ₂₆ Cl ₅ Cr N ₂ O ₂	
Formula weight	603.72	
Temperature	150(2) K	
Wavelength	0.71073 Å	
Crystal system	Monoclinic	
Space group	P2 ₁ /n	
Unit cell dimensions	a = 8.4910(3) Å	α = 90°.
	b = 24.2220(8) Å	β = 99.989(2)°.
	c = 13.5340(5) Å	γ = 90°.
Volume	2741.33(17) Å ³	
Z	4	
Density (calculated)	1.463 Mg/m ³	
Absorption coefficient	0.929 mm ⁻¹	
F(000)	1236	
Crystal size	0.30 x 0.20 x 0.10 mm ³	
Theta range for data collection	2.77 to 21.74°.	
Index ranges	-8 ≤ h ≤ 8, -23 ≤ k ≤ 25, -14 ≤ l ≤ 14	
Reflections collected	5895	
Independent reflections	3181 [R(int) = 0.0541]	
Completeness to theta = 21.74°	98.1 %	
Max. and min. transmission	0.9128 and 0.7680	
Refinement method	Full-matrix least-squares on F ²	
Data / restraints / parameters	3181 / 66 / 339	
Goodness-of-fit on F ²	1.121	
Final R indices [I > 2σ(I)]	R ₁ = 0.0898, wR ₂ = 0.1848	
R indices (all data)	R ₁ = 0.1132, wR ₂ = 0.1958	
Largest diff. peak and hole	1.018 and -1.001 e.Å ⁻³	

Table 2. Atomic coordinates ($\times 10^4$) and equivalent isotropic displacement parameters ($\text{\AA}^2 \times 10^3$) for kjc0913. $U(\text{eq})$ is defined as one third of the trace of the orthogonalized U^{ij} tensor.

	x	y	z	$U(\text{eq})$
C(1)	4060(10)	1972(4)	6759(7)	28(2)
C(2)	3684(14)	1826(5)	5767(9)	57(3)
C(3)	2365(17)	1485(6)	5437(10)	74(4)
C(4)	1418(17)	1314(6)	6096(12)	79(5)
C(5)	1751(13)	1475(5)	7059(10)	58(4)
C(6)	3041(12)	1800(4)	7413(9)	43(3)
C(7)	5445(11)	2352(4)	7038(7)	27(2)
C(8)	6811(11)	2197(4)	7885(7)	30(2)
C(9)	6244(13)	2225(6)	8884(8)	59(4)
C(10)	7345(13)	1605(4)	7658(9)	50(3)
C(11)	9643(11)	2429(4)	8602(7)	28(2)
C(12)	10695(11)	2824(4)	8523(7)	27(2)
C(13)	8419(10)	3030(4)	7449(6)	24(2)
C(14)	10876(10)	3661(4)	7451(7)	25(2)
C(15)	11912(11)	3377(4)	6767(7)	32(2)
C(16)	11859(12)	3933(4)	8381(7)	39(3)
C(17)	9831(11)	4085(4)	6825(7)	26(2)
C(18)	10487(11)	4631(4)	6568(7)	28(2)
C(19)	12116(13)	4734(4)	6560(7)	39(3)
C(20)	12575(15)	5244(5)	6224(8)	48(3)
C(21)	11437(16)	5644(4)	5930(7)	46(3)
C(22)	9846(14)	5554(4)	5928(7)	40(3)
C(23)	9370(12)	5043(4)	6235(7)	34(3)
O(1)	5435(7)	2758(3)	6487(5)	27(2)
O(2)	8409(7)	4004(3)	6468(4)	28(2)
Cr(1)	6828(2)	3411(1)	6410(1)	23(1)
Cl(1)	8037(3)	2934(1)	5249(2)	31(1)
Cl(2)	5834(3)	3826(1)	7716(2)	36(1)
Cl(3)	4921(3)	3830(1)	5148(2)	30(1)
N(1)	8223(8)	2553(3)	7937(5)	24(2)
N(2)	9938(8)	3207(3)	7819(5)	24(2)
C(24)	7814(19)	4990(9)	8647(15)	142(2)
Cl(4)	9474(9)	5439(3)	8929(6)	136(2)

CI(5)	6449(9)	5115(4)	9473(7)	153(3)
C(24A)	8260(30)	5433(15)	8870(40)	140(2)
CI(4A)	8970(40)	4890(30)	9710(40)	430(40)
CI(5A)	6280(30)	5290(9)	8265(16)	148(2)

Appendix C

Publication

A cw EPR and ENDOR investigation on a series of Cr(I) carbonyl complexes with relevance to alkene oligomerization catalysis: $[\text{Cr}(\text{CO})_4\text{L}]^+$ ($\text{L} = \text{Ph}_2\text{PN}(\text{R})\text{PPh}_2, \text{Ph}_2\text{P}(\text{R})\text{PPh}_2$)[†]

Lucia E. McDyre,^a Tracy Hamilton,^a Damien M. Murphy,^{*a} Kingsley J. Cavell,^a William F. Gabrielli,^b Martin J. Hanton^c and David M. Smith^c

Received 12th March 2010, Accepted 9th June 2010

First published as an Advance Article on the web 21st July 2010

DOI: 10.1039/c0dt00127a

The preparation and characterisation of the Cr(I) complexes $[\text{Cr}(\text{CO})_4\text{L}]^+$ ($\text{L} = \text{Ph}_2\text{PN}(\text{R})\text{PPh}_2, \text{Ph}_2\text{P}(\text{R})\text{PPh}_2$), which are used as pre-catalysts for the selective oligomerization of ethylene, are reported. The electronic properties and structural features of these complexes in frozen solution have been established *via* continuous wave X-band Electron Paramagnetic Resonance (cw-EPR) and continuous wave ¹H, ¹⁴N and ³¹P Electron Nuclear Double Resonance (cw-ENDOR) spectroscopy. The EPR spectra are dominated by the *g* anisotropy, with notably large ^PA couplings from the two equivalent ³¹P nuclei. The spin Hamiltonian parameters ($g_{\perp} (g_{xx} = g_{yy}) > g_e > g_{\parallel} (g_{zz})$) are consistent with a low-spin *d*⁵ system possessing C_{2v} symmetry, with a SOMO where the metal contribution is primarily *d*_{xy} for all complexes. The isotropic Fermi contact term (^P*a*_{iso}, determined by EPR and ENDOR) was found to be largest for complexes containing ligands **e**, **d**, **f** and **g**, indicating that the ³¹P 3 s character in the SOMO is higher for the PNP type ligands than the PCP type. Subtle structural differences in the complexes were also identified through variations in the Δ*g* shifts (identified by EPR), and through differences in the phenyl ring conformations (identified by ¹H ENDOR). Attempts to correlate trends in EPR-derived parameters with data measured for catalysis using these pre-catalysts are also made, but no clear connections were found.

Introduction

A current focus in olefin oligomerization is the design of highly selective catalysts for the formation of single chain length α-olefins such as the Phillips Cr based catalyst system, for the highly selective trimerization of ethylene into 1-hexene.¹ Recently, new Cr complexes containing P–N–P, P–S–P and S–N–S bidentate and tridentate ligands have been developed as catalysts for 1-hexene formation,² and even more excitingly, 1-octene formation (*i.e.* selective tetramerization of ethylene).³ Chromium based catalysts dominate the field, although active Ti and Ta trimerization catalysts have also been reported.^{4,5} In notable recent studies, Wass and coworkers have furthermore demonstrated the trimerization and co-trimerization of substrates other than ethylene.^{6,7} For example, ethylene/styrene cotrimerization and isoprene trimerization have been reported.^{6,7}

It is clear that an entirely different mechanism, to the traditional *Cossee-Arlman* mechanism, must be operating and a mechanism involving Cr-metallo-cycles is favoured.^{1,8,10} Evidence to support this mechanism is growing, with the isolation of Cr 5- and 7-

membered metallocycles; the 7-membered metallocycle decomposes to give 1-hexene.^{8,9} Chromium catalysed trimerization with 1:1 C₂D₄ and C₂H₄ gave only the even numbered isotomers C₆D₁₂, C₆D₈H₄, C₆D₄H₈ and C₆H₁₂ in the ratio 1:3:3:1, in total agreement with the metallocycle mechanism.¹⁰ However, an important unknown in this mechanism is the oxidation state of Cr during the catalytic cycle. The active catalyst is generated *in situ* from a Cr(III) compound, added ligand, and cocatalyst (commonly, MAO - methylaluminoxane). Cr(III)–Cr(v),⁹ Cr(I)–Cr(III)^{11,12} and Cr(II)–Cr(IV)^{13,14} couples have been suggested as the principle oxidation states involved. Cr(v) and Cr(I) complexes are rare and generally unstable; Cr(v) complexes typically have oxygen or halide ligands, whereas Cr(I) complexes with isocyanides and bipy ligands are known.¹⁵

At present, a Cr(I)–Cr(III) couple is favoured. However, this is by no means certain, and it may be that different couples operate with different catalyst systems or operating conditions. X-ray photoelectron spectroscopy studies on the Phillips catalyst support a Cr(I)–Cr(III) couple¹⁶ and elegant studies by Köhn and coworkers lend further weight to a Cr(I)–Cr(III) mechanism.¹⁷ Several molecular modelling studies have been undertaken,^{14,18–21} in one study the Cr(II)–Cr(IV) system was assumed,¹⁴ while in others Ta¹⁸ and Ti^{19–21} systems were considered. The main aim of the latter study was to understand why insertion of a third ethylene occurs in preference to liberation of 1-butene, and then why additional insertions did not occur. Catalytic 1-octene formation is extremely new, however, and a creditable mechanism has only recently been published.²² The proposed mechanism is able to explain the observed by-products, and there is a self-consistency in the explanations.

^aSchool of Chemistry, Cardiff University, Main Building, Park Place, Cardiff, UK CF10 3AT. E-mail: murphydm@cardiff.ac.uk

^bSasol Technology (Pty) Ltd, R&D Division, 1 Klasie Havenga Road, Sasolburg, 1947, South Africa

^cSasol Technology (UK) Ltd, Purdie Building, North Haugh, St Andrews, UK KY16 9ST

[†] Electronic supplementary information (ESI) available: Figure S1: FSED EPR spectra; Figure S2a–S2g: Experimental and simulated cw EPR spectra; Figure S3a–S3g: Additional ¹H ENDOR data; Figure S4: Additional ¹⁴N ENDOR data; Figure S5: Additional ³¹P ENDOR data; Table S1: Catalysis data. See DOI: 10.1039/c0dt00127a

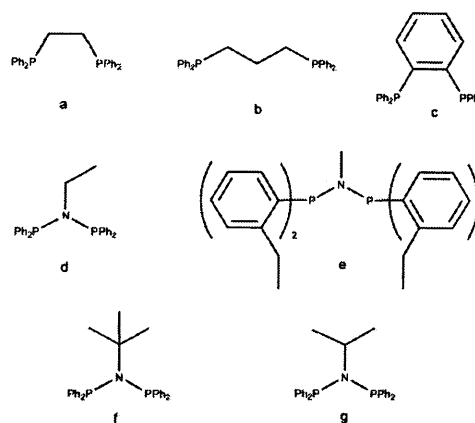
Undoubtedly, one of the most versatile and important analytical tools for characterising the above catalytic systems remains magnetic resonance techniques. In the case where paramagnetic oxidation states are involved, the commonly used NMR methods are rendered less effective or difficult to apply. Determination of ligand structure near a paramagnetic centre has historically been difficult because the standard techniques of spectral assignment and NOE-based distance constraints used for diamagnetic compounds are not readily applied to paramagnetically perturbed resonances. However, this type of information can be readily obtained by EPR and the related hyperfine techniques of ENDOR, HYSCORE, ESEEM and ELDOR detected NMR. Similar to NMR, these EPR techniques can be used to study the Cr based catalyst systems under a variety of conditions (variable temperatures, variable pressures, in solution, *etc.*), providing information not only on the principle oxidation states involved but also a structural description on the complexes in solution. To date most of the available EPR literature pertaining to Cr complexes has focussed on Cr(III)^{23,24} and Cr(V)²⁵ compounds, and to a much lesser extent on low spin Cr(I).²⁶ Bruckner *et al.*,²⁴ have recently monitored the structure and valence state of a Cr(III) oligomerization system *via in situ* EPR. They found that upon addition of MMAO acting as a co-catalyst to activate Cr(acac)₃/PNP, the Cr(III) EPR intensity decreased, with a concomitant increase of new signals between 3200–3600 G. This axial signal with $g_{\perp} = 2.0127$ and $g_{\parallel} = 1.9868$ was similar to that observed from low spin Cr(I) complexes.^{26,27} Thus it was shown that Cr(III) is reduced to Cr(I) in the presence of MMAO. As the reduction of Cr(III) is much faster than Cr(I) formation, it was postulated that the major species formed may be an antiferromagnetic Cr(I) dimer or a Cr(II) species.²⁴

Whilst EPR offers valuable insights into the redox and electronic properties of the Cr complexes in the catalytic reaction, ENDOR (Electron Nuclear Double Resonance) provides further complementary information on the structure of the paramagnetic complex. This information can be accessed *via* analysis of the hyperfine coupling tensor from remote ligand nuclei.^{28,29} The paucity of literature pertaining to ENDOR studies of Cr(I) compounds is remarkable (and there are none using the pulsed hyperfine methods). In this study we will therefore use cw-EPR and ENDOR to study the electronic properties and ligand structure on the series of paramagnetic Cr(I) carbonyl complexes $[\text{Cr}(\text{CO})_4\text{L}]^+$ ($\text{L} = \text{Ph}_2\text{PN}(\text{R})\text{PPh}_2$, $\text{Ph}_2\text{P}(\text{R})\text{PPh}_2$, abbreviated hereafter as P–N–P and P–C–P ligands respectively) which can be used as model catalytic systems for the selective oligomerization of ethylene.

Results and discussion

EPR Spectroscopy: the g matrix

The ligands **L** used for the synthesis of the $[\text{Cr}(\text{CO})_4\text{L}]^+$ complexes are shown in Scheme 1, labelled **a–g**. Syntheses of chromium(0) and chromium(I) complexes of these ligands (**1a–g** and **2a–g** for Cr(0) and Cr(I) respectively) followed published procedures^{30–32} and are described in the experimental section. Cr(0) complexes are quite stable and can be freely handled under an inert atmosphere; however, care must be taken in the manipulation of the Cr(I) complexes, which are air and thermally sensitive. For EPR analysis, each complex **2a–g** was dissolved in dry dichloromethane–toluene



Scheme 1

in the EPR tube under an argon atmosphere. The resulting solutions were deep blue in colour for all $[\text{Cr}(\text{CO})_4\text{a–g}]^+$ complexes.

The cw-EPR spectrum for $[\text{Cr}(\text{CO})_4\text{b}]^+$ is shown in Fig. 1. The low temperature FSED pulsed EPR and room temperature cw EPR spectra were also recorded, but no improved resolution was observed compared to the low temperature cw-measurement (see Electronic Supplementary Information; ESI, Figure S1 & S2h†). The spectrum shown in Fig. 1 can be approximately described as possessing an axial g matrix with well resolved superhyperfine structure in both the perpendicular and parallel components. The corresponding EPR simulation is also displayed in Fig. 1 and the resulting spin Hamiltonian parameters are listed in Table 1.

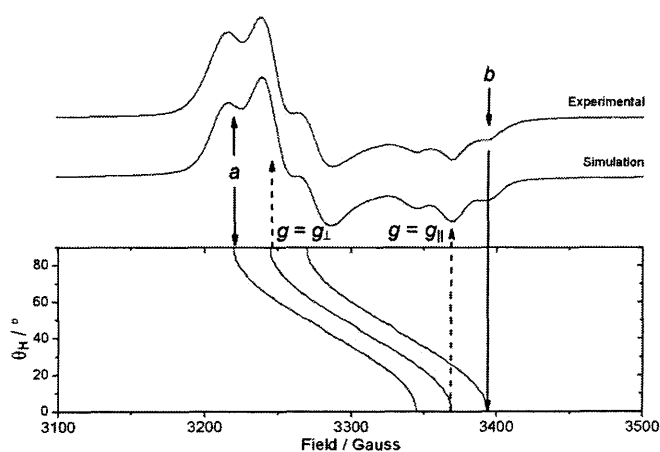


Fig. 1 Experimental and simulated cw-EPR spectra (140 K) of $[\text{Cr}(\text{CO})_4\text{b}]^+$ recorded in dichloromethane–toluene at a microwave frequency of 9.371 GHz. The angular dependency curves calculated for the Cr(I) g matrix and the ^{31}P A matrix are shown in the lower trace.

Each component of the g matrix is split into an unmistakable 1 : 2 : 1 triplet pattern arising from the superhyperfine interaction with two equivalent ^{31}P nuclei ($I = \frac{1}{2}$) in the P–C–P based ligand **b**. Since the natural abundance of ^{53}Cr ($I = 3/2$) is only *ca.* 9.5%, coupled with the large linewidths associated with the ^{31}P hyperfine pattern, no anisotropic hyperfine interaction associated with ^{53}Cr was detected in the frozen solution spectrum.

The EPR spin Hamiltonian parameters (g and A) for any paramagnetic complex will depend on the coordination state and

Table 1 Spin Hamiltonian parameters obtained by simulation for the compounds $[\text{Cr}(\text{CO})_4\text{a-g}]^+$

Complex	Ligand	g_{\perp}	g_{\parallel}	$^{\text{P}}A_{\perp}/\text{G}^{\text{a}}$	$^{\text{P}}A_{\perp}/\text{MHz}$	$^{\text{P}}A_{\parallel}/\text{G}^{\text{a}}$	$^{\text{P}}A_{\parallel}/\text{MHz}$	a_{iso}/G	$a_{\text{iso}}/\text{MHz}$	% s character
2e	PNP	2.089	1.983	29.0	84.8	24.0	66.6	27.3	78.7	0.573
2c	PCCP	2.084	1.989	25.5	74.4	25.0	69.6	25.3	72.8	0.532
2a	PCCP	2.083	1.989	24.8	72.3	24.5	68.2	24.8	70.9	0.518
2d	PNP	2.077	1.985	27.7	80.5	25.5	70.8	27.0	77.3	0.534
2g	PNP	2.072	1.988	27.0	78.3	25.5	71.0	26.5	75.9	0.556
2f	PNP	2.068	1.988	27.0	78.1	25.5	71.0	26.5	75.8	0.556
2b	PCCCP	2.063	1.987	24.9	72.0	24.5	68.1	24.7	70.7	0.520

^a A values ± 0.2 G.

symmetry of the metal centre. For the six coordinate $[\text{Cr}(\text{CO})_4\text{b}]^+$ complex, the strong ligand fields are expected to cause a large splitting between the t_{2g} orbitals and the e_g orbitals resulting in a low spin (LS) d^5 state ($S = \frac{1}{2}$). High spin (HS) or intermediate spin d^5 states ($S = 5/2$ or $3/2$) could only occur in the presence of a weak ligand field, which is not expected in the $[\text{Cr}(\text{CO})_4\text{b}]^+$ case. Furthermore, the LS Cr(I) complex could exist in two possible electronic ground states: a $(d_{xz}, d_{yz})^4(d_{xy})^1$ or $(d_{xy})^2(d_{xz}, d_{yz})^3$ configuration. Simple crystal field arguments would suggest that the expected ground state for the $[\text{Cr}(\text{CO})_4\text{b}]^+$ complex is $(d_{xz}, d_{yz})^4(d_{xy})^1$.²⁶ It is proposed that π -back donation to CO helps to stabilize d_{xz} and d_{yz} relative to the d_{xy} based HOMO. This is borne out by the observed g matrix. For a SOMO where the metal contribution is primarily d_{xy} , the components of the g matrix are given by the following equations:^{26,27}

$$g_{xx} - g_e = 2\lambda \sum_{m=0} \frac{(c_{xy})^2 (c_{xz}^m)^2}{E_0 - E_m} \quad (1a)$$

$$g_{yy} - g_e = 2\lambda \sum_{m=0} \frac{(c_{xy})^2 (c_{yz}^m)^2}{E_0 - E_m} \quad (1b)$$

$$g_{zz} - g_e = 8\lambda \sum_{m=0} \frac{(c_{xy})^2 (c_{x^2-y^2}^m)^2}{E_0 - E_m} \quad (1c)$$

In these equations g_e is the free electron g value, λ is the spin-orbit coupling constant for the free Cr(I) ion (-185 cm^{-1}), c_{xy}^m is the LCAO coefficient, E_0 is the energy of the SOMO and m sums over the other MOs with energies E_m . Spin-orbit coupling mixes in d_{xz} , d_{yz} and $d_{x^2-y^2}$ character, but for a low spin d^5 system, d_{xz} and d_{yz} will lie just below the SOMO, while $d_{x^2-y^2}$ will be empty and much higher in energy. As a result the above equations predict that the g_{xx} and g_{yy} values should be significantly higher than g_e while g_{zz} should be slightly less than g_e . These trends are indeed observed experimentally, with g_{\perp} ($g_{xx} = g_{yy}$) = 2.063 and $g_e > g_{\parallel}$ (g_{zz}) = 1.987 (Table 1), agreeing with a d_{xy} ground state of $[\text{Cr}(\text{CO})_4\text{b}]^+$.

The cw-EPR spectra for all the remaining complexes, **2a-g**, are shown in Fig. 2. In all cases, axial g matrices ($g_{\perp} > g_e > g_{\parallel}$) are observed and the corresponding spin Hamiltonian parameters for each complex are listed in Table 1 (the individual simulated spectra are given in the ESI†). Similar to the above discussion on $[\text{Cr}(\text{CO})_4\text{b}]^+$, it appears that the ground state in all the complexes can therefore be described as d_{xy} . It should be noted however, that the resolution of the spectra, and indeed the spin Hamiltonian values, are found to be highly dependent on the ligand type (Table 1). The difference in g values (defined as $\Delta g = g_{\perp} - g_{\parallel}$), for

example, is greatest for $[\text{Cr}(\text{CO})_4\text{e}]^+$ and smallest for $[\text{Cr}(\text{CO})_4\text{b}]^+$ (see Fig. 2 and Table 1).

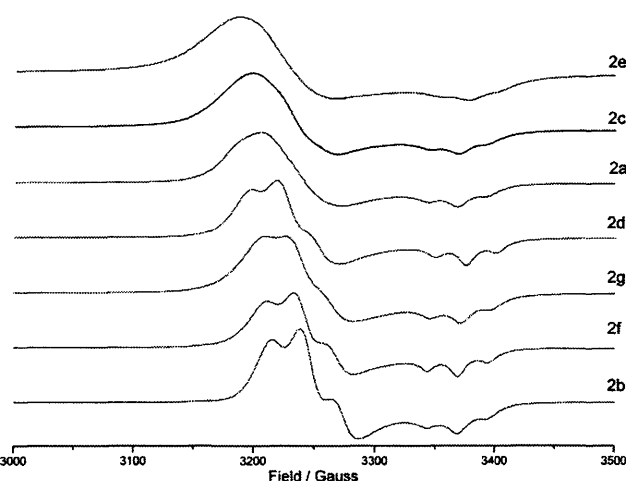


Fig. 2 cw-EPR spectra (140 K) of $[\text{Cr}(\text{CO})_4\text{a-g}]^+$ recorded in dichloromethane-toluene. The spin Hamiltonian parameters obtained by simulation are shown in Table 1.

Despite these clear differences in the Δg shift, caused by the extent of tetragonal distortion in the complexes, no obvious correlation emerges between the observed spectral shifts and the ligand type (*i.e.*, P-N-P or P-C-P based ligands). Some correlations were identified with respect to the $^{\text{P}}A$ hyperfine values, and these will be discussed later.

ENDOR Spectroscopy

The ^1H , ^{14}N and ^{31}P cw-ENDOR spectra were also recorded for all complexes in frozen (deuterated) dichloromethane-toluene at 10 K. Analysis of these ENDOR spectra was based on the observed orientational selection in the EPR spectra. It should be recalled that the powder EPR spectra (shown in Fig. 1 and 2 above) reflect an average of all molecular orientations of the complex with respect to the external field (\mathbf{B}). If the g (and A) matrix is known, one can then easily associate distinct sets of molecular orientations with a given resonant field value. For example when the applied field (\mathbf{B}) = B_{\perp} the specific orientations corresponding to the xy molecular direction ($g = g_{\perp}$) are chosen. Similarly when $\mathbf{B} = B_{\parallel}$, specific orientations corresponding to the z molecular direction ($g = g_{\parallel}$) are selected. These two resonant field positions (sometimes referred to as 'single-crystal like' positions in the powder pattern^{29,33,34}) are indicated in Fig. 1. This set of molecular

orientations can then be selected at fixed magnetic field settings for nuclear resonance (in the ENDOR experiment). The result is a hyperfine spectrum that contains only one part of the powder pattern, or at least very few molecular orientations.

Whilst the current $[\text{Cr}(\text{CO})_4\text{a-g}]^+$ complexes are dominated by the g anisotropy at X-band, the ^1A coupling is appreciable at this frequency (Table 1) and this complicates the choice of field position for the ENDOR measurements. In this case, when the applied field (B) = B_1 at least two sets of specific orientations are selected (as seen in the angular dependency plot for the Cr g matrix combined with the ^1A superhyperfine lines in the lower trace of Fig. 1). However, when the ENDOR spectra are recorded at the field position labeled *a* in Fig. 1, only a single orientation (corresponding to $\theta_{\text{H}} = 90^\circ$) is selected: effectively a field position analogous to $g = g_{\perp}$. Similarly when the ENDOR spectra are recorded at the field position labeled *b* in Fig. 1, only a single orientation (corresponding to $\theta_{\text{H}} = 0^\circ$) is selected: effectively a field position analogous to $g = g_{\parallel}$. Although the ENDOR spectra were measured at several (mixed) field positions, these latter two unique field positions greatly simplify the analysis of the subsequent ENDOR data.

^1H ENDOR. The ^1H ENDOR spectra of each complex recorded at the field position *a* (effective $g = g_{\perp}$ position) are shown in Fig. 3 for comparison. The spectra contain a matrix ^{19}F peak (labeled * in Fig. 3; $\nu_{\text{N}} = 14.0272$ MHz for ^{19}F at 3500 G) which arises from the $[\text{Al}(\text{OC}(\text{CF}_3)_3)_4]^-$ counter ion used in the preparation of the Cr(I) complex (see experimental section). All of the spectra appear to be qualitatively similar, containing couplings from weakly interacting protons. The outer ENDOR peaks are quite broad, and this is usually indicative of a distribution of proton environments, producing a minor strain on the ^1A values. The weakly coupled protons, responsible for the outer lines in the ENDOR spectra, most likely originate from the phenyl substituents on ligand *a-g*, since they are common to all complexes and closest to the Cr centre (see Scheme 2). The methyl and methine protons in the P–N–P ligand backbone (*d-g*) are, for example, more than 5 Å away from the Cr centre (too remote to account for the observed hyperfine couplings). Although the methine protons in the P–C–P ligand backbone (*a* and *b*) are

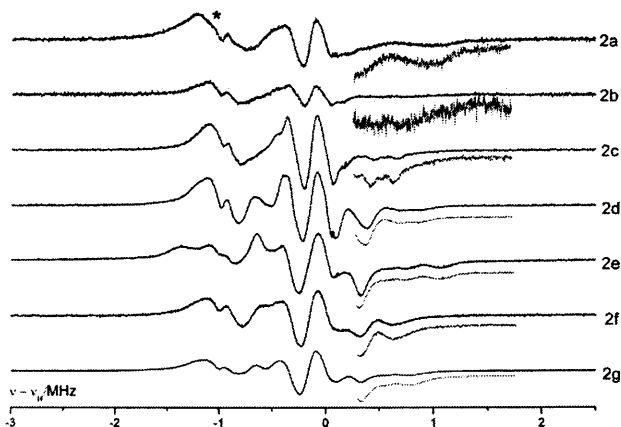
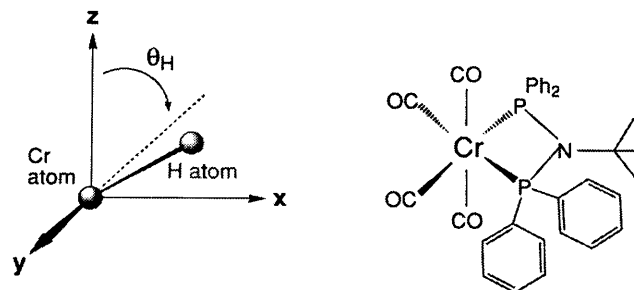


Fig. 3 cw ^1H ENDOR spectra (10 K) of $[\text{Cr}(\text{CO})_4\text{a-g}]^+$ recorded in deuterated dichloromethane-toluene. The spectra were obtained at the effective field position corresponding to $g = g_{\perp}$ for each system. * = ^{19}F matrix peak from the $[\text{Al}(\text{OC}(\text{CF}_3)_3)_4]^-$ counter ion.

closer to Cr (*ca.* 4.5 Å), their interaction would be expected to be predominantly dipolar in character and once again unlikely to account for the observed couplings.



Scheme 2

According to the published crystal structure of $[\text{Cr}(\text{CO})_4\text{g}]^+$,³¹ the two sets of phenyl groups in the complex are twisted with respect to each other. As a result, the two protons in the *ortho*-position of each phenyl ring are structurally inequivalent. This results in substantially different $\text{Cr}\cdots^1\text{H}_{\text{o-phenyl}}$ distances; *i.e.*, for each phenyl ring one of the *ortho*-protons has a shorter $\text{Cr}\cdots^1\text{H}_{\text{o-phenyl}}$ distance compared to the other. The four shortest $\text{Cr}\cdots^1\text{H}_{\text{o-phenyl}}$ distances from the crystal structure are reported to be 3.30, 3.54, 3.71 and 4.18 Å,³¹ and these distances are all easily within range of weakly coupled nuclei detectable by cw-ENDOR. Since the experimental ^1H hyperfine tensor will contain both isotropic (arising from spin polarisation) and anisotropic (arising from dipole-dipole interactions) terms, the observed differences in Fig. 3, must therefore arise either from changes to the relative conformation of the phenyl groups or due to changes in the electronic spin delocalisation in the complexes. In order to examine these changes in more depth, detailed simulations of the ENDOR data were performed.

The ^1H ENDOR spectra recorded at several field positions for $[\text{Cr}(\text{CO})_4\text{g}]^+$, as a representative example, are shown in Fig. 4 along with the associated simulations. Two distinct proton environments account for the spectra.

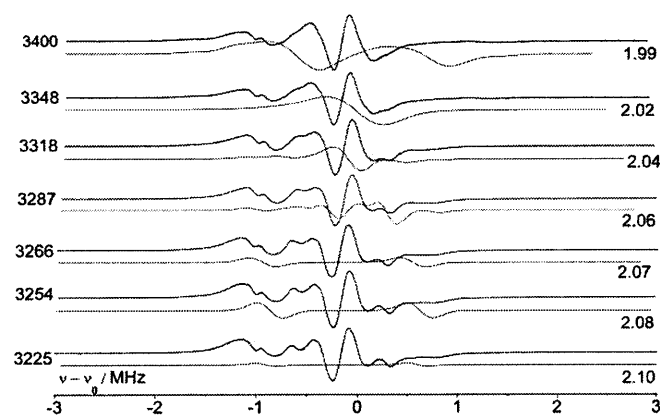


Fig. 4 Experimental and simulated cw ^1H ENDOR spectra (10 K) of $[\text{Cr}(\text{CO})_4\text{g}]^+$ recorded in deuterated dichloromethane-toluene. The angular selective spectra were obtained at the magnetic field positions (B in Gauss) and corresponding g values shown in the Figure.

However, owing to the broad linewidths observed, only the nuclei with the largest couplings can be simulated with any

accuracy (*i.e.*, the error associated with the simulated hyperfine couplings for the second set of protons, responsible for the inner peaks, is too large and suggests a $\text{Cr}\cdots^1\text{H}$ distance of >4 Å). The nucleus responsible for the largest couplings contains a small a_{iso} contribution (-0.05 MHz), and the resulting A_{\parallel} term (3.4 MHz) gives an estimated $\text{Cr}\cdots^1\text{H}$ distance of 3.58 Å (calculated using a simple point-dipole approximation based on the principal hyperfine components of $A_1 = -1.5$, $A_2 = -2.0$, $A_3 = 3.35$ MHz). Analysis of the ENDOR spectra for the remaining complexes reveals small a_{iso} values in all cases and this suggests that the variations observed in Fig. 3 for the different ligands must originate from slight differences in the phenyl group conformations. As mentioned earlier, distinctive $\text{Cr}\cdots^1\text{H}$ distances of 3.30, 3.54, 3.71 and 4.18 Å, were identified in the single crystal of $[\text{Cr}(\text{CO})_4\text{g}]^+$. It is highly likely that the main proton observed in the frozen solution ENDOR spectra, with the $\text{Cr}\cdots^1\text{H}$ distance of 3.58 Å, represents an averaged distribution of the single crystal distances. This would certainly account for the unusually broad linewidths of the ENDOR spectra.

^{14}N couplings. The ^{14}N ENDOR spectra were also recorded for the P–N–P containing ligands ($[\text{Cr}(\text{CO})_4\text{d-g}]^+$). As the ^{14}N nuclei are not directly coordinated to Cr, their couplings are expected to be weak. In such weak coupling cases, pulsed hyperfine techniques such as ESEEM and HYSCORE are ideally suited to extract the full hyperfine (A) and quadrupole (Q) matrices. Nevertheless, a good estimate can also be extracted from the more poorly resolved cw ENDOR spectra. The ^{14}N ENDOR spectra for $[\text{Cr}(\text{CO})_4\text{f}]^+$, recorded at four different field positions are shown in Fig. 5.

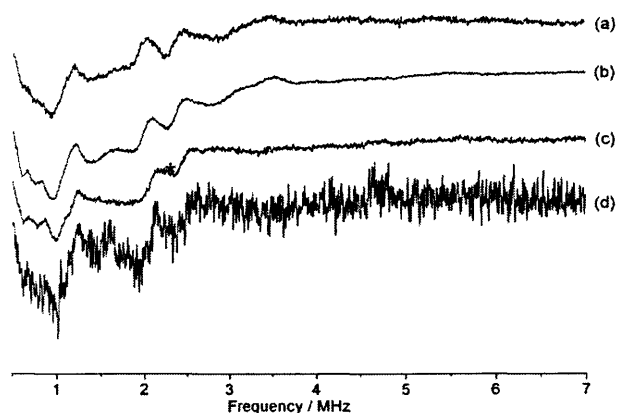


Fig. 5 Experimental cw ^{14}N ENDOR spectra (10 K) of $[\text{Cr}(\text{CO})_4\text{f}]^+$ recorded in deuterated dichloromethane–toluene. The angular selective spectra were obtained at the magnetic field positions and corresponding g values of (a) 3220 G, $g = 2.10$ (b) 3260 G, $g = 2.08$ (c) 3370 G, $g = 2.01$ and (d) 3394 G, $g = 1.99$. * = ^2H matrix peak.

As deuterated solvents were used, a deuterium matrix peak is clearly visible in the spectra (labeled * in Fig. 5; $\nu_{\text{N}} = 2.2876$ MHz for ^2H at 3500 G). The remaining features in the spectra are attributed to the superimposed A and Q terms. To a first and very crude approximation, the values obtained were $A_1 = \pm 4.38$ MHz, $A_2 = \pm 4.41$ MHz, $A_3 = \pm 6.65$ MHz and $Q_1 = \pm 0.13$ MHz, $Q_2 = \pm 0.19$ MHz, $Q_3 = \pm 0.32$ MHz.

However, since the quadrupole value contains important information on the electronic structure of the complex, these ^{14}N spectra will become more important and meaningful in later

studies devoted to the activation of the complex. In that case, the structural and electronic changes in the complex may be better monitored *via* the changes to the ^{14}N A and Q values *via* pulsed hyperfine methods.

^{31}P couplings. The ^{31}P couplings are sufficiently large, that they are clearly visible in the EPR spectra (Fig. 1 and 2). However, they are also present in the ENDOR spectra, as shown in Fig. 6 for $[\text{Cr}(\text{CO})_4\text{f}]^+$. Owing to the higher resolving powers of ENDOR, in principle their couplings, and possibly orientations, can be determined with more accuracy. The isotropic ^{31}P hyperfine couplings should arise from ^{31}P 3s character in the SOMO, from polarisation of inner shell P s orbitals by spin density on the metal or in P 3p orbitals. These summed contributions can then be analysed by EPR to account for the observed spin densities. However, as discussed by Rieger *et al.*,²⁶ reliable interpretation of the ^{31}P hyperfine matrix should be treated carefully as the anisotropies are often small and the g matrix anisotropy is much greater than the A^{P} matrix (hence observed spectral features correspond to orientations of the magnetic field along one of the g matrix principal axes). This will depend on the symmetry of the complex. Assuming an approximate C_{2v} symmetry for the $[\text{Cr}(\text{CO})_4\text{L}]^+$ complexes (since the C_2 axis runs from Cr through the N atom bridging the two P atoms, with one vertical mirror plane containing the two P atoms and another containing the two CO molecules) the g matrix axes are necessarily along the x , y and z molecular axes, with the Cr–P vectors lying approximately midway between the x and y axes (Scheme 2). However, at the low X-band frequency used in this work, the symmetry of the complex can be treated as axial for analysis purposes.

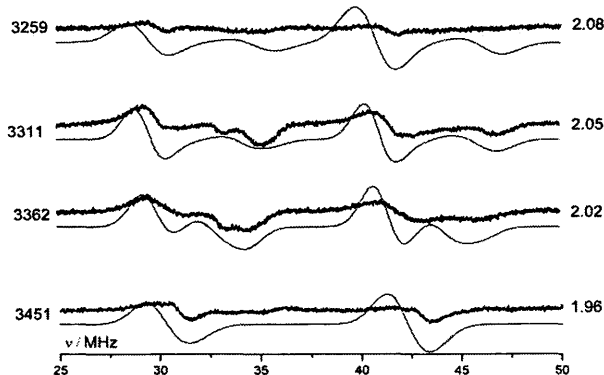


Fig. 6 Experimental and simulated cw ^{31}P ENDOR spectra (10 K) of $[\text{Cr}(\text{CO})_4\text{c}]^+$ recorded in deuterated dichloromethane–toluene. The angular selective spectra were obtained at the magnetic field positions (B in Gauss) and corresponding g values shown in the Figure.

The cw ^{31}P ENDOR spectra were simulated at a number of field positions for $[\text{Cr}(\text{CO})_4\text{f}]^+$ (Fig. 6). Although the observed linewidths were broad, the matrix is largely axially symmetric with $A_1 = 70 \pm 1$, $A_2 = 72 \pm 1$ and $A_3 = 83 \pm 1$ MHz ($a_{\text{iso}} = 75$ MHz $\cong 26.75$ G). This isotropic value is similar to that observed by EPR (see Table 1, $a_{\text{iso}} = 26.5$ G, allowing for the larger error in the EPR spectra). Interestingly the $^{\text{P}}A_{\parallel}$ value is calculated as 8 MHz, giving an estimated $\text{Cr}\cdots\text{P}$ bond length of 2.02 Å. Clearly this is an under estimation of the distance compared to the known crystal structures of $[\text{Cr}(\text{CO})_4\text{g}]^+$ ³¹ ($\text{Cr}\cdots\text{P}$ bond lengths of 2.26 and 2.66 Å) and $[\text{Cr}(\text{CO})_4(\text{diphos})]^0$ ³⁶ ($\text{Cr}\cdots\text{P}$ distance of 2.36 Å). This

discrepancy arises primarily from the dominant a_{iso} contribution to the hyperfine tensor, resulting in a higher degree of error associated with the dipolar term, and due to the limitations in the point-dipole approximation at such short electron-nuclear distances. For example, with a hyperfine tensor of $A_1 = 70$, $A_2 = 72$ and $A_3 = 81$ MHz, then $A_1 = 6.0$ MHz giving a Cr...P distance of 2.2 Å. For these reasons, it is qualitatively more meaningful to compare in detail the a_{iso} values rather than the anisotropic $^{\text{P}}A$ terms.

It should be noted that the small degree of anisotropy observed in the $^{\text{P}}A$ matrix is analogous to the experimental and calculated values for a series of Cr(I) carbonyl phosphine and phosphonite complexes as reported by Cummings *et al.*^{26b} The $[\text{Cr}(\text{CO})_4(\text{dppe})]^+$ complex had reported g values of 2.09, 2.08 and 1.988 and $^{\text{P}}A$ values of 66, 66 and 68 MHz. In all cases, the calculated anisotropies were small while the predicted a_{iso} values were analogous to those experimentally observed in this work.

As seen in Table 1, the a_{iso} values appear to be larger for the P–N–P type ligands compared to the P–C–P ligands. These results indicate that the electronic $3^{\text{P}}3s$ character in the SOMO is higher for the P–N–P type ligands (**2e** > **2g** ~ **2f** > **2d**) compared to the P–C–P type ligands (**2b** ~ **2a**); although **2c** has a slightly higher a_{iso} values in this expected trend. A similar correlation does not exist with respect to the g values (Table 1). Since the g matrix depends on the energy of the SOMO, which in turn is affected by the extent of tetragonal distortion in the complex, then any perturbation or changes in the coordination and symmetry of the system will be manifested in the g_1 components. Therefore ligands **a–g**, appear to alter the electronic properties of the complexes $[\text{Cr}(\text{CO})_4\text{L}]^+$ in a very subtle and delicate manner.

Structure function relations

The ligands chosen for study were done so on the basis that catalytic ethylene tetramerization data has been previously reported,^{31,37,38} and furthermore that they represent significantly different variations of the diphosphine scaffold capable of enabling this reaction. Pertinent catalytic data was tabulated³⁸ and a correlation searched for between the measured EPR-derived parameters (specifically the g values, phosphorus spin densities and % s orbital character (Fermi contact term), see Table 1) and various parameters of significance to the tetramerization reactions (activity, % C_6 , % C_8 , % 1- C_6 , % 1- C_8 , % C_6 -cyclics, 1- C_8 :1- C_6 ratio and PE formation). However, no meaningful correlation in trends could be identified between any combination of parameters. Given the significant perturbation to the chromium environment when $[\text{Cr}(\text{CO})_4\text{L}][\text{Al}(\text{OC}(\text{CF}_3)_3)_4]$ is activated for catalysis using excess trialkylaluminium and then placed under elevated pressure of ethylene, this lack of correlation is perhaps not surprising, and suggests that more meaningful analysis can only be achieved by studying species that have been activated in the first instance, and secondarily under pressure of ethylene. For this reason ongoing work will extend this initial study of the precatalyst to monitor the changes to electronic and structure properties after activation of the catalysts.

Conclusions

Reactive Cr(I) bis(diphenylphosphine) species, labelled $[\text{Cr}(\text{CO})_4\text{a–g}]^+$, were prepared and the paramagnetic complexes

characterised *via* cw-EPR and ENDOR spectroscopies. Subtle differences were identified between the complexes, most notably in the shifts to the g components and the changes to the $3^{\text{P}}3s$ character. The spin Hamiltonian parameters were found to be consistent with a low-spin d^5 system of C_{2v} symmetry, possessing a SOMO where the metal contribution is primarily d_{xy} . The isotropic Fermi contact term ($^{\text{P}}a_{\text{iso}}$) was found to be largest for complexes containing ligands **d**, **f**, **e** and **g**, indicating that the $3^{\text{P}}3s$ character in the SOMO is higher for the P–N–P type ligands than the P–C–P types. Observed changes in the g matrix did not however follow the same trends of ligand type, indicating that g is dependent not just on the energy of the SOMO but also on the structural differences in ligand which influence the extent of tetragonal distortion in the complexes. Structural differences in the $[\text{Cr}(\text{CO})_4\text{a–g}]^+$ complexes were also revealed through ^1H ENDOR, where the observed spectral changes were attributed to variations in the phenyl ring conformations as a function of ligand type. These EPR and ENDOR results reveal that the ligands **a–g** impart very subtle electronic and structural alterations to this class of complex, but that these parameters do not correlate with any trend in catalytic data at least for the parent pre-catalyst prior to activation.

Experimental section

General procedures

All manipulations were performed using standard Schlenk techniques under an argon atmosphere, or under a nitrogen atmosphere in a MBraun UNILAB glovebox with less than 0.1 ppm water and O_2 . Solvents were dried using a Braun Solvent Purification System, and degassed prior to use. Ligands **a**, **b** and **c** were purchased from Aldrich and used as received; **d** and **f** were prepared according to a literature procedure;³⁵ **e** was prepared according to a literature procedure;³⁷ **g** was prepared according to a literature procedure.³⁹ The corresponding chromium(0) **1a–1g** and chromium(I) compounds **2a–2g** were prepared according to literature procedures.^{30,31} $\text{Ag}[\text{Al}(\text{OC}(\text{CF}_3)_3)_4]$ was prepared according to a literature procedure.³²

Instruments

NMR spectra were recorded at 298 K on Bruker Avance AMX 400 or Jeol Eclipse 300 spectrometers. Chemical shift values are given relative to residual solvent peak. ESI-MS were performed on a Waters LCT Premier XE instrument. Infra-red spectra were recorded using a JASCO FT/IR-660 *Plus* spectrometer and analysed in solution (dichloromethane).

EPR/ENDOR measurements

Each complex **2a–g** was dissolved in 200 μl DCM–toluene in the EPR tube and a frozen solution produced by placing the tube in liquid nitrogen. Each spectrum was recorded at 140 K (EPR) or 10 K (ENDOR).

Instruments. All continuous-wave (cw) EPR spectra were recorded on an X-band Bruker EMX spectrometer operating at 100 kHz field modulation, 10 mW microwave power and equipped with a high sensitivity cavity (ER 4119HS). EPR computer

simulations were performed using the SimEPR32 program.⁴⁰ g values were determined using a DPPH standard. All cw ENDOR measurements were performed on a Bruker ESP300E series spectrometer operating at 12.5 kHz field modulation and equipped with an ESP360 DICE ENDOR unit in an EN-801 ENDOR cavity. The spectra were recorded at 10 K, using 8 dB RF power from an ENI A-300 RF amplifier, 251 kHz modulation depth and 4mW microwave power. The ENDOR spectra were simulated using an in-house programme based on the resonance expressions given in.³⁴ The EPR linewidths used in the ENDOR simulations were 5 G.

Representative synthesis of chromium(0) tetracarbonyl species

[Cr(CO)₄(Ph₂PN(*i*Pr)PPh₂)] (1g). Toluene (20 ml) was added to chromium hexacarbonyl [Cr(CO)₆], (350 mg, 1.59 mmol) and **g** (500 mg, 1.17 mmol) and the stirred mixture was heated under reflux for 48 h. The solution was cooled to 0 °C and filtered to remove excess [Cr(CO)₆]. Solvent was removed under reduced pressure and the product extracted into dichloromethane (5 ml). Methanol (10 ml) was added to precipitate the product, which was isolated by filtration and dried *in vacuo* to yield the yellow solid [Cr(CO)₄(Ph₂PN(*i*Pr)PPh₂)] (1 g):

Yellow solid (260 mg, 38%); ¹H NMR (CDCl₃, 400.8 MHz, 298 K): δ (ppm) 0.62 (d, 6H, CH₃, $J_{\text{HH}} = 6.8$ Hz), 3.52 (sept, 1H, CH, $J_{\text{HH}} = 7.0$ Hz), 7.41 (m, 12H, *meta*-, *para*-C₆H₅), 7.69 (m, 8H, *ortho*-C₆H₅); ³¹P {¹H} NMR (CDCl₃, 121.7 MHz, 298 K): δ (ppm) 112.70 (s); ¹³C NMR (CDCl₃, 125.8 MHz, 298 K): δ (ppm) 22.54 (CH₃), 54.79 (CH), 127.39 (*meta*-C₆H₅), 129.52 (*para*-C₆H₅), 130.86 (*ortho*-C₆H₅), 136.09 (*ipso*-C₆H₅), 221.89 (*cis*-CO), 227.40 (*trans*-CO); High Resolution ESI_{pos}-MS (MeCN): found 591.0796 (calc 591.0820 dev: -4.1 ppm); IR (CH₂Cl₂): $\nu = 1887$ (s) (CO), 1923 (s) (CO), 2006 (s) (CO) cm⁻¹.

All other Cr(0) complexes were synthesised using an analogous method to give **1a–f**. Analytical data are provided below.

[Cr(CO)₄(Ph₂PCH₂CH₂PPh₂)] (1a). Yellow solid (300 mg, 42%); ¹H NMR (CD₂Cl₂, 400.8 MHz, 298 K): δ (ppm) 2.00 (t, 4H, CH₂CH₂, $J = 4.1$ Hz), 7.20–7.35 (m, 16H, *ortho*- and *meta*-C₆H₅), 7.50 (m, 4H, *para*-C₆H₅); ³¹P {¹H} NMR (CD₂Cl₂, 121.7 MHz, 298 K): δ (ppm) 80.35 (s); ¹³C NMR (CD₂Cl₂, 125.8 MHz, 298 K): δ (ppm) 27.30 (CH₂CH₂), 127.76 (*meta*-C₆H₅), 130.36 (*para*-C₆H₅), 131.88 (*ortho*-C₆H₅), 137.63 (*ipso*-C₆H₅), 219.61 (*cis*-CO), 228.30 (*trans*-CO); High Resolution ESI_{pos}-MS (MeCN): found 562.0542 (calc 562.0555 dev: -2.3 ppm); IR (CH₂Cl₂): $\nu = 1870$ (s) (CO), 1902 (s) (CO), 2005 (s) (CO) cm⁻¹.

[Cr(CO)₄(Ph₂PCH₂CH₂CH₂PPh₂)] (1b). Yellow solid (400 mg, 57%); ¹H NMR (CDCl₃, 400.8 MHz, 298 K): δ (ppm) 1.88 (m, 2H, CH₂), 2.34 (m, 4H, CH₂), 7.32 (m, 20H, C₆H₅); ³¹P {¹H} NMR (CDCl₃, 121.7 MHz, 298 K): δ (ppm) 42.38 (s); ¹³C NMR (CDCl₃, 125.8 MHz, 298 K): δ (ppm) 18.57 (CH₂), 29.64 (CH₂), 127.31 (*meta*-C₆H₅), 128.42 (*para*-C₆H₅), 130.78 (*ortho*-C₆H₅), 136.72 (*ipso*-C₆H₅), 220.70 (*cis*-CO), 225.07 (*trans*-CO); High Resolution ESI_{pos}-MS (MeCN): found 576.0717 (calc 576.0711 dev: 1.0 ppm); IR (CH₂Cl₂): $\nu = 1885$ (s) (CO), 1913 (s) (CO), 2005 (s) (CO) cm⁻¹.

[Cr(CO)₄(Ph₂PBzPPh₂)] (1c). Yellow solid (320 mg, 47%); ¹H NMR (CD₂Cl₂, 400.8 MHz, 298 K): δ (ppm) 7.30 (m, 20H, *ortho*-, *meta*-C₆H₅, C₆H₄), 7.45 (m, 4H, *para*-C₆H₅); ³¹P {¹H}

NMR (CD₂Cl₂, 121.7 MHz, 298 K): δ (ppm) 83.33 (s); ¹³C NMR (CD₂Cl₂, 125.8 MHz, 298 K): δ (ppm) 127.39 (*meta*-C₆H₅), 127.60 (*para*-C₆H₅), 128.93, 129.65, 131.33 (C₆H₄), 131.37 (*ortho*-C₆H₅), 135.60 (*ipso*-C₆H₅); High Resolution ESI_{pos}-MS (MeCN): found 610.0564 (calc 610.0555 dev: 1.4 ppm); IR (CH₂Cl₂): $\nu = 1893$ (s) (CO), 1916 (s) (CO), 2012 (s) (CO) cm⁻¹.

[Cr(CO)₄(Ph₂PN(Et)PPh₂)] (1d). Yellow solid (350 mg, 50%); ¹H NMR (CDCl₃, 400.8 MHz, 298 K): δ (ppm) 0.75 (t, 3H, CH₃, $J_{\text{HH}} = 7.3$ Hz), 3.00 (m, 2H, CH₂), 7.41 (m, 20H, C₆H₅); ³¹P {¹H} NMR (CDCl₃, 121.7 MHz, 298 K): δ (ppm) 114.36 (s); ¹³C NMR (CDCl₃, 125.8 MHz, 298 K): δ (ppm) 15.12 (CH₃), 43.99 (CH₂), 127.52 (*meta*-C₆H₅), 129.65 (*para*-C₆H₅), 130.86 (*ortho*-C₆H₅), 135.55 (*ipso*-C₆H₅), 221.24 (*cis*-CO), 227.22 (*trans*-CO); High Resolution ESI_{pos}-MS (MeCN): found 577.0656 (calc 577.0664 dev: -1.4 ppm); IR (CH₂Cl₂): $\nu = 1891$ (s) (CO), 1915 (s) (CO), 2007 (s) (CO) cm⁻¹.

[Cr(CO)₄(Ar₂PN(Me)PAr₂)] Ar = 2-C₆H₄(Et) (1e). Yellow solid (350 mg, 53%); ¹H NMR (CD₂Cl₂, 400.8 MHz, 298 K): δ (ppm) 0.85 (br s, 12H, CH₃), 2.46 (s, 3H, CH₃), 2.61 (br s, 8H, CH₂), 7.32 (m, 16H, *Ar*-H); ³¹P {¹H} NMR (CD₂Cl₂, 121.7 MHz, 298 K): δ (ppm) 103.4 (br s); ¹³C NMR (CD₂Cl₂, 125.8 MHz, 298 K): δ (ppm) 13.27 (CH₃), 26.03 (CH₂), 33.55 (CN), 124.89 (*meta*-C₆H₅), 129.05 (*para*-C₆H₅), 134.47 (*ortho*-C₆H₅), 144.59 (*ipso*-C₆H₅), 219.76 (*cis*-CO), 227.72 (*trans*-CO); IR (CH₂Cl₂): $\nu = 1864$ (s) (CO), 1895 (s) (CO), 2006 (s) (CO) cm⁻¹; High Resolution ESI_{pos}-MS (MeCN): found 675.1746 (calc 675.1759 dev: -1.9 ppm).

[Cr(CO)₄(Ph₂PN(*i*Bu)PPh₂)] (1f). ³¹P {¹H} NMR (CD₂Cl₂, 121.7 MHz, 298 K): δ (ppm) 115.86 (s). The supply of ligand was limited, therefore the entire complex **1f** was converted to the Cr(I) complex as priority was given to EPR/ENDOR measurements.

Synthesis of Ag[Al(OC(CF₃)₃)₄]²². LiAlH₄ (1.0 g, 0.026 mol) was suspended in hexane (60 ml), cooled to 253 K and HOC(CF₃)₃ (15 ml, 0.11 mol) added slowly. The mixture was stirred for 45 min then heated under reflux overnight using a condenser set at 253 K. The solution was filtered, the product washed with hexane and solvent removed *in vacuo* to yield the white solid Li[Al(OC(CF₃)₃)₄] (20.0 g, 80%); ¹⁹F NMR ((CD₃)₂SO, 250 MHz, 298 K): δ (ppm) -75.06.

Li[Al(OC(CF₃)₃)₄] (10.0 g, 0.01 mol) and AgF (1.7 g, 0.013 mol) were suspended in CH₂Cl₂ (50 ml) in the dark and mixed in an ultrasonic bath overnight. The solution was filtered and the solvent removed *in vacuo* to yield the white solid Ag[Al(OC(CF₃)₃)₄] (8.3 g, 77%).

Representative synthesis of chromium(I) tetracarbonyl species

Cr(CO)₄(Ph₂PN(*i*Pr)PPh₂)[Al(OC(CF₃)₃)₄] (2g). Complex **1g** (100 mg, 0.17 mmol) and Ag[Al(OC(CF₃)₃)₄] (220 mg, 0.23 mmol) were dissolved in dichloromethane (5 ml) to give a dark blue solution. The Schlenk tube was covered with foil to reduce exposure of the reaction mixture to light. The solution was stirred at room temperature overnight, then filtered and the solvent removed *in vacuo* to yield the blue solid [Cr(CO)₄(Ph₂PN(*i*Pr)PPh₂)[Al(OC(CF₃)₃)₄] (**2g**): Dark blue powder (105 mg, 40%); High Resolution ESI_{pos}-MS (MeCN): found 591.0824 (calc 591.0820 dev: 0.6 ppm); IR (CH₂Cl₂): $\nu = 1964$ (s) (CO), 2032 (s) (CO), 2086 (s) (CO) cm⁻¹.

All other Cr(I) complexes were synthesised *via* an analogous method (using either 100 mg or 50 mg Cr(0) complex) to give **2a–f**: Analytical data is provided below.

[Cr(CO)₄(Ph₂PCH₂CH₂PPh₂)]₂[Al(OC(CF₃)₃)₄] (2a**). Dark purple powder (90 mg, 66%); High Resolution ESI_{pos}-MS (MeCN): found 562.0562 (calc 562.0555 dev: 1.2 ppm); High Resolution ESI_{neg}-MS (MeCN): found 966.9030 (calc 966.9037 dev: -0.7 ppm); IR (CH₂Cl₂): ν = 1971 (s) (CO), 2034 (s) (CO), 2085 (s) (CO) cm⁻¹.**

[Cr(CO)₄(Ph₂PCH₂CH₂CH₂PPh₂)]₂[Al(OC(CF₃)₃)₄] (2b**). Dark blue powder (145 mg, 54%); High Resolution ESI_{pos}-MS (MeCN): found 576.0706 (calc 576.0711 dev: -0.8 ppm); High Resolution ESI_{neg}-MS (MeCN): found 966.9084 (calc 966.9037 dev: 4.8 ppm); IR (CH₂Cl₂): ν = 1954 (s) (CO), 2046 (s) (CO), 2086 (s) (CO) cm⁻¹.**

[Cr(CO)₄(Ph₂PBzPPh₂)]₂[Al(OC(CF₃)₃)₄] (2c**). Dark blue powder (65 mg, 50%); High Resolution ESI_{pos}-MS (MeCN): found 610.0540 (calc 610.0555 dev: -2.4 ppm); IR (CH₂Cl₂): ν = 1969 (s) (CO), 2032 (s) (CO), 2086 (s) (CO) cm⁻¹.**

[Cr(CO)₄(Ph₂PN(Et)PPh₂)]₂[Al(OC(CF₃)₃)₄] (2d**). Dark blue powder (120 mg, 45%); High Resolution ESI_{pos}-MS (MeCN): found 577.0648 (calc 577.0664 dev: -2.7 ppm); IR (CH₂Cl₂): ν = 1968 (s) (CO), 2036 (s) (CO), 2089 (s) (CO) cm⁻¹.**

[Cr(CO)₄(Ar₂PN(Me)PAr₂)]₂[Al(OC(CF₃)₃)₄] Ar = 2-C₆H₄(Et) (2e**). Dark blue powder (150 mg, 62%); High Resolution ESI_{pos}-MS (MeCN): found 675.1773 (calc 675.1759 dev: 2.0 ppm); IR (CH₂Cl₂): ν = 1975 (s) (CO), 2022 (s) (CO), 2052 (s) (CO), 2082 (s) (CO) cm⁻¹.**

[Cr(CO)₄(Ph₂PN(*i*Bu)PPh₂)]₂[Al(OC(CF₃)₃)₄] (2f**). The supply of complex was limited, therefore priority of use of **2f** was given to EPR/ENDOR measurements.**

Acknowledgements

L. McDyre and T. Hamilton would like to thank Sasol Technology (Pty) Ltd. for funding. We are grateful to the referees for their extensive and helpful comments, and particularly for providing further confirmation on the magnitude and sign of the *g* matrix.

Notes and references

- M. E. Lashier, EP 0780353A1, 1997, Phillips Petroleum; J. T. Dixon, M. J. Green, F. M. Hess and D. H. Morgan, *J. Organomet. Chem.*, 2004, **689**, 3641.
- D. S. McGuinness, P. Wasserscheid, W. Keim, C. Hu, U. Englert, J. T. Dixon and J. J. C. Grove, *Chem. Commun.*, 2003, 334; J. T. Dixon, J. J. C. Grove, P. Wasserscheid, D. S. McGuinness, F. M. Hess, H. Maumela, D. H. Morgan, A. Bollmann, WO 03053891A1 2003; D. S. McGuinness, P. Wasserscheid, W. Keim, D. Morgan, J. T. Dixon, A. Bollmann, H. Maumela, F. Hess and U. Englert, *J. Am. Chem. Soc.*, 2003, **125**, 5272; J. T. Dixon, P. Wasserscheid, D. S. McGuinness, F. M. Hess, H. Maumela, D. H. Morgan, A. Bollmann, WO 03053890A1, 2003 (Sasol Technology).
- M. J. Overett, K. Blann, A. Bollmann, J. T. Dixon, F. M. Hess, E. Killian, H. Maumela, D. H. Morgan, A. Neveling and S. Otto, *Chem. Commun.*, 2005, 622.
- P. J. W. Deckers, B. Hessen and J. H. Teuben, *Angew. Chem., Int. Ed.*, 2001, **40**, 2516.
- C. Andes, S. B. Harkins, S. Murtuza, K. Oyler and A. Sen, *J. Am. Chem. Soc.*, 2001, **123**, 7423.
- L. E. Bowen and D. F. Wass, *Organometallics*, 2006, **25**, 555.
- L. E. Bowen, M. Charernsuk and D. F. Wass, *Chem. Commun.*, 2007, 2835.
- R. Emrich, O. Heinemann, P. W. Jolly, C. Krüger and G. P. J. Verhovnik, *Organometallics*, 1997, **16**, 1511.
- N. Meijboom, C. J. Schaverien and A. G. Orpen, *Organometallics*, 1990, **9**, 774.
- T. Agapie, S. J. Schofer, J. A. Labinger and J. E. Bercaw, *J. Am. Chem. Soc.*, 2004, **126**, 1304.
- R. M. Manyik, W. E. Walker and T. P. Wilson, *J. Catal.*, 1977, **47**, 197.
- R. D. Köhn, M. Haufe, S. Mihan and D. Lilge, *Chem. Commun.*, 2000, 1927.
- D. H. Morgan, S. L. Schwikkard, J. T. Dixon, J. J. Nair and R. Hunter, *Adv. Synth. Catal.*, 2003, **345**, 939.
- W. J. van Rensburg, C. Grove, J. P. Steynberg, K. B. Stark, J. J. Huyser and P. J. Steynberg, *Organometallics*, 2004, **23**, 1207.
- R. A. Cotton, G. Wilkinson, C. A. Murillo, M. Bochmann, *Advanced Inorganic Chemistry*, Wiley, 1999, 1355.
- Y. Fang, Y. Liu, Y. Ke, C. Guo, N. Zhu and Y. Hu, *Appl. Catal., A*, 2002, **235**, 33.
- R. D. Köhn, M. Haufe, G. Kociok-Köhn, P. Wasserscheid and W. Keim, *Angew. Chem. Int. Ed.*, 2000, **39**, 4337.
- Z. Yu and K. N. Houk, *Angew. Chem., Int. Ed.*, 2003, **42**, 808.
- A. N. J. Blok, P. H. M. Budzelaar and A. W. Gal, *Organometallics*, 2003, **22**, 2564.
- T. J. M. de Bruin, L. Magna, P. Raybaud and H. Toulhoat, *Organometallics*, 2003, **22**, 3404.
- S. Tobisch and T. Ziegler, *Organometallics*, 2003, **22**, 5392.
- M. J. Overett, K. Blann, A. Bollmann, J. T. Dixon, D. Haasbroek, E. Killian, H. Maumela, D. S. McGuinness and D. H. Morgan, *J. Am. Chem. Soc.*, 2005, **127**, 10723.
- T. Weyhermüller, T. K. Paine, E. Bothe, E. Bill and P. Chaudhuri, *Inorg. Chim. Acta*, 2002, **337**, 344.
- A. Bruckner, J. K. Jabor, A. E. C. McConnell and P. B. Webb, *Organometallics*, 2008, **27**, 3849.
- M. Branca, M. Fruianu, S. Sau and M. A. Zoroddu, *J. Inorg. Biochem.*, 1996, **62**, 223; M. Branca, G. Micera and D. Sanna, *Inorg. Chem.*, 1993, **32**, 578.
- P. H. Rieger, *Coord. Chem. Rev.*, 1994, **135–136**, 203; A. L. Rieger and P. H. Rieger, *Organometallics*, 2002, **21**, 5868; D. A. Cummings, J. McMaster, A. L. Rieger and P. H. Rieger, *Organometallics*, 1997, **16**, 4362.
- B. R. McGarvey, *Coord. Chem. Rev.*, 1998, **170**, 75.
- A. Schweiger, G. Jeschke, *Principles of pulse electron paramagnetic resonance*, Oxford University Press, 2001.
- D. M. Murphy and R. D. Farley, *Chem. Soc. Rev.*, 2006, **35**, 249.
- L. E. Bowen, M. F. Haddow, A. G. Orpen and D. F. Wass, *Dalton Trans.*, 2007, 1160.
- A. J. Rucklidge, D. S. McGuinness, R. P. Tooze, A. M. Z. Slawin, J. D. A. Pelletier, M. J. Hanton and P. B. Webb, *Organometallics*, 2007, **26**, 2782.
- I. Krossing and A. Reisinger, *Coord. Chem. Rev.*, 2006, **250**, 2721.
- B. M. Hoffman, J. Martinsen and R. A. Venters, *J. Mag. Reson.*, 1984, **59**, 110.
- G. C. Hurst, T. A. Henderson and R. W. Kreilick, *J. Am. Chem. Soc.*, 1985, **107**, 7294; T. A. Henderson, G. C. Hurst and R. W. Kreilick, *J. Am. Chem. Soc.*, 1985, **107**, 7299.
- M. J. Overett, K. Blann, A. Bollmann, J. T. Dixon, F. M. Hess, E. Killian, H. Maumela, D. H. Morgan, A. Neveling and S. Otto, *Chem. Commun.*, 2005, 620.
- M. J. Bennett, F. A. Cotton and M. D. LaPrade, *Acta Crystallogr., Sect. B: Struct. Crystallogr. Cryst. Chem.*, 1971, **27**, 1899.
- K. Blann, A. Bollmann, H. de Bod, J. T. Dixon, E. Killian, P. Nongodlwana, M. C. Maumela, H. Maumela, A. E. C. McConnell, D. H. Morgan, M. J. Overett, M. Prétorius, S. Kuhlmann and P. J. Wasserscheid, *J. Catal.*, 2007, **249**, 244.
- M. J. Overett, K. Blann, A. Bollmann, R. de Villiers, J. T. Dixon, E. Killian, M. C. Maumela, H. Maumela, D. S. McGuinness, D. H. Morgan, A. Rucklidge and A. M. Z. Slawin, *J. Mol. Catal. A: Chem.*, 2008, **283**, 114.
- M. S. Balakrishna, T. K. Prakasha and S. S. Krishnamurthy, *J. Organomet. Chem.*, 1990, **390**, 203.
- T. P. P. Spalek and Z. Sojka, *J. Chem. Inf. Model.*, 2005, **45**, 18.